Model Reduction in Chemical Engineering

Case studies applied to process analysis design and operation

Cover design by JM&BD

Model Reduction in Chemical Engineering

Case studies applied to process analysis design and operation

Proefschrift

ter verkrijging van de graad van doctor
aan de Technische Universiteit Delft,
op gezag van de Rector Magnificus, prof. ir. K.C.A.M. Luyben,
voorzitter van het College voor Promoties
in het openbaar te verdedigen op maandag 4 juli 2010 om 15:00 uur

door

Bogdan DORNEANU

Inginer diplomat
(Universitatea Politehnica din Bucureşti, Roemenië)
geboren te Medgidia (Roemenië)

Dit proefschrift is goedgekeurd door de promotor:

Prof. ir. J. Grievink

Samenstelling promotiecommissie:

Rector Magnificus	**Voorzitter**
Prof. ir. J. Grievink	**Technische Universiteit Delft, promotor**
Dr. ir. C.S. Bildea	**University Politehnica of Bucharest, copromotor**
Prof. dr. ir. P.M.J. van den Hof	**Technische Universiteit Delft**
Prof. dr. F. Kapteijn	**Technische Universiteit Delft**
Dr. ir. H.J.M. Kramer	**Technische Universiteit Delft**
Prof. dr. ir. P.M.M. Bongers	**Technische Universiteit Eindhoven / Unilever**
Prof. dr. P.D. Iedema	**Universiteit van Amsterdam**
Dr. ir. P.J.T. Verheijen	**Technische Universiteit Delft, reservelid**

Keywords: model reduction, process modelling, plantwide control, dynamic optimization, alkylation, ice cream freezing

An electronic version of this thesis is available from http://www.library.tudelft.nl

ISBN 978-90-8570-771-4

Copyright ©2011 by Bogdan Dorneanu

All rights reserved. No part of the material protected by this copyright notice may be reproduced or utilized in any form or by any means, electronic or mechanical, including photocopying, recording or by any information storage and retrieval system, without the prior written permission from the author.

Printed in The Netherlands by CPI Wöhrmann Print Service

Motto

"It can scarcely be denied that the supreme goal of all theory is to make the irreducible basic elements as simple and as few as possible without having to surrender the adequate representation of a single datum of experience."

A. Einstein

A significant part of the research was carried out within the framework of MRTN-CT-2004-512233 (PRISM – Towards Knowledge-Based Processing Systems). The financial support of the European Commission and Unilever R&D Vlaardingen is gratefully acknowledged.

Table of contents

Summary i

Samenvatting v

Rezumat ix

Chapter 1 – Introduction 1
1. Role of modelling in chemical engineering 2
   1.1. Model applications and benefits 2
   1.2. Efforts and cost factors for model development and application 5
2. Requirements for model use in chemical engineering 5
3. Process models and modelling 6
   3.1. Process models 6
   3.2. Model classification 8
   3.3. Model development steps 9
   3.4. Dual way of modelling: decomposition and aggregation over detail levels 13
4. Motivation and formulation of the research problem 15
5. Research approach and outline of the thesis 18
6. References 20

Chapter 2 – Process modelling and model reduction 25
1. Introduction 26
2. A design view on process modelling 27
   2.1. Levels of decomposition in the modelling procedure 28
3. Contextual and structure levels of decomposition 30
   3.1. Contextual level 30
   3.2. Structure level 31
      3.2.1. Process decomposition and physical structure of the model 31
      3.2.2. Behavioural structure of the model 36
      3.2.3. Model connectivity 37
4. Mathematical, numerical and software implementation levels 39
   4.1. Mathematical level: behavioural models of nodes 40
      4.1.1. Coordinates 40
      4.1.2. Classification of quantities 41
      4.1.3. Classification of equations 42
      4.1.4. Validity and applicability conditions (knowledge constraints) 46
      4.1.5. Types of operations in model equations 46
      4.1.6. Model classification 46
   4.2. Mathematical level: Connectivity 47
   4.3. Mathematical level: Aggregation at system level 49
   4.4. Relationship between the structure and the complexity of the model 51
      4.4.1. Number of equations 52
      4.4.2. Number of terms in the model equations 52
      4.4.3. Connectivity of the model equations 53
   4.5. Numerical level 53
   4.6. Software implementation level 54
5. Existent model reduction techniques 55
   5.1. Approaches to model reduction of process models 55
   5.2. Contextual level 55
   5.3. Structure level 56
      5.3.1. Model reduction at physical structure level 56
      5.3.2. Model reduction at behavioural structure level 58
   5.4. Mathematical level 59

5.4.1. Model simplification techniques 60
5.4.2. Model order-reduction techniques 61
5.5. System level 62
5.6. Numerical level 62
6. Model reduction for chemical engineering applications 63
7. Selected research problems in model reduction 64
8. Conclusions 66
9. References 67

Chapter 3 – Application of model reduction to design of plantwide control systems 73
1. Introduction 74
1.1. Model reduction for complex processes 74
1.2. Design of the plantwide control systems 74
2. Model reduction 75
2.1. Model simplification 76
2.1.1. Linearization 76
2.1.2. Approximation of functional expressions 77
2.1.3. Simplification of physical properties model 77
2.1.4. Simplification of chemical kinetics 77
2.2. Model-order reduction 77
2.2.1. Linear model-order reduction 78
2.2.2. Nonlinear model-order reduction 79
2.3. Linear model-order reduction by balanced realization 79
3. Model reduction with process knowledge 81
3.1. Classical model reduction algorithm for chemical plants 81
3.1.1. Obtaining the rigorous model 81
3.1.2. Obtaining the linear model 82
3.1.3. Obtaining the balanced state space model 82
3.1.4. Obtaining the reduced-order model 82
3.1.5. Plantwide control structures 83
3.2. Structure-retaining model reduction algorithm 83
A. Identification of units or groups of integrated units to which local control is applied 84
B. Application of tailored reduction techniques to individual units or groups of aggregated units 84
C. Obtaining the reduced model of the full plant 85
4. Case study: plantwide control of iso-butane - butene alkylation plant 87
4.1. Process description and the rigorous model 87
4.2. The linear model 90
4.3. The balanced model 90
4.4. Exploiting the structure 91
4.4.1. The reactor sub-system 91
4.4.2. The distillation columns 95
4.5. Assessment of the plantwide control structure 97
5. Conclusions 101
6. References 102

Chapter 4 – Dynamic optimization using a reduced process model 105
1. Introduction 106
2. Dynamic optimization 107
2.1. Numerical methods for dynamic optimization 108
2.2. Single-shooting dynamic optimization 109
3. Model reduction for dynamic optimization 110
3.1. The rigorous model 111
3.2. The reduced model 113

3.2.1. The reactor sub-system 113
3.2.2. The distillation columns 114
3.2.3. Performance of the reduced model 114
4. The dynamic optimization 115
5. Conclusions 119
6. References 120

Chapter 5 – Development of a reduced model for ice cream freezing 125
1. Introduction 126
1.1. Model reduction for complex units and products 126
1.2. Ice formation in a scraped surface heat exchanger 126
2. Physical aspects and modelling approach 128
2.1. Ice cream structure 129
2.1.1. Ice particles 129
2.1.2. Liquid matrix 129
2.1.3. Fat droplets 129
2.1.4. Air bubbles 130
2.2. Scraped-surface heat exchanger 130
2.3. Freezing mechanism 131
2.4. Scope and approach to modelling of the ice cream freezing unit 132
3. Specification of the 5-D model of the ice cream freezing unit 135
3.1. Spatial domains with thermodynamic phases 135
3.2. The generic equation of conservation for the physical resources 137
3.3. Mass 138
3.3.1. The bulk domain 140
3.3.2. The frozen layer domain 140
3.3.3. The equipment related domains and phases 141
3.4. Momentum 141
3.5. Energy 141
3.5.1. The bulk domain 143
3.5.2. The ice particles in the bulk domain 143
3.5.3. The rotor 144
3.5.4. The frozen layer domain 144
3.5.5. The freezer's wall 144
3.5.6. The coolant 144
3.6. Overview of the reductions in the 5-D model 144
4. Specification of the 3-D model of the ice cream freezing unit 145
4.1. Mass 147
4.1.1. The bulk domain 147
4.1.2. The frozen layer domain 150
4.2. Momentum 153
4.3. Energy 155
4.3.1. The bulk domain 156
4.3.2. The frozen layer domain 161
4.3.3. The freezer wall 163
4.3.4. The coolant 163
4.4. Overview of the model reduction for the conservation equations in the 3-D model 164
5. Constitutive equations for the 3-D model 165
5.1. Thermodynamic equations of state 166
5.1.1. Density of phases 166
5.1.2. Specific heat and enthalpy 168
5.1.3. Ice-water-sugar phase equilibrium 170
5.2. Fluxes in a spatial direction 170

5.2.1. Mass flux in axial direction 170
5.2.2. Mass flux along the internal coordinate 171
5.2.3. Energy flux in axial direction 171
5.2.4. Energy flux in radial direction 171
5.2.5. Energy flux in radial direction over the frozen layer and the metal wall 172
5.3. Rate laws 172
5.3.1. Mass transfer and ice melting processes 173
5.3.2. Energy transfer processes 182
5.4. Conductivities and transfer coefficients 186
5.4.1. Mass transfer coefficients 186
5.4.2. Viscosity 188
5.4.3. Thermal conductivity 189
5.4.4. Heat transfer coefficients 190
5.5. Overview of the reductions for the constitutive equations in the 3-D model 192
6. Summary of the mathematical structure of the 3-D model 193
7. Input-output structure of the reduced model for model use 197
8. Conclusions 199
9. References 200

Chapter 6 – Numerical application of the reduced model for ice cream freezing 203
1. Introduction 204
2. Development of a numerical scheme and implementation 206
2.1. Discretization of coordinates and mathematical operators 206
2.2. Discretization of model equation for the steady state model 209
2.3. Discretization of the population balance equation for the ice particles 210
2.3.1. Finite volume method 211
2.4. Software environment 213
2.5. Verification of the model implementation 214
3. Model applications 215
3.1. Model simulation 215
3.1.1. Simulation scenario 215
3.1.2. Simulation results and discussion 217
3.2. Parametric sensitivity analysis for validation purposes 223
3.2.1. Sensitivity analysis by singular value decomposition 224
3.2.2. Results of the parametric sensitivity analysis and discussion 226
4. Conclusions 233
5. References 233

Chapter 7 – Conclusions and recommendations 235
1. Research questions and approach 236
2. Conclusion on model reduction approach with test results 237
2.1. Generation of model reduction options by a decomposition approach 237
2.2. Application fo the structure-retaining model reduction approach 238
2.2.1. Model reduction for complex processes with simple products 238
2.2.2. Model reduction for simple processes with complex products 239
3. Recommendations 241
3.1. Model reduction for complex processes with simple products 241
3.2. Model reduction for a single unit with complex products 242
3.2.1. Application of the structure-retaining approach 242
3.2.2. Selective model refinement 242
3.2.3. Preparing for model validation and application 243
3.3. Decomposition of the process for model reduction 243
4. References 245

Chapter 8 - Appendix **247**
1. Summary of differential operations involving the mathematical operators in cylindrical coordinates 248
2. Mass and population conservation equations 249
   a. The population balance equations for the dispersed phase 249
   b. The mass conservation equations for the pseudo-continuous phase 250
   c. The mass conservation equations for the frozen layer domain 252
3. Momentum conservation equations 253
4. Energy conservation equations 254
   a. The energy conservation equations for the fluid bulk 254
   b. The energy conservation equations for the ice particles in the bulk domain 255
   c. The energy conservation equations for the frozen layer domain 257
   d. The energy conservation equations for the freezer wall 258
   e. The energy conservation equations for the coolant 258
5. Averaging procedure along the radial and angular coordinates 259
6. Overview of coordinate-averaged mass conservation equations 261
   a. The averaged conservation equations for the bulk domain 261
   b. The averaged conservation equation for the frozen layer 262
7. Coordinate-averaged conservation equation for dispersed phases 263
8. Coordinate-averaged conservation equation for the pseudo-continuous phase 268
9. Averaging of the conservation equation for the ice phase in the frozen layer 271
10. Expression of the volume flow rate 273
11. Physical properties for the simulation of the ice cream freezing model 276
12. The shrinking core model for the melting of an ice particle 277
13. Mass conservation equations for the bulk domain expressed per unit length of freezer 278
14. Conservation property of the overall amount of water 280
15. Singular vectors for the SVD on the model parameters 282
   15.1. Operational parameters 282
   15.2. Input parameters 282
   15.3. Freezer design parameters 283
   15.4. Empirical parameters 283
16. References 283

Curriculum Vitae **285**

Publications **286**

Acknowledgement **287**

SUMMARY

Model Reduction in Chemical Engineering

Case studies applied to process analysis, design and operation

During the last decades, mathematical models have become widely used for supporting a broad range of chemical engineering activities, such as product and process design and development, process monitoring and control, real time optimization of plant operation or supply chain management. The use of models for these applications allows for a rapid screening of the design alternatives, better-informed decisions, low cost and time-to-market of the products and processes, and finally, a better design and operation. Chapter 1 of this thesis discusses the role and the aspects of the modelling in the chemical engineering area and the continued need for model reduction.

Tremendous advancements have been made in the past years in the development of numerical techniques, in computing speed and data storage. However, along with the increase in the speed of computing, the process models have become more extensive and more complicated. Process models increasingly cover a wider scope, represent a deeper process integration and intensification and have more details at much smaller spatial scales. Such rigorous models of complicated systems cannot always be effectively used for applications such as design and optimization. These "inverse problems" require repetitive solution of the model in numerous iterative passes and remain critical in computing time and use of resources. A reduction of the model complexity is required to make a model-based solution practical.

Finding such a reduction in a systematic way is not at all obvious and it often demands a significant effort without a fully satisfactory outcome. In many of the current approaches in systems engineering order-reduction is applied to a model in its entirety, without preserving the underlying network structure of the process or its multi-scale decomposition. Retaining the meaningful structural features of a process in a reduced model is a necessity for practical applications, associated with the (re-)usability over a longer time span.

The first goal of this work is to explore the landscape and reveal a trade-off between two opposing and unsatisfactory extremes of performing model reduction:

(a) without any regard for underlying process structure

(b) to account for the process structure up to the smallest level, but forcing to perform model reduction to very small sub-systems, with issues of overall consistency over time-scales upon re-aggregation into a process model

The second, more practical goal is to show that such reduced process models, accounting for relevant process structure can be obtained and are indeed suitable for use in design and control. These goals are the motivation for the research and lead to the results presented in this thesis.

The novelty of the thesis is in systematizing and exploiting the essential structural features in model reduction for a chemical process. The structural features of the chemical process models are classified in Chapter 2 of the thesis in groups of attributes on several levels of model decomposition:

(a) *Contextual level,* offering information related to the model goals and applications, hypothesis to be tested, performance indicators

(b) *Structure level*, which consists of the information related to the following attributes:

- Systemic connectivity (flowsheet, units, streams)
- Physical attributes (coordinates, resources, species, phases, etc.)
- Behavioural attributes (sources-and-sinks type of phenomena, such as reactions, transfer, transport, etc.)

(c) *Mathematical level*, including the mathematical variables and relations (differential & algebraic equations, domain of applicability etc.) representing the behaviour of the process

(d) *Numerical level,* covering numerical methods used for solving the model and the model applications

(e) *Software implementation level,* having computationally efficient implementations of the model and solver

This gradual model reduction approach aims first at simplifying the systemic and physical attributes of the structure level of the chemical process model. Only then additional mathematical (lower number of equations and simplified terms) and numerical (scheme) reductions are selectively applied to individual compartments or units. In the following step, the reduced models of the individual units are connected at system level and the reduced model of the full process is obtained. In this way, the model reduction procedure is able to preserve the essential structural features of the process. Moreover, the physical meaning of the variables and equations is kept as much as possible.

The pragmatic criteria chosen for the success of a reduction approach are to develop a model which: (i) is solved successfully in an acceptable amount of time, (ii) is used effectively for practical applications, and (iii) retains the topological and physical structure of the process to a sufficient level of detail

The feasibility and the advantages of the approach are tested for two types of process applications:

(1) A complex process with a relatively simple (one-phase) product, with the *iso*-butane alkylation process as a case study

(2) A second single operation process with a complex product, exemplified on the freezing step in ice cream manufacture

For the first type of processes, the simplification acts mostly on the representation of the systemic and the higher level of the physical structure (units) of the chemical process in the model. The process is decomposed in units in the process flowsheet and these units are modelled individually. If required, model reduction is applied to the model of these units as well. The resulted reduced models of the units are then connected in order to obtain the reduced model of the full process.

The application and the advantages of the new reduction approach are tested in Chapter 3 for the assessment of the plantwide control structures for the *iso*-butane alkylation plant. Chapter 4 discusses the application of the approach when dealing with the dynamic optimization of the plant's operation. The behaviour of this reduced model is compared with a rigorous model of the process. Moreover, a comparison is done with another reduced model obtained by applying the "classical" model order-reduction approach to the rigorous model of the plant as a whole. The application in Chapter 3 is solved successfully in a very short amount of time, while the dynamic optimization in Chapter 4 requires a longer computation time, due to initialization issues.

For the second type of processes (complex product formation) the simplification acts on the lower levels of the physical structure (species, phases, domains, compartments), as well as on the behavioural level (phenomena).

The development of a dynamic model to support process design and operation for the freezing step in ice cream manufacture is described in Chapter 5 of this thesis. For this particular application, the development of a rigorous model covering all the phenomena in detail is conceptually quite conceivable. Nevertheless, it is currently impossible to solve such a rigorous model because many high-dimensional laws of conservation will arise and the knowledge regarding the parameters of the rate phenomena occurring inside the system is still limited. For this reason, a model reduction is performed; in this case both conceptually during the model development, as well as during the numerical stage of the modelling procedure. For this application, a reduced model is solved in steady state (Chapter 6), in an acceptable amount of time, being able to predict the right trends for the model outputs. In addition, the model is used successfully for a sensitivity analysis of the model parameters type of problem.

Follow-up questions are related to (a) what is lost in the model's predictive accuracy when the reduction is done by decomposition of the process in entities, (b) how deep a decomposition should go for a particular application, and (c) whether the models of process units were reduced enough to achieve the desired goals. The issue of consistent reduction over models of the decomposed elements and their re-aggregation should also be investigated further. Moreover dynamic model solution, model validation and optimization-type of applications of the ice cream freezing model are still

required to demonstrate further the applicability of the reduced model for process and product design and operation applications.

SAMENVATTING

Model Reduction in Chemical Engineering

Case studies applied to process analysis, design and operation

In de laatste decennia worden wiskundige modellen steeds meer gebruikt ter ondersteuning van een brede reeks van chemisch technologische activiteiten, zoals product- en procesontwerp en –ontwikkeling, procesbewaking en –regeling, real-time optimalisatie van procesvoering en integraal ketenbeheer. Gebruik van modellen voor deze toepassingen kan leiden tot een snelle screening van ontwerp alternatieven, beter geïnformeerde besluiten, lage kosten en korte marktintroductietijden van producten en processen en, ten slotte, tot betere ontwerpen en procesvoering. Hoofdstuk 1 van dit proefschrift bespreekt de rol en inhoudelijke aspecten van modelbouw in het chemisch technologische vakgebied en de aanhoudende behoefte aan modelreductie.

Er zijn geweldige vooruitgangen geboekt in de voorbije jaren in de ontwikkeling van numerieke technieken, in rekensnelheid en data opslag. Echter, parallel met de toename van rekensnelheid zijn de procesmodellen omvangrijker en ingewikkelder geworden. Procesmodellen bestrijken in toenemende mate een breder gebied, representeren diepere procesintegratie en -intensificatie en bevatten meer details op een veel kleinere ruimtelijke schaal. Zulke grondige modellen van ingewikkelde systemen kunnen niet altijd effectief worden gebruikt voor toepassingen zoals ontwerp en optimalisatie. Deze omgekeerde (‘inverse’) problemen vereisen het herhaald oplossen van het model in talloze iteraties en blijven zo kritiek in rekentijd en gebruik van andere hulpmiddelen. Reductie van de rekencomplexiteit van het model is nodig om een modelgebaseerde oplossing praktisch mogelijk te maken.

Het vinden van een dergelijke reductie op een systematische manier is zeker niet vanzelfsprekend. Het vereist vaak een aanzienlijke inspanning zonder een volledig bevredigende uitkomst. Want, bij veel van het huidige aanpakken in systems engineering wordt modelreductie toegepast op een model in zijn geheel, zonder de onderliggende netwerkstructuur van het proces of zijn meerschaligheid te behouden. Het bewaren van zinvolle structuuraspecten van een proces in een gereduceerd model is noodzakelijk voor praktische toepassingen in verband met bruikbaarheid van het model over een langere periode.

Het eerste doel van dit werk is het landschap te verkennen en een afweging duidelijk te maken tussen twee tegenovergestelde en onbevredigende uitersten bij het uitvoeren van een modelreductie:

(a) Zonder enig aandacht voor de onderliggende processtructuur

(b) De processtructuur tot op het fijnste niveau meenemen, maar daardoor gedwongen te zijn de modelreductie uit te voeren op heel kleine subsystemen, met kwesties als overall consistentie over tijdschalen bij het weer samenvoegen tot een procesmodel.

Het tweede, meer praktische doel is aan te tonen dat zulke gereduceerde procesmodellen, die rekening houden met de relevante processtructuur, kunnen worden verkregen en inderdaad geschikt worden bevonden voor gebruik bij ontwerp en regeling. Deze doelen zijn de motivatie voor dit onderzoek en leiden tot de resultaten die in dit proefschrift staan.

Het nieuwe van dit proefschrift is gelegen in het systematiseren en benutten van essentiële structuuraspecten bij modelreductie voor een chemisch proces. De structuuraspecten van chemische procesmodellen worden geclassificeerd in Hoofdstuk 2 van dit proefschrift in termen van groepen van attributen op verscheidene niveaus van modelcompositie:

(a) *Context niveau*, dat informatie biedt met betrekking tot het doel en de toepassing van het model, de hypothese die moet worden getest en indicatoren voor de geleverde prestaties

(b) *Structuur niveau*, dat informatie verschaft over de volgende kenmerken:
- Knopen en verbindingen in het systeem (flowsheet, eenheden en stromen)
- Fysische attributen (coördinaten, type behoudsvariabelen, componenten, fasen, etc.)
- Gedragsattributen (bron en putverschijnselen zoals reacties, overdrachten, transporten, etc.)

(c) *Wiskundig niveau*, dat gaat over variabelen en relaties die in de vorm van differentiaal en algebraïsche vergelijkingen het procesgedrag beschrijven, met ongelijkheden als afbakening van het toepasbaarheid gebied

(d) *Numeriek niveau*, betreffende numerieke methoden voor het oplossen van het model voor toepassingen

(e) *Software niveau*, voor realisatie van een rekenkundig efficiënte implementatie van model en oplossingsmethoden in software

Deze gefaseerde aanpak van modelreductie beoogt eerst de systeemkundige en fysische attributen op het structuur niveau van het chemische proces en zijn model te vereenvoudigen. Pas daarna worden selectief mathematische (minder vergelijkingen en vereenvoudigde termen) en numerieke (algoritmisch) reducties toegepast op individuele bouwstenen in het model. In de vervolgstap worden de gereduceerde modellen van de afzonderlijke eenheden weer verbonden op systeem niveau en wordt het gereduceerde model voor het complete proces verkregen. Op deze wijze is de modelreductieprocedure in staat essentiële structuuraspecten van het proces te behouden. Bovendien blijft de fysische betekenis van variabelen en vergelijkingen zoveel mogelijk bewaard.

De pragmatisch gekozen criteria voor het succes van een reductieaanpak zijn dat een model wordt ontwikkeld dat (i) wordt opgelost in een aanvaardbare tijdspanne, (ii) effectief kan worden gebruikt voor praktische toepassingen en (iii) de topologische en fysische structuur van het proces in voldoende mate van detail behoudt.

De haalbaarheid en de voordelen van de ontwikkelde aanpak van modelreductie worden getoetst aan twee types van procestoepassingen:

(1) Een complex proces met relatief simpele (een-fase) producten, met als voorbeeld het *iso*-butaanalkylatie proces
(2) Een enkele proceseenheid met een complex product, met de vriesstap bij het make van roomijs als voorbeeld

Voor het eerste type proces richt de vereenvoudiging zich in hoofdzaak op de representatie van het systeem en van de hogere niveaus van de fysische structuur (eenheden) van het chemische proces in het model. Het proces wordt ontbonden in eenheden in de procesflowsheet en deze eenheden worden afzonderlijk gemodelleerd. Zonodig, wordt modelreductie toegepast op de modellen van deze eenheden. De zo verkregen gereduceerde modellen van de eenheden worden dan weer verbonden tot een gereduceerd model van het gehele proces.

De toepassing en de voordelen van de nieuwe reductieaanpak worden getoetst in Hoofdstuk 3 voor de beoordeling van alternatieve fabrieksbrede regelstructuren voor het *iso*-butaanalkylatie proces. Hoofdstuk 4 bespreekt de toepassing van deze aanpak wanneer het dynamische gedrag bij procesvoering wordt geoptimaliseerd. Het gedrag van het gereduceerde model wordt vergeleken met dat van een grondiger model van het hele proces. Bovendien wordt een vergelijking gemaakt met het gedrag van een ander gereduceerd model, dat is verkregen door toepassing van een "klassieke" reductiemethode op de orde van een grondig model van het gehele proces. De toepassing in Hoofdstuk 3 wordt succesvol opgelost in zeer korte tijd, terwijl de dynamische optimalisatie in Hoofdstuk 4 een langere rekentijd vereist als gevolg van rekenkundige initialisatie kwesties.

Voor het tweede type proces (vorming van een complex product) werkt de vereenvoudiging op zowel de diepere niveaus van de fysische structuur (chemische componenten, fasen, domeinen, compartimenten) als de beschrijving van de verschijnselen die het gedrag bepalen.

De ontwikkeling van een dynamisch model ter ondersteuning van ontwerp en procesvoering voor de vriesstap bij het maken van roomijs wordt beschreven in Hoofdstuk 5 van dit proefschrift. Voor deze specifieke toepassing is de ontwikkeling van een zeer grondig model dat alle relevante verschijnselen in detail beschrijft conceptueel zeer wel denkbaar. Niettemin is het thans praktisch onmogelijk een dergelijk model te op te lossen omdat er veel hoogdimensionale behoudswetten in zullen voorkomen en kennis van de snelheidswetten van de verschijnselen en hun parameters beperkend is. Daarom is op voorhand modelreductie nodig; in dit geval zowel conceptueel bij de modelformulering als bij de numerieke fase van de modelontwikkeling. Voor deze toepassing wordt in Hoofdstuk 6 het gereduceerde model onder stationaire omstandigheden in voldoend korte tijd

opgelost, waarbij de juiste fysische trends van de modeloutputs worden verkregen. Bovendien is het gereduceerde model met succes gebruikt voor een gevoeligheids analyse met betrekking tot bepaling van parameters met dominante effecten op de outputs.

De vragen met betrekking tot vervolgonderzoek zijn gerelateerd aan welke informatie verloren gaat in het voorspellende vermogen van een gereduceerd model als een reductie wordt uitgevoerd door een ontbinding van een proces in zijn eenheden. Aan hoe diep een decompositie moet worden doorgevoerd voor een specifieke toepassing en aan de diepte van reductie van modellen van proceseenheden om het gewenste doel te bereiken. De kwestie van een consistente reductie over de modellen van de ontbonden eenheden en hun samenvoeging moet ook verder onderzocht. Bovendien, voor het model van de vriesstap voor roomijs is het nodig de mogelijkheden van dynamische simulatie, model validatie en optimalisatie toepassingen aan te tonen ten behoeve van proces en product ontwerp en toepassingen bij procesvoering.

REZUMAT

Model Reduction in Chemical Engineering

Case studies applied to process analysis, design and operation

În ultimele decenii, modelele matematice sunt folosite pe scară tot mai largă pentru o gamă extrem de extinsă de aplicaţii în ingineria chimică. Câteva exemple în acest sens sunt proiectarea şi dezvoltarea de procese şi produse, monitorizarea şi controlul proceselor, optimizarea în timp real a operării proceselor sau managementul aprovizionării. Utilizarea modelelor în aceste situaţii permite o evaluare rapidă a alternativelor de proiect, decizii informate, costuri reduse şi lansare rapidă pe piaţă a produselor şi proceselor. Toate acestea au ca rezultat o mai bună proiectare şi operare a proceselor chimice. Capitolul 1 al acestei teze tratează rolul şi particularităţile folosirii modelelor în ingineria chimică, precum şi necesitatea continuă de a le reduce complexitatea.

Un progres extraordinar a fost făcut în ultimii ani în domenii precum dezvoltarea de metode numerice pentru rezolvarea modelelor, creşterea vitezei de calcul şi stocarea datelor. O consecinţă a acestor evoluţii este că modelele proceselor au devenit mult mai detaliate mai complicate. Modelele au un scop din ce în ce mai larg, descriu procese integrate şi intensificate şi consideră tot mai multe detalii la scale din ce în ce mai mici. Astfel de modele exacte ale unor sisteme complexe nu pot fi întotdeauna utilizate într-un mod eficient pentru aplicaţii precum proiectarea sau optimizarea de proces. Aceste „probleme inverse" necesită rezolvarea în mod repetată a modelului într-un număr mare de iteraţii şi reprezintă încă un punct critic în ceea ce priveşte folosirea resurselor de calcul. Reducerea complexităţii reprezintă un pas necesar în abordarea unei probleme de inginerie chimică utilizând modele matematice.

Reducerea la nivel sistemic a unui model nu este întotdeauna evidentă, de cele mai multe ori rezultatul final nefiind satisfăcător în ciuda unui efort considerabil. Numeroase metode din ingineria sistemelor consideră modelul întregului proces, urmărind reducerea numărului de ecuaţii, fără a ţine cont de structura procesului sau de modul în care acesta se poate descompune la diverse scale. Păstrarea caracteristicilor structurale ale procesului este o necesitate pentru utilizarea modelului redus în aplicaţii practice, asociată cu posibilitatea de a (re-)utiliza modelul pe o perioadă mai lungă de timp.

Un prim scop al acestei teze este analiza domeniului pentru a dezvălui o imagine de ansamblu a posibilităţilor de reducere a complexităţii modelului. Două extreme au fost identificate în acest caz:

(a) Metode care nu iau în considerare structura internă a procesului

(b) Metode care iau în considerare structura internă a procesului până la cel mai mic detaliu şi reducând complexitatea unui număr mare de subsisteme foarte mici. Dezavantajul unei astfel de abordări este pierderea consecvenţei globale de-a lungul scalelor de timp în momentul reasamblării subsistemelor pentru a obţine modelul întregului proces

Un al doilea scop mult mai practic este de a arăta că astfel de modele cu complexitate redusă, care ţin cont de structura internă a procesului, pot fi obţinute şi sunt într-adevăr potrivite pentru utilizarea în proiectare şi control. Aceste scopuri reprezintă motivarea pentru cercetare şi a condus la rezultatele prezentate în această teză.

Noutatea acestei teze constă în sistematizarea şi utilizarea caracteristicilor structurale fundamentale ale modelelor proceselor chimice în scopul reducerii complexităţii acestora. Aceste caracteristici sunt clasificate în Capitolul 2 în grupuri de atribute, pe diverse nivele de descompunere a modelului:

(a) Nivelul *contextual,* care oferă informaţii referitoare la scopul şi aplicaţiile modelului, ipotezele care sunt verificate, indicatorii de performanţă

(b) Nivelul *structural*, compus din informaţii legate de următoarele caracteristici:

- Conectivitate la nivel sistemic (flowsheet, operaţii unitare)
- Fizice (coordonate, resurse, specii, faze etc.)
- Comportamentale (fenomene de generare sau consum de resurse, precum reacţii chimice, transfer, transport etc.)

(c) Nivelul *matematic*, alcătuit din informaţiile legate de variabilele şi relaţiile matematice (ecuaţii diferenţiale şi algebrice, domeniul de aplicabilitate etc.) care definesc comportamentul procesului

(d) Nivelul *numeric,* cuprinzînd metodele folosite pentru rezolvarea modelului şi a aplicaţiilor practice

(e) Nivelul *implementării software* a modelului, care include modul de aplicare a algoritmilor de rezolvare folosind tehnica de calcul

Reducerea complexităţii modelului urmăreşte, într-un prim pas, simplificări la nivel structural, în special al conectivităţii sistemului şi al structurii fizice, a modelului procesului chimic ce trebuie modelat. O dată ce acest pas a fost realizat, tehnici de reducere suplimentară a complexităţii la nivel matematic (număr de ecuaţii şi termeni simplificaţi), respectiv numeric (metode matematice) sunt aplicate în mod selectiv modelelor de operaţii unitare sau compartimente. La pasul următor, modelele reduse ale operaţiilor unitare sunt conectate la nivel sistemic pentru a obţine modelul redus al întregului proces. În acest fel, procedura de reducere a complexităţii poate păstra caracteristicile structurale fundamentale ale procesului chimic şi semnificaţia fizică a variabilelor şi ecuaţiilor.

Din punct de vedere practic, o metodă de reducere este performantă dacă: (i) modelul redus este rezolvat într-un timp acceptabil, (ii) modelul redus poate fi utilizat în mod eficient pentru aplicaţii

practice şi (iii) modelul redus păstrează structura topologică şi structura fizică a procesului la un nivel de detaliu suficient de ridicat.

Aplicabilitatea şi avantajele acestei proceduri de reducere a complexităţii modelelor sunt testate pe două tipuri de procese:

(1) Un proces complex cu un produs relativ simplu (monofazic), folosind procesul de alchilare a izobutanului drept exemplu

(2) Un proces simplu (o singură operaţie) cu un produs complex (multifazic), având drept exemplu operaţia de congelare parţială din procesul de fabricare a îngheţatei

Pentru primul tip de proces, simplificarea consideră în principal modul de reprezentare a nivelului structural, în general conectivitatea la nivel sistemic şi nivelele superioare (operaţii unitare) ale structurii fizice a procesului chimic de modelat. Procesul este descompus în operaţii unitare care apoi sunt modelate individual. Reducerea complexităţii se aplică modelelor individuale, acolo unde este cazul. Aceste modele reduse sunt apoi combinate pentru a obţine modelul redus al întregului proces.

Capitolul 3 testează modul de aplicare şi avantajele procedurii de reducere atunci când se doreşte evaluarea structurilor de reglare a instalaţiei de alchilare a izobutanului. Capitolul 4 tratează modul de aplicare al procedurii de reducere în scopul optimizării dinamice a procesului. Răspunsul modelului redus este comparat cu cel al unui model detaliat al procesului şi cu un model redus obţinut prin aplicarea procedurilor „clasice" de reducere a complexităţii, care acţionează asupra modelului întregului proces. Aplicaţia practică din Capitolul 3 este rezolvată cu succes într-un timp de calcul foarte scurt, în timp ce optimizarea dinamică din Capitolul 4 necesită un timp ceva mai lung, din cauza unor probleme de iniţializare.

În cazul celui de-al doilea tip de proces (formarea unui produs complex) simplificarea acţionează la nivelele inferioare ale structurii fizice (specii, faze, domenii, compartimente), precum şi la nivel comportamental (al fenomenelor). Obţinerea unui model dinamic redus utilizabil pentru proiectarea şi operarea procesului de congelare parţială a îngheţatei este descrisă în Capitolul 5 al tezei. Pentru acest tip de aplicaţie, deducerea unui model riguros al procesului, care să descrie toate fenomenele în detaliu, este conceptual posibilă. Cu toate acestea, rezolvarea unui astfel de model detaliat nu este posibilă în prezent din cauza numeroaselor ecuaţii de conservare şi a informaţiilor limitate asupra vitezei fenomenelor care au loc în proces. Din aceste motive, reducerea complexităţii se face atât la nivel conceptual pe parcursul dezvoltării modelului, cât şi la nivel matematic. Pentru această aplicaţie, modelul redus prezice corect variaţia variabilelor de ieşire ale modelului, în regim staţionar (Capitolul 6), şi poate fi rezolvat într-un timp relativ scurt. În plus, modelul redus este folosit cu succes pentru analiza senzitivităţii parametrilor modelului.

Rămân de investigat în continuare chestiuni referitoare la: (a) ce se pierde în capacitatea de prezicere a modelului atunci când reducerea complexităţii se face prin descompunerea modelului în unităţi individuale, (b) cât de detaliat trebuie realizată această descompunere şi (c) dacă modelele

individuale au fost reduse suficient pentru atingerea scopurilor dorite. Descompunerea modelului în elementele componente într-un mod consistent şi re-conectarea acestora trebuie investigate în continuare. În plus, pentru a demonstra aplicabilitatea la proiectarea şi operarea procesului de congelare parţială a îngheţatei, sunt necesare rezolvarea în regim dinamic, validarea folosind date experimentale şi aplicarea pentru rezolvarea unor probleme de optimizare.

1

INTRODUCTION

The reduction of chemical process models is investigated in this PhD thesis. In view of the inherent complexity of model reduction, an exploratory approach is chosen by means of case studies. The motivation for this research came from the particularities of the model development for chemical engineering applications. This Introduction sets the stage for the use of models in chemical engineering. It outlines the main benefits models bring for applications in the chemical engineering area. It then shows there is a continuing need of developing techniques to model process systems with wider scope, deeper integration, more detailed scales. Process models are increasingly used in "inverse problems" implying a need for reduced computation times. The possibilities for model reduction are presented in the framework of the generic model development steps. The key driver of this thesis research is a wish to preserve the (topological) structure in model reduction. Modelling is often done at different scales of resolution. Therefore, a dual way of modelling of process models is highlighted, based on decomposition/aggregation of structure and reduction/refinement of behaviour. It is from this dual perspective that the scope of this thesis is introduced together with a statement of the scientific questions that are dealt with in the thesis. The chapter is concluded with an outline of the thesis.

1. Role of modelling in chemical engineering

Mathematical modelling has a long history in chemical engineering. In their review of 50 years of mathematics in chemical engineering (Ramkrishna & Amundson, 2004) wrote: *"The beginning of this era was marked by the concerted effort of a few to raise the mathematical consciousness of the profession to think fundamentally about processes"*. With the advent of fundamental insights in transport phenomena and reaction kinetics and the introduction of the digital computers in the 1960's, mathematical modelling in chemical engineering became a pillar in process development, design and operation.

At first, the use of mathematics aimed at formulating models that could be solved analytically (Constales, Marin, Nicolis, Van Keer & Yablonsky, 2003). The efforts were focused on circumventing the limitations of early computers, mainly the lack of speed and storage capacity for handling very large problems (Ponton, 1995). Mathematics and chemical engineering developed in parallel, chemical engineering becoming the source of inspiration for new developments in areas like nonlinear science (Constales, Marin, Nicolis, Van Keer & Yablonsky, 2003). In (Ilievski, 2010), the advances in numerical algorithms satisfy a "law" that is similar to the Moore's law describing the advances in chip technology. Moreover, with the increase in computational power, wider ranges of applications become possible to solve, not only for chemical processes, but also for materials and products as well (Ramkrishna & Amundson, 2004).

In spite of tremendous advancements in the development of both numerical techniques and in computing and data storage, the complexity of process models, and hence of the model applications has risen as well. For this reason, the reduction of the model continues to play an important role in modelling applications.

1.1. Model applications and benefits

In recent decades, models have become widely used for handling chemical engineering activities at all levels, during the entire product and process lifecycle, as shown in Table 1.1. The references presented in this table are primarily chosen for being good illustrations of the model application in chemical engineering area, and not necessarily for all being "state-of-the art" reviews.

The use of models for all these applications has several important advantages: saving of time, efforts and costs; enhanced pace of innovation; deeper understanding of the phenomena that take place inside the systems; better designs and manufacturing excellence. Significant savings or enhanced revenue is achieved during the process lifecycle by using models (Cameron & Ingram, 2008). However, models do not come free. The modelling requires very significant efforts, with associated costs. It is often an iterative process to reach the specified goals and functions of the models. In addition, model applications may constrain available resources, such as computing times and, mainly, human efforts to formulate a problem and analyse the computational results in an effective and timely manner.

Table 1.1. Model applications in chemical engineering activities

Model applications	References
Understanding fundamental phenomena	Betlem, Rijnsdorp & Azink, 1998; Heiszwolf, Engelvaart, van den Eijnden, Kreutzer, Kapteijn & Moulijn, 2001; Van den Bergh, Ban, Vlugt & Kapteijn, 2009
Product development and design	Gani, 2004; Eden, Jørgensen, Gani & El-Halwaqi, 2004; Costa, Moggridge & Saraiva, 2006; Charpentier, 2009
Product applications	Bongers, 2009; Bongers & Almeida-Rivera, 2009
Process research and development	Jaksland, Gani & Lien, 1995; Bałdyga & Bourne, 1997; Van Goethem, Barendregt, Grievink, Moulijn & Verheijen, 2008; Lutze, Gani & Woodley, 2010
Process design and engineering	Kiparissides, 1996; Saldivar & Ray, 1997; Taylor & Krishna 2000l; Bermingham, Verheijen & Kramer, 2003; Van Lith, Betlem & Roffel, 2003; Almeida Rivera, Swinkels & Grievink, 2004; Bildea & Dimian, 2008
Process operations: monitoring, control, real-time optimization	Henson, 1998; Qin, 1998; Sørensen, Macchietto, Stuart & Skogestad, 1996; Jockenhövel, Biegler & Wächter, 2003; Mendez, Cerda, Grossmann, Harjunkoski & Fahl, 2006; Bos, 2006; Martin Rodriguez, Cano & Matzopoulos, 2010
Production planning and scheduling	Mendez, Henning & Cerda, 2000; Pinto, Joly & Moro, 2000; Kopanos, Puigjaner & Georgiadis, 2010
Supply chain management and integration	Applequist, Pekny & Reklaitis, 2000; Chen & Lee, 2004; Georgiadis, Tsiakis, Longinidis & Sofioglou, 2011

The advantages of modelling in chemical engineering applications will be explained further in more detail, with a focus on process engineering.

Modelling makes possible the understanding of the fundamental phenomena and their interactions that take place in the process. The models capture and retain quantitative and qualitative technological knowledge. Thus, better-informed decisions can be taken at all levels of design and operation.

The process models are usually developed from fundamental chemical engineering, physics and chemistry relationships and validated against observed data. The experimental effort that is required for supporting the selection of unit operations, their scale-up, or the development of process policies and control systems could increase a lot during the development stage (Marquardt, 1996). When developing a new process, the knowledge regarding the nature and behaviour of relevant phenomena that take place inside the system is often limited, hence the possibility of modelling them from first principles is limited too. As a result, most of these systems are represented by empirical models based on experimental data. A high number of experiments for obtaining the necessary data will increase the cost and the time-to-market of the product or process. This number is reduced, for

example, by using the model for the design of optimal experiment procedures & experimental conditions for determining its parameters, like for example in (Francheschini & Macchietto, 2008).

Moreover, the use of models accelerates innovation by examining the design space and rapidly screening the design alternatives. In order to improve customers' satisfaction, companies need to develop new ranges of products, different from what is already on the market. In the same time, the products are required to meet tighter environmental and safety regulations. In this case, it has to be decided the best alternative to meet requests for designing new processes and equipment or for making simple improvements to existing ones. In some cases, processing units or even the whole plant is redesigned in order to improve the performance (for example, the production of fuels by Fischer-Tropsch synthesis – Dry, 2002).

Process models are also used for support of plant operation in process simulators, in process state estimation and performance monitoring, and in real time optimizers, as shown in table 1.1.

The focus of the thesis will be on the modelling of *process engineering* aspects, where process engineering is taken in a broad sense, covering process development, design and support of operations. Models for product design and development can be separated into two distinct categories: *performance – structure* and *structure – processing*. The relationships between product performance, expressed in quality factors, as appreciated by customers, and product structure remain outside the purpose of this thesis. Regarding the *structure – processing* group, the formation of the product structure and composition in a process is seen as a normal part of the processing operation, and thus covered by process modelling.

In chemical engineering applications, the system is usually equivalent with a chemical process. A chemical process is defined as a series of successive physical and chemical operations in which raw materials are transformed into products. The transformations take place in units such as reactors, distillation columns, heat exchangers, etc. These units form the core operations of the process. Often the performance of the product is characterised only by properties such as temperature and chemical composition, which in turn define density, heat capacity, and viscosity. These products will be called "simple products" as their performance depends on the thermodynamic state of a single phase. In other cases, these properties are not sufficient to describe fully the product. For a product with a complex internal structure, consisting of different components and phases, more information will be required to define the relationship between the performance, and the structure and composition. These types of products will be called "complex products".

The characteristics of the chemical process and its modelling are influenced by both the process and the product's structures. For this reason, the processes will be classified as:

(1) processes with simple products
(2) processes with complex products

Applications from both classes will be discussed in this thesis.

1.2. Efforts and cost factors for model development and application

The development and the application of a model require significant effort. This effort comes in terms of human efforts and skills, as well as in terms of time required for the model development. There is always a trade-off between the cost and the expected benefit of the model. Two stages can be distinguished when trying to evaluate the effort and the costs: (a) the initial model development and (b) the model applications with maintenance.

The efforts and costs of the initial model development stage are quite visible: it takes time, it requires good modelling skills and (expensive) human labour time, and there must be an infrastructure for model implementation (hardware, licensed software, etc.) and computing (in some cases massive computing is required). These efforts and costs are quite considerable and must be explicitly allocated upfront by the problem owner.

The efforts and costs in the second stage, the model application and maintenance are less visible. The most visible is the cost with tuning a model to its applications. However, the most important cost factor at this stage is in fact a loss factor. For example, potential benefit and generation of income is lost by having a model that is performing below its target level.

Time is playing also a critical role in two ways:

(1) Required time for the delivery of a planned application

(2) Required computing times for solving a problem. This can be an important factor in real-time applications. However, for off-line applications a slow turn-around time for a model computation will slow down the project execution and the generation of critical results.

2. Requirements for model use in chemical engineering

The obvious presumption is that the costs of the model development, use and maintenance will be offset by the benefits of the model applications. The requirements for model development, use and maintenance are:

a) At system and goal level: Specifications of the boundaries for the system to be modelled and the kind of problems to be solved by the model, such as simulation and optimization of performance for specified external scenarios.

b) At network structure level: Graphical and textual representation of the inner network of the system being modelled (such as a process flowsheet). This network may have a layered structure. For example, the nodes in the network represent a process unit, which in itself is a sub-network of interconnected sub-nodes. These sub-nodes can be geometric domains in units.

c) At network behaviour level: Textual representation of the understanding of the relevant mechanistic structures (co-existing thermodynamic phases), phenomena and behaviour of nodes and connecting streams. The model must account for the “true” system. This means that the model should predict the behaviour of the process accurately enough for the model application goals. A model must

account for the uncertainty of the experimental observations. It is very important to understand which properties of the system are modelled accurately and which are treated superficially (Hjalmarsson, 2005). Moreover, how this affects the performance of the resulted model should be clear. The understanding of the behaviour of the system can be succinctly captured in *modelling assumptions*.

d) At mathematical level: Representation of the variables, operators and equations, which form a *mathematical model* of the system. Alternative model formulations are well possible. There is a trade-off between model completeness (in terms of coverage of phenomena) and computing efforts for solving the model. Once several model alternatives are available, the user should be able to select them in a systematic way (Verheijen, 2003) in order to guarantee the model performance.

e) At numerical level: The mathematical model(s) can be classified in certain categories (for example, NLA, ODE, DAE, MINLP) for which classes of numerical methods exist. The mathematical model is transformed to a corresponding numerical version. This transformation often involves the replacement of the mathematical operators in the model by equivalent numerical operations.

f) At software level: The numerical model and the solution methods are coded in different ways into different software environments. The implemented model has a clear structure for potential re-use of the model parts.

g) Availability of interfaces to enter problem data into the implemented model and to present computed results in suitable formats to the model users.

h) Documentation: The implemented model must be well documented. All the assumptions and decisions, and the model structure are clearly stated, as well the assessment of the models' performance. Though in many cases background decisions are not reported (Cameron & Ingram, 2008), better documentation of the intermediate steps could provide helpful for future model development. The information on the different versions of the model is easily retrieved in order not to have to repeat previous work should model improvement or re-use prove necessary. The different model alternatives usually derive from each other by detailing and aggregation, by changing or moving scale, or by reduction within the same scale. It is important that these relationships between model alternatives are clear, to allow the ease of switching between different versions and simulations.

In the following, the focus will be on developing models to be used for applications with time critical computations.

3. Process models and modelling

3.1. Process models

A (process) system Σ is defined as a finite region in some space characterized by a set of quantifiable variables. This space can be a conjunction of several spaces, among which a physical

space, a signal space, and a design space. The system that evolves in time is called a dynamic system. The definition of a dynamic system includes (Katok & Hasselblatt, 1996):

(1) A *phase space – X* - (also called *state space*), a set of elements (called "points") that represent possible states of the system in any moment in time
(2) *Time – t* -, which can be either continuous (real) or discrete (integer)
(3) A *law of evolution – g -,* which is a rule allowing, when the state of the system at some moment in time is known, to determine the state of the system at any other moment in time. The existence of this law is equivalent to the assumption that the process is deterministic in the past and in the future. It is assumed that the structure of the law of evolution does not depend on time.

The formal definition of a dynamical system (Katok & Hasselblatt, 1996) is in this case:

A dynamical system is a triple (*X, T, G*), where *X* is a set (*phase space*), *T* is either integer or real, and *G* is a one-parametric group of transformation of *X* (with discrete time if *T* is integer).

Moreover, the system is a combination of interconnected entities, integrated to perform a specific function.

The model of a system will be defined by a set of relations between properties of the system that are measured in particular domains (Yang & Marquardt, 2009). The relations between the properties of the system are written in the form of mathematical equations. Moreover, the interactions between the system itself and the surrounding environment are written in mathematical form as well. The set of equations (*the mathematical model*) is the result of the modelling, defined as a goal oriented activity to describe the fundamental behaviour of real or hypothetical systems. Modelling is both a conceptual process and a work process, with the goal of delivering a model suitable for an application goal. During the modelling procedure, the modeller gathers information from the system of reference for the development of a model suitable for a defined goal.

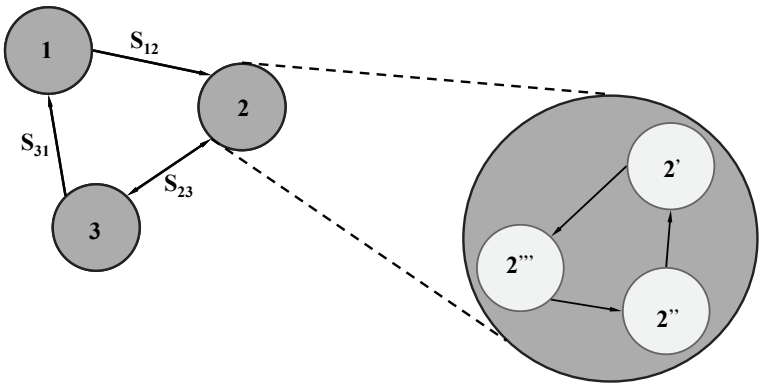

Figure 1.1.Structure model of a process

A common way of visualising a process system is as a multi-level network. The process units are the nodes of the network, while the connecting streams of resources are the network edges (Figure 1.1). Starting from this network view, a *structure model* of the process is developed. This model shows which kind of nodes are present and how are they connected (which streams of resources are connecting the different units in the process). The structure model of the process is represented visually by the *process flowsheet* or topologically by the *Boolean connectivity*. Moreover, each of the nodes performs a specific function, which defines a *behavioural model* of the node. The overall behavioural model of the process is a combination of the behavioural models of the nodes and the structure/connectivity model. This pattern can repeat itself several times at different levels of detail. The behavioural model of a node in a process network may be the result of the structure and behavioural models of sub-nodes at a lower level of structure. The typical levels that can be considered for a chemical process are presented in Figure 1.2: process system, units, compartments in units, phase domains (droplets, bubbles, films, etc.) and interfaces, rate phenomena, etc.

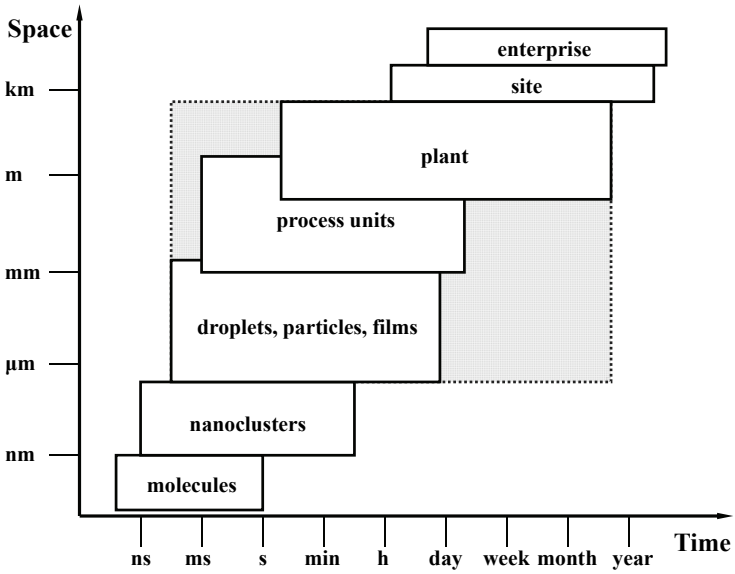

Figure 1.2. Scales in process modelling (After Marquardt, see Grossmann, 2004)

Having defined the structure model for the process, the different laws defining the *mathematical model* are easily written and implemented into a software environment that allows for both the solution and the use of the model by a user. The modelling is often iterative and can lead to several alternatives of the model for a specific application. The different stages of the model development will be detailed in Section 3.3 of this chapter.

In the following, the focus of the thesis will be on dynamic physical-chemical models with description of the process units in continuous space and time. The process units will be integrated through a network structure into a process flowsheet. The spatial scale runs from particle (micrometers) to plant size (< kilometre), while the time scale runs from fast (milliseconds) to slow (hours/days), as shown in Figure 1.2.

3.2. Model classification

Several criteria can be defined in order to classify models: the intended use of the model (model goals); the internal information (physical, chemical, etc.) contents, including scales; the mathematical features; the computational features of the model.

Models are related to specific types of transformation that take place in the process. On this basis, one can distinguish:

(1) Physical- chemical models, which cover the transformation of mass, energy, momentum, electrical charge, exergy, etc.
(2) Economic models, which cover the transformation of capital
(3) Signal/information based models, covering the monitoring and control actions
(4) Safety, reliability, maintenance models that focus on the availability of operational states
(5) Planning and scheduling type of models focused on the allocation and withdrawal of resources in time and location

Based on understanding the phenomena inside the system, process models are classified in three distinct categories (Cameron, Wang, Immanuel & Stepanek, 2005):

(1) *Mechanistic or fundamental* – the model is based on the underlying understanding of the physics and chemistry of the process. In this case, the conservation of resources and the rate phenomena are derived from first principles.
(2) *Empirical or black box* – the model is based on experimental data, typically in the form of time series of input and output data.
(3) *Grey-box* – the model is based on a combination of both experimental data and underlying physics. Usually, the conservation of resources is derived from first principles, while the rate phenomena are data generated.

Generally, the mechanistic models are preferred since they will be accurate over a much larger range of conditions than the empirical models (Bequette, 1998). However, the knowledge regarding the physics and chemistry of the real case does not always allow for the development of a mechanistic model. It may also happen that developing fundamental models is too expensive and preference is given to black box or grey-box models when enough empirical data is available. For this reason,

many models are of either black- or grey-box type. The models presented in this thesis are of the grey-box type.

3.3. Model development steps

In order to identify the justification and the options for model reduction it is required to understand how models are being developed. During the modelling procedure, the modeller gathers information from existing experimental data, literature and experience to define the structure and behavioural model of the process. The mathematical model is further implemented into a software environment that allows for use of the model by a user, as presented in Figure 1.3.

The development of the model for a process takes place in several iterative steps (Lohmann & Marquardt, 1996; Foss, Lohmann & Marquardt, 1997; Hangos & Cameron, 2001; Preisig, 2010) each of them having as a result one or more model alternatives. For the following discussions, the development steps considered are, as summarised in Figure 1.4:

a) Model specification and design. During this step, the scope of the model and its physical and mathematical content are defined. Different models are used for different purposes. It is important to have the goal defined as clearly as possible before the actual modelling procedures are performed. It is customary to identify also future scenarios for business or scientific applications.

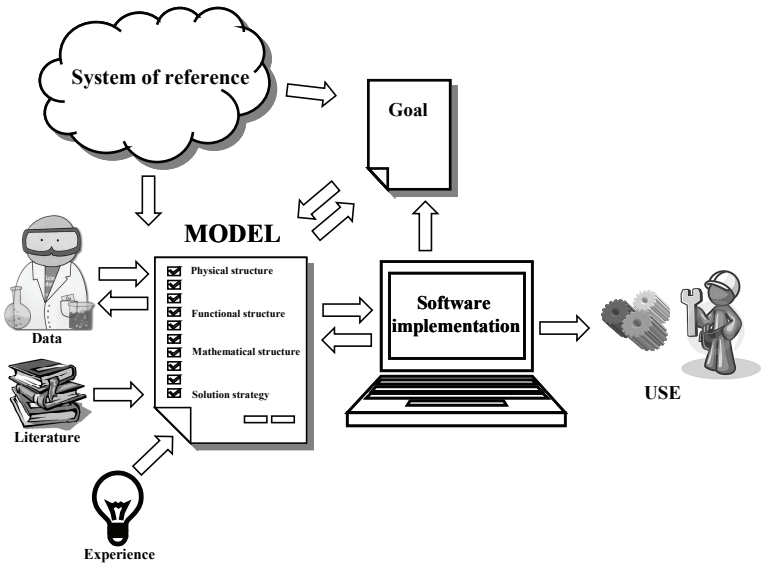

Figure 1.3. Process modelling environment

A reference system is chosen and the system demarcation from the environment is defined. The functional specifications, such as inputs, outputs and the performance indicators are specified

according to the goal of the model. The different entities that form the system and the connections between them are specified. This represents the internal network of the system, or the topology. Decisions regarding the assumptions of the model (type of resources, scales of resolution for the system and the sub-systems, time and geometric space, fundamental state, reactions, etc.) are taken and the behavioural laws (equations) for the different model components are defined. The degrees of freedom and the policy for the optimal decision-making are identified. A part of the variables is defined as known in such way that the number of equations is equal to the number of the unknowns. Moreover, it is investigated if the model is well posed and if it can be solved (Leitold & Hangos, 2001). The existence of a solution or the multiplicity of solutions is examined (Unger, Kröner & Marquardt, 1995; Bildea & Dimian, 1998; Kiss, Bildea, Dimian & Iedema, 2002). Once these checks have been done, for cases when dealing with an inverse problem, some of the prespecified variables can be released to allow embedding of the model in a nonlinear programming problem (NLP). Lastly, testing scenarios are specified, for testing the model's functionality and applicability. During this step several model alternatives will be developed, according to the decisions taken. The result of the model specification and design step is the *mathematical model alternative(s)*. Two mathematical model alternatives differ by the equations of the model. The different model alternatives of a specific system are related and derived from each other, either by model expansion and detailing or by model reduction.

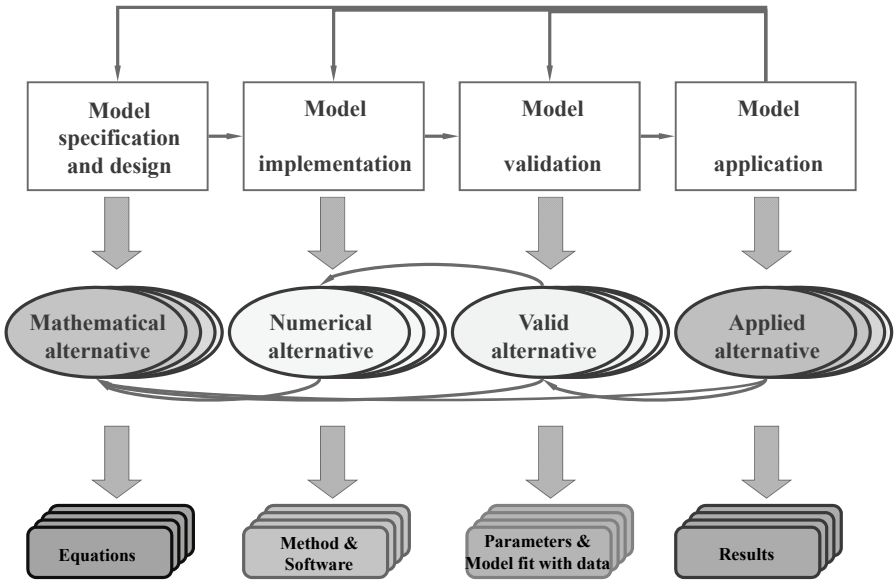

Figure 1.4. Model development cycle

b) Implementation of the model for numerical solutions. This step includes the selection of the software environment and of the suitable numerical methods that will be used for solving the model

and using it for applications. The numerical methods should be stable, accurate and fast enough for the specified model application. Commercial packages, such as differential algebraic equation solvers, linear algebra packages, large-scale simulators, NLP solvers etc. are usually used for this step. Often, further manipulation of the model is required in order to make the numerical implementation of the model possible. The model can be simplified by applying mathematical manipulations (Marquardt, 2001) such as model reduction, re-arrangement of the model equations or transformation to alternative representations of the model. Once the model is implemented, the correctness of the implementation is verified via case studies with known solutions. This implies comparing the results of the model with experimental data or just experience. Similar to the previous step, different mathematical model alternatives will lead to different numerical implementations of the model. Moreover, depending on the choice of the numerical methods and software environment, the same mathematical alternative could lead to several numerical alternatives. The result of this step is the *numerical model alternative(s)*. Two numerical model alternatives differ by the numerical method used for the solution of the model and by the software environment used for solving the model, while the mathematical model is the same.

c) Validation of the model. In this step, the verification of the numerical implementation of the model is performed, as well as the validation of the model in the domain of applications. The model validation involves the following steps: (1) qualitative assertion of correct behaviour at the domain boundaries or at other asymptotic conditions; (2) tuning of model parameters using experimental data, with estimation of the errors and covariance; (3) testing of model predictive power using other independent experimental data; (4) obtaining information on the predictive uncertainty over the window of validation. The different parameters of the model are determined from experimental data and the model is tested by comparing its behaviour with known cases. Model discrimination of the different mathematical and numerical model alternatives is performed in order to decide which of them performs satisfactorily for the desired application. Different approaches (Stewart, Henson & Box, 1996; Burke, Duever & Penlidis, 1997; Stewart, Shon & Box, 1998; Asprey & Maccietto, 2002; Lakner, Hangos & Cameron, 2005; Ye, Meyer & Neuman, 2008) have been developed and reported for applications in the area of process engineering. Limitations of the model applications are identified during this step as well. The resulting *valid model* should fulfil a set of performance specifications; otherwise, the procedure is iterated to one of the previous steps. A first attempt is rarely successful in obtaining a proper model; hence, the modelling can also be a time-consuming task. For this reason, it is very important to spend enough time on collecting all the necessary information to define it properly. In general, empirical models are valid only for a limited range, depending on the set of data used to obtain the model. The mechanistic models are valid for a wider range, but their development is far more complex and time-consuming (Cameron, Wang, Immanuel & Stepanek, 2005). The result of this step is called a *valid model alternative(s)*. The different valid model alternatives differ by the values and the number of the model parameters

obtained during the validation. When working with one model alternative, different values of the model parameters are obtained when applying different methods of estimation, or when using different data sets to validate the model. For use of several model alternatives, the number and the meaning of the model parameters may differ from one alternative to the other.

d) Application of the model with documentation. During this step, the model is used in two ways:

(1) For routine computational applications, such as simulation, parameter identification or control. This can be done in a "direct" way, by simulation, or in an "inverse" way, by achieving a performance and output related target. The "direct" way implies the specification of all degrees of freedom, including initial and boundary conditions. The "inverse" use of the model implies the use of a performance criterion, which is optimised by varying over degrees freedom in a model. Such an optimization can be performed with respect to economics, parameter fitting, data-model reconciliation applications, etc.

(2) The model or parts of the model can be re-used for other types of applications.

After this step, the *alternative model & applications* are obtained. The applied alternatives of a specific model differ by the type of results obtained for alternative scenarios.

3.4. Dual way of modelling: decomposition and aggregation over detail levels

Under certain goals and conditions, for a certain application, different models are obtained that adequately describe features of the process. This can range from very extensive and fundamental models with attention to the finest details of phenomena to lumped, input-output type of models, with a minimum of internal mechanisms represented in the model. The result is a family of models, where one should be able to distinguish the kinds of relationships that can be obtained between different models of the same process (Aris, 1994). One way of representing the relationships between the models of the same process is presented in Figure 1.5. In explaining this Figure, the terminology of (Aris, 1994) will be followed, which means that the word *hypothesis* captures *modelling goal(s) and assumptions*.

The complexity of a model depends on a series of attributes. Firstly there are physical attributes (entities), related to the process considered: number of units, number of physical resources to be considered (mass, energy, momentum, etc.), number of domains, phases, and species, as well as the number and type of phenomena which need to be taken into account. Secondly, there is a second group of attributes relating to the mathematical structure of the model (type of equations, number of variables, and complexity of the problems to be solved, etc.). The attributes that affect the model complexity will be discussed in more detail in Chapter 2 of the thesis.

Starting from the process Σ, with a set of hypotheses H_1, a first model M_1 is obtained.

For example, the model M_1 is formed by the full set of differential equations obtained from applying conservation laws for mass, energy and momentum over the system Σ along a spatial

coordinate. Assuming that the model obtained in this way is too complex (for example the momentum conservation equation is defined by a rigorous Navier-Stokes equation) a second set of hypotheses ($H_3 - H_5$), is required to obtain versions of the model which are easier to solve.

For example, hypothesis H_3 leads to a steady state version of the conservation equations, while hypotheses H_4 and H_5 simplify the momentum conservation equations.

The models can be simplified further (hypotheses $H_7 - H_9$) until a desired ratio of complexity versus accuracy is achieved. The models $M_3 - M_8$ are derived from model M_1 by letting certain parameters take on a limiting value (Aris, 1994). This procedure of obtaining simple models will be called *reduction*.

It is possible to derive a second model, M_2 of the process Σ from a set of hypotheses H_2 .

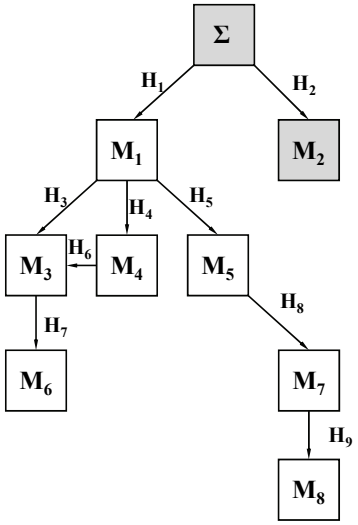

Figure 1.5. Relationships between models (adapted from Aris, 1994)

This set of hypotheses affects the way the system is defined, for example when the model M_1 is so complicated (number or complexity of equations, number of parameters, etc.), that it seems that better insight is gained by drastic simplification. In this way, important features of M_1 are extracted in a way that allows for easier analysis (Aris, 1994). Once the model M_2 is available, its complexity can be increased by adding more detail, going in the opposite way to reduction. This procedure will be called *refinement*. Once the model reaches a desired level of complexity versus accuracy, this refinement stops.

In chemical engineering applications, the mathematical modelling of physical systems is performed by decomposition and aggregation of the system across a hierarchy of appropriately chosen levels (Klatt & Marquardt, 2009).

The *decomposition* is performed by breaking the process into smaller entities, which are modelled individually. Once the model of each entity is available, the original model can be re-constructed by coupling these individual models. This is performed through *aggregation*.

To conclude, four operations are performed on process models, in sets of two:

Decomposition and ***Aggregation*** of **STRUCTURE** over levels

Refinement and ***Reduction*** of detail/complexity of **BEHAVIOUR**

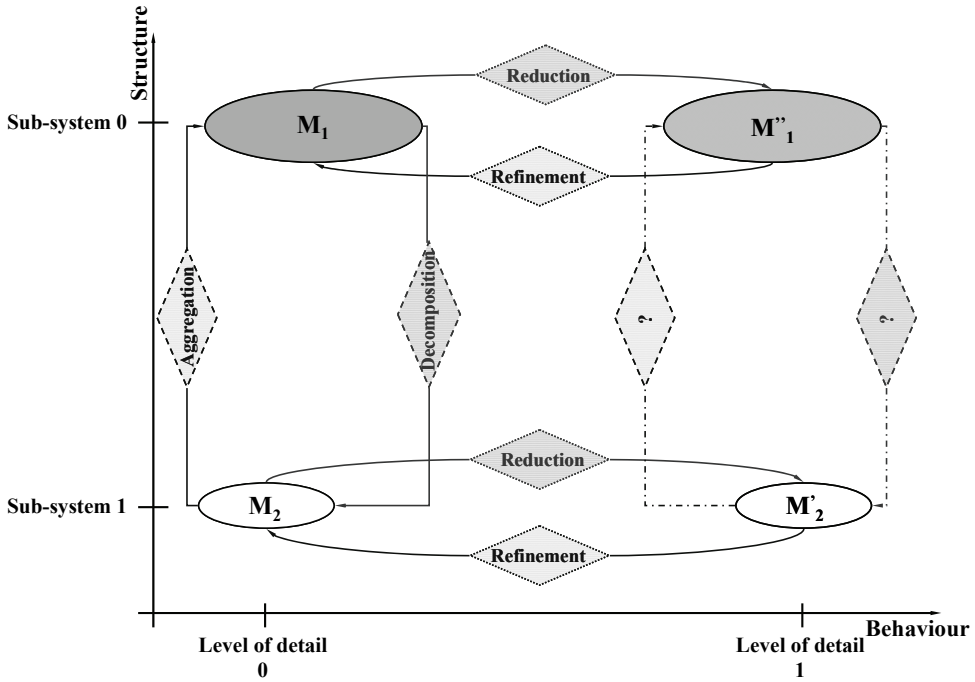

Figure 1.6. Dual way of modelling of chemical processes
0 = reference level; 1 = reduced/simplified

These four operations are shown in Figure 1.6, where the decomposition and the aggregation are vertically oriented, while the refinement and the reduction are horizontally presented.

This approach has several advantages. By decomposing the system into smaller entities, the understanding of the behaviour and the function of each hierarchical level is easier. It is possible to standardise models of entities (reactors, distillation columns, etc.) which can be easily re-used for building a different aggregated (complex) model. Once a standardization is available, the modelling procedures become easier and faster. In the same time, the modelling procedures are flexible. Commercial software packages, such as Aspen Dynamics® or gProms® make use of standard model libraries, which can be easily (re)used and interconnected for developing complex process models.

Lastly, the two previous approaches (refinement and reduction) can be combined when some parts of the model are reduced and others are refined.

In the following discussion, model reduction approaches will be considered, with focus on the model attributes.

4. Motivation and formulation of the research problem

Societal demands for better performance of engineering systems pushes for wider integration at upper scales of systems, while the developments in science and engineering offer opportunities for

high precision and intensification at smallest scales. Thus, chemical engineering systems become more complicated, having repercussion for the modelling. The models are required to cover a wider scope and because of the deeper integration between scales in a node of a network and of stronger interactions between different nodes. In addition, the range of scales is continuously expanding, covering more details of the phenomena at the micro-scale and supply chain integration at the upper scale. The conceptual and the mathematical capability to model such complicated systems is not always matched by the computational power to handle such models in practical applications, like model validation, design and optimization. Table 1.2 presents some features of the model that makes them hard to solve.

Model reduction consists of a series of approaches and techniques used for obtaining accurate, yet computationally less expensive models of process systems.

The state-of-the-art of the model reduction involves a host of diverse methods and techniques, which can be classified in two distinct categories:

- Dedicated *conceptual approaches* in the physical-mathematical domain. These approaches are often related to the level of detail of specific phenomena (physical or kinetic lumping, reduction of the reaction networks, etc.) in chemical engineering systems. Often, the modelling and the model reduction are focused on one single phenomenon (for example lumping of species or of reactions).
- *Numerical, data driven techniques* in systems engineering (projection and balancing methods, etc.)

Table 1.2. Model-inherent complications when solving models

What makes a model "harder" to solve?		
Mathematical perspective	***Behaviour***	Non-linear terms in equations; e.g. chaotic behaviour by a single logistic equation
		Mathematical operations on functions, like differentiation and integration
		Loss of stability
		"Stiffness" by a wide range of scales
	Structure	High degree of coupling between several equations by some variables, especially when the coupling induces an irreducible set
		Large number of variables and equations
Numerical perspective		Numerical stability
		Convergence
		Discrete approximations of continuous mathematical operations

The traditional approaches for reducing the complexity of process models do not always exploit the structural and the discrete features of the models. The systems engineering model

reduction techniques consider the model of the process as a whole when attempting to simplify it. The starting point is a rigorous model of the process. This rigorous model is obtained considering relevant phenomena that take place in the process at pre-selected ranges of time and spatial scales. In a first group of approaches, the reduction focuses on the reducing the number of model equations (model-order reduction techniques), without accounting for the inner structure of the process. Although significant reduction of the number of equations can be achieved, attention must be paid on the internal structure of the problem, as well as on retaining the physical meaning of the variables (Wattanwar, 2010). Often, the differential equations are being transformed into equally hard to solve sets of non-linear algebraic equations (Van den Bergh, 2005).

The second group of techniques focuses on reducing the complexity of the model equations (model simplification techniques), without affecting their number. In this case, the physical insight is retained by the obtained model, as well as the number of equations.

The standard methods for reducing the model complexity are reviewed in Chapter 2 of the thesis.

Sometimes, the knowledge on the phenomena that take place in the process is limited and it is not possible to obtain a fully rigorous model. The information on the phenomena or the physical properties is yet to be obtained. From the first stages of the modelling procedure, the modeller has to take some decisions on how these properties are modelled. Decisions are being made based on experience, trial-and-error, etc. on the different attributes of the model, leading to a "conceptual model". Once this model is available, a second step in the model reduction procedure is focused on reducing the mathematical structure, leaving unexploited the physical insight.

To conclude, the computational efficiency of the models is improved *conceptually* or/and *numerically*. The conceptual model reduction approaches are usually used during the model specification and design stage. The procedure involves the reduction of the discrete attributes of the model (species, resources, phases, reactions, domains, coordinates, transfer phenomena, connectivity, etc.). The number of such discrete structural attributes of a model determines in a multiplicative way the number of variables and equations. The numerical model reduction techniques come into use as soon as the mathematical model alternatives are obtained. The procedure involves in this case the reduction of the number and of the complexity of the functional expressions in the model equations.

The structural aspects of a process model are present in chemical engineering textbooks. Although model structure is being present to some extent (Aris, 1994; Rice & Do, 1995; Weiss & Preisig, 2000; Hangos & Cameron, 2001; Yang & Marquardt, 2009), the structuring is not yet treated satisfactorily in the context of model reduction. Often, the starting point of the modelling is represented by the equations and the variables as a predefined set.

The overall ambition of this thesis is to take a more fundamental and domain specific approach than just applying numerical data driven techniques for model order reduction, and to look

at and exploit the underlying chemical engineering structure elements of a model in developing reduced models as well.

Two extremes of performing model reduction can be considered:

(a) The underlying structure of the process model is not taken into account at all. The numerical model (order-) reduction techniques are facing a problem of enormous size. Even when results are obtained, the reduced model has no clear relationship to the underlying flowsheet structure. When it comes to having an understanding about the reduction criteria, the benefit of this approach is that these criteria have been consistently applied to the entire model. From the cut-off criteria used for the model reduction, it is clear which modes of behaviour have been ignored or simplified.

(b) The structure of the process model is taken fully into account up to the smallest level of detail. The conceptual model reduction is followed by a numerical (order-) reduction and is applied to each behavioural model in the various nodes and sub-nodes of the network. This approach is very labour-intensive. Furthermore, the question arises on how to reduce the numerous sub-models individually in a consistent way (are the corresponding modes of behaviour retained or ignored?). There is another problem with respect to the interaction between levels of detail. The behaviour of the nodes at the smallest level is determined by their imbedding at larger scales. It is a function of the interaction between the nodes and the emerging conditions. As these are a priori unknown, it is difficult to tell which phenomena and rate processes are dominant and what can be neglected.

It is obvious that neither extreme is satisfactory. The key issue is how to find a good balance between dealing with the structural effects while having a consistent approach to the behavioural reduction. Answering this issue by sheer theory development is yet too demanding in a general setting, even for chemical process systems. Therefore, in this thesis an exploratory approach has been chosen, aiming to identify the interactions in the STRUCTURE-BEHAVIOUR reduction problem by using specific cases. The main research question is:

Are there ways to develop or adapt model reduction methods to better preserve essential (spatial) structure elements in chemical engineering models?

Model Reduction in Chemical Engineering – Case studies applied to process analysis, design and operation

The theme is addressed through several research questions:

1) What are the main structural features of chemical process models that are co-determine the model size and the computational efforts? Where is the structure being addressed in the modelling procedures?

2) How does the model structure reflect in the reduction approaches?

3) Is it possible to exploit efficiently these structural features when reducing the complexity of the process model?

4) Are the reduced models fit for purpose, and what are the suitable criteria for such fitness?

5. Research approach and outline of the thesis

Finding answers to these research questions is attempted through a case driven approach.

The main topics and contributions of the research are:

a) To identify and systematize the main structural features of process models

b) To identify and systematize the model reduction approaches and techniques, as used for chemical engineering applications

c) To develop a new, more comprehensive approach that accounts for both the structural and behavioural features of the process models as well as for their the numerical attributes (number and structure of the equations), capturing specific contributions of existent techniques

d) To investigate and test the application of these model reduction approaches for common chemical engineering applications

The focus of the research will not be on developing new numerical model reduction approaches, but on the conceptual use of the existent techniques. Moreover, automated model building with reduction approaches is beyond the scope of the thesis.

The first three topics will be addressed in Chapter 2, *Process modelling and model reduction*, of the thesis. The network concept with nodes and edges, presented in Figure 1.1, is used for the process representation, and the main attributes of the process structure are defined. The way the structure affects the model size and the most important existent reduction approaches are systematized. A *structure-retaining model reduction approach* that exploits the essential structural features of a process is developed in this chapter as well. This approach brings together existent model reduction techniques and uses them within their specific context and applicability.

The main body of this work, Chapters 3 – 6, will address the fourth topic. Chapter 3, *Application of model reduction to design of plantwide control systems*, describes a new procedure of applying model reduction that takes into account the inner structure of the process. The idea behind it is to decompose the model into smaller entities and to apply model reduction to these entities individually. The resulting reduced models of the entities are connected according to the process structure in order to obtain the reduced model of the full process. The application of this procedure for two chemical process applications is presented in Chapters 3 and 4. The assessment of the plantwide control structures of a complex process with simple structured products is the focus of Chapter 3.

Chapter 4, *Dynamic optimization using a reduced process model*, presents the design and implementation of the optimum dynamic operation profile in a large-scale chemical plant. The same

process is considered for both applications: the *iso*-butane alkylation process, though a different model is obtained for each application. The starting point of the model reduction procedure is, for both cases, a rigorous model of the chemical plant.

Chapter 5, *Development of a reduced model for ice cream freezing*, presents the conceptually driven development of the reduced model for a process unit with products with a complex structure. The freezing step in the ice cream manufacture process is the case study for the model reduction. For this particular application, it is not possible to develop a rigorous model of the process for two reasons:

(a) The knowledge regarding many of the phenomena that take place inside the system is limited

(b) The full model with all fundamental conservation laws for all the thermodynamic phases present will become so complicated that solving it is still far beyond current computational feasibility for practical applications. The model reduction is performed in this case conceptually, during the model development.

Chapter 6, *Numerical application of the reduced model for ice cream freezing*, solves the steady state version of this reduced ice cream freezing model and tests the numerical feasibility of applying the model for validation purposes.

Chapter 7, *Conclusions and recommendations*, summarises the main results and limitation of the thesis research and recommends directions for future development.

6. References

Almeida-Rivera, C.P., Swinkels, & P.L.J., Grievink, J. (2004). Designing reactive distillation processes: present and future, *Computers and Chemical Engineering* 28, 1997

Applequist, G.E., Pekny, J.F., Reklaitis, G.V. (2000). Risk and uncertainty in managing chemical manufacturing supply chains, *Computers and Chemical Engineering* 24, 2211

Aris, R. (1994). Mathematical modelling techniques, Dover Publications

Asprey, S.P., & Macchietto, S. (2002). Designing robust optimal dynamic experiments, *Journal of Process Control* 12, 545

Bałdyga, J. & Bourne, J.R. (1997). Interaction between chemical reactions and mixing on various scales, *Chemical Engineering Science* 52, 457

Bequette, B.W. (1998). Process dynamics: modelling, analysis and simulation, *Prentice Hall*, 5

Bermingham, S.K., Verheijen, P.J.T., & Kramer, H.J.M. (2003). Optimal design of solution crystallization processes with rigorous models, *Chemical Engineering Research and Design* 81, 893

Betlem, B.H.L., Rijnsdorp, J.E., & Azink, R.F. (1998). Influence of tray hydraulics on tray column dynamics, *Chemical Engineering Science* 53, 3991

Bildea, C.S. & Dimian, A.C. (1998) Stability and multiplicity approach to the design of heat-integrated PFR, *AIChE Journal* 45, 2662

Bildea, C.S. & Dimian, A.C. (2008). Chemical process design: Computer-aided case studies, *Wiley-VCH*, Weinheim

Bongers, P.M.M. (2009). Process and equipment design optimising product properties and attributes, *Computer Aided Chemical Engineering* 26, 225

Bongers, P.M.M., Almeida-Rivera, C.P. (2009). Product driven process synthesis methodology, *Computer Aided Chemical Engineering* 26, 231

Bos, R. (2006). Monitoring of industrial processes using large scale first principles models, *PhD Thesis*, Delft University of Technology, The Netherlands

Burke, A.L., Duever, T.A., Penlidis, A. (1997). Choosing the right model: Case studies on the use of statistical model discrimination experiments, *The Canadian Journal of Chemical Engineering* 75, 422

Cameron, I.T., Wang, F.Y., Immanuel, C.D., Stepanek, F. (2005) Process systems modelling and applications in granulation: A review, *Chemical Engineering Science* 60, 3723

Cameron, I.T., Ingram, G.D. (2008). A survey of industrial process modelling across the product and process lifecycle, *Computers and Chemical Engineering* 32, 420

Charpentier, J.C. (2009). Perspective on multiscale methodology for product design and engineering, *Computers and Chemical Engineering* 33, 936

Chen, C.L., Lee, W.C. (2004). Multi-objective optimization of multi-echelon supply chain networks with uncertain product demands and prices, *Computers and Chemical Engineering* 28, 1131

Constales, D., Marin, G.B, Nicolis, G., Van Keer, R., & Yablonsky, G.S. (2003). Mathematics in chemical kinetics and engineering: An introduction to the special issue dedicated to papers presented at the MaCKiE-2002 conference, *Chemical Engineering Science* 58, 4747

Costa, R., Moggridge, G.D., & Saraiva, P.M. (2006). Chemical product engineering: An emerging paradigm within chemical engineering, *AIChE Journal* 52, 1976

Dry, M.E. (2002). The Fischer-Tropsch process: 1950 – 2000, *Catalysis Today* 71, 227

Eden, M.R., Jørgensen, S.B, Gani, R., & El-Halwaqi, M.M. (2004). A novel framework for simultaneous separation process and product design, *Chemical Engineering and Processing: Process Intensification* 43, 595

Foss, B.A., Lohmann, B., Marquardt, W. (1997). A field study of the industrial modelling process, *Journal of Process Control* 19, 153

Franceschini, G., Macchietto, S. (2008). Model based design of experiments for parameter precision: State of the art, *Chemical Engineering Science* 63, 4846

Gani, R. (2004).Chemical product design: challenges and opportunities, *Computers and Chemical Engineering* 28, 2441

Georgiadis, M.C., Tsiakis, P., Longinidis, P., & Sofioglou, M.K. (2011). Optimal design of supply chain networks under uncertain transient demand variations, *Omega* 39, 254

Hangos, K.M., Cameron, I.T. (2001). Process modelling and model analysis, *Academic Press*

Heiszwolf, J.J., Engelvaart, L.B., van den Eijnden, M.G., Kreutzer, M.T., Kapteijn, F., Moulijn, J.A. (2001) Hydrodynamic aspects of the monolith loop reactor, *Chemical Engineering Science* 56, 805

Henson, M.A. (1998). Nonlinear model predictive control: Current status and future directions, *Computers and Chemical Engineering* 23, 187

Hjalmarsson, H. (2005). From experiment design to closed-loop control, *Automatica* 41, 393

Ilievski, Z. (2010). Model order reduction and sensitivity analysis, *PhD Thesis*, Eindhoven University of Technology, The Netherlands

Jaksland, C.A., Gani, R., Lien, K.M. (1995). Separation process design and synthesis based on thermodynamic insights, *Chemical Engineering Science* 50, 511

Jockenhövel, T., Biegler, L.T., & Wächter, A. (2003). Dynamic optimization of the Tennessee Eastman process using the OptControlCentre, *Computer and Chemical Engineering* 27, 1513

Katok, A., & Hasselblatt, B. (1996). Introduction to the modern theory of dynamical systems, Cambridge University Press

Kiparissides, C. (1996). Polymerization reactor modelling: A review of recent developments and future directions, *Chemical Engineering Science* 51, 1637

Kopanos, G.M., Puigjaner, L., & Georgiadis, M.C. (2010). Optimal production scheduling and lot-sizing in dairy plants: The yoghurt production line, *Industrial and Engineering Chemistry Research* 49, 701

Kiss, A.A., Bildea, C.S., Dimian, A.C., & Iedema, P.D. (2002). State multiplicity in CSTR – separator – recycle polymerisation systems, *Chemical Engineering Science* 57, 535

Klatt, K.U. & Marquardt, W. (2009). Perspectives for process systems engineering – Personal views from academia and industry, *Computers and Chemical Engineering* 33, 536

Lakner, R., Hangos, K.M., Cameron, I.T. (2005). On minimal models of process systems, *Chemical Engineering Science* 60, 1127

Leitold, A., Hangos, K.M. (2001). Structural solvability analysis of dynamic process models, *Computers and Chemical Engineering* 25, 1633

Lohmann, B., Marquardt, W. (1996). On the systematization of the process of model development, *Computers and Chemical Engineering* 20, S213

Lutze, P., Gani, R. & Woodley, J.M. (2010). Process intensification: A perspective on process synthesis, *Chemical Engineering and Processing* 49, 547

Marquardt, W. (2001). Nonlinear model reduction for optimization based control of transient chemical processes, *Proceedings of the 6th international Conference of Chemical Process Control, AIChe Symp. Ser. 326*, Vol. 98, 12

Martin Rodriguez, H., Cano, A., & Matzopoulos, M. (2010). Improve engineering via whole-plant design optimization, *Hydrocarbon Processing* 89, 43

Mendez, C.A., Henning, C.P., & Cerda, J. (2000). Optimal scheduling of batch plants satisfying multiple product orders with different due-dates, *Computers and Chemical Engineering* 24, 2223

Mendez, C.A., Cerda, J., Grossmann, I.E., Harjunkoski, I., & Fahl, M. (2006). State-of-the-art review of optimization methods for short-term scheduling of batch processes, *Computers and Chemical Engineering* 30, 913

Pinto, J.M., Joly, M., Moro, L.F.L. (2000). Planning and scheduling models for refinery operations, *Computers and Chemical Engineering* 24, 2259

Ponton, J. (1995). Process systems engineering: Halfway through the first century, *Chemical Engineering Science* 50, 4045

Preisig, H.A. (2010). Constructing and maintaining proper process models, Computers and Chemical Engineering 34, 1543

Ramkrishna, D. & Amundson, N.R. (2004). Mathematics in chemical engineering: A 50 year introspection, *AIChE Journal* 50, 7

Rice, R.G., Do, D.D. (1995). Applied mathematics and modelling for chemical engineers, *John Wiley & Sons*

Qin, S.J. (1998). Control performance monitoring – a review and assessment, *Computer and Chemical Engineering* 23, 173

Saldivar,E. & Ray, W.H. (1997). Mathematical modelling of emulsion copolymerization reactors: Experimental validation and application to complex systems, *Industrial and Engineering Chemistry Research* 36, 1322

Sørensen, E., Macchietto, S., Stuart, G., & Skogestad, S. (1996). Optimal control and on-line operation of reactive batch distillation, *Computers and Chemical Engineering* 20, 1491

Stewart, W.E., Henson, T.L., Box, G.E.P. (1996). Model discrimination and criticism with single-response data, *AIChE Journal* 42, 3055

Stewart, W.E., Shon, Y., Box, G.E.P. (1998). Discrimination of fit of multiresponse mechanistic models, *AIChE Journal* 44, 1404

Taylor, R., Krishna, R. (2000). Modelling reactive distillation, *Chemical Engineering Science* 55, 5183

Unger, J., Kröner, A., Marquardt, W. (1995). Structural analysis of differential-algebraic equation systems – Theory and applications, *Computers and Chemical Engineering* 19, 867

Van den Bergh, J. (2005). Model reduction for dynamic real-time optimization of chemical processes, *PhD Thesis*, Delft University of Technology, The Netherlands

Van den Bergh, J., Ban, S., Vlugt, T.J.H., & Kapteijn, F. (2009). Modelling the loading dependency of diffusion in zeolites: The relevant site model, *Journal of Physical Chemistry C* 113, 17840

Van Goethem, M.W.M., Barendregt, S., Grievink, J., Moulijn, J.A., Verheijen, P.J.T. (2008). Towards synthesis of an optimal thermal cracking reactor, *Chemical Engineering Research and Design* 86, 703

Van Lith, P.F., Betlem, B.H.L., Roffel, B. (2003). Combining prior knowledge with data driven modelling of a batch distillation column including start-up, *Computers and Chemical Engineering* 27, 1021

Verheijen, P.J.T. (2003). Model selection: An overview of practices in chemical engineering, *Computer-Aided Chemical Engineering* 16, 85

Wattanwar, S. (2010). Identification of low order models for large scale processes, *PhD Thesis*, Eindhoven University of Technology, The Netherlands

Weiss, M., Preisig, H.A. (2000). Structural analysis in the dynamical modelling of chemical engineering systems, *Mathematical and Computer Modelling of Dynamical Systems* 6, 325

Yang, A., Marquardt, W. (2009). An ontological conceptualization of multiscale models, *Computers and Chemical Engineering*, 33, 822

Ye, M., Meyer, P.D., Neuman, S.P. (2008). On model selection criteria in multimodel analysis, *Water Resources Research* 44

2

PROCESS MODELLING AND MODEL REDUCTION

The development of chemical process models is performed in a sequence of stages, leading to a specific internal structure of the model. In this chapter a framework to analyze the model structure, focusing on the elements that offer opportunities for model reduction is presented. The chapter introduces as well the most important techniques that are used for model reduction in the chemical engineering area. A novel approach to perform model reduction is introduced, which is trying to balance the model structural (nodes and edges) and behavioural (equations) characteristics to obtain a computationally feasible model. This approach takes an integrative look at all options for model reduction from the outset. It first covers the conceptual phase, where a mathematical model is developed addressing structural and behavioural features. Then, in the numerical phase, classical numerically driven (model order-) reduction techniques are applied. The application of this procedure will be studied in the following chapters of the thesis with the help of case studies that are outlined at the end of the chapter.

1. Introduction

A chemical process can be defined as a system that manufactures chemical products from feeds, supported by utilities and directed by automatic and human control. Any system has a boundary and an interior. The inside of a process can be seen as a multi-level network. The process units are the nodes of the network, while the network edges are formed by the streams connecting these units between themselves and with the outside environment across the boundary. These streams transport physical resources (species, mass, energy, momentum) or signals. The units effect the transformations in the states of these resources or signals. The multi-level aspect of the system appears because many nodes (units) have an internal network structure as well, comprising interconnected compartments and thermodynamic phases with transfer of resources between them. Sensors and actuators link the state of the physical resources to signals and reversely.

In this chapter, the term *process model* relates to a mathematical description of the behaviour of the internal part of the system, while accounting for the multi-level network structure. The process model is supposed to have *predictive power* regarding the evolution of the process behaviour, given enough conditions at the system boundaries. These boundary conditions reflect the state of the external environment, to which the process responds. A specification of an adequate set of boundary will be called a *scenario*.

Often, model applications in the process engineering area deal with a high dimensionality and a high degree of coupling between the different nodes of the process (Charpentier & McKenna, 2004; Vlachos, 2005; Klatt & Marquardt, 2009). This increases the complexity of the models, which depends not only on the total number of equations that need to be solved, but on the number of terms in these equations as well. These are determined by both the physical structure (process network) and the behavioural features (phenomena taking place in the process).

The number of equations and their complexity can be influenced in each model development step. The model development stage can be sometimes time consuming (Cameron, Wang, Immanuel & Stepanek, 2005). Predictive accuracy has to be balanced against model complexity and computational speed, often in iterative modes between model refinements and reductions.

Model reduction is deemed necessary when the computing times for solving a model become critical for the success of the applications. This is the case in so-called inverse problems, where a model may be solved very many times to meet target conditions or an optimal performance. Another case for reduction involves model applications where a model user needs very short turn-around time of a model simulation because of required fast and frequent interpretation of modelling results (like at stock exchange trading or in real time control).

Model reduction consists of a set of approaches and techniques that can be used for obtaining a model that represents the process and its behaviour in a way that is computationally feasible (Marquardt, 2001; Antoulas, Sorensen & Gugercin, 2000). In this chapter, an inventory of the most important model reduction techniques available is presented. The procedures will be presented from a

chemical engineering point of view, identifying the structural and behavioural model elements that can be subject to reduction.

The chapter is structured in the following way: Section 2 introduces the decomposition of a physical system for applications in process modelling. Moreover, definitions of the models attributes are introduced for the contextual and structure levels in Section 3, and for the mathematical, numerical and software implementation levels in Section 4. The main outcome of this section is a list of discrete model building attributes that can be used for model reduction or refinement. Section 5 explores existing model reduction techniques and their use for applications in chemical engineering, taking into account the model decomposition presented in Sections 3 and 4. A *structure-retaining approach* to perform model reduction taking into account both the structural and behavioural features of the process models is presented in Section 6. A case study approach is used in this thesis to assess the application of the model reduction approach. The selection and motivation of the chosen problems is elaborated in Section 7, while conclusions are summarised in Section 8.

2. A design view on process modelling

Process modelling is a systematic activity to study, analyse and optimize the behaviour of a physical system by mathematical and computational means. The first outcome is a mathematical model whose features can be analysed. The second outcome is a software implementation of the model that can perform computations for a pre-specified class of operating scenarios. The third outcome is data obtained from model applications by users in simulations and optimizations.

The inside of a process system Σ is seen as a network of individual entities, which will be called “nodes”, connected by “edges”, as presented in Figure 1.1 in Chapter 1. For chemical engineering applications, the modelling of the process Σ is performed by developing models for the individual nodes separately and connecting the resulting models, according to the network structure, in order to obtain the full model of the process.

In the following, a design view on process modelling and model reduction is introduced. The underlying philosophy is that the development of a mathematical model for a process is very similar to an engineering design procedure. A modeller has to make decisions regarding the creation of structure and behaviour in the model, reflecting the structure and behaviour in the object of modelling, just as a designer makes decisions regarding the object under design. The engineering design procedures are often organised in a hierarchical manner, working from an overall perspective towards fill in of details. This hierarchical decomposition is usually domain specific and takes advantage of the structure and geometric scales that commonly occur in the class of objects. The result is a sequence of decision making at increasing levels of detail. One well-known example in chemical engineering is the hierarchical design method of Douglas (Douglas, 1988) for the conceptual design of chemical processes. Alternative designs may arise in parallel due to the preferred design decisions.

In presenting this view, a decomposition of the model development in a sequence of stages is the common thread. The different levels of decomposition and the different structures obtained during the modelling procedure are shown. The outcome is an overview of the design decision variables in model building which can be used for model reduction (or refinement) purposes. Alternative competitive models may arise due to the decisions taken during the model development.

When reading the following sections, a distinction must be kept in mind with respect to the decomposition of the modelling procedure (and the model itself) and the structural decomposition of the object of modelling.

2.1. Levels of decomposition in the modelling procedure

The creation of models and model alternatives is done in the first two stages of the model development cycle: *Model specification and design* and *Model implementation*, shown in Figure 1.4. Several alternative process models result from the modelling procedure, depending on the development stage and the model's specifications (goal, assumptions, performance, etc.), each with its own qualities, performance and behaviour.

However, the models of the same process share a common structure, which is extended or reduced through the modelling process, for a desired set of specifications. This common structure in process models is related to the generic features of the physical system of reference.

In the following, six sub-levels of decomposition (Figure 2.1) will be discussed: the contextual level, the structure level, the mathematical level, the aggregation at the system level, the numerical level and the software implementation level.

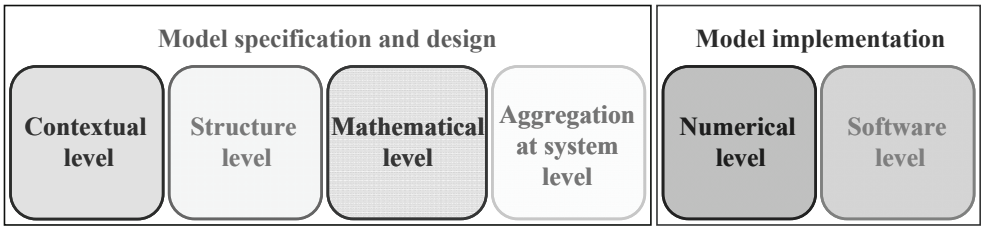

Figure 2.1. Levels of decomposition of the modelling procedure

For every level of decomposition, a set of decisions regarding the model are being taken and a representation of the model is obtained. This decomposition of the modelling process is done to identify the model design options that can be used for model reduction.

At contextual level, information related to the goal and application of the model is contained. The structure level offers information on the physical structure of the system and the phenomena (behaviour) considered by the model. The mathematical level includes all the mathematical relationships describing the structure and the behaviour of the system. At numerical level, decisions

related to the computational solution strategy of the model are taken, while at software level information on the implementation of the model in software environment is specified.

An overview of the activities and the outcome for each level of decomposition in Figure 2.1 is presented in Table 2.1.

Table 2.1. Levels of decomposition of the modelling procedure

Level		Activity in the level	Outcome	
Model specification and design	***Contextual***	1. Define process system to be modelled 2. Define the boundaries of the process with the system's environment 3. Define model goal(s) & application(s) 4. Define hypothesis and scenarios to be tested 5. Specify model inputs & outputs 6. Specify performance criteria	***Input-output representation***	**Mathematical alternative**
	Structure	1. Derive a suitable network model structure by decomposing the process 2. Select the phenomena that take place in the process which are relevant for the intended model use	***Physical (internal) and functional structure***	
	Mathematical	1. Define the mathematical relationships for the physical entities' behaviour 2. Define the mathematical relationships for the connectivity	***Mathematical model structure***	
	Aggregation at system level	1. Connect the different model attributes	***Network-type model structure***	
Model implementation	***Numerical***	1. Model analysis with transformations and scaling to improve solvability 2. Select the numerical methods/algorithms for solving per node 3. Model reductions in sub-sets of equations (per node) 4. System-wide aggregation of the numerical model (for example, up to multi-scale simulation)	***Solution strategy***	**Numerical alternative**
	Software	1. Implement the model in a software environment 2. Implement the numerical methods in a software environment	***Software implementation***	

In Section 3, an inventory of the discrete attributes of the contextual and structure levels is presented. Section 4 offers an inventory and classification of the attributes at the mathematical level,

as well as the inventory of the model attributes at system, numerical and software implementation levels. To support the understanding of the decomposition of the modelling process the same modelling example of a chemical process is presented all along these sections, together with the exposure of the decomposition approach. For every level detailed in the following, the *iso*-butane alkylation process is used as an example.

3. Contextual and structure levels of decomposition

3.1. Contextual level

This level (Figure 2.2) includes the specification of the process system to be modelled, the goal of the model and the applications it will be used for (dynamics, steady-state simulation, design, process control, etc.). For each application, the hypothesis to be tested and the performance indicators are specified. The boundaries of the process system need to be specified, as well as the interaction between the process system and its environment.

The concept of *boundary* will be defined as part of the structure level of decomposition in Section 3.2.1.

The "inputs" and the "outputs" are fixed as well at this level of decomposition. The inputs comprise information related to feeds, utilities, mode of operation, set points for operation, etc. The outputs include chemical products, energy products (steam, power), waste, emissions, operational and economic performance indicators, etc.

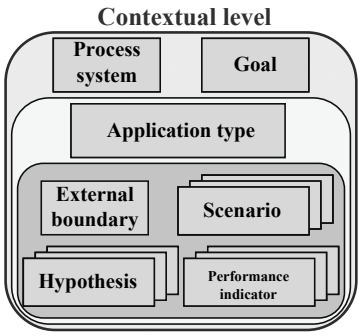

Figure 2.2. Structure of the contextual level

In the same time, the scenarios for testing are defined. The result of this step is an input-output type of structure of the process, as shown in Figure 2.3.

The alkylation process is used to produce high-octane blending component for gasoline by liquid phase conversion of n-butene with excess iso-butane, using acid catalyst. The goal of the model is the understanding the behaviour of an *iso*-butane/butene alkylation plant. The desired product is the *iso*-octane. The raw materials are the *iso*-butane and the olefin (1- and 2-butene). The fresh feed also contains propane and *n*-butane.

The present commercial routes for alkylation rely on the use of sulphuric acid (H_2SO_4) or anhydrous hydrogen fluoride (HF) as catalysts (Hommeltoft, 2001). The process takes place usually at high pressure, to ensure the liquid phase and low reaction temperatures. For the further development, the sulphuric acid route is chosen. The alkylation reaction requires a high interfacial surface area between the acid catalyst and the hydrocarbon. Current commercial alkylation processes the dispersions are acid-continuous with dispersed hydrocarbon droplets (Albright, 2002).

The plant behaviour will be studied for two scenarios: steady state and dynamic operation. Two applications are envisaged: the assessment of the plantwide control structures and the design and implementation of the optimal dynamic operation.

3.2. Structure level

The simplest way of representing the process is by using an input – output type of structure (I-O), as shown in Figure 2.3, which is a result of the contextual level of decomposition. Since usually the process is seen as a network of interconnected nodes, the model should be able to represent this as well.

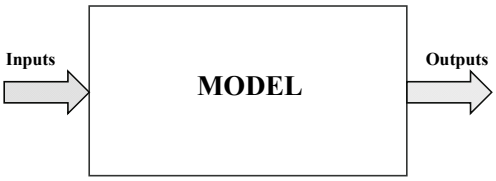

Figure 2.3. Input – output representation of the process

In the same time, each individual node in the process structure performs a specific function, which can be defined through a mathematical relationship.

The structure level specifies the nodes of the network and the connections between them. Moreover, the specific functions (behaviour) of each individual node are defined.

Further, the mathematical relationships defining the behaviour of the network nodes, as well as the connectivity are specified, at mathematical and system level, respectively.

Two sub-levels are identified for the structure of the model:

(1) P*hysical* structure of the model, which relates to the nodes considered and the connections between them;

(2) *Behavioural* structure of the model, including the function performed by each individual node.

3.2.1. Process decomposition and physical structure of the model

It is assumed that the process (flowsheet) structure is available. The process decomposition is performed leading to a reduced/simplified network structure from which the process model can be built. The physical structure level consists of all the information regarding the nodes in the process network, as well as the connectivity.

A series of discrete attributes are identified at this level of decomposition. These are specified according to the way the process network is defined and depending on the type of application which is considered. When looking at levels in a process flowsheet one commonly distinguishes between: (0) Process as a system; (1.a) Units in the process (nodes); (1.b) Connections transporting resources (edges).

Within a unit, the following levels can be distinguished: (2) compartments (for example trays in the distillation column) and (3) domains (for example the hold-up of process fluids and the heating agent inside of a heat exchanger).

Inside the domain, one may have: (4) region, (5) phase, (6) species, (7) interface, and (8) coordinate.

Table 2.2 presents the relations between the different attributes of the model, as considered in this thesis. Each of the attributes presented in the table are detailed in the following sections.

Table 2.2. Relations between attributes of the model at structure level

Level		Attribute		Unit	Compartment	Domain	Region	Phase
Structure	Physical	Resource	Mass	✓	✓	✓	✓	✓
			Species	✓	✓	✓	✓	✓
			Population	✓	✓	✓	✓	✓
			Energy	✓	✓	✓	✓	✓
			Momentum	✓	✓	✓	✓	✓
			Information	✓	✓	✓	✓	
		Unit						
		Compartment		■				
		Domain		■	■			
		Region		■	■	■		
		Phase		■	■	■	■	
		Interface		■	■	■	■	■
		Coordinate		■	■	■	■	■
	Behaviour	*Sources and sinks*		◘	◘	◘	◘	◘
		Buffer effect		◘	◘	◘	◘	◘
Connectivity	Physical	*Stream*		►				
	Behaviour	*Transfer*		►	►	►	►	►
		Transport		►	►	►	►	►

✓ = uses resource; ■ = contains attribute; ◘ = involves phenomena; ► = is connected by

The delimitation between the attributes is done by means of boundaries and interfaces, as shown in Figure 2.4. The *interface* is a physical means of delimitation between attributes inside the system, where the different attributes in the model come in contact.

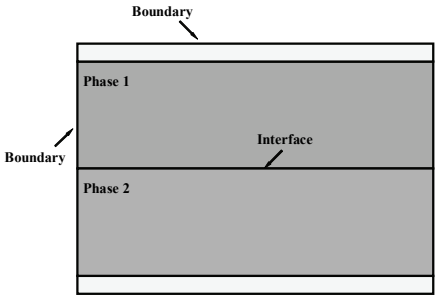

Figure 2.4. Boundaries and interfaces

The interface is defined as a very steep transition region between two thermodynamic phases, leading to a jump in physical properties.

A *boundary* represents a conceptual mean of separating among different attributes and between attributes and the outer world. The boundary is defined in geometric terms and has no behavioural features. As such it does not influence the number of equations in a model.

For the applications of the iso-butane alkylation plant, the external boundary of the model is taken as the battery limit of the plant, excluding the utility generation and waste treatment systems while including all processing operations to turn C_3-C_4 feeds into alkylates.

Since the process is defined by the transformations it causes to the resources and by means of these resources, a definition of a resource should be given before discussing the structure in more detail.

A *resource* represents any physical or information entity, R , of limited availability that needs to be used in order to obtain a transformation inside the process.

The most important *physical* resources considered in modelling of chemical processes are the mass, energy, momentum. For particular applications, other types of resources can be considered, such as electrical charge in electrochemical processes. Mass, energy and momentum are treated as field quantities, being locally continuously distributed over space and time.

The most important *information* resource is the signal, distributed over time, as used in control applications.

Some of these resources can be classified into smaller sub-divisions (kinetic energy, potential energy, work, etc.).

A special, though very relevant in some practical cases, mass resource is showing up as a population of particulates, being small discrete lumps of matter having an internal state, like mass or size or energy. Examples are crystals, droplets of liquid dispersed in another phase or gas bubbles in a liquid phase.

The *species* represent another group of resources. A species σ is defined as an ensemble of identical chemical or biochemical entities that are generated or consumed through a transformation called reaction.

In the case of the alkylation example, the resources that will be taken into account are the mass, the energy and the momentum. Since for the reaction the hydrocarbons are dispersed inside the acid, the hydrocarbon droplets population should be also considered.

Moreover, the utilities: energy (hot, cold), process water, power are available from both external sources, as well as co-generated in the process.

Alkylation serves to dispose of the C_3-C_4 cut from the FCC (fluid catalytic cracking) unit by converting much of this cut into alkylates. The alkylation usually converts *iso*-butane and *n*-butenes into products. Light hydrocarbons such as propane are present as inert. Liquid sulphuric acid is used as catalyst.

The main constituents of the alkylation product are trimethylpentanes (Dimian & Bildea, 2008). Undesired byproducts, including light (C_3-C_5) paraffins and isoparaffins, acid-soluble oils and pseudo-alkylates (mixtures of C_5-C_{16}) are produced in variable amounts, depending on the employed feed and on the operating conditions (Albright & Wood, 1997).

The composition of alkylate obtained in the process depends on the operating conditions, the number of passes in the reactor.

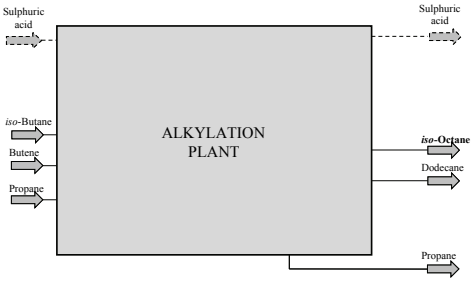

Figure 2.5. Input-output diagram for the iso-butane alkylation plant

Table 2.3. Typical alkylate composition

Type		Species
Reactant		*iso*-Butane (A)
		Butenes(B) 1- & 2Butene
Product	***Light ends (LE)***	*iso*-Pentane
		2,3-Dimethylbutane
		2- & 3-Methylpentane
		2,3 & 2,4-Dimethylpentane
		2,2,3-Trimethylbutane
		2- & 3-Methylhexane
		2,2,4-Trimethylpentane
		2,2,3-Trimethylpentane
		2,3,4-Trimethylpentane
		2,3,3-Trimethylpentane
	Dimethyl hexanes (P)	2,5-Dimethylhexane
		2,4-Dimethylhexane
		2,3-Dimethylhexane
		3,4-Dimethylhexane
	Heavy ends (R)	2,2,5-Trimethylhexane
		2,2,4-Trimethylhexane
		2,4,4-Trimethylhexane
		2,3,5-Trimethylhexane
Others	***Catalyst (C)***	Sulphuric acid
		Water
		SO_2
	Inert (I)	Propane

A typical composition (Albright, Spalding, Faunce & Eckert, 1988) is shown in Table 2.3.

The input-output diagram of the alkylation plant is presented in Figure 2.5, showing the main feeds and the products of the process.

a1) Process unit U represents a part of the process system Σ where a transformation of one or more resources, R takes place. Each unit has a function (or scope) assigned within the structure of the system, which is related to the transformation taking place inside the unit. The units can be classified according to the type of resources are transformed in: (a) physical units, where physical resources are transformed, and (b) information units, where signals are generated, transformed and applied.

Once the physical units have been defined, information units are added to the process flowsheet if required. These units are used for the control of quantities such as reactor feed, pressure, temperature, concentration of the distillation columns outlet streams, etc.

The STRATCO effluent refrigerated sulphuric acid alkylation unit (Caton, Racen & Troutman, 2008) is taken as an example. Five major sections are considered, as shown in Figure 2.6. The sections presented in Figure 2.6 do not always represent single process units, but groups of such units.

(1) Reaction section – the reacting hydrocarbons are brought into contact with sulphuric acid catalyst under controlled conditions

(2) Refrigeration section – the heat of reaction is removed & the light hydrocarbons are purged

(3) Effluent treating section – the free acid, alkyl and di-alkyl sulphates are removed from the net effluent stream to avoid downstream corrosion and fouling

(4) Fractionation section – *iso*-butane is recovered for recycle to the reaction section and remaining hydrocarbons are separated into the desired products

(5) Blowdown section – spent acid is degassed, the waste water pH is adjusted and acid vent steams are neutralized before being sent off-site

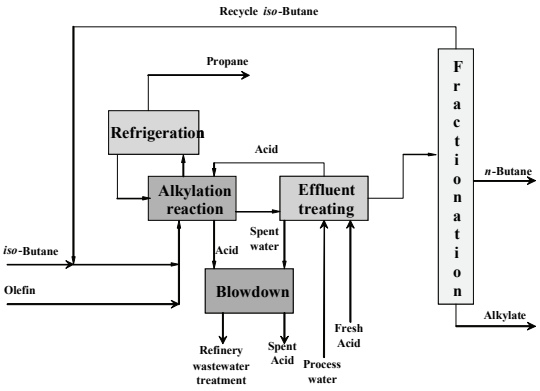

Figure 2.6. Block flow diagram of a STRATCO effluent refrigerated sulphuric acid alkylation unit (Caton, Racen, & Troutman, 2008)

a2) Compartment C represents a spatially distinct subdivision of the process unit U that is separated by a boundary from the rest of the unit.

a3) Domain D represents a spatially distinct subdivision of the geometric space of the compartment C that is separated by an interface I from another domain. Usually, a domain consists of a single phase. A second phase may be present, where usually one is continuous, while the other is dispersed.

To illustrate the concepts of compartment and domain for the alkylation plant a heat exchanger will be considered.

Table 2.4. Domains inside a heat exchanger

Compartment	Domain			
	Process stream	*Heating agent*	*Wall*	*Insulation*
Tubes	***Liquid phase 1***			
Shell		***Fluid phase 2***		
Wall			***Solid phase 1***	
Insulation				***Solid phase 2***

The following compartments are identified in this case: the tubes, the shell, the wall and the insulation.

Four domains are present (Table 2.4): the process stream whose temperature needs to be increased, the heating agent, the exchanger wall and the insulation. Each of these domains is characterised by a different type of phase that is present inside the domain.

a4) Region ρ represents a subdivision of a domain D of a compartment C characterized by a common characteristic behaviour inside the region. As well as the domains, two distinct regions are separated by an interface. The domain is a *spatial* notion, while the region is contained inside a domain and has certain distinctive *behavioural* features, for example the transition from laminar to

turbulent flow, or the sudden extinction of reactions. The interface of the region cannot be specified in terms of a function of a spatial or time coordinates, but it is defined by the passing of an inequality constraint on a set of state variables. A region may also be defined as a physical boundary layer within a domain and forming an interface between a wall and the bulk of a fluid.

a5) Phase φ represents thermodynamic phase as a subdivision of a region or a domain. A system may be characterized as "homogeneous" (single phase with $\varphi = 1$) or "heterogeneous" (multiphase with $\varphi \geq 2$) according to the number of distinct phases. Two different phases are separated by an interface I through which transfer of resources may take place. The interface may be a planar interface (as shown in Figure 2.7b) or a domain structure with regular or irregular islands of one phase embedded in a surrounding matrix of a different phase, as shown in Figure 2.7a).

The alkylation reaction takes place in liquid phase, with the hydrocarbons dispersed in the acid. Two phases are considered in this case (see Figure 2.7a): (1) a continuous liquid acid phase and (2) the dispersed hydrocarbon liquid droplets. In case of the distillation columns, two interconnected phases are considered for each tray (see Figure 2.7b): (1) a liquid and (2) a vapour phase. Mass and energy are transferred through the interface between the two phases.

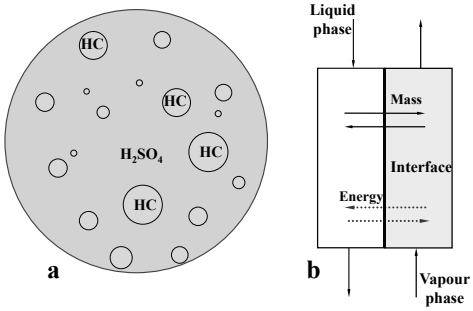

Figure 2.7. Schematic representation of phases considered in the alkylation process: a) Reactor; b) Distillation tray

3.2.2. Behavioural structure of the model

The attributes of the behavioural level correspond to the transformations that take place inside the nodes considered inside the process' network. The following groups can be distinguished in this case:

b1) Sources and sinks ξ. This group of attributes generates or consumes resources, such as reactions or birth and death processes in case of particulates. For example, a reaction k is defined as a mechanism through which a set of species, called reactants, are being transformed into a set of different species, called products. Depending on the level of decomposition desired, reactions take place at phase, region, domain, or unit level.

The production of iso-octane involves the liquid-phase reaction of 1-butene with iso-butane un the presence of a second liquid phase of sulphuric acid. The alkylation reaction is accompanied by several other acid-catalyzed reactions such as olefin oligomerization, product cracking and product isomerisation, all of which result in the formation of several inferior products. The mechanism usually cited for iso-butane alkylation involves a carbenium ion chain mechanism initiated by the protonation of the olefin (Hommeltoft, 2001). Some basic reactions are (Lee & Harriott, 1977):

A) Chain initiation:

$$C_4^{=} + H_2SO_4 \underset{k_{-1}}{\overset{k_1}{\rightleftharpoons}} C_4^{+} + HSO_4^{-} \tag{2.1}$$

B) Main chain:

$$i - C_4^{+} + C_4^{=} \underset{k_{-2}}{\overset{k_2}{\rightleftharpoons}} C_8^{+} \tag{2.2}$$

$$C_8^{+} + i - C_4 \underset{k_{-3}}{\overset{k_3}{\rightleftharpoons}} i - C_4^{+} + C_8 \tag{2.3}$$

C) By-product reactions:

$$C_8^{+} + C_4^{=} \underset{k_{-4}}{\overset{k_4}{\rightleftharpoons}} C_{12}^{+} \tag{2.4}$$

$$C_{12}^{+} \underset{k_{-5}}{\overset{k_5}{\rightleftharpoons}} C_5^{+} + C_7^{=} \tag{2.5}$$

$$C_{12}^{+} \underset{k_{-6}}{\overset{k_6}{\rightleftharpoons}} C_6^{+} + C_6^{=} \tag{2.6}$$

$$C_{12}^{+} \underset{k_{-7}}{\overset{k_7}{\rightleftharpoons}} C_7^{+} + C_5^{=} \tag{2.7}$$

b2) Buffer effects (change in hold-up). A resource R can be stored or depleted in a region or domain. The determination of hold-ups and changes therein are done only in dynamic models considering time derivatives of hold-ups of resources.

3.2.3. Model connectivity

The final group of attributes offers information related to the way the different entities inside the process network are connected between themselves and with the environment.

c1) Streams. The stream S represents a moving quantity of resource R that is being transferred from a process unit to another, as shown in Figure 2.8. The streams are also transferred between the process Σ and the environment Δ.

Three categories of streams are considered in most of the process application: material, energy and information streams. In case of the material streams, the decomposition can go even further.

A material stream S can be subdivided into different phases, φ and species σ. For the purpose of this research, the stream is considered just as an interconnection between different entities of the network. In some cases, within a physical stream, a transformation of the resource R may take place. If this happens, the stream will be considered as a unit. A stream has two components:

(1) *Topological component*, which defines the units connected by a particular stream, and the direction of the stream

(2) *Behavioural component*, which indicates the amount of resource being moved from one unit to the other

c2) Transfer. A transfer process θ is defined as a mechanism through which a resource is being transported, through a boundary or interface, from one node of the system to the other. Species mass diffusion between phases and radiation from a hot surface into a fluidic volume are examples of transfers. Depending on the level of decomposition desired, the transfer takes place at phase, region, domain, or unit level. In tranfer, the diffusive flow is usually dominant.

c3) Transport. A transport process J is defined as a mechanism through which a resource R is being transported into, through and out of a distinct region. Depending on the level of decomposition desired, the transport takes place at phase, region, and domain or unit level. Physically, transport is achieved by convective and diffusional flows. While the transfer takes place between phases, for example, the transport is possible inside of a single phase. The convective flow is usually dominant in transport.

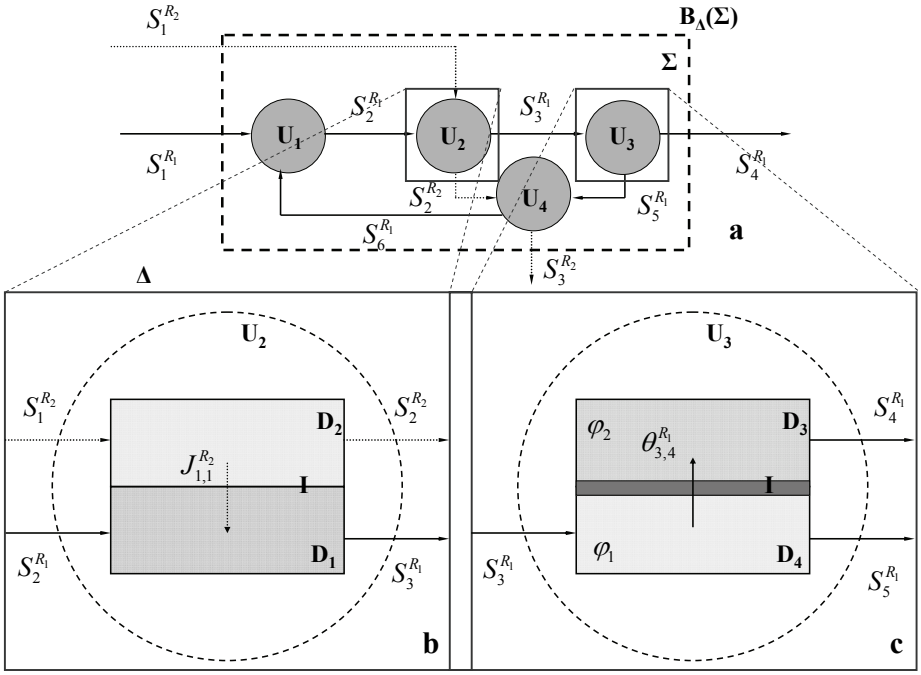

Figure 2.8. Model decomposition:
a) Streams and units; b) Domains and transport; c) Phases and transfers

For the iso-butane alkylation, the streams are visualised in Figure 2.9, which presents an example of the plant's flowsheet from Dimian & Bildea, 2008. A more detailed flowsheet is presented in Caton, Racen & Troutman, 2008.

Examples of transformations that involve the transfer of a resource for the *iso*-butane alkylation plant are presented in Table 2.5. The table is not complete, but offers an idea of the variety of units required in the process.

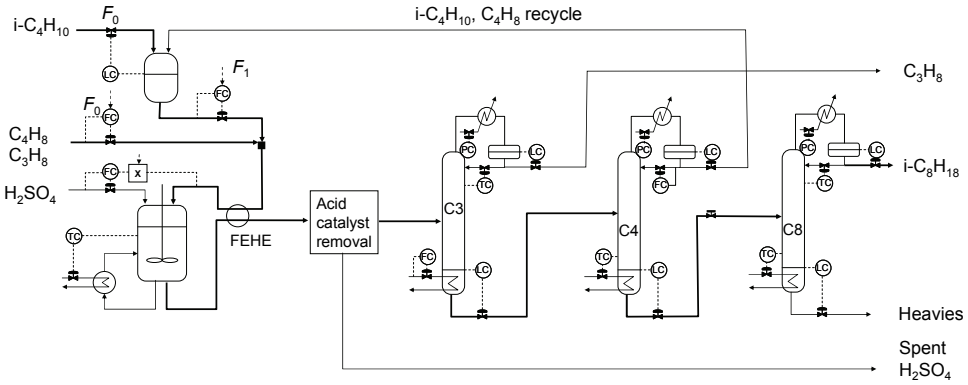

Figure 2.9. Flowsheet for the iso-butane alkylation plant (Dimian & Bildea, 2008)

Table 2.5. Examples of physical process units for the alkylation plant

Unit	Function	Transformation	Resource	Type of transformation
Reactor	Alkylation	***Reaction***	***Mass***	**Rate process**
Heat exchanger	Feed cooling	***Heat exchange***	***Energy***	**Transfer**
	Condense depropanizer feed			
	Remove heat of reaction			
Flash	Remove propane	***Separation***	***Mass***	
Distillation column	Remove iso-butane			
	Remove n-butane			
	Remove alkylate			
Settler	Acid removal			
Coalescer	Feed water removal			
Mixer	Feed mixing	***Mixing***		
Pump	Reactor inlet stream	***Pressure change***	***Momentum***	
Compressor	Reactor vapour stream			
Pipe	Transport feed & products	***Transport***	***Mass***	**Transport**
PID controller	Control process operation	***Computation***	***Information***	

4. Mathematical, numerical and software implementation levels

This section aims to present a systematic overview of the structure and attributes of a process model and its implementation. A discussion of common elements of this structure and certain attributes can be found in textbooks on process modelling (Hangos & Cameron, 2001) as well. There it is spread out over several chapters. The purpose of presenting this concise overview is to set the stage for a systematic subsequent discussion of model reduction options, according to the presented structure and attributes. Furthermore, the systematic presentation of the model equations plays also a vital role in Chapter 3, 4 and 5 of this thesis. The mathematical level is split in the behavioural models of nodes (Section 4.1), connectivity of nodes to a network (Section 4.2) and the aggregated network model (Section 4.3)

4.1. Mathematical level: behavioural models of nodes

Once the information related to the physical structure level is defined, the result is a network-type of representation of the model similar to the one in Figure 2.8, together with details on the phenomena that take place in each individual block.

At this point, the mathematical relations defining the behaviour of the nodes are written. In many cases, for a certain type of entity a general equation is written, which is further refined according to a specific case. The mathematical relations relate closely to the structure of the model, accounting for the number and the nature of the model discrete attributes.

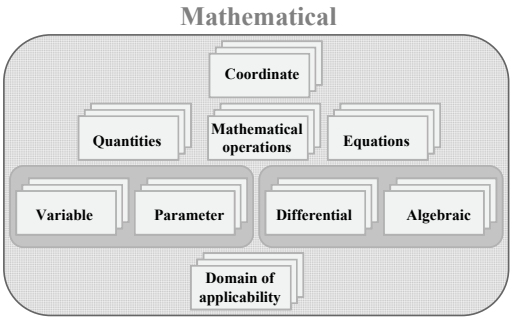

Figure 2.10. Structure of the mathematical level

At the *behavioural mathematical level*, the main attributes that are identified are the model equations, which can be classified in differential and algebraic, as seen in Figure 2.10.

Within an equation, one can identify the different quantities (variables and parameters), as well as the mathematical operations (differentiation, integration, summation, power, etc.).

In the following, a classification of the different components of the model's equations is presented.

4.1.1. Coordinates

The coordinate system consists of a set of variables used to determine in a unique way the position (in time and in space) within units of the process Σ. The most common used coordinates in product and process modelling are: (a) the time coordinate t; (b) the spatial coordinate $\vec{z}$; and (c) the internal coordinate $\vec{s}$ of a particulate.

Except for the time, the coordinates presented above are usually vectors, containing a number of components related to the degree of detail used or desired in the decomposition of the process.

There can be a generic set of coordinates for the entire system or the various nodes considered in the process network may have a different set of coordinates. For a specific process unit, a domain has its own set of coordinates. For example, in a fixed bed reactor, the fluid phases flowing through the bed have one set of spatial coordinates and the catalyst particles have another set of spatial coordinates, while sharing time as a joint coordinate.

The coordinates have two main roles when defining the model. They may occur as variables in the equations, as in explicit functions in initial and boundary conditions or in rate functions. The second role is in the definition of the mathematical operators occurring in the model equations, such as differentiation or integration.

4.1.2. Classification of quantities

The mathematical structure of the model represents relationships between quantities describing the system. These quantities are classified in two categories: variables and parameters. The classification of the quantities does not offer model reduction options.

b1) Variables. This category contains the quantities that vary along the system's coordinates. The following groups are identified, following the concept of a state space model:

1) State variables x. Represent quantities indicating the hold-up of a resource in a region or domain, for a dynamic system. Conservation laws are written for the state variables and the behaviour of the system is characterised by the evolution of its states along the coordinates. From the way system variables change with the coordinates, the systems can be classified in two categories (Bequette, 1998):
   i) Lumped systems – none of the variables of interest depends on any spatial coordinate
   ii) Distributed systems – at least one variable of interest depends on the spatial position z or on an internal coordinate s

2) Input variables, u. An input variable represents the quantity that is linked and determined by the "external environment" of the system considered for the model. The variation of the input variables affects the value of the state variables. The evolution in time of an input variable must be specified before a problem can be solved. Inputs are usually chosen based on the knowledge of the system considered. This group of variables is classified in:
   i) Control (manipulated) variables - are (externally) modified in a controlled way as part of a scenario, in order to achieve desired performance. In this category, one can distinguish between (a) inflow variables, on which the user does not necessarily have a direct influence, and (b) operational variables on which the user has a direct influence.
   ii) Disturbances - the modification does not take place in a controlled way. This group of variables may have a stochastic nature.

3) Output variables y. The output variables represent the quantities derived from the state variables, which are of direct interest to the model user. The inputs modify the state of the system that further has an effect on the outputs. The output variables offer information related to the performance of the model and represent a link to the external environment. They are used for the extraction of relevant information for the user of the model. Two categories are identified: (a) the outflow variables, and (b) the quantities that relate to the quality of the (product) output.

4) Algebraic variables (as co-states related to the constitutive equations). The algebraic (or the auxiliary) variable v represents a group of quantities derived from the input and state variables. Within this category one can distinguish:

   (a) Thermodynamic state variables v_1 (enthalpy, entropy)

   (b) Physical property variables v_2 (density, specific heat, viscosity, conductivity, diffusion)

   (c) Rate of change variables r, represent the rates by which the resources are produced or consumed inside the system. A typical example of change variables are the chemical reaction kinetic rates.

   (d) Fluxes of resources in transport and transfer rate processes

5) Algebraic variables related to the connectivity by streams, Φ. This group of variables involves quantities such as the composition and the flow rate variables of streams connecting process unit.

6) Boolean or logical variables related to the nodes and edges being active in a flow sheet. These variables are useful in modelling for process synthesis by means of a topological superstructure. The nodes and streams have each logical variables, whose value (on/off) indicate whether a node or a stream is considered to be active in the flowsheet. Such variables are not considered in this thesis.

b2) Parameters. Represent quantities that do not vary along the system's coordinates or with changing external conditions. These quantities are completely specified in the context of use, in order to be able to solve the problem mathematically. Parameters are often "adjusted" to achieve desired performance of the model. This group is classified in:

i) Design parameters, δ, representing the sizing and the number of the units

ii) Empirical behavioural parameters, α, taking away uncertainties in the model equations by tuning to experimental data

b3) Range and units. This category offers information related to the lower and upper limits for the variation of the different quantities. Units of measurement are also required.

4.1.3. Classification of equations

The number and the variety of the attributes at physical structure level influence the number of variables, as well as the number and the complexity of the equations. The complexity of a set of equations depends more on the nonlinearity and the number of the terms occurring in an equation, on the mathematical type of operation within such terms (derivatives, integrals, etc.), and on the coupling between the equations by jointly occurring variables, than on the number of equations. Three views on defining the types of equations are possible:

(1) Functional, systems view: input, change, output

(2) Mathematical view: linear, nonlinear, algebraic, differential, integral

(3) The physical view: conservation laws, constitutive equations for thermodynamic state and equilibrium, property relations, rate expressions

In the following section, the focus is on the mathematical view in presenting the equations, while the classification will be done taking into account the physical view. The classification of the model equations does not offer model reduction options.

c1) Differential equations. This group of equations arises from conservation laws or from mathematical transformations. The behaviour of the domain is modelled by applying the conservation principles to the resources of the system. The resource as such is conserved in the domain, although it may change its amount. The conservation of the resource signifies that what enters the domain should leave, is transformed into another quantity, or it accumulates in the domain. The mass, energy and momentum are strictly conserved, while the species amounts may transform.

In general, a conservation equation is written in the form of a resource balance, often called an equation of change:

$$\left\{\begin{matrix}accumulation\\ of\\ resource\end{matrix}\right\}=\left\{\begin{matrix}resource\ in\\ through\ boundary\end{matrix}\right\}-\left\{\begin{matrix}resource\ out\\ through\ boundary\end{matrix}\right\}+\left\{\begin{matrix}resource\\ generation\end{matrix}\right\}-\left\{\begin{matrix}resource\\ consumption\end{matrix}\right\} \quad (2.8)$$

For a general input-state-output system, the set of differential equations will be written as:

$$\frac{dx(t,z,s)}{dt}=f\left(x(t,z,s),\nabla_z x(t,z,s),\nabla_s x(t,z,s),u(t,z,s),v(t,z,s),\alpha,\delta\right) \quad (2.9)$$

Here t is the time variable, z is the spatial coordinate vector, and s is the internal coordinate. The variable $x(t,z,s)\in\mathbb{R}^n$ is the state variable vector, $u(t,z,s)\in\mathbb{R}^m$ is the input variable vector, $v(t,z,s)\in\mathbb{R}^q$ is the algebraic (co-state) variable vector, $\alpha\in\mathbb{R}^p$ is the empirical parameters vector, while δ is the design parameter vector. In the above equation n is the state space dimension. The function f describes the dynamics of the domain.

In case of distributed systems, a (parabolic or hyperbolic) partial differential equation (PDE) is obtained in the form of equation (2.9). For lumped systems, the result is an ordinary differential equation (ODE):

$$\frac{d\tilde{x}(t)}{dt}=f\left(\tilde{x}(t),u(t),v(t),\alpha,\delta\right) \quad (2.9.a)$$

In the following, the focus will be on the physical interpretation of the model equations. When modelling process systems, the most important quantities for which conservation equations are written are the mass (for pseudo-continuous phases) or the population (for distributed phases), the energy, the momentum and the electrical charge. For the purpose of this thesis the Maxwell-type of equations for electro-magnetic fields are not considered.

1) Mass balances. When mass is considered as a resource being transformed, the generic balance equation is written for any of the species present in the domain, in the form of the mass balance equation (see Appendix 1). The number of independent balances is equal to the number of species considered.

2) Population balances. The population balance equation (Appendix 2) is the form the generic balance equation takes for any of the populations of entities of dispersed phases considered in a domain, when these entities have a distributed internal state.

3) Momentum balances. In a similar way, a generic momentum balance can be written for the cases when the momentum is the resource transformed inside the domain. The generic momentum balance equation is presented in Appendix 3. The number of the independent balances is equal to the number of spatial coordinates considered.

4) Energy balances. In the generic form, the balance equation (see Appendix 4) is written for the total energy. The total energy is the sum of internal, kinetic and potential energy, all of which are associated to the mass. Work is a summation of various other energy effects, such as mechanical work, volume work, electrical work, etc.

c2) Initial and boundary conditions

Together with the differential equations of the domain, additional relations should be specified to complete the model to define known values of the state variables x on the domain's boundaries. Depending on the type of boundary being used, these additional constraints are classified as follows:

i) Initial conditions. These constraints define the values of the state variables at the lower boundary of the time axis:

$$0 = f_0\left(x, u, v, \alpha, \delta\right)\Big|_{t=0} \tag{2.10}$$

ii) Boundary conditions. These constraints define the values of the state variables on a specific geometric boundary of the domain. They appear in three major forms (Hangos & Cameron, 2001): (a) first type or Dirichlet, (b) second type or Neumann, and (c) third type or Robbins.

$$0 = f_{BC}\left(x, \nabla x, u, v, \alpha, \delta\right)\Big|_{B} \tag{2.11}$$

c3) Algebraic equations for co-states. A third set of equations characterizing the processes occurring in a domain is represented by relationships expressing thermodynamic equilibrium, reaction rates, transport rates for heat, mass, momentum, physical properties and so on. Several alternatives are available for writing these equations for a particular physico-chemical system.

In general, this type of equations is written in the following form:

$$0=h\left(x\left(t,z,s\right),u\left(t,z,s\right),v\left(t,z,s\right),\alpha,\delta\right) \tag{2.12}$$

The function h describes the (algebraic) constitutive equations for the rates, the thermodynamic equilibrium and the physical properties of the phases.

The algebraic equations for co-states are classified as follows:

1) Thermodynamics equations of state. The equations of state are thermodynamic equations between state variables of the system, for a given set of physical conditions (O'Connell & Haille, 2005).

2) Physical property equations. The physical properties of a system are not constants. Processing condition may vary in a wide range during operation. Moreover, the system consists of a variety of materials (pure species, mixtures, and phases) in any state (liquid, solid, gas). Information regarding the physical properties (for example density, viscosity, thermal conductivity, diffusivity, etc.) of the materials is required to complete the model. Equation (2.12) will be used to write this type of relations.

3) Equilibrium equations. These equations are written for systems with chemical, thermal, mechanical or electrical potential equilibrium.

4) Rates of transfer, transport and change. The differential equations describing the system (see Appendix 1-4) consider a number of terms of transfer. This number of terms is determined by the number of distinct rate phenomena that influence the system Σ. Examples of such terms that appear in a typical process are sources and sinks like net convection, diffusion (or dispersion), interfacial transfer of resources, generation (or consumption) in reactions, etc. Relations describing these types of transfer are derived and added to the model. The complexity of these terms adds to the overall complexity of the model.

   All these terms will be written in the general form expressed in equation (2.12).

c3) Output equations. The relations between the state variables x and the output variables y are usually defined by algebraic equations. This can be written in a general form as:

$$y\left(t,z,s\right)=g\left(x\left(t,z,s\right),v\left(t,z,s\right),\alpha,\delta\right) \tag{2.13}$$

Here $y(t,z,s) \in \mathbb{R}^p$ is the output variable vector. The function g describes the way in which the observations are deduced from the state and the algebraic variables. The dimension of the input vector, m and the dimension of the output variable vector p, are much smaller than n, and usually $m \geq p$.

It has to be mentioned that the output equations in (2.13) do not show the internal gradients of the states with respect to the coordinates (t,z,s). Mathematically, this would be consistent with the state differential equations for a distributed system in equations (2.9). However, in practice, such gradients are not easy to measure. For this reason, the use of the states is a more adequate choice for the output equations.

These equations do not always have to be written in an explicit form, but an expression relating the state variables to the output variables should always be possible to derive.

4.1.4. Validity and applicability conditions (knowledge constraints)

The knowledge constraints are usually defined as inequalities, which result from the translation of the modelling assumptions (Hangos & Cameron, 2001). These inequality constraints define a set in the space of all variables entering a constitutive equation (rate equation, thermodynamic equation, equation of state) over which the equations can be reliably applied.

$$0 \leq j\left(x(t,z,s), v(t,z,s), \alpha, \delta\right) \tag{2.14}$$

4.1.5. Types of operations in model equations

Another set of attributes at mathematical level is represented by the different type of operations present in the model equations, which are determined by the behaviour of the attributes in the physical structure.

The operations range from simple algebraic operations such as addition/subtraction $\{+,-\}$, multiplication/division $\{*,/\}$, derivation/integration $\left\{\frac{\partial}{\partial}, \int\right\}$, power/logarithm $\{\hat{},\log\}$ and to more complex special functions such as Bessel functions, etc.

4.1.6. Model classification

Depending on the type of functional expression on the right-hand side of the set of differential and algebraic equations, the models are classified in:

i) Linear models – contain models for which the functional expressions in equations (2.9) – (2.14) are written as a linear combination of the variables. For a linear model, the model equations are written in the following way:

$$\frac{dx(t,z,s)}{dt} = A(t,z,s)\cdot x(t,z,s) + B(t,z,s)\cdot u(t,z,s) + C(t,z,s)\cdot v(t,z,s)$$

$$y(t,z,s) = D(t,z,s)\cdot x(t,z,s) + E(t,z,s)\cdot v(t,z,s) \qquad (2.15)$$

$$0 = F(t,z,s)\cdot x(t,z,s) + H(t,z,s)\cdot u(t,z,s) + G\cdot v(t,z,s)$$

ii) Nonlinear models – for these models the functional expressions are not written in linear form. Most of the real systems are of nonlinear nature. Explicit solutions to nonlinear differential equations can rarely be obtained (Bequette, 1998).

4.2. Mathematical level: Connectivity

The connection between the nodes of the networks (shown in Figure 2.11) is an important feature of the chemical processes. In the following, a way of accounting for the connectivity between the different units (attributes) of the model in the model equations will be presented.

The connectivity needs to be accounted for in the process model as well. Two types of streams are considered in Figure 2.11: (1) streams that connect the *unit* k to the outside environment, and (2) streams that connect the unit k to other units in the process network. The first type of streams is defined by the input variables u, while the second type is defined by the *flow* of resources being transported through stream $\Phi_j^{(R)}$. This vector of streams $\Phi_j^{(R)}$ is made up of flow rates of the species, momentum, energy, etc. in this stream.

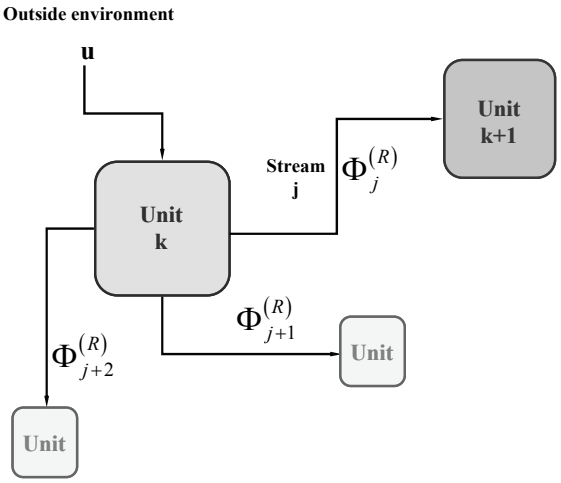

Figure 2.11. Connection of units by streams

The stream vectors are ordered in a stream matrix, $M_{\Phi}^{(R)}$:

$$M_{\Phi}^{(R)} = \left[\Phi_1^{(R)} \quad \Phi_2^{(R)} \quad \Phi_3^{(R)} \quad ... \quad \Phi_j^{(R)} \right] \tag{2.16}$$

A unit (as a node) will have some *gates* through which it is connected with streams inside the network. A new *flow* vector is introduced, representing the set of flows per node *k* through its gates *g*. There is one flow per gate and there may be several gates for a node. A flow through a gate *g* of a node *k*, is denoted by $\Theta_{g,k}^{(R)}$.

These flows will be arranged in a flow matrix:

$$M_{\Theta}^{(R)} = \begin{bmatrix} \Theta_{1,1}^{(R)} & \Theta_{1,2}^{(R)} & \Theta_{1,3}^{(R)} & ... & \Theta_{1,g}^{(R)} \\ \Theta_{2,1}^{(R)} & \Theta_{2,2}^{(R)} & \Theta_{2,3}^{(R)} & ... & \Theta_{2,g}^{(R)} \\ ... & ... & ... & ... & ... \\ \Theta_{k,1}^{(R)} & \Theta_{k,2}^{(R)} & \Theta_{k,3}^{(R)} & ... & \Theta_{k,g}^{(R)} \end{bmatrix} \tag{2.17}$$

The *flows* must be connected with streams inside the network, and they belong to a node.

For a *lumped system*, a differential equation, containing the matrix of *flows* $M_{\Theta}^{(R)}$ is written. This matrix is post-multiplied with the unit vector, I to obtain a linear addition of flows.

$$\frac{d\tilde{x}(t)}{dt} = f\left(\tilde{x}(t), M_{\Theta}^{(R)} \cdot \mathrm{I}, u(t), v(t), \alpha, \delta \right) \tag{2.18}$$

For a *distributed system*, the internal balance equation does not change:

$$\frac{dx(t,z,s)}{dt} = f\left(x(t,z,s), \nabla_z x(t,z,s), \nabla_s x(t,z,s), u(t,z,s), v(t,z,s), \alpha, \delta \right) \tag{2.19}$$

In this case, the flows appear in the model equations through the boundary conditions:

$$0 = f_{BC}\left(x, \nabla x, M_{\Theta}^{(R)}, \alpha, \delta \right)\Big|_B \tag{2.20}$$

When the boundary conditions are given at the inlet only, it is necessary to add an additional set of outlet boundary conditions. The function of this additional set is to relate an outgoing flow, $\Theta_{g,k}^{(R)}$ with the internal state *x* at the outlet.

Obviously, the *flow* vectors $\Theta_{g,k}^{(R)}$ are unknown and must be specified by making a connection with the *streams*. Each *flow* through a gate, $\Theta_{g,k}^{(R)}$ will be connected with a stream, $\Phi_j^{(R)}$. This can be

done by means of a connectivity matrix for a node, $C_k^{(R)}$. This matrix has entries *c* that can take the following values:

$$c = \begin{cases} -1 & out \\ 0 & no\ \ connection \\ 1 & in \end{cases} \tag{2.21}$$

The connectivity matrix of node *k* is build up in the following way:

$$C_k^{(R)} = \begin{pmatrix} c_{1,1}^{(R)} & c_{1,2}^{(R)} & \cdots & c_{1,j}^{(R)} \\ c_{2,1}^{(R)} & \vdots & \vdots & c_{2,j}^{(R)} \\ \vdots & \vdots & \vdots & \vdots \\ c_{g,1}^{(R)} & c_{g,2}^{(R)} & \cdots & c_{g,j}^{(R)} \end{pmatrix}_k \tag{2.22}$$

The row index counts the flows, while the column index counts the streams. Each row and column of this connectivity matrix have only one non-zero element. A row (of length j) is associated with a gate g and the non-zero element in this row selects the stream j that will be connected to the *flow* through this gate. A column (of length g and having a single non-zero element) is associated with a stream and indicates through which gate g of a unit k this stream is passing.

The flow matrix is connected to the stream matrix for each node *k*:

$$M_{\Theta,k}^{(R)} = C_k^{(R)} \cdot \left[M_{\Phi}^{(R)} \right]^T \tag{2.23}$$

$$M_{\Theta}^{(R)} = C^{(R)} \cdot \left[M_{\Phi}^{(R)} \right]^T \tag{2.24}$$

The matrix $C^{(R)}$ is a column wise matrix, collecting $C_k^{(R)}$, with $k = 1,...,K$. The matrix $C^{(R)}$ can have only two non-zero elements of opposite signs (-1 for a *source* and +1 for a *sink*). The matrix $M_{\Theta}^{(R)}$ is a matrix collecting all the flow matrices $M_{\Theta,k}^{(R)}$, with $k = 1,...,K$.

4.3. Mathematical level: Aggregation at system level

The model equations presented in the relations (2.9) – (2.14) do not account for the model connectivity. Since the connectivity is an important property of the chemical process models, as mentioned in the previous sections, the equations will be rewritten in order to account for this feature. The result is a set of differential and algebraic equations (PDAE's) shown in Figure 2.12, which represents both the internal and behavioural structure of the model.

Once the models of the single entities (nodes and streams) are available, the next step in the model specification and design step (see Figure 1.2 in Chapter 1) is the coupling of these individual

models to obtain the full model (see Figure 2.12) of the process Σ, presented in Figure 2.8. The coupling is performed by connecting the individual entities through the streams of resources (material, energy, momentum, information). The output stream of one entity is the input stream of the following entity, as the flowsheet of the application shows.

At mathematical level, the interconnection is represented as an algebraic equation (equality) between sub-models variables such as mass flow, mass fraction, specific enthalpy, heat flow, temperature, entropy, pressure, etc. These equations act as constraint equations for the state variables and can lead to a high index problem.

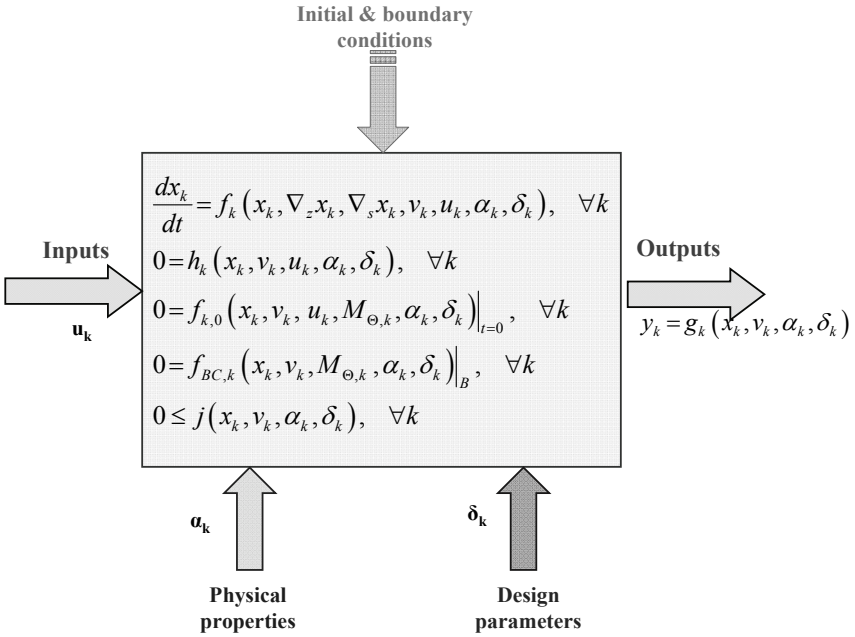

Figure 2.12. Input-output and behavioural structure of the model

For this reason, it is important to know which input variables sets do not result in a high index problem and how to interconnect the sub-models in such way to ensure that the resulting model does not have a high index structure. The requirement for an index of at most one is that equation (2.12) can be solved in implicit form. This is equivalent to the algebraic equation set should have Jacobian of full rank with respect to the algebraic variables (Hangos & Cameron, 2001).

To detect the cause of the high index problem it is important to know (Soetjahjo, 2006):

a) if the state variables constraints are due to internal constraint equations within the model, or due to the choice of the input variables, or due to the interconnection of the sub-models
b) which variables appear in state variables constraints
c) how to solve the index problem, either by symbolic index reduction or by special numerical handling

In practical terms, avoiding high index problems is equivalent to specifying the variables that can be manipulated in practice. For example, for the dynamics of the distillation column the reflux must be specified, and not the composition of the distillate. The occurrence of high index problems can create a trade-off in model reduction: by simplifying equations by elimination of fast phenomena and imposing constraints on state variables, a reduction in the number of variables and equations can be obtained. This potential gain can, however, be removed by the creation of a high-index problem.

4.4. Relationship between model structure and computational complexity

In the previous sections, a classification of the model equations was introduced. It has to be noted that the classification is useful for understanding the model structure, but does not offer handles or structural elements to change the number of model equations.

The complexity of the model is determined by the following factors:

(1) Number of model equations

(2) Number of terms in the model equations

(3) Type of operations in the model equations

Table 2.6. Discrete decision attributes at model structure level

Level	Attribute	Counter
Physical structure	*Resource, R*	$n_R + n_\sigma$
	Unit, U	n_U
	Compartment, C	n_C
	Domain, D	n_D
	Region, ρ	n_ρ
	Phase, φ	n_φ
	Coordinate, C	n_C
	Boundary, B	n_B
(Scalar) Phenomena	*Sources & sinks, ξ*	k_ξ
	Buffer effect, ω	k_ω
Connectivity (directional phenomena)	*Stream, S*	n_S
	Transfer, θ	k_θ
	Transport, J	k_J

For this reason, a formal counting variable (integer) of the number of attributes is introduced in Table 2.6. These are discrete decision variables available for making model changes, for either reduction or refinement.

4.4.1. Number of equations

The total number of variables and equations of the model is determined by the physical structure of the model. The number of model equations is calculated using a combinatorial product over a set of counting variables of the relevant attributes.

a) *The number of state equations* (differential equations) is determined by the product of the number of physical attributes and the number of resources considered:

$$NDE = \sum_{n_U}\left(\sum_{n_C}\left(\sum_{n_D}\left(\sum_{n_\rho}\left(\sum_{n_\varphi}\left(n_R + n_\sigma\right)\right)\right)\right)\right) \tag{2.25}$$

b) *The number of algebraic equations* is determined by the number of sources and sink terms, the number of transfer and transport phenomena, the phase and reaction equilibria, the physical and transport properties considered in the model. In practice the number of algebraic variables is three to ten times the number of differential equations (Van den Bergh, 2005), depending on the implementation of the physical properties (as hidden module or as explicit equations in the model). The number of initial conditions is equal to the number of state variables considered, while the number of the boundary conditions is equal to the product between the number of state variables and the number of boundaries.

$$NAE = \left(n_\varphi + n_\zeta\right) + \left(k_\theta + k_J\right) + n_{pp} + \ldots \tag{2.26}$$

List of symbols

NDE = number of differential equations

NAE = number of algebraic equations

n_{pp} = number of physical and transport properties

4.4.2. Number of terms in the model equations

The number of terms and the type of operations in the model equations are determined by the behavioural structure (phenomena), as well as the connectivity attributes of the model.

The number of terms in differential equations is determined by the number of coordinates considered, the number of sources, sinks, transfer, and transport phenomena considered in the model.

4.4.3. Connectivity of the model equations

The incidence matrix of the model shows which variables occur in which equations. If this matrix is manipulated by permutations into a lower-block triangular form, the numerical solution process is decomposed in solving a sequence of smaller sub-problems. Usually, a process has recycles inside the units (such as counter current connections between compartments) and between units as well as heat and power integration between the units. The more of these connections arise, the denser the incidence matrix becomes and prospects on decomposition are lost. Removing weak recycles between far removed downstream and upstream units in the process from the model can be more than proportional beneficial in reducing computational efforts.

4.5. Numerical level

The third level of decomposition considered in the modelling procedure is the numerical level (see Figure 2.13).

An important step in modelling the process Σ involves the decisions regarding the numerical methods that will be available and chosen for solving the model. Most of the models of chemical processes contain a large number of nonlinear differential and algebraic equations (DAE's). The numerical solution of the model implies transformation, substitutions and other types of manipulation of the model equations in a form that can be dealt with by the respective numerical method or environment.

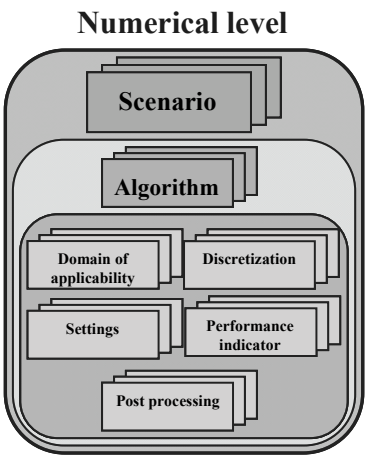

Figure 2.13. Structure of numerical level

For example, when dealing with a set of partial differential equations (PDE's), one numerical approach involves the discretization of the model equations along one or more coordinates and transforming the equations into a set of ordinary differential equations (ODE's). The transformation will lead to an increase of the number of ODE's to be solved proportional to the number of discretized coordinates.

This approach involves also a decision on which coordinate will NOT be discretised and used as the continuous coordinate in the numerical integration of the resulting ODE set.

An alternative approach in solving (P)DAE's is by application of functional approximations with minimization of weighted residuals. This leads, among others, to orthogonal collocation methods on finite elements. Here, decisions are needed regarding the kind of support functions, the distribution of collocation points along the coordinates and more.

For these reasons, the numerical implementation of the model can be a time consuming task as well. At this level, information related to the chosen set of suitable numerical solution algorithms, the

settings of the numerical algorithms parameters (tolerances, maximum number of iterations, discretization steps, domains of applicability, etc.) should be included. Information concerning the post processing of the results should be defined at this level as well.

Two issues need to be considered when solving a system of DAE's (Rascol, Meyer, Le Lann, & Prevost, 1998): the high order index and the consistent initial conditions.

The differential index of the DAE system is the minimum number of system differentiation with respect to time in order to convert it into an explicit set of first order ODE's (Leitold & Cameron, 2001).

There are three main causes for a high index DAE (Soetjahjo, 2006):

a) internal state constraints
b) non causal relation of the chosen "input" variables of the model
c) interconnection of the DAE sub-models

Avoiding high index DAE is also a matter of proper modelling, as discussed in Section 4.3.

The calculation of consistent initial values, equation (2.10), is important for applications such as optimal control or parameter identification problems. For the solution of the DAE system is required a set of initial conditions (2.10). The input variables are specified and from equation (2.12) the algebraic variables can be calculated if the model is well defined. Once these variables are known, the differential equation (2.9) is solved.

4.6. Software implementation level

The final level of decomposition for the modelling process is the software implementation. Once the strategy of solving the model is clear after the numerical level of decomposition, the following step is to write the model equations into a software environment. A distinction is kept between the implementation of the (scaled and discretised) model equations and of the numerical technique to solve these equations. The latter are often pre-packaged. The writing of the model equations into the software environment often requires an important amount of work. The variables and the equations should be written in a certain way, specific to the software.

Depending on the software environment to be used, the model equations are implemented in two ways:

a) Open-model format - the model equations are written completely, with their mathematical operators. Sometimes the equations are rewritten to avoid division (by zero), and transforming them into multiplications.

b) Model library format – the software environment has a library of models of the different entities inside the process network available. The user chooses the desired models and connects them as the topological structure specifies, specifying which are the inputs, the outputs and the parameters.

In both cases, the software environment have available a built-in library of solvers for differential equations, solving linear systems of equations, etc. In some cases (for example in gProms®) tools for other applications such as (dynamic) optimization or parameter estimation are available as well.

5. Existent model reduction techniques

As seen from the previous sections, every choice, at each level of decomposition will have an effect on the final model. Moreover, different decisions lead to different resulting models for the same application.

In practice, the model should be able to preserve the input-output behaviour over specified windows of inputs and outputs and represent the reality in a not very computationally intense way, having in the same time a low maintenance cost.

Model reduction is one of the approaches used to obtain such a model. This approach has a long history in the area of systems and control. Though very extensive, the systems and control literature related to model reduction focuses to a large extent on the reduction at the mathematical structure level, more specifically on reducing the number of equations of the system. In addition, since this is usually done in an aggregated way, it can prove unsuccessful in many cases, as it will be shown further.

5.1. Approaches to model reduction of process models

Several ways of classifying the model reduction techniques can be envisaged, but for the further section, the following is considered (Marquardt, 2001):

(1) Model simplification. This category includes all the techniques used to reduce the model complexity by reducing the complexity of the functional expressions, represented by the functions f, g, h in the model equations. Model simplification preserves the total number of model equations, but may diminish the number of terms and their nonlinearity.

(2) Model order-reduction. The techniques in this category replace the original large-scale model with a model having less number of differential equations. They will operate on a priori given mathematical models and aim for a (significant) reduction in computational times.

There must be a clear distinction between model *order-reduction*, the group of techniques that reduce the size (number of differential equations) of the model, and model *reduction*, which includes all methods that can be used for reducing the model complexity (acting on both the number and the "quality" of these equations).

Sections 3 and 4 of this section introduce the discrete decision attributes that allow modification of the model. In the following, the way each of these groups of attributes can be used for performing model reduction is identified.

5.2. Contextual level

Model reduction is performed from the first steps of the model development cycle. All the choices taken at the contextual level will affect the outcome of the modelling procedure.

Table 2.7. Typical applications for model use

Application type / Variable type	*Analysis of performance*	*Optimization of performance*	*Improvement of design*	*Feasibility of new design*	*Parameter estimation*
Input	✓	✓	✓	**?**	✓
Operating conditions	✓	**?**	✓	**?**	✓
Design parameters	✓	✓	**?**	**?**	**?**
Physical properties	✓	✓	✓	✓	✓
Output	**?**	✓	✓	✓	✓

At this level, the real system is reduced to a model with a single application or groups of applications that will be analysed using the model.

The decisions regarding the application and the goal(s) will have an effect on the input-state-output structure of the final model. Depending on the application the model will be used for, different groups of variables will act as known (✓) and unknown (**?**) for the model, as shown in Table 2.7. For the most important applications in process engineering (analysis and optimization of performance, improvement and feasibility of design), the variables that act as inputs and outputs are defined.

Moreover, the choice to operate in steady- or dynamic state will have an effect on the number of coordinates considered by the model. This is one of the few options for model reduction at this stage.

5.3. Structure level

The number of equations depends strongly on the number of discrete attributes at the structure level, as shown in equations (2.25) and (2.26). In the chemical engineering area, the reduction is being performed at both the physical, behavioural and the mathematical structure level.

The decisions regarding the physical structure of the system Σ will affect both the number of model equations and the complexity of the differential and algebraic equations (PDAE's) system that is obtained.

The existent techniques at structure level are summarised in Table 2.8 together with papers where each technique is used. The references in Table 2.8 are for exemplification purpose only.

5.3.1. Model reduction at physical structure level

The physical structure level affects the number of model equations. Starting from the initial levels of decomposition, model reduction is performed in several ways:

a) Resources

The number of resources directly affects the number of differential equations that have to be solved. The reduction in this case is performed by ignoring resources that are not important for the application considered (Yermakova & Anikeev, 2005). In chemical engineering often, the momentum balance is replaced by (algebraic equation) information related to the flow regime. For applications that take place in isothermal conditions, the energy balance is ignored as well.

Table 2.8. Model reduction options in chemical engineering applications at structure and system level

Options			**Approach**	**Example**
Level		Attribute		
Physical	**Structure**	*Resource*	Ignore	Yermakova &Anikeev, 2005; Okino & Mavrovouniotis, 1998
		Unit	Lumping	Ranzi, Dente, Goldaing, Bozzano & Faravelli, 2001; Henda & Falcioni, 2006; Dones & Preisig, 2010
		Compartment		
		Domain		
		Region		
		Phase		
		Coordinate	Steady state assumption	Gerstlauer, Mitrović, Motz & Gilles, 2001
			Integrate/average out	Mercenier & Michel, 1994; Housiadas, Klidis & Tsamopoulos, 2007
			Symmetry assumption	
	Connectivity	*Transfer*	Ignore terms Average	Baur, Higler, Taylor & Krishna, 2000; Schrefler, 2004
		Transport		
	Behaviour	*Sources and sinks*	Lumping	Okino & Mavrovouniotis, 1998
			Time-scale analyis	
			Sensitivity analysis	
System	**Structure**	*Unit*	Lumping/Aggregation	Antelo,Banga &Alonso,2008
	Connectivity	*Stream*	Lumping	Altimari & Bildea 2008; Altimari & Bildea, 2009

b) Species

Although considered as a resource in this thesis, the model reduction of the species is well developed in the chemical engineering literature, hence a separate section is required. Lumping of

species into pseudo-species is one way of reducing the model at this level. The lumping is performed using a continuum or a discrete view (Okino & Mavrovouniotis, 1998). In the first approach, a complex mixture is treated as a continuum. The species are not identified as a specific individual, but only as a distribution of species. The mixture is described in terms of rate constants, or physical constants such as boiling point, molecular structure or molecular weight. In the discrete lumping, the components of the mixture are treated individually. On basis of the reactivity, the species vector size is reduced to one of lower dimensions. Often the reduction of species is related to the reduction of the number of reactions, as shown in the next section.

c) Units, compartments, domain and regions

The number of physical blocks considered in the model has an effect on the number of equations that have to be solved, as well as the number of boundary conditions that have to be considered. An example is the separation of a mixture of two components. This can be performed in two ways: (1) using a distillation column, for which rigorous transfer equations are written for each try or (2) using a simple separation type of unit for which the equilibrium between the gas and the liquid phase at operation conditions define the output flows of the unit. Lumping different individual blocks will decrease the problem size.

d) Phases

The reduction is performed in this case by lumping distinct, dispersed phases into pseudo-continuous phases (Henda & Falcioni, 2006). In this way, there is no need for writing balance equations for each separate phase, separately. The system of PDE's that has to be written for the dispersed phases is replaced in most cases by a single PDE and a set of algebraic equations defining the composition of different species inside the pseudo-continuous phase. For example, in the case of the iso-butane alkylation, the reaction takes place in liquid phase.

e) Coordinates

Model reduction options emerge in the choice of the coordinate system by assuming certain geometric symmetries and thus reducing the required number of coordinates. Assuming steady state instead of dynamic behaviour (Gerstlauer, Mitrović, Motz & Gilles, 2001) or imposing symmetry assumptions (Housiadas, Klidis & Tsomopoulos, 2007) or going from Eulerian to Lagrangian coordinates are techniques used to transform the system from a number of n coordinates to a much smaller number as well.

Another option is to work with averaged values of functions over a sub-space (Mercenier & Michel, 1994; Housiadas, Klidis & Tsomopoulos, 2007). By performing averaging over this sub-space, the coordinates spanning this sub-space drop out and are replaced by a single scalar (an area or a volume of the sub-space). This latter reduction option is applied in Chapter 5 of this thesis.

5.3.2. Model reduction at behavioural structure level

The behavioural structure level affects the number of algebraic equations as well as the number of terms in the differential equations. At this level, the following reduction approaches are identified:

a) Sources & sinks

The use of complex reaction sets will have a strong effect on the complexity of the resulting model, due to the presence of different time scales and uncertainties regarding the kinetic parameters. The model reduction techniques are linked in this case with the identification of the key reactions and the sets of species that give insight into the behaviour of the process.

Three strategies have been pursued in the context of chemical reaction systems: lumping, sensitivity analysis and time-scale analysis (Okino & Mavrovounitis, 1998). Lumping transforms the original variables to a lower dimensional vector. The sensitivity analysis is used for the identification and elimination of the insignificant reactions and species based on their impact on the system, while the time-scale analysis identifies the different scales over which the species react and the fast-time scale reactions and species are assumed to be at steady state.

b) Transfer & transport terms

The reduction is done in this case by neglecting significant terms that have no practical interest or by averaging (integrating) the equations over suitable scales in time and space. A common example is the case of the reactive distillation column. Two different approaches are available for modelling of the unit (Baur, Higler, Taylor & Krishna, 2000): (1) the equilibrium stage model, in which the vapour and liquid phases are assumed to be in thermodynamics equilibrium, and (2) the non-equilibrium stage model, in which the finite mass-transfer rates across the vapour-liquid interface are accounted for.

c) Derivatives

Depending on the time scales of interest, some derivatives for the states that settle very fast into a steady state, a pseudo-steady state hypothesis can be applied. On the other hand, for states changing very slowly relative to other states, a pseudo-constant state can be applied. A similar approach can be followed for spatial coordinates.

5.4. Mathematical level

Since the equations are the core of any model, it is obvious that an important effort in reducing the complexity will focus at this level of decomposition.

As mentioned in Section 4.3 of this chapter, a system Σ is represented in mathematical form as a set of differential and algebraic equations (PDAE's), shown in Figure 2.12. In the following

sections model reduction techniques used to reduce the complexity of this PDAE system will be discussed.

The existent techniques for model reduction at mathematical lever are summarised in Table 2.9. The references in Table 2.9 are for exemplification purpose only.

Table 2.9. Model reduction options in chemical engineering applications at mathematical and numerical level

Options			Approach			Example
Level		Attribute				
Numerical	**Mathematical**	*Differential equation*	Order-reduction	Linear	Projection-based	Marquardt, 2001; Sandberg & Rantzer, 2004; Antoulas, 2005; Astolfi, 2007; Wattamwar, Weiland & Backx, 2010
					Non-projection based	
				Nonlinear		Hedengren & Edgar, 2005; Brüls, Duysinx & Golinval, 2007
			Simplification	Linearization		Marquardt, 2001
				Approximation of functional expressions		
		Algebraic equation	Linearization			Marquardt, 2001
			Approximation of functional expressions			
			Simplification of chemical kinetics			Nafe & Maas, 2002; Bhattacharjee, Schwer, Barton & Green, 2003
			Simplification of physical properties models			Marquardt, 2001
		Domain of applicability	Focus on domain of interest			Bildea, Dimian & Iedema, 2001
	Numerical scheme		Discretization			Motz, Mitrović, Gilles, 2002; Kasiri & Bashiri, 2010
			Functional approximation			Seferlis & Grievink, 2001; Dalaouti & Seferlis, 2006
			Operator approximation			Qamar, Elsner, Angelov, Warnecke & Seidel-Morgenstern, 2006; Mesbah, Kramer, Huesman & Van den Hof, 2009

5.4.1. Model simplification techniques

This is a very popular technique since in many applications, such as dynamic optimization, the repeated evaluation of the right-hand side of the model described by Figure 2.12 is the main computational effort. Hence, by reducing the complexity of the functions to be evaluated, an

important reduction of the costs can be achieved. This is done by techniques such as linearization or by approximation of the functional expressions, for the differential equations of the model. For the algebraic equations, techniques such as simplification of chemical kinetics (Nafe & Maas, 2002; Bhattacharjee, Schwer, Barton & Green, 2003) or of physical properties models (Marquardt, 2001) are used as well.

5.4.2. Model order-reduction techniques

The simplification of the (algebraic) right-hand side of the model equations is not always enough to make the model computationally effective. For this reason, methods to reduce the number of equations in the PDAE system have been developed. Two groups of techniques are often used for the model-order reduction, depending on the type of the model:

a) Linear model order-reduction

These techniques are dedicated to linear models and are classified in two categories:

1) projection-based methods, including methods such as balanced realization-based methods (Antoulas, 2005), proper orthogonal decomposition (POD)-based methods (Wattamwar, Weiland & Backx, 2010), Krylov-subspace (Phillips, 1998) or momentum matching methods (Astolfi, 2007)

2) non-projection methods, such as the Hankel optimal model reduction method (Benner, Quintana-Orti, & Quintana-Orti, 2004), the singular perturbation methods (Cao & Schwartz, 2005) or various optimization-based methods (Sootla, Rantzer & Kotsalis, 2009)

More details on the methods in this category can be found in Chapter 3, Section 2.2.1 of this thesis.

b) Nonlinear model order-reduction

Most nonlinear model order-reduction methods are extensions of linear methods for model reduction (Brüls, Duysinx & Golinval, 2007). For example, some reduction techniques apply linear projection to the nonlinear model as if it were a linear model.

The simplest approach for generating reduced order models for nonlinear systems is based on linearization of systems nonlinearity and subsequent application of linear model-order reduction methods. The main drawback of this approach is that the obtained reduced model is valid only locally, around the initial operating point of the nonlinear system. However, these techniques do not work for cases when the models have a strongly nonlinear behaviour.

Since these approaches are not always successful, due to the high nonlinearity of the chemical and biochemical plant models, some particular methods have been developed, for example the use of neural networks (Padhi & Balakrishnan, 2002), or the use of hybrid models (Vega, Lima & Pinto, 2008; Romijn, Özkan, Weiland, Ludlage & Marquardt, 2008).

However, the main issue in working with nonlinear model-order reduction is that the reduced models obtained can be even more difficult to solve than the full models (Marquardt, 2001).

5.5. System level

The existent techniques are also summarised in Table 2.8, together with papers where each technique is used. The references in Table 2.8 are for exemplification purpose only.

a) Units

The lumping of different individual process units, presented in the previous section, is a technique used at system level as well.

b) Streams

Different streams can be lumped together into a single stream, as shown in (Bildea, Dimian & Iedema, 2000) or in (Altimari & Bildea, 2008) where the different recycle streams were coupled as one big recycle.

5.6. Numerical level

a) Discretization

The approximation of the set of partial differential equations (PDE's) defining the chemical process system, by a set of ordinary differential equations is often needed in order to reduce excessive demand for computation time required by the solution of the systems. The PDE's are solved numerically using two types of techniques (Motz, Mitrović & Gilles, 2002):

(1) While keeping the time derivatives, the space coordinates are discretized by methods such as finite difference, finite element, and orthogonal collocation, to obtain a set of ordinary differential equations (ODE's). Such schemes are referred to as the method of lines.

(2) Both space and time coordinates are discretized to obtain a set of nonlinear algebraic equations.

The reduced (discrete) system is obtained using different discretization approaches for which parameters such as time step, grid spacing, node distribution, etc. need to be adequately selected, taking into account the nature of the application and the physical system under consideration.

b) Functional approximation

These techniques are trying to transform the set of PDE's into a set of ODE's. The state variables are rewritten as a set of known support functions Ψ_i, which are chosen to satisfy as many conditions (symmetry, boundary) of the problem as it is feasible:

$$x = \sum_{i=1}^{n} a_i \cdot \Psi_i \tag{2.27}$$

For example, in the case of the orthogonal collocation the support functions are orthogonal polynomials (Finlayson, 1974). The variables a_i become the new unknowns of the system.

c) "Operator" approximation

These techniques are trying to approximate the operations in the equations in such way that they are easier to solve. For example, for the differentiation:

$$\frac{\partial x}{\partial z} = \frac{x(z_{k+1}) - x(z_k)}{z_{k+1} - z_k} \tag{2.28}$$

In a similar way, the approximation of the integration operator is also possible.

6. Model reduction for chemical engineering applications

As seen in the previous sections, the state-of-the-art of the model reduction approaches involves a host of diverse methods and techniques that act on both the conceptual, structural level of the process models, as well as on the numerical level.

Traditionally, the procedure is to apply order-reduction to a model in its entirety (Marquardt, 2001), without preserving the underlying network structure of the process or its-multi scale decomposition.

Although in many cases significant reduction of the number of equations is achieved, the benefit is often limited, because the internal structure of the problem is destroyed, the physical meaning of the variables is lost and there is little or no decrease in the solution time (Van den Bergh, 2005). Attention must be paid on the internal structure of the problem, as well as on retaining the physical meaning of the variables (Wattanwar, 2010).

For this reason a *structure-retaining model reduction approach* has been developed. The approach aims first at simplifying the physical (units, domains, phases, etc.) and the systemic (connectivity) level of the chemical process model, as well as the behavioural (phenomena) structure, with the help of the options summarised in Table 2.8. Only then additional mathematical (number of equations) and numerical scheme reductions are selectively applied to individual compartments or units, using the options presented in Table 2.9. In the following step, the reduced models of the individual units are connected at system level and the reduced model of the full process is obtained. In this way, the reduction procedure is able to preserve the essential structural features of the process. Moreover, the physical meaning of the variables and equations can be preserved as much as possible.

This signifies that the model M_1 is firstly decomposed on the Structure axis in the sub-models M_2 to M_4, as shown in Figure 2.14. The model M_1 is either a rigorous model of the process system of be studied, or a conceptual version of it, for the cases when the rigorous model cannot be obtained. In the following step, each individual sub-model is reduced at behavioural level. At this point, the phenomena that take place inside the system defined by the model, which are relevant for the

application considered, are preserved. Thirdly, the resulting models are further reduced at mathematical level by applying model-order reduction techniques, if still required. As a result, the reduced sub-models $M_2^{'}$ to $M_4^{'}$ will be obtained. Finally, these reduced models are connected to obtain the reduced model $M_1^{'}$ of the initial process defined by the conceptual model M_1.

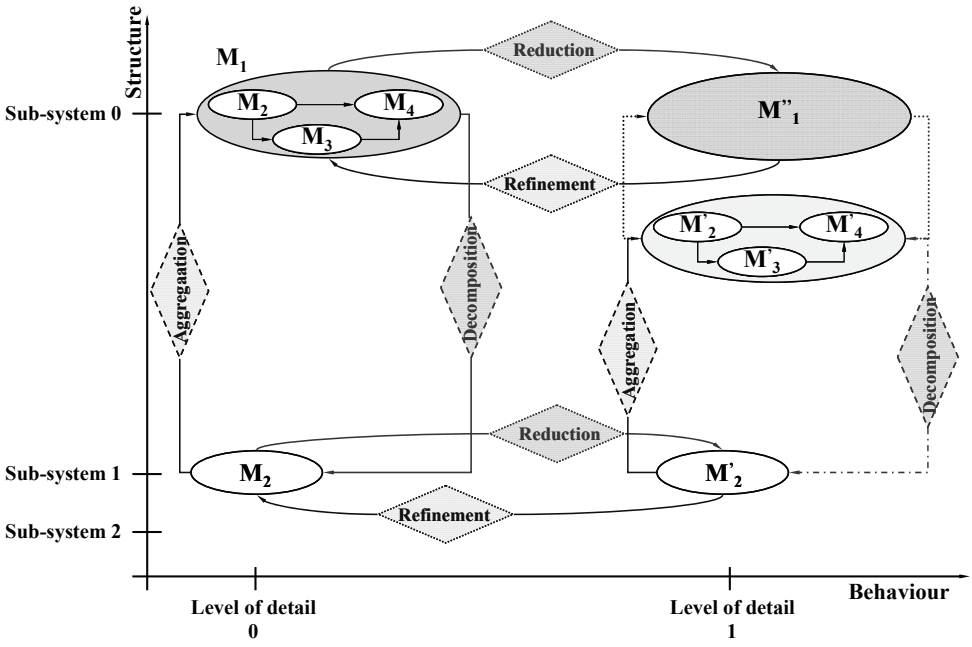

Figure 2.14. Approaches to model reduction of process models
0 = reference level; 1 = refined level

The following criteria are defined and used in this thesis for assessing the success of the reduction approach:

(1) The reduced model $M_1^{'}$ retains a satisfactory predictive accuracy

(2) the reduced model $M_1^{'}$ is solved successfully in an acceptable amount of time

(3) the reduced model $M_1^{'}$ is used successfully for practical applications

7. Selected research problems in model reduction

The proposed structure-retaining model reduction approach covers a host of decisions, involving mainly discrete elements: which attributes, connectivities, terms to reduce or to simplify. This makes it very hard to develop a *synthesis theory for process model reduction* with associated tools to manipulate the discrete model objects, like with mixed integer nonlinear programming

(MINLP), as for instance in process synthesis. To test the practical feasibility of this approach in an explorative manner, case studies have been performed from which lessons will be learned.

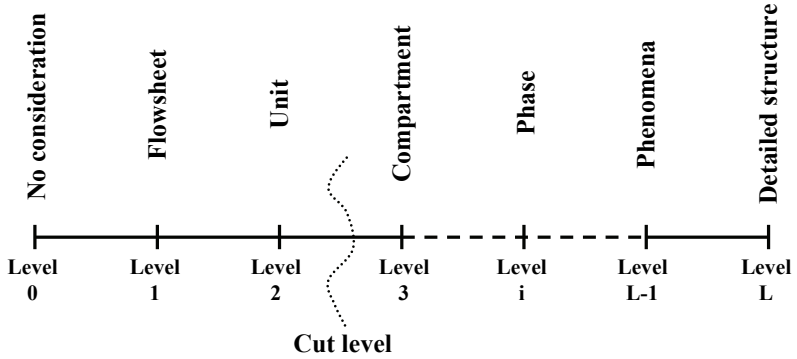

Figure 2.15. Line of exploration for the model structure

Within this set-up of doing case studies, there are generic issues for each process. A first decision that needs to be taken while performing the model reduction is how far one should go in decomposing the model structure. An intuitive answer is that the choice for the cut level (Figure 2.15) is most likely application goal dependent. Scales below the cut level are ignored in the reduced model.

For processes with relatively simple internal structure of the products (for example single-phase), the cut level should go at least to the unit level. In case of processes with a more complex internal structure of the products, the cut level must be taken at a lower level (phase, species, molecular level, etc.). This lower level is required by the presence of the detailed scales inside the product.

The cut-off criteria for details, size and time between the different attributes should be done in a consistent way. On how to perform this, a generic answer is difficult to give at this stage. For this reason, a case study approach will be used in the following chapters to study the application of the model reduction procedure presented in Section 6.

The selected case studies are not the outcome of a carefully crafted *design of experiments* to test and evaluate the model reduction approach in the most effective way. The cases are practically chosen to match the funding conditions for the thesis project. Nevertheless, the cases represent very interesting and relevant extremes of the spectrum of chemical processes. Two types of applications will be studied for this assessment:

(1) complex (multiple unit) processes with relatively simple (one-phase, similar components) products

(2) simple (single unit) processes with complex (multiphase, multi-component) products

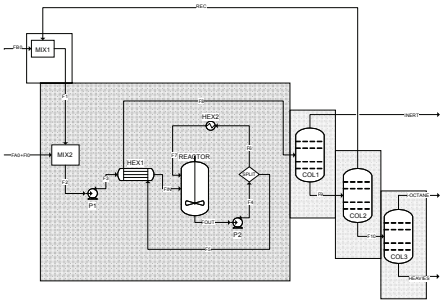

Figure 2.16. The iso-butane alkylation plant

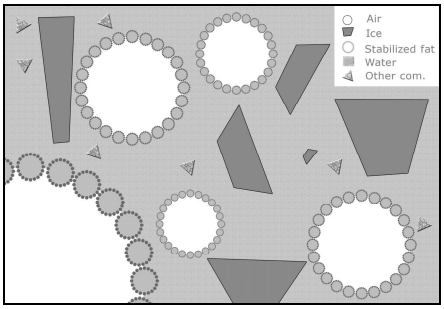

Figure 2.17. Ice cream structure

For the first type of process, the *iso*-butane alkylation process will be studied. The details of the process are presented in Section 3 of this chapter. The process flowsheet (Figure 2.16) consists of some of the most common process units: chemical reactors, distillation columns, heat exchangers, mixers, pumps, etc. Another source of complexity is the presence of a recycle of raw materials, which have to be reused in the process.

Two types of generic inverse applications are considered for the use of the process model: (a) *the assessment of the plantwide control structures*, and (b) *the dynamic optimization of the plant's operation*.

For the second type of process, the freezing step in ice cream manufacture is selected. The complexity lays in this case not in number of units in the process flowsheet, but in the number of phases of the product (Figure 2.17), the distributive nature of its product structure as well as the many interactive phenomena that need to be taken into account.

8. Conclusions

Current numerical reduction approaches focus on the (process) model in its entirety, without trying to preserve the underlying network structure of the process or its multi-scale decomposition. Retaining the meaningful structural features in a reduced model of a process is a necessity for long-term practical use of the model, certainly in a practical manufacturing environment where adaptations in process unit models will occur regulary.

In this chapter, the most important features of the chemical process model structure have been identified and the opportunities for performing model reduction have been described. A structure-retaining model reduction has been presented. The approach aims first at simplifying the physical (units, domains, phases, etc.) and the systemic (connectivity) level of the chemical process model, as well as the behavioural (phenomena) structure. Only then additional mathematical (number of equations) and numerical scheme reductions are selectively applied to individual compartments or units. In the following aggregation step, the reduced models of the individual units are connected at system level and the reduced model of the full process is obtained. In this way, the reduction

procedure maintains the essential structural features of the process and the physical meaning of the variables is preserved as much as possible.

The reduction must be performed in such way that the resulting model retains the predictive accuracy of the original up to a satisfactory level. Moreover, the reduced model should be solved sufficiently fast for practical applications.

The applicability and the effectiveness of the structure-retaining model reduction will be studied in the following chapters by means of case studies. This approach allows for an easy identification of the characteristics of applying the reduction procedure for specific cases, which can be further extrapolated to generic applications.

9. References

Albright, L.F., Spalding, M.A., Faunce, J., & Eckert, R.E. (1988). Alkylation of isobutene with C_4 olefins. 3. Two-step process using sulphuric acid as catalyst, *Industrial and Engineering Chemistry Research* 27, 391

Albright, L.F. (2002). Alkylation of isobutene with C_3-C_5 olefins: Feedstock consumption, acid usage, and alkylate quality for different processes, *Industrial and Engineering Chemistry Research* 41, 5627

Albright, L.F. & Wood, K.V. (1997). Alkylation of isobutene with C_3-C_4 olefins: identification and chemistry of heavy-end production, *Industrial and Engineering Chemistry Research* 36, 2110

Altimari, P., & Bildea, C.S. (2008). Coupling exothermic and endothermic reactions in plug-flow reactor – separation – recycle systems, *Industrial and Engineering Chemistry Research* 47, 6685

Altimari, P. & Bildea, C.S. (2009). Integrated design and control of plantwide control Systems coupling exothermic and endothermic reactions, *Computers and Chemical Engineering* 33, 911

Antelo, L.T., Banga, J.R., & Alonso, A.A. (2008). Hierarchical design of decentralized control structures for the Tennessee Eastman Process, *Computers and Chemical Engineering* 32, 1995

Antoulas, A.C. (2005). An overview of approximation methods for large-scale dynamical systems, *Annual Reviews in Control* 29, 181

Asprey, S.P., Macchietto, S. (2002). Designing robust optimal dynamic experiments, *Journal of Process Control* 12, 545

Astolfi, A. (2007). A new look at model reduction by moment matching for linear systems, *Proceedings of the 46th IEEE Conference on Decision and Control*, 4361

Baur, R., Higler, A.P., Taylor, R., & Krishna, R. (2000). Comparison of equilibrium stage and nonequilibrium stage models for reactive distillation, *Chemical Engineering Journal* 76, 33

Benner, P., Quintana-Orti, E.S., & Quintana-Orti, G. (2004). Computing optimal Hankel norm approximations of large-scale systems, *Proceedings of the IEEE Conference on Decision and Control* 3, 3078

Bequette, B.W. (1998). Process dynamics: modelling, analysis and simulation, *Prentice Hall*, 5

Bhattacharjee, B., Schwer, D.A., Barton, P.I., & Green, Jr., W.H.G. (2003). Optimally- reduced kinetic models: reaction elimination in large-scale kinetic mechanisms, *Combustion and Flame*, 135, 191

Bildea, C.S., Dimian, A.C., & Iedema , P.D. (2000). Nonlinear behaviour of reactor-separator-recycle Systems, *Computers and Chemical Engineering* 24, 209

Bildea, C.S., Dimian, A.C., & Iedema, P.D. (2001). Multiplicity and stability approach to the design of heat-integrated multibed plug flow reactor, *Computers and Chemical Engineering* 25, 41

Bongers, P.M.M., Almeida-Rivera, C. (2009). Product driven process synthesis methodology, *Computer-Aided Chemical Engineering* 26, 231

Brüls, O., Duysinx, P., & Golinval, J.P. (2007). The global model parameterization for non-linear model-order reduction in flexible multibody dynamics, *International Journal for Numerical Methods in Engineering* 69, 948

Burke, A.L., Duever, T.A., Penlidis, A. (1997). Choosing the right model: Case studies on the use of statistical model discrimination experiments, *The Canadian Journal of Chemical Engineering* 75, 422

Cameron, I.T., Wang, F.Y., Immanuel, C.D., Stepanek, F. (2005) Process systems modelling and applications in granulation: A review, *Chemical Engineering Science* 60, 3723

Cao, L. & Schwartz, H.M. (2005). Reduced-order models for feedback stabilization of linear systems with a singular perturbation model, *Asian Journal of Control* 7, 326

Caton, J., Racen, B., Troutman, G. (2008). Introduction to sulphuric acid alkylation unit process design,*http://www2.dupont.com/Clean_Technologies/en_US/assets/downloads/Intro%20to%20H2 S04%20Unit%20Design.pdf*

Charpentier, J.C. & McKenna, T.F. (2004). Managing complex systems: Some trends for the future of chemical and process engineering, *Chemical Engineering Science* 59, 1617

Christofides, P.D., Daoutidis, P. (1998). Robust control of hyperbolic PDE systems, *Chemical Engineering Science* 53, 85

O'Connell, J.P., Haille, J.M. (2005). Thermodynamics: fundamentals and applications, *Cambridge University Press,* 72

Dalaouti, N. & Seferlis, P. (2006). A unified modelling framework for the optimal design and dynamic simulation of staged reactive separation processes, *Computers and Chemical Engineering* 30, 1264

Dimian, C.A. & Bildea, C.S. (2008). Chemical Process Design. Computer-aided cases studies, *Wiley-VCH*, 261

Dones, I. & Preisig, H.A. (2010). Model simplification and time-scale assumptions applied to distillation modelling, *Computers and Chemical Engineering* 34, 732

Douglas, J.M. (1988). Conceptual design of chemical processes, *McGraw-Hill*

Finlayson, B. A. (1974). Orthogonal collocation in chemical reaction engineering, *Catalysis Review* 10, 69

Gerstlauer, A., Mitrović, A., Motz, S., & Gilles, E.D. (2001). A population model for crystallization processes using two independent particle properties, *Chemical Engineering Science* 56, 2553

Gopal, V., & Biegler, L.T. (1998). A successive linear programming approach for initialization and reinitialization after discontinuities of differential-algebraic equations, *SIAM Journal on Scientific Computing* 20, 447

Hangos, K., Cameron, I. (2001). Process modelling and model analysis, *Academic Press*, 51

Hangos, K., Cameron, I. (2001). A formal representation of assumptions in process modelling, *Computers and Chemical Engineering* 25, 237

Hedengren, J.D. & Edgar, T.F. (2005). Order reduction of large-scale DAE models, *Computers and Chemical Engineering* 29, 2069

Henda, R. & Falcioni, D.J. (2006). Modelling of heat transfer in a moving packed bed: Case of the preheater in nickel carbonyl process, *Journal of Applied Mechanics* 73, 47

Hjalmarsson, H. (2005). From experiment design to closed-loop control, *Automatica* 41, 393

Hommeltoft, S.I. (2001). Isobutane alkylation. Recent developments and perspectives, *Applied Catalysis A: General* 221, 421

Housiadas, K.D., Lidis, G., Tsamopoulos, J. (2007). Two- and three-dimensional instabilities in the film blowing process, *Journal of Non-Newtonian Fluid Mechanics* 141, 193

Kasiri, N. & Bashiri, A. (2010). Comparative study of different techniques for numerical reservoir simulation, *Petroleum Science and Technology* 28, 494

Kiss, A.A., Bildea, C.S., Dimian, A.C. (2005). Design of recycle systems with parallel and consecutive reactions by nonlinear analysis, *Industrial and Engineering Chemistry Research* 44, 576

Klatt, K.U. & Marquardt, W. (2009). Perspectives for process systems engineering – Personal views from academia and industry, *Computers and Chemical Engineering* 33, 536

Lakner, R., Hangos, K.M., Cameron, I.T. (2005). On minimal models of process systems, *Chemical Engineering Science* 60, 1127

Lee, L. & Harriott, P. (1977). The kinetics of isobutene alkylation in sulphuric acid, *Industrial and Engineering Chemistry Process Design and Development* 16, 282

Leitold, A., Hangos, K.M. (2001). Structural solvability analysis of dynamic process models, *Computers and Chemical Engineering* 25, 1633

Marquardt, W. (1996). Trends in computer-aided process modelling, *Computers and Chemical Engineering*, 20, 591

Marquardt, W. (2001). Nonlinear model reduction for optimization based control of transient chemical processes, *Proceedings of the 6th international Conference of Chemical Process Control, AIChe Symp. Ser. 326*, Vol. 98, 12

Mercenier, J. & Michel, P. (1994). A criterion fro time aggregation in intertemporal dynamic models, *Mathematical Programming* 64, 179

Mesbah, A., Kramer, H.J.M., Huesman, A.E.M., Van den Hof, P.M.J. (2009). A control oriented study on the numerical solution of the population balance equation for crystallization processes, *Chemical Engineering Science* 64, 4262

Motz, S., Mitrović, A., & Gilles, E.D. (2002). Comparison of numerical methods for the simulation of dispersed phase systems, *Chemical Engineering Science* 57, 4329

Nafe, J., & Maas, U. (2002). A general algorithm for improving ILDMs, *Combustion Theory and Modelling*, 6, 697

Okino, M.S., Mavrovouniotis, M.L. (1998). Simplification of mathematical models of chemical reaction systems, *Chemical Reviews* 98, 391

Padhi, R. Balakrishnan, S.N. (2002). Proper orthogonal decomposition based feedback optimal control synthesis of distributed parameter systems using neural networks, *Proceedings of the American Control Conference* 6, 4389

Phillips, J.R. (1998). Model reduction of time-varying linear systems using approximate multipoint Krylov-subspace projectors, *IEEE/ACM International Conference on Computer-Aided Design, Digest of Technical Papers*, 96

Prasad, V., & Wayne Bequette, B. (2003). Nonlinear system identification and model reduction using artificial neural networks, *Computers and Chemical Engineering*, 27, 1741

Qamar, S., Elsner, M.P., Angelov, I.A., Warnecke, G., Seidel-Morgenstern, A. (2006). A comparative study of high-resolution schemes for solving population balances in crystallization, *Computer and Chemical Engineering* 30, 1119

Ranzi, E., Dente, M., Goldaniga, A., Bozzano, G., & Faravelli., T. (2001). Lumping procedures in detailed kinetic modelling of gasification, pyrolysis, partial oxidation and combustion of hydrocarbon mixtures, *Progress in Energy and Combustion Science*, 27, 99

Rascol, E., Meyer, M., Le Lann, J.M., & Prevost, M. (1998). Numerical problems encountered in the simulation of reactive absorption: DAE index reduction and consistent initialisation, *Computers and Chemical Engineering* 22, S929

Romijn, R, Özkan, L., Weiland, S., Ludlage, J. & Marquardt, W. (2008). A grey-box modelling approach for the reduction of nonlinear systems, *Journal of Process Control* 18, 906

Sandberg, H. & Rantzer, A. (2004). Balanced truncation of linear time-varying systems, *IEEE Transactions on Automatic Control*, 49, 217

Scherpen, J.M.A. (1994). Balancing for nonlinear systems, *PhD Thesis*, University of Twente, Enschede, The Netherlands

Schrefler, B.A. (2004). Multiphase flow in deforming porous material, *International Journal for Numerical Methods in Engineering* 60, 27

Seferlis, P. & Grievink, J. (2001). Optimal design and sensitivity analysis *of reactive distillation units using collocation models, Industrial* and Engineering Chemistry Research 40, 1673

Soetjahjo, A.T.M.J. (2006). Mathematical analysis of dynamic process models – Index, inputs and interconnectivity, *PhD Thesis*, Delft University of Technology, The Netherlands

Sootla, A., Rantzer, A., & Kotsalis, G. (2009). Multivariable optimization-based model reduction, *IEEE Transactions on Automatic Control* 54, 2477

Stewart, W.E., Henson, T.L., Box, G.E.P. (1996). Model discrimination and criticism with single-response data, *AIChE Journal* 42, 3055

Stewart, W.E., Shon, Y., Box, G.E.P. (1998). Discrimination of fit of multiresponse mechanistic models, *AIChE Journal* 44, 1404

Unger, J., Kröner, A., Marquardt, W. (1995). Structural analysis of differential-algebraic equation systems – Theory and applications, *Computers and Chemical Engineering* 19, 867

Van den Bergh, J. (2005). Model reduction for dynamic real-time optimization of chemical processes, *PhD thesis*, Delft University of Technology, The Netherlands

Vlachos, D.G. (2005). A review of multiscale analysis: Examples from systems biology, materials engineering and other fluid-surface interacting systems, *Advances in Chemical Engineering* 30, 1

Vega, M.P., Lima, E.L., & Pinto, J.C. (2008). Use of bifurcation analysis for development of nonlinear models for control applications, *Chemical Engineering Science* 63, 5129

Wattanwar, S.K. (2010). Identification of low-order models for large-scale processes, *PhD Thesis,* Eindhoven University of Technology, The Netherlands

Wattanwar, S.K., Weiland, S., Backx, T. (2010). Identification of low-order parameter-varying models for large-scale systems, *Journal of Process Control* 20, 158

Willard, S. (2004). General topology, *Dover Publications*, 28

Yang, A., Marquardt, W. (2009). An ontological conceptualization of multiscale models, *Computers and Chemical Engineering*, 33, 822

Ye, M., Meyer, P.D., Neuman, S.P. (2008). On model selection criteria in multimodel analysis, *Water Resources Research* 44

Yermakova, A. & Anikeev, V.I. (2005). Analysis of the CSTR with two-phase flow under phase equilibrium conditions, *Chemical Engineering Science* 60, 3199

3

APPLICATION OF MODEL REDUCTION TO DESIGN OF PLANTWIDE CONTROL SYSTEMS

The chapter proposes an approach for obtaining reduced-order models of chemical processes, with application to the design of plantwide control systems. The approach is based on the inherent structure that exists in a chemical plant and identifies units or groups of units that determine the steady state and dynamic behaviour of the plant. Specific reduction techniques with different accuracy are applied to each unit, followed by the coupling of the reduced models, according to the process flowsheet structure. By means of a case study, the *iso*-butane - butene alkylation plant, it is shown that the approach retains the nonlinearity of the original plant model and preserves the significance of important model variables. These features make the reduced model a valid option for the effective assessment of plantwide control structures.

1. Introduction

1.1. Model reduction for complex processes

The discussion in Chapters 1 and 2 of the thesis showed that, for the case of complex processes, the reduction procedures focus on the upper levels of the network structure of the process: process units, compartments, domains.

In this chapter, the focus will be on developing a reduced model for a complex process with a single-phase product, in order to highlight the characteristics of the model reduction approach when dealing with this type of processes. The influence of the product's internal structure is not important in this case, and will be neglected. The main attribute of such a model is the many network-like aspects of the process structure, which features units with a reduced number of distinct compartments and domains, like trays in distillation columns.

The reduction procedure is illustrated by means of a case study: the *iso*-butane alkylation plant. It will be demonstrated that an important decrease of the simulation time is obtained while the reduced model preserves the behaviour of the original model. Moreover, having reduced models of the units connected accordingly to process structure is a natural way of simplifying the adaptation to future plant changes.

1.2. Design of the plantwide control systems

In today's competitive environment, high economical performance of chemical and biochemical plants is achieved by cost-effective steady-state integrated design and by continuously responding to the market conditions through dynamic operation. The desired policy of operation is accomplished by control systems that maintain the steady state or implement the optimal dynamic behaviour (Engell, 2007).

The synthesis, design and optimization of the plantwide control system require dynamic models of the chemical / biochemical plant. Often, the models are very complex, and therefore call for high computational speed and high memory storage capacity. Moreover, the problems are likely to be ill conditioned, since the applications involve solving an inverse problem. This often results in significant numerical troubles, unstable convergence and eventually, unreliable results.

Because of numerical and time constraints, it is not always possible to consider models of the highest complexity. The model must be adapted to the specific purpose (Baldea, Daoutidis & Kumar, 2006) although in many cases it is not evident which simplifications are suitable. Therefore, for particular simulations, it is necessary to find an appropriate technique to reduce these effects. To achieve these objectives, the model quality is crucial. The model should predict with good accuracy the behaviour of the real system it describes. Moreover, some process models that are developed from experimental observations are far from being highly accurate. For this reason, it is important for the reduced model to take into account this uncertainty (Nagy and Braatz, 2003, 2007). In the same time,

the problems that need to be solved often imply repeated solution of the process model. Thus, it is important that the complexity of the model be limited, in order to allow solution during a restricted time. Another requirement for the process models is the low cost of maintenance, which implies that the effort to adapt the model to future plant changes must be kept as small as possible. Additionally, in many applications of the chemical industry, the process is highly nonlinear and it is important that this characteristic be preserved (Nagy, Mahn, Franke & Allgöwer, 2007).

Model reduction is one technique that can be used for obtaining such a model (Marquardt, 2001; Antoulas, Sorensen & Gugercin, 2000). In this chapter, a new approach to model reduction, with applicability to the dynamic models of chemical processes and plantwide control, is presented. This approach makes use of the inherent flowsheet structure that exists in a chemical plant in the form of units or groups of units that are connected by material streams. The decomposition mirrors the decentralization of the control problem. The recommended procedure exploits the knowledge about the process and applies the model reduction techniques to individual units of the plant, and then couples these reduced models.

The chapter is structured in the following way: Section 2 explores existing model reduction techniques and the application of model reduction to chemical plants. Next, the proposed approach to model reduction is introduced in Section 3. The algorithm is applied to the *iso*-butane alkylation plant in Section 4. Finally, conclusions are presented in Section 5.

2. Model reduction

The models of dynamical systems contain a large number of equations, both differential and algebraic, and, quite often, these equations contain complex functional expressions. Such models can be written in the following, general form:

$$\begin{aligned} \frac{dx}{dt} &= f\left(x(t), u(t), \alpha\right) \\ y(t) &= g\left(x(t), u(t), \alpha\right) \end{aligned} \tag{3.1}$$

Here t is the time variable, $x(t) \in \mathbb{R}^n$ is the state vector, $u(t) \in \mathbb{R}^m$ is the input vector, $y(t) \in \mathbb{R}^p$ the output variable vector, α is the parameters vector, and n is the state space dimension. The dimension of the input vector, m and the dimension of the output variable vector p, are much smaller than n, and usually $m \geq p$. The function f describes the dynamics of the system, while the function g describes the way in which the observations are deduced from the state and the input.

To this set, new algebraic equations are added to the dynamic model to describe the physical and thermodynamic relations:

$$0 = h\left(x(t), u(t), \alpha\right) \tag{3.2}$$

Model reduction has a long history in the systems and control literature. The main idea of this technique is to reduce the complexity of the dynamic model, while preserving its input-output behaviour. The review on model reduction techniques in Marquardt (2001) is recommended. One can find several ways of classifying the model reduction methods, but probably the best way is the one presented in the above-cited paper:

- *Model simplification* – a technique that preserves the number of equations of the original model, but reduces the complexity of the functional expressions in the model equations
- *Model-order reduction* – a technique that replaces the original large-scale model with a model having (much) less equations

2.1. Model simplification

The *model simplification* techniques are very popular in the area of chemical engineering. In many applications (for example in dynamic optimization), the repeated evaluation of the right-hand side of the model described by equation (3.1) is often the main computational effort. Hence, by reducing the complexity of the functions to be evaluated, the model simplification methods are as important as the ones that reduce the number of equations.

Among these techniques, one can distinguish the linearization around a nominal operating point, the approximation of functional expressions and the simplification of chemical kinetics (Nafe and Maas, 2002) and/or physical properties models. In addition, significant model reduction is also possible by model lumping (Ranzi, Dente, Goldainga, Bozzano & Faravelli, 2001), in which thermodynamic phases and chemical components are taken together into pseudo-phases and lumped species. However, such lumping can increase the complexity of the functional expressions in the remaining model equations.

2.1.1. Linearization

The linearization around a nominal operating point is one of the most often used methods to simplify nonlinear models. The main idea of this procedure is to rewrite the system presented in equation (3.1) under the following form:

$$\begin{aligned} \frac{d\tilde{x}(t)}{dt} &= A\cdot\tilde{x}(t) + B\cdot\tilde{u}(t) \\ \tilde{y}(t) &= C\cdot\tilde{x}(t) + D\cdot\tilde{u}(t) \end{aligned} \tag{3.3}$$

where $$\tilde{x}(t) = x(t) - x_{nom}(t) \tag{3.4}$$

$$\tilde{u}(t) = u(t) - u_{nom}(t) \tag{3.5}$$

$$\tilde{y}(t) = y(t) - y_{nom}(t) \tag{3.6}$$

In the previous equations A, B, C and D are the system matrices, with $A \in \mathbb{R}^{n \times n}$, $B \in \mathbb{R}^{n \times m}$, $C \in \mathbb{R}^{p \times n}$ and $D \in \mathbb{R}^{p \times m}$, while the subscript nom represents the nominal operating point.

One way of realizing the transformation is by using the Taylor series expansion.

The linearization reduces drastically the computational effort. The simulation is more reliable since the nonlinear system it is replaced by a linear system, easier to solve. However, the linear models do not adequately predict the process dynamics for the cases when the system is far away from the nominal operating point.

2.1.2. Approximation of functional expressions

This technique implies the replacement of a complicated, nonlinear model equation by simpler functional expressions. This simple functional expression has to approximate the original up to a user specified tolerance, which leads to a multi-variate nonlinear approximation problem.

2.1.3. Simplification of physical properties model

The most common method of simplifying the physical properties models is the development of local thermodynamic models. The use of local thermodynamics reduces significantly the computational effort, while maintaining the accuracy at an acceptable level.

The easiest way of reducing the complexity is to re-write the functional expression of a property in a polynomial form.

2.1.4. Simplification of chemical kinetics

In many applications, large-scale chemical kinetic models are quite common. The complexity arises from the large number of reactions and components, and it can be reduced both by eliminating from the reaction network: *a) reactions* (Bhattacharjee, Schwer, Barton & Green, 2003), which is a task of the model simplification, and *b) species*, which is a special case of model-order reduction. The use of moments in population balance models, for eliminating the distributed nature of the population balance, is an example of this technique.

2.2. Model-order reduction

Reducing the complexity of the functional expressions in the model equations is not always enough to achieve the model reduction. In many cases, the number of the model equations needs to be reduced also. In the *model-order reduction* class, two main groups of methods can be distinguished: *linear* and *nonlinear* model-order reduction, depending on the type of the full model.

2.2.1. Linear model-order reduction

The largest group of order-reduction methods applies to the linear systems. The problem can be stated in the following form:

Given the linear dynamical system (3.3)*, one should find an approximation*

$$\begin{aligned} \frac{d\hat{x}(t)}{dt} &= \hat{A}\cdot\hat{x}(t) + \hat{B}\cdot\tilde{u}(t) \\ \tilde{y}(t) &= \hat{C}\cdot\hat{x}(t) + \hat{D}\cdot\tilde{u}(t) \end{aligned} \tag{3.7}$$

with $\hat{A}\in\mathbb{R}^{k\times k}$, $\hat{B}\in\mathbb{R}^{k\times m}$, $\hat{C}\in\mathbb{R}^{p\times k}$, $\hat{D}\in\mathbb{R}^{p\times m}$ *and* $k \ll n$ *such that the following properties are satisfied (Antoulas, 2000):*

- The approximation error is small, and a global error bound can be defined.
- System properties, like stability, are preserved.
- The procedure is computationally stable and efficient.

The approach has many advantages. First, the linear models are easy to be obtained, for example through Taylor series expansion, as mentioned in the previous section. In the same time, there is a considerable large range of "treatment" techniques for linear models, which spreads from the backward Euler method to multistep methods of solving the ordinary differential equations (ODE's) that describe the system. In addition, finally yet importantly, stable and well-understood numerical linear algebra algorithms allow the analysis, control or simulation of such a system.

Many methods of obtaining the approximation presented in equations (3.7) have been developed in different fields, including control, fluid dynamics, and chemical engineering. They can be classified into two categories: *(a) projection-based methods* and *(b) non-projection based methods*.

(a) The common feature of the projection-based methods is that they are trying to find such k and $n-k$ dimensional subspaces S_1 and S_2 of the state space, S that the reduced system will result from the projection of the state onto S_1 and the residual onto S_2, and the elimination of the states in S_2. In this category, one can mention techniques such as Krylov-subspace or momentum matching methods, balanced realization-based methods or proper orthogonal decomposition (POD)-based methods (Skogestad & Postlethwaite, 1996; Antoulas & Sorensen, 2001; Rathinam & Petzold, 2003; Penzl, 2006).

(b) In the non-projection methods, the state-space of the approximation has no connection with the unreduced system. The most used techniques in this category are the Hankel optimal

model reduction method, the singular perturbation method or various optimization-based methods (Mäkilä, 1991; Marquardt, 2001).

Each of the methods above has advantages and drawbacks. For example, the Krylov subspace-based methods can be applied for a very high-order system, but have robustness, stability and efficiency issues (Bai, 2002). In the case of the Hankel-norm approximation and balanced realization methods, very low-rank approximations are possible and accurate low-order models will result, but the solution require dense computations and can be carried out only for low-dimension (few hundreds equations) models (Antoulas & Sorensen, 2001). In the same time, the accuracy of the result is guaranteed by theoretical results and can be calculated a priori (Skogestad & Postlethwaite, 1996). The POD-based methods are not system invariant, the resulting simplification being heavily dependent on the initial excitation, but can be applied for high-complexity systems (Antoulas & Sorensen, 2001).

2.2.2. Nonlinear model-order reduction

Since the real world applications require the use of nonlinear models, ways to reduce the complexity of such models had to be developed as well. Some of them apply linear projections to the nonlinear model as if it were a linear model (Scherpen, 1994).

Since these approaches are not always successful, due to the high nonlinearity of the chemical and biochemical plant models, some particular methods have been developed, for example the use of neural networks (Prasad & Bequette, 2003), or the use of hybrid models (Nagy, Mahn, Franke & Allgöwer, 2007). However, the main issue in working with nonlinear model-order reduction is that the reduced models obtained can be even more difficult to solve than the full models (Marquardt, 2001).

2.3. Linear model-order reduction by balanced realization

The linear model-order reduction methods are easy to apply and the accuracy of the obtained reduced models is guaranteed by theoretical results. The linear model is easy to obtain, sometimes only by means of Taylor series expansion. In the same time, the model is easy to solve and analyze, by means of stable, well-understood numerical linear algebra algorithms.

In the following, methods for obtaining reduced-order models by balanced realization will be presented. In this approach, a new state-space description is obtained in such a way that the controllability and observability gramians are equal and diagonal. The balanced realization can be easily obtained by simple state similarity transformations, and routines for doing this are available in commercial software, such as MATLAB®.

The most important property of a balanced realization is that after the balancing, each state is as controllable as it is observable, and the measure of state's observability and controllability is given by its associated Hankel singular value (Skogestad & Postlethwaite, 1996). This property becomes

interesting for the model reduction techniques, which remove the states with little effect on the system's input-output behaviour.

Considering the balanced linear model, which can be described by equations (3.3), the state space vector $\tilde{x}$ is partitioned into $\begin{bmatrix} \tilde{x}_1 \\ \tilde{x}_2 \end{bmatrix}$, where $\tilde{x}_2$ is the vector of the states to be removed. After partitioning the matrices A, B and C, equation (3.3) is rewritten as follows:

$$\begin{aligned} \frac{d\tilde{x}_1(t)}{dt} &= A_{11}\cdot\tilde{x}_1(t) + A_{12}\cdot\tilde{x}_2(t) + B_1\cdot\tilde{u}(t) \\ \frac{d\tilde{x}_2(t)}{dt} &= A_{21}\cdot\tilde{x}_1(t) + A_{22}\cdot\tilde{x}_2(t) + B_2\cdot\tilde{u}(t) \\ \tilde{y}(t) &= C_1\cdot\tilde{x}_1(t) + C_2\cdot\tilde{x}_2(t) + D\cdot\tilde{u}(t) \end{aligned} \tag{3.8}$$

Two main approaches to reduce the order of the model by balanced realization can be mentioned in this case:

(a) Balanced truncation – removes all the states corresponding to the small Hankel singular values. By eliminating the states with little effect on the system's input-output behaviour ($\tilde{x}_2$), equations (3.8) become equations (3.7), with $\hat{x}(t) \equiv \tilde{x}_1(t)$, $\hat{A} \equiv A_{11}$, $\hat{B} \equiv B_1$, $\hat{C} \equiv C_1$ and $\hat{D} \equiv D$. An important property of the truncation is that it retains the system behaviour at high frequency.

(b) Balanced residualization – sets to zero the derivatives of the states with little effect on the system's input-output behaviour. An important property of the residualization is that it preserves the steady-state gain of the system. In this case, the matrices in equation (3.7) are calculated as follows:

$$\begin{aligned} \hat{A} &\equiv A_{11} - A_{12}\cdot A_{22}^{-1}\cdot A_{21} \\ \hat{B} &\equiv B_1 - A_{12}\cdot A_{22}^{-1}\cdot B_2 \\ \hat{C} &\equiv C_1 - C_2\cdot A_{22}^{-1}\cdot A_{21} \\ \hat{D} &\equiv D - C_2\cdot A_{22}^{-1}\cdot B_2 \end{aligned} \tag{3.9}$$

It must be mentioned that an important advantage of using the balanced realization techniques for obtaining the reduced models is that the error can be calculated a-priori. The infinite norm of the

error between the original model and the reduced-order model is twice the sum of the Hankel singular values of the eliminated states (Skogestad & Postlethwaite, 1996).

3. Model reduction with process knowledge

As seen in the previous section, many reduction techniques have been developed, in order to obtain models that:

- predict the behaviour of the plant with good accuracy
- have limited complexity, to allow repeated solution during a restricted time

Although significant reduction of the number of equations can be achieved, the benefit is often limited, because the structure of the problem is destroyed, the physical meaning of the model variables is lost and there is little or no decrease in the solution time (Van den Bergh, 2005). Moreover, especially in the case of nonlinear model-order reduction, the obtained reduced model is often difficult to solve.

Another desired quality of the reduced model is the adaptability to future plant changes. If in an industrial application, one of the units in the plant flowsheet is replaced, a new reduced model of the plant has to be obtained.

3.1. Classical model reduction algorithm for chemical plants

In the following sections, the focus will be on obtaining reduced-order models that can be used to determine the plantwide control structure of the plant. The main steps of a classical approach to model reduction will be presented, together with the most common issues that appear when applying the procedure.

3.1.1. Obtaining the rigorous model

The starting point of the approach is a rigorous dynamic model of the plant. This dynamic model is obtained using a commercial package, such as Aspen Dynamics® or gPROMS®.

Usually, a basic control of inventory at unit level is included. In the same time, depending on the package that is used, some model reduction is already present, such as the use of flow-driven simulation instead of the rigorous pressure-driven mode, the local thermodynamic models, the simplified chemical kinetics or the instantaneous models for mixers, pumps, valves or heat exchangers. Very often, the user is able to insert own equations and data to describe parts of the plant.

Under these conditions, the plant model still contains thousands of differential and algebraic equations, with initial conditions derived from a nominal steady-state operating point. The size of the model can lead to numerical difficulties when trying to find a solution. When this happens, the search for the cause of the difficulties and for a remedy is a time-demanding task. Finding a solution of the dynamic model implies solving numerically a system of differential and algebraic equations (DAE's).

The numerical algorithms often require an initial guess for the algebraic variables. Depending on the problem, finding the best starting point for the algorithms can also be a challenging task.

3.1.2. Obtaining the linear model

The linear model in state-space formulation is obtained easily with the help of the dynamic simulators discussed above. Determining the stability of the model is also an easy task. All it takes is to calculate the eigenvalues of the system matrix, obtained after the linearization. However, for unstable systems, the origin of the instability is often very difficult to identify.

It has to be stressed that many chemical and biochemical plants have a strongly nonlinear behaviour. Some of the most common features are the high parametric sensitivity and the state multiplicity. These effects are enhanced by coupling the units through heat integration or material recycles. For this reason, the linear models are reliable near the linearization point, but their accuracy is poor for large disturbances.

3.1.3. Obtaining the balanced state space model

The balanced realization methods for model reduction are now a well-developed and relatively simple group of techniques.

For linear systems, the approach requires only matrix computation. In the same time, the error bounds between the original and the reduced model can be easily and a-priori calculated with the help of the induced Hankel norm (Skogestad & Postlethwaite, 1996).

For stable systems, the balancing of the state space is straightforward. If the system is unstable, the stable part is isolated, balanced, and added back to the unstable part of the model.

For very large models, the algorithm often fails due to the ill conditioning of the Lyapunov equation solved while calculating the gramians (Mullhaupt & Riedel, 2004).

3.1.4. Obtaining the reduced-order model

In the next step, the reduced-order model is obtained from the balanced space model. Reduction of the system is achieved by retaining only certain states in the representation. This operation is equivalent to defining a certain subspace within the state space. Small Hankel singular values in the balanced realization indicate state variables with little contribution to the input-output behaviour.

The reduced-order model is obtained by equating to zero these variables (truncation) or their time-derivatives (residualization). Truncation is more accurate in representing the initial part of the dynamic response, but residualization preserves the steady-state gain. If the dynamics of the systems is high-order, no significant reduction can be achieved.

3.1.5. Plantwide control structures

The term plantwide control refers to all the structural and strategic decisions that have to be taken in order to accomplish a desired policy of operation. Two approaches are often used for the assessment of the plantwide control structures (Skogestad & Larsson, 1998):

(a) Several alternatives for the plantwide control structure are evaluated, for a given design of the plant. The main disadvantage of this approach is the large number of alternatives to be generated and assessed. In the same time, it is difficult to have a precise problem definition. This can lead to several solutions for the same plantwide control problem (Larsson & Skogestad, 2000).

(b) The plantwide control and the design are carried on in the same time. This approach (Bansal, Perkins, Pistikopoulos, Ross & van Schijndel, 2000; Schweiger & Floudas, 1997) involves, very often, solving multi-objective optimization problems, based on full nonlinear dynamic model of the process.

The design of the plantwide control structures also brings some particularities when model reduction is considered. Although the goal is a control structure for the whole plant, many control loops are local to certain units. For example, instabilities arising from heat-integration are solved by manipulating local heat duties; in distillation, composition of product streams is controlled by reflux rate or reboiler duty.

From a plantwide viewpoint, the design of the control structure is mainly concerned with the inventory of reactants, products, impurities and by-products (Bildea & Dimian, 2003). The solution is much simpler by excluding the local control loops from the analysis. This can be done by including these local control loops into the reduced model of the unit.

Both approaches need, however, a dynamic model of the plant. In the same time, this model has to be solved many times until a solution of the plantwide control problem is reached. If the model is solved fast, the control structure alternatives are easily evaluated.

3.2. Structure-retaining model reduction algorithm

After presenting the classical method to obtain the plantwide control structure of the plant using the model reduction and the main difficulties that can be encountered, a new approach is further introduced. This approach uses the knowledge about the structure that exists in a chemical plant in the form of units that are connected by material streams, which mirrors the decentralization of the control problem (Vasbinder & Hoo, 2003). The recommended procedure is to apply model-order reduction and/or model simplification to individual units, and then to couple these reduced models. The result of this coupling is a reduced model of the full plant. The effectiveness of the approach will be proven by means of a case study: the *iso*-butane – butene alkylation plant.

To obtain the reduced model of the plant, the following steps have to be considered:

A. Identification of units or groups of integrated units to which local control is applied

There are several ways to split the plant flowsheet into units. For example, the flowsheet is divided into units according to the equipment type: mixers, pumps, reactors, heat exchangers, distillation columns etc. For the distillation columns, an even more detailed decomposition can be considered: reboiler, trays, and condenser. Another idea is to split the flowsheet considering the main operations: mixing section, reaction section, separation section etc.

Therefore, the number of individual blocks to be further analyzed depends on the criteria used for flowsheet decomposition. For the case of a very fine decomposition, a large number of blocks are obtained, which lead to a large increase of the time allocated for individual block analysis. When the decomposition is too raw and the number of blocks is too small, the added value of the approach is insignificant.

One way of achieving the flowsheet decomposition is by using the concept of controlled group of units (CGU, Naka, Lu & Takiyama, 1997). The concept of CGU represents an independently operable part of the flowsheet, which provides an inventory control function to maintain it at a certain steady state for some time. Each CGU has an internal structure comprised of a number of processing units and control loops. The decomposition into CGU's should be done in such way that the dynamic interactions between them are minimized (Naka Lu & Takiyama, 1997, Seki & Naka, 2006). To achieve this, the connection between the parts of the plant through mass and energy streams are considered. Then decomposition is done by "cutting" streams of material, while units connected by an energy stream are kept together.

B. Application of tailored reduction techniques to individual units or groups of aggregated units

Each of the models of the units has smaller size compared to the original full model. Therefore, simple methods such as the reduction of the balanced state space model (which are not suitable for large-scale models) are easy to apply and to implement numerically for the purpose of the model reduction.

Moreover, since the error bounds between the original and the reduced-order model can be calculated a priori (see above), the cut-off criteria for the smaller Hankel singular values for different process units is defined in a consistent way. For the units with a strongly nonlinear behaviour, the use of model simplification or nonlinear model-order techniques can be a very good solution. In addition, due to the smaller size of the unit model, the chances of obtaining a reduced model that is difficult to solve decrease significantly.

C. Obtaining the reduced model of the full plant

The reduced model of the full plant is obtained by connecting the reduced models of the individual units. The connection is realized through streams characterized by the flowrates of each chemical species, temperature and pressure. To assess the quality of the reduced-order model, various disturbances are applied on one of the feed streams of the unit or plant. The responses in the outlet stream are recorded and compared further with the responses predicted by the full-order model, for the same disturbances.

Figure 3.1 introduces the algorithm of model reduction with process knowledge. The steps that need to be performed in order to obtain the reduced model are:

(1) A rigorous dynamic (nonlinear) model of the plant is developed. This step is performed using several commercial packages, as mentioned in Section 3.1.
(2) Identify the CGU's in the plant flowsheet. The concept of CGU's is presented above.
(3) Achieve the decomposition of the plant flowsheet. This decomposition should "cut" only material streams.
(4) The rigorous dynamic model of each CGU is developed using commercial packages. At this point, control structures for the CGU are added, if necessary.
(5) Proceed to the model reduction of each CGU. The following sub-steps have to be performed:
    a. Obtain a linear model of the CGU. As mentioned above, many commercial packages can perform this task easily.
    b. The balanced realization of the linear model of the CGU is obtained.
    c. The model reduction of the balanced model is performed.
(6) Check if the resulting reduced models of the CGU's are accurate enough. This can be achieved by comparing the behaviour predicted by the reduced and the rigorous models of each CGU, in the time domain or in the frequency domain (or both). The comparison can be graphical or statistical. If the resulting reduced model is not accurate enough, another technique should be used.
(7) If the reduced models of the CGU's are accurate, the full model of the plant is reconstructed by coupling together the reduced model of the CGU's.
(8) Check if the obtained full model of the plant is accurate. This is done by validation against the original nonlinear model. If the full model is not accurate enough, return to
    a. Step (5): A different model reduction of the CGU's is attempted;
    b. Step (3): The balanced realization of the linear model of the CGU is obtained.
    c. Step (2): Different CGU's are identified.
(9) If the full model is accurate enough, the algorithm stops.

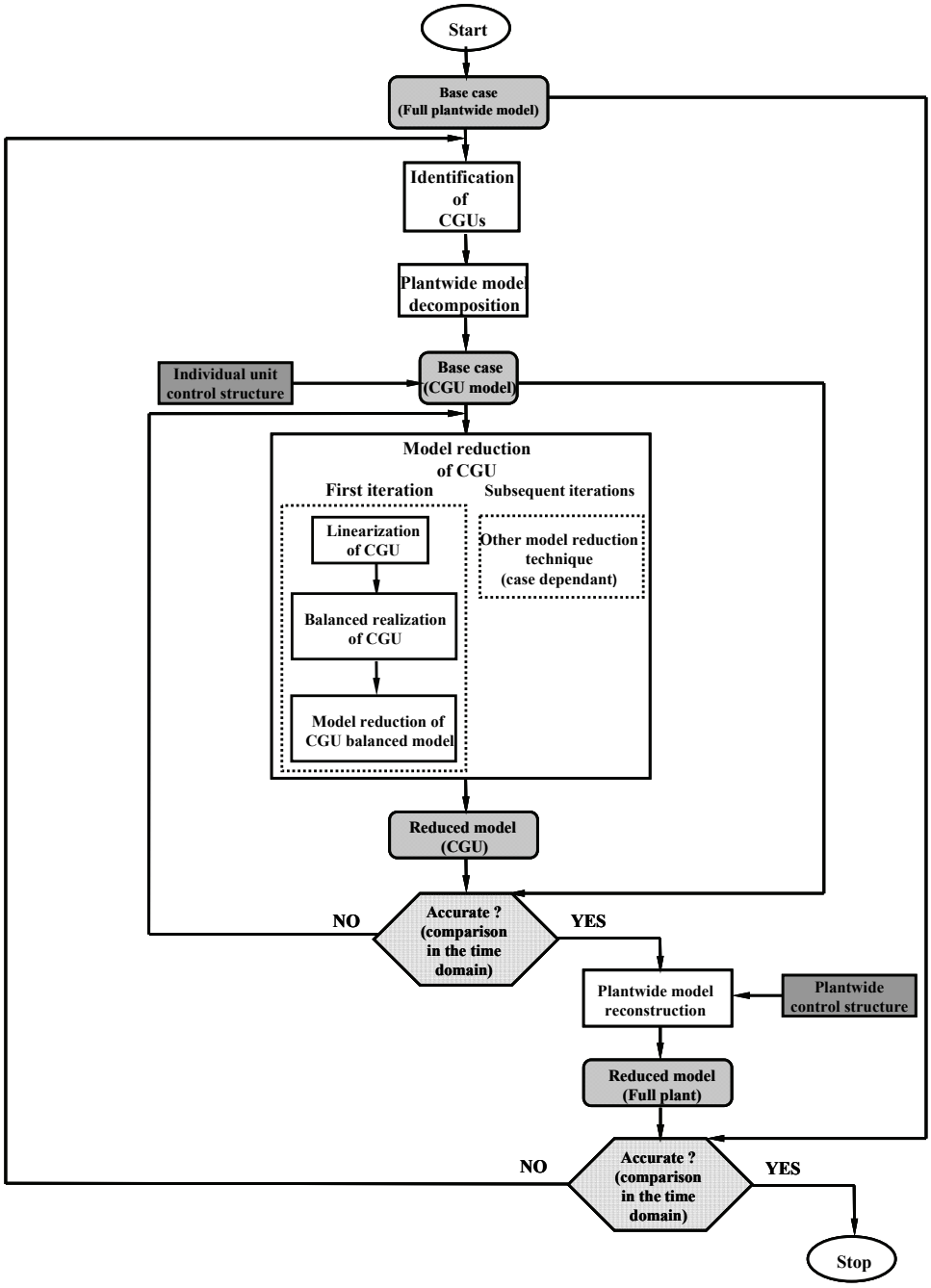

Figure 3.1.The algorithm of the structure retaining model reduction approach

In the following section, the effectiveness of the approach will be proven by means of a case study.

4. Case study: plantwide control of *iso*-butane - butene alkylation plant

The alkylation of *iso*-butane with butene is a widely used method for producing high-octane blending component for gasoline. In industrial practice, the modern processes use the sulphuric acid as a catalyst. Although the chemistry of alkylation is very complex, for our purposes, the following reactions will be used for the overall chemistry:

$$\underset{(A)}{C_4H_8} + \underset{(B)}{i-C_4H_{10}} \rightarrow \underset{(P)}{i-C_8H_{18}} \tag{3.10}$$

$$\underset{(A)}{C_4H_8} + \underset{(P)}{i-C_8H_{18}} \rightarrow \underset{(R)}{C_{12}H_{26}} \tag{3.11}$$

This particular case study has been chosen because the plant structure includes the most common units that can be seen in the industry: heat integrated reactor, distillation columns, mixers, pumps, recycles. The structure of the plant flowsheet will be presented in the following, while a detailed description of the process can be found in the book of Dimian and Bildea (2008).

In the classical approach to model reduction, in the control community, the reduced model is developed for controller tuning. In the following, a reduced model of the alkylation process will be developed, to be used for the analysis of plantwide control structures. Several different plantwide control structures are proposed and the behaviour of the reduced model of the plant is assessed. This is done for deciding the control strategy, and not the controller tuning, which means that steady state behaviour characteristics, such as sensitivity, are important. Moreover, the plantwide control structures do not control the different units in the plant flowsheet (like the reactor, or the distillation columns), but the way the reactants are introduced into the process. Once the reduced model of the plant is obtained, the plantwide control structure is added and the behaviour of the model is assessed.

4.1. Process description and the rigorous model

The plant produces 26 kton/year *iso*-octane, with a selectivity of 85% for a yearly run of 8000 hours. The raw materials are the butene and the *iso*-butane. The butene stream has a large amount of propane, which is an inert for the reaction, as impurities (10%). The main product is the *iso*-octane. Since the selectivity of the process is not 100%, some heavy products (modelled as dodecane) are formed.

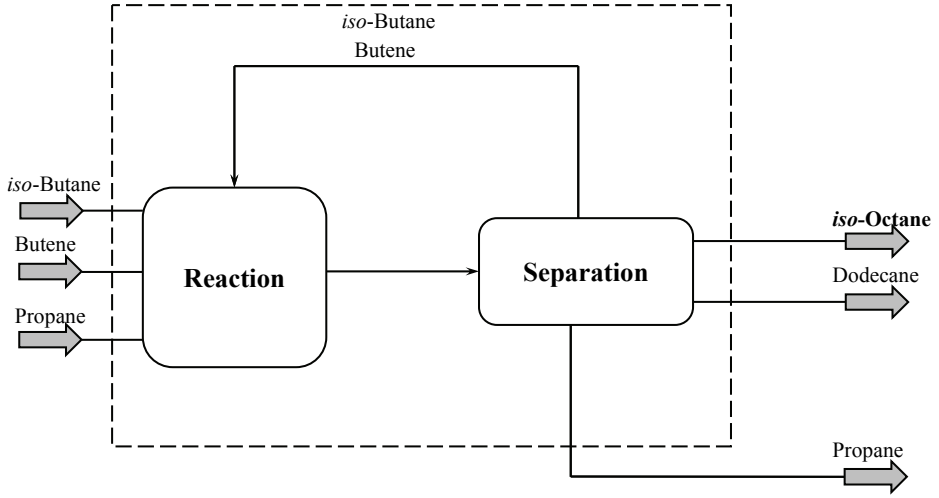

Figure 3.2. The basic iso-butane alkylation plant flow scheme

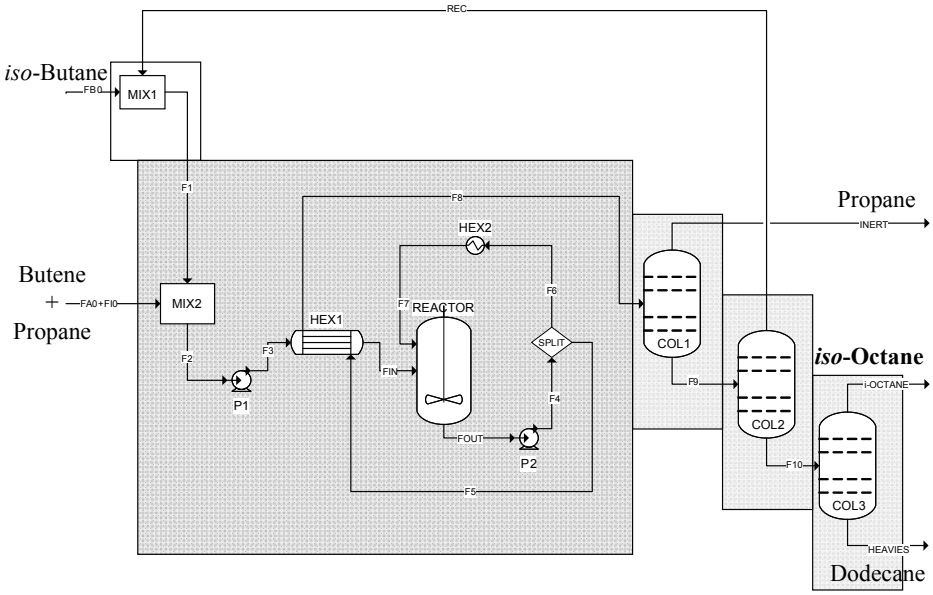

Figure 3.3. The iso - butane – butene alkylation plant flowsheet

The process consists of two basic operations (Figure 3.2). The main operation is the alkylation of *iso*-butane with butene to *iso*-octane and dodecane, which occurs in the reaction section. The two reactants are converted into products at low temperature, in a reactor modelled as a CSTR. The reaction volume is 4 m^3 and the reaction pressure is 8 bar. In practice, the temperature ranges between 0 and -10 ^{0}C. In this study, the reaction temperature is chosen to be -5 ^{0}C. The cooling is achieved in

an external heat exchanger. For heat integration purposes, the reactor outlet stream acts as coolant to the reactor inlet stream, as seen in Figure 3.3.

Table 3.1. Distillation column design specifications

Column specifications	Units	Column 1 (COL1)	Column 2 (COL2)	Column 3 (COL3)
Number of stages	$[-]$	28	29	24
Feed stage	$[-]$	18	10	11
Reflux ratio	$[-]$	110	0.1	0.2
Distillate to feed ratio	$[-]$	0.017	0.95	0.91
Reboiler duty	$[MW]$	6.65	3.8	0.09
Condenser duty	$[MW]$	-6.28	-3.54	-0.33

After reaction, the main product is separated from the reactor outlet stream. The separation is done by distillation, through the direct sequence. The inert is removed in the first column, while the reactants, having similar volatilities, are removed next.

In this way, only one recycle stream appears in the flowsheet. The third column separates the product from the heavies. A summary of the distillation columns design specifications is presented in Table 3.1.

Table 3.2. Stream summary for the iso-butane alkylation plant

Stream	Temperature $[^0C]$	Pressure $[bar]$	Mass flow $\left[kg/s\right]$				
			A	*B*	*P*	*R*	*I*
F_{B0}	25.0	8.0	-	0.580	-	-	-
$F_{A0} + F_{I0}$	25.0	8.0	0.550	-	-	-	0.108
F_{IN}	2.3	8.0	1.378	10.662	0.001	Traces	0.110
F_{OUT}	-5.0	8.0	10.409	126.461	11.564	1.734	1.379
F_8	48.9	9.0	0.833	10.117	0.925	0.139	0.110
INERT	26.8	8.0	0.001	0.054	Traces	Traces	0.108
F_9	61.1	9.0	0.832	10.063	0.925	0.139	0.002
REC	57.0	8.0	0.828	10.054	0.001	Traces	0.002
F_{10}	194.3	8.3	0.004	0.008	0.924	0.139	Traces
IOCTANE	93.5	1.2	0.004	0.008	0.923	0.00	Traces
HEAVIES	228.2	1.5	Traces	Traces	0.001	0.139	Traces

Once the plant structure has been decided, the next step is the equipment design and sizing. This was achieved using Aspen Plus®. A summary of the main streams composition is presented in Table 3.2.

After obtaining a steady-state model in Aspen Plus®, a dynamic model of the *iso*-butane alkylation plant is developed in Aspen Dynamics®. Aspen Dynamics® creates a very basic plantwide control structure consisting of a push flow control scheme on the raw material feeds, pressure control and where required, level control. However, this basic control structure does not involve any quality control loops. This basic dynamic model will be called the "open-loop" model and will be analyzed further.

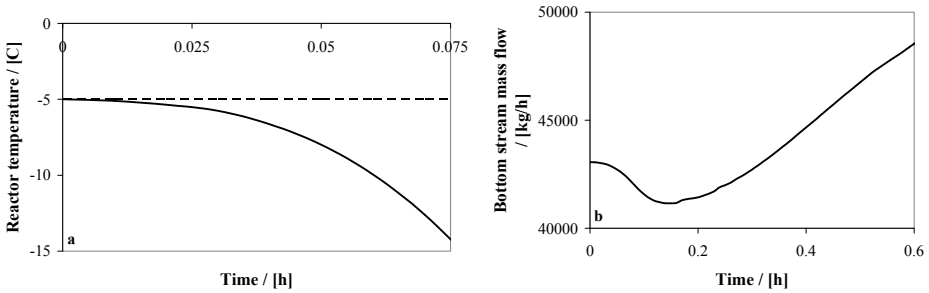

Figure 3.4.Instability of the "open-loop" plant:
a) The temperature of the reactor; b) The mass flow of the first column bottom stream

The simulation of the "open-loop" plant shows that the plant is unstable. Starting from the nominal (steady-) state, the reactor temperature drops fast and all flow rates dramatically increase (Figure 3.4). Soon, one level control loop reaches its limits, and overflow occurs.

4.2. The linear model

The original plantwide model is linearized around the nominal operating point (steady state). This step is done using the linearization toolbox provided by Aspen Dynamics®. The system matrix A has three positive eigenvalues, with unclear origin. The instability could be determined by the heat-integrated reactor, which presents a strongly nonlinear behaviour, as it will be shown later. Another source of instability could be the reactor-separation-recycle structure. It is also possible that one or more distillation columns present multiple steady states, phenomenon that is accompanied by instability (Jacobsen & Skogestad, 1995). An experienced modeller will consider other possible causes of the plant's instability. The issue of the three positive eigenvalues needs to be analyzed further.

4.3. The balanced model

Obtaining the balanced model using MATLAB® fails: the algorithm complains about ill-conditioned matrices. A balanced realization of the linear model of the original plant, which has 554 states, cannot be obtained. The cause is not easy to be determined.

As seen above, the use of reduced-order models, in a classical way, for designing the plantwide control seems to be hopeless. It looks difficult to develop a reduced model for the *iso*-butane alkylation plant using this approach. For the assessment of the plantwide control structure, other methods of obtaining the reduced model have to be used. The following steps will make use of the knowledge about the process while achieving the model reduction.

4.4. Exploiting the structure

For obtaining the plantwide control structure, the flowsheet of the *iso*-butane alkylation plant is decomposed into units and groups of units to which local control is applied. The decomposition does not cut the connection between units that are heat integrated.

The plant model is split into the following units: mixers, reactor (together with the heat integration around it), distillation columns, and pumps (Figure 3.3). The mixers and the pumps are assumed instantaneous, so they are not interesting from the point of view of the model reduction. For the models of each unit, the molar flowrates of each component, the temperature and the pressure for the inlet stream are considered as inputs, while the molar flowrates of each component, the temperature and the pressure of the outlet stream/streams are considered as outputs. Inputs that are usually considered for control, such as reflux rate or reboiler duties, are already assigned to local control loops. Therefore, from a plantwide control perspective, the set points of these local control loops are available as manipulated variables.

The model reduction techniques will be applied further to the reactor and each distillation column, individually.

4.4.1. The reactor sub-system

The analysis of the reactor subsystem shows instability. However, the unit can be easily stabilized by adding a temperature controller manipulating the cooling duty. After the stabilization, the unit is linearized around the steady-state point. The linear model that is obtained has 15 states, and the agreement with the nonlinear model is good, as seen in Figure 3.5.a.

Further, the reduction of the linear balanced model is attempted. The reduced-order model has only seven states, but the agreement with the full nonlinear model is questionable (Figure 3.5.a). It can be concluded that, for this case, no significant order-reduction at high accuracy can be achieved.

A second approach is considered in order to reduce the size of the reactor system model, preserving in the same time its nonlinearity. This reduction is based on model simplification.

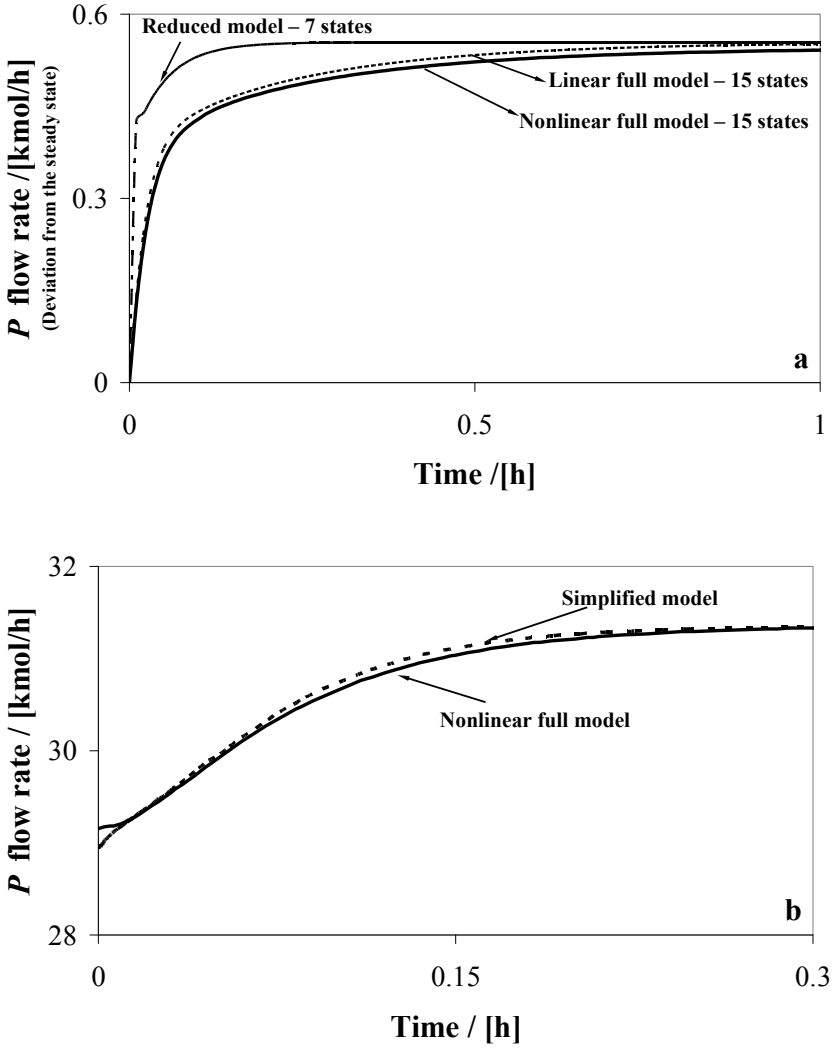

Figure 3.5. Model reduction of the reactor sub-system: iso-Octane molar flow in the outlet stream: a) Time response of the nonlinear, linear and reduced model for a step of 1 kmol/h on the butene in the feed; b) Time response of the nonlinear and simplified model for a step of 5 kmol/h on the butene in the feed.

A new dynamic model is written, consisting of five component balances, and considering constant temperature and physical properties:

$$\frac{dn^{(A)}}{dt} = F_{IN}^{(A)} - F_{OUT}^{(A)} - V \cdot r_1 - V \cdot r_2$$
$$\frac{dn^{(B)}}{dt} = F_{IN}^{(B)} - F_{OUT}^{(B)} - V \cdot r_1$$
$$\frac{dn^{(P)}}{dt} = F_{IN}^{(P)} - F_{OUT}^{(P)} + V \cdot r_1 - V \cdot r_2 \qquad (3.12)$$
$$\frac{dn^{(R)}}{dt} = F_{IN}^{(R)} - F_{OUT}^{(R)} + V \cdot r_2$$
$$\frac{dn^{(I)}}{dt} = F_{IN}^{(I)} - F_{OUT}^{(I)}$$

where:

$F_{IN}^{(i)}$ = the molar flow of component i in stream F_{IN}, $\left[kmole/h \right]$

$F_{OUT}^{(i)}$ = the molar flow of component i in stream F_{OUT}, $\left[kmole/h \right]$

$n^{(i)}$ = the number of moles of component i, $[kmole]$

$i = A, B, P, R, I$

V = the volume occupied by the reaction mixture, $[m^3]$

r_j = the rate of reaction j, $\left[kmole/m^3 \cdot h \right]$

$j = 1,2$

t = time, $\left[h \right]$

The volume occupied by the reaction mixture is calculated as a function of the number of moles of component i as:

$$V = \sum_i \left(n^{(i)} \cdot v_\mu^{(i)} \right) \qquad (3.13)$$

where:

$v_\mu^{(i)}$ = the molar volume of component i, $\left[m^3/kmole \right]$

The values for the molar volumes are presented in Table 3.3.

The reaction rates are assumed proportional to the reactant concentrations:

$$r_1 = k_1 \cdot c^{(A)} \cdot c^{(B)} \qquad (3.14)$$

$$r_2 = k_2 \cdot c^{(P)} \cdot c^{(R)} \qquad (3.15)$$

Table 3.3. The molecular volumes of component i

Component	Units	Molecular volume
Propane (I)	$\left[m^3/kmole\right]$	0.082
***iso*-Butane (A)**		0.089
1-Butene (B)		0.098
***iso*-Octane (P)**		0.158
Dodecane (R)		0.222

where: $c^{(i)}$ = the molar concentration of component i, $\left[kmole/m^3\right]$

k_j = the rate constant of reaction j, $\left[m^3/kmole \cdot h\right]$

The rate constant of reaction j it is assumed to be following an Arrhenius-type dependence on temperature:

$$k_j = k_{j,0} \cdot e^{-\frac{E_{a,j}}{R \cdot T}} \tag{3.16}$$

The values for the pre-exponential factors, $k_{j,0}$ and the activation energies, $E_{a,j}$ are taken from (Mahajanam, Zheng & Douglas, 2001) and are presented in Table 3.4.

Table 3.4. Kinetic parameters for reactions j

Component	Units	Reaction 1	Reaction 2
Pre-exponential factor $k_{j,0}$	$\left[m^3/kmole \cdot s\right]$	$1.62 \cdot 10^9$	$4.16 \cdot 10^{12}$
Activation energy $E_{a,j}$	$\left[kJ/kmole\right]$	$6.5 \cdot 10^4$	$8.1 \cdot 10^4$

The molar concentration of component i is determined as:

$$c^{(i)} = \frac{n^{(i)}}{V} \tag{3.17}$$

with: $k_{j,0}$ = the pre-exponential factor for reaction j, $\left[m^3 / kmole \cdot h \right]$

$E_{a,j}$ = the activation energy of reaction j, $\left[kJ / kmole \right]$

The molar flow of component i in the outlet flow is calculated in the following way:

$$F_{OUT}^{(i)} = F_{OUT} \cdot \frac{c^{(i)}}{\sum_i c^{(i)}} \tag{3.18}$$

In practice, a constant temperature inside the reactor is achieved by the use of a temperature controller. In this way, there is no need for the energy balance equation, and one differential variable becomes an algebraic one. Moreover, the equations for determining the temperature-dependent physical properties of the components are no longer necessary.

The control of the heat-integrated reactor consists of a temperature controller, manipulating the cooling duty, and a level controller, manipulating the outlet flow.

One extra differential equation is added to the model in order to ensure level control on the reactor's outlet flow. A PI controller is considered for this purpose. This extra equation is defined as follows:

$$F_{OUT} = F_{OUT,0} + K \cdot \left(\varepsilon(t) + \frac{1}{t_i} \int_0^t \varepsilon(\tau) d\tau \right) \tag{4.19}$$

where: F_{OUT} = the molar flow of the reactor outlet stream, $\left[kmole / h \right]$

F_{OUT} = the bias, $\left[kmole / h \right]$

K = the gain, $\left[kmole / m^3 \cdot h \right]$

ε = the error between the measured and the desired value, $\left[m^3 \right]$

t_i = the integral time, $\left[h \right]$

With the error between the measured and the desired value is determined as:

$$\varepsilon = V^* - V \tag{4.20}$$

where: V^* = the specified reactor volume, $[m^3]$

V = the measured reactor volume, $[m^3]$

As seen in the Figure 3.5.b, the agreement with the AspenDynamics® nonlinear model is excellent.

4.4.2. The distillation columns

Unexpectedly, the first and the third distillation column are also unstable. It should be remarked that the dynamic model specifies, realistically, the reflux on a mass basis, in contrast to the steady-state simulation, which uses moles.

Realizing the large relative volatilities and the very different molar weights, the existence of multiple or unstable steady states becomes a possibility (Jacobsen and Skogestad, 1995). Indeed, switching to mole-based specifications stabilizes the columns (Figure 3.6).

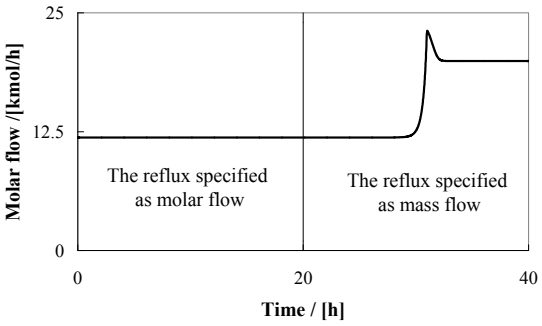

Figure 3.6.The instability of first column: Distillate stream molar flow

However, in the following the distillation columns will be modelled with mass-based reflux specification. Temperature controllers will be used to obtain a closed-loop stable system. Therefore, the control of the three distillation columns consists of temperature control both in the top and in the bottom of the columns, in addition to the inventory control loops (pressure, levels in the reflux drum and column sump).

As well as for the reactor system, the model of each distillation column is linearized, and then the reduced-order model of the balanced realization is obtained.

For the distillation columns, a significant order-reduction is achieved with excellent accuracy, as seen in Figure 3.7.a, where results are presented for the first distillation column. From a nonlinear model with about 200 states, the reduced-order model is linear and has around 20 states.

Table 3.5.Model reduction results

Unit	Model reduction technique	Full nonlinear model	Reduced model
CSTR	Model simplification	15 states	**5** states
COL1	Model-order reduction	185 states	**20** states
COL2		191 states	**25** states
COL3		163 states	**22** states
Simulation time, (s)		150	**30**

A summary of the model reduction results is presented in Table 3.5.

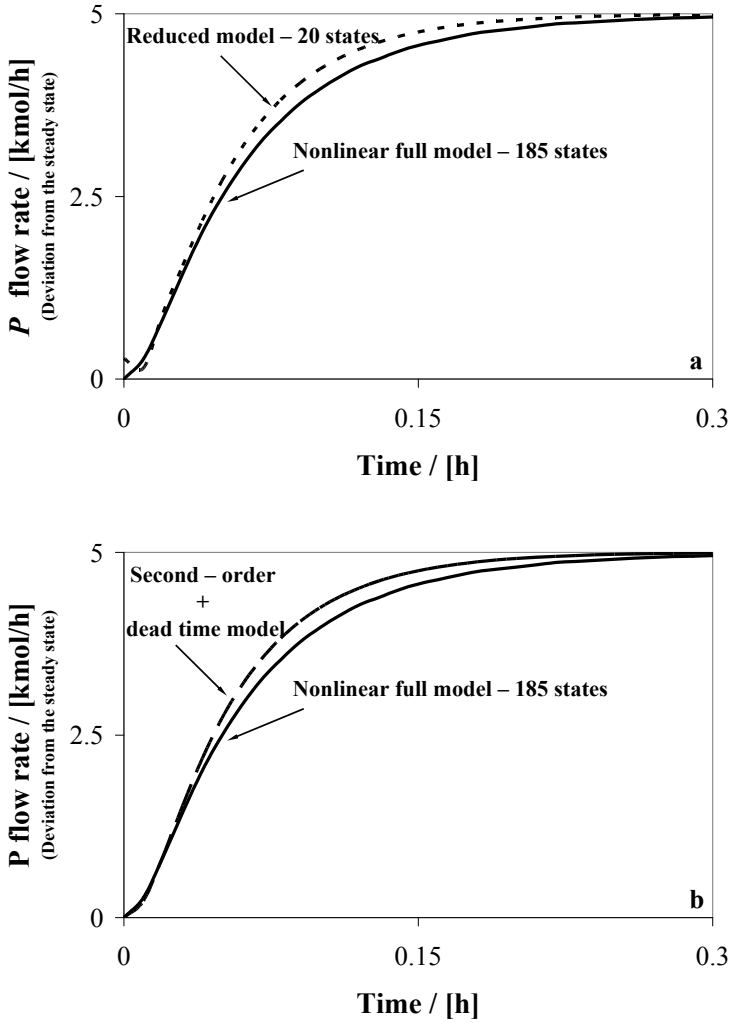

Figure 3.7. Model reduction for COL1: iso-octane molar flow in the bottom stream:
a) Time response for the full nonlinear and reduced model for a step of magnitude 5 kmol/h (~10%) on the feed stream molar flow; b) Time response for the full nonlinear and the small order model for a step of magnitude 5 kmol/h (~10%) on the feed stream molar flow

However, from the appearance of the time response of the full nonlinear model (Figure 3.7.a.), it should be remarked that the behaviour can be well approximated by a model of even lower order, such as a second-order plus dead-time model with parameters estimated with the help of the system identification toolbox provided by MATLAB®.

Figure 3.7.b. compares the predictions of the nonlinear and the second-order and dead-time models of the first distillation column, considering the *iso*-octane molar flowrate in the bottom stream as output. The agreement between the two models is excellent.

For the further steps in the assessment of the plantwide control structures, the order-reduced models obtained from the balanced realization of the linear models will be used.

4.5. Assessment of the plantwide control structure

At this point, three different models are available:

(a) The original nonlinear model (R)

(b) The reduced-order linear model (M1)

(c) The reduced-order nonlinear model (M2)

The original nonlinear model, R, is developed in AspenDynamics® and will be taken as reference. Model M1 contains the reduced-order linear model of each unit in the flowsheet, while model M2 contains the reduced-order linear models of the distillation columns and the simplified, nonlinear model of the reactor.

Different plantwide control structures are considered and evaluated. In the following, two of them will be discussed (Figure 3.8).

In control structure CS1, the fresh feeds of both reactants are fixed. This has the advantage of setting directly the production rate and the product distribution. The disadvantage of this control structure is that is highly sensitive to disturbances, as it will be shown later.

In control structure CS2, the butene fresh feed is fixed, but the iso-butane is brought into the process on inventory control. This eliminates the disadvantage of the previous control structure.

As the two control structures presented above differ only in the way the reactants are being brought into the process, the reduced-order models of the reaction and separation section can be easily reused.

In order to assess the quality of the reduced models M1 and M2 and their applicability to plantwide control design, the control structures CS1 and CS2 are applied and the predictions of the full and reduced models are compared.

When the butene feed is decreased by 10%, the full model predicts that control structure CS1 is not able to control the plant: the amount of butene in the process is not enough to consume the *iso*-butane. The reactant is accumulating in the plant and the recycle flow is continuously increasing. While simulating the full nonlinear model R, because of the high increase of the recycle flow, the Aspen Dynamics® simulation crashes and has to be stopped. This is also the reason for the smaller amount of data available for this model. The nonlinear model M2 is correctly predicting the high sensitivity to disturbances of this control structure, as shown in Figure 3.9. However, the linear model M1 wrongly indicates that a new steady state is reached. In other words, having a linear reduced-order for the reactor does not preserve the system's behaviour.

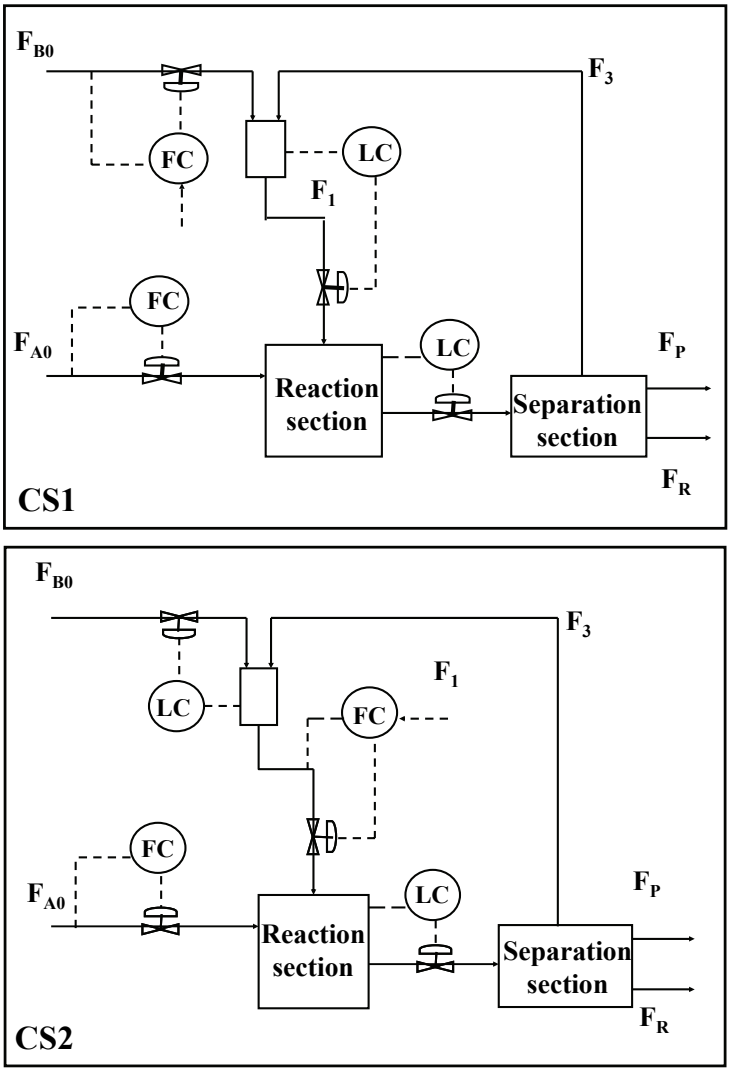

Figure 3.8.Control structures for the alkylation plant

It can be concluded that the reduced-order model must be able to preserve the nonlinear behaviour of the full model.

When the same disturbance is applied to the control structure CS2, a new steady state is reached in a relatively short time for the nonlinear model R and M2, as seen in Figure 3.10. The excellent accuracy of the nonlinear reduced-order model, M2, is obvious. In the same time, an important reduction of the computation time, from less than 3 minutes to about 30 seconds, should be also remarked, as shown in Table 3.5. This reduction of the computation time could result from the use of linear reduced-order models for the distillation columns. The linearization has as a result the

reduction of the computational effort, as discussed above. In addition, the use of a simple model for the reactor, which consists only of five mass balance equations, has an important contribution to this reduction of the computation time.

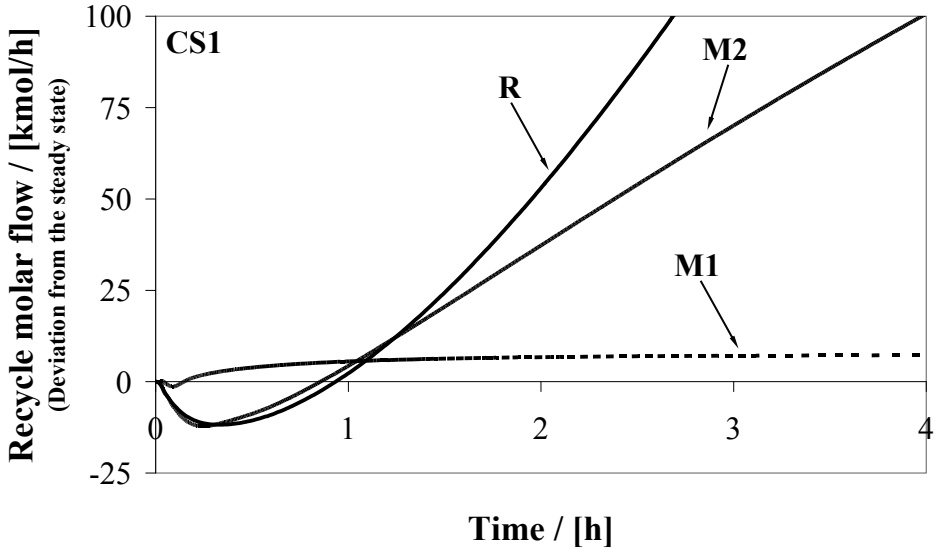

Figure 3.9.Dynamic simulation results, for 10% decrease of the fresh butene flowrate: Recycle flowrate.

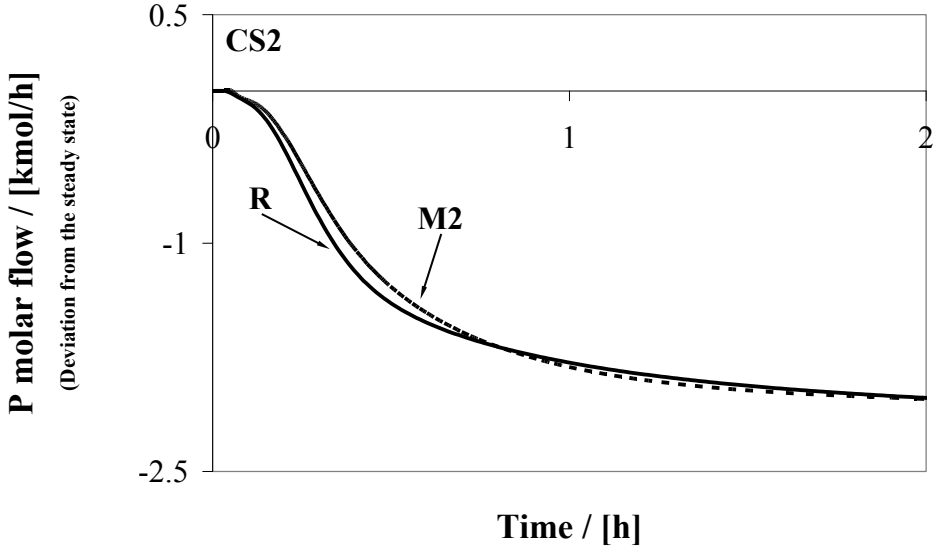

Figure 3.10.Dynamic simulation results, for 10% decrease of the fresh butene flowrate: Production rate.
(a) The reduced model M1 does not predict the sensitivity of control structure CS1, while M2 does
(b) The reduced model M2 correctly predicts the behaviour of control structure CS2

From the results presented in Figure 3.9 and Figure 3.10 it can be concluded that the control structure CS2 performs better than the control structure CS1 for the case presented above. This control structure is recommended for use further.

In the discussion above, the way the rigorous, the linear and the reduced models were obtained has been discussed. Since for the purpose several tools were used, in the following the way these tools were connected in order to achieve the goal will be summarised.

The rigorous model was obtained using the Aspen Engineering Suite®. Aspen Plus® and Aspen Dynamics® were used for obtaining the steady state and the dynamic model of the alkylation plant, respectively. The linear models were determined with the help of the linearization toolbox in Aspen Dynamics®. The balanced realization of the state space model and the model reduction were performed in MATLAB®, as well as the parameter identification for the reduced models of the distillation columns. Finally, the simplified reactor model and the complete reduced model of the alkylation plant were obtained using SIMULINK®.

The connection between these tools was done through the matrices of the state space representation of the system (the alkylation plant). The output of Aspen Dynamics® linearization tool is the set of matrices presented in equation (3.3). With the help of these matrices, the linear system is very easy to be implemented in MATLAB®, as a state space model. The model reduction performed in MATLAB® to this state space returns another set of smaller size matrices, which are also easy to turn into a state space model. SIMULINK® is a dynamic simulation package that allows the user to specify a block diagram representation of a dynamic process. As an extension to MATLAB®, the state space models obtained previously are fully compatible.

Another point that needs to be discussed is the time needed for the development of the reduced-order model using the structure-retaining approach, assuming that a full nonlinear model is already available. It is estimated that an experienced modeller will develop the reduced-order model of the alkylation plant is not more than two days. However, obtaining a nonlinear reduced model of a unit can be more time consuming.

5. Conclusions

The chapter proposes and demonstrates the advantage of considering the structure of a process flowsheet when developing reduced-order models to be used during the design of the plantwide control system.

The recommended procedure is to apply the model reduction to the individual units or groups of units of the plant, and then to connect together the reduced models. The reduction for the individual units consisted in a linear model-order reduction of the distillation column models and a simplification of the integrated reactor model.

Some advantages of applying this procedure have been highlighted by means of a case study:

- The procedure is flexible. Tailored model reduction techniques are applied to different plant units. In the case presented above, the reactor model was reduced by model simplification, while linear model-order reduction of the balanced realization was used for the distillation columns. The dynamics of the mixers, pumps and the heat exchangers was neglected.
- The solution time is significantly reduced, by factor 5.
- The nonlinearity of the model can be preserved. This feature is highly desirable since many units of chemical and biochemical plants have a strongly nonlinear behaviour, such as state multiplicity or parametric sensitivity, behaviour that is enhanced by the coupling through heat integration and/or material recycles. It was shown that considering a linear model for the reactor in the reduced model of the plant did not preserve essential behavioural features of the system. After applying a disturbance for the control structure CS1, the linear reduced-order model did not predict the system sensitivity, in contrast to the predictions of the full-order and the reduced-order nonlinear models.
- The maintenance and adaptation to future plant changes is facilitated by the modularity of the reduced model. Once one of the units in the plant flowsheet needs to be replaced, its reduced model can be easily inserted in the reduced model of the plant.
- The modularity of the reduced model is also useful for the case when a rigorous model for one of the plant units is not available. However, if a simplified model of the unit is available and accurate enough, it can be easily inserted in the reduced model of the whole plant.

After demonstrating the advantages of using this model reduction technique for the assessment of the plantwide control structure of a chemical plant, the next step is to use it for other applications in the chemical industry. For example, dynamic optimization of plant operation is another time consuming task for which the advantage of using reduced models is obvious.

6. References

Antoulas, A.C., & Sorensen, D.C. (2001). Approximation of large-scale dynamical systems: An overview, *Technical report*, *http://www-ece.rice.edu/~aca/mtns00.pdf* (last visited 29.09.2008)

Antoulas, A.C., Sorensen, D.C., & Gugercin, S. (2000). A survey of model reduction methods for large-scale systems. Structured Matrices in Operator Theory, Numerical Analysis, Control, Signal and Image Processing, Contemporary Mathematics, *AMS Publications* 280, 193

Bai, Z. (2002). Krylov subspace techniques for reduced-order modelling of large-scale dynamical systems, *Applied Numerical Mathematics* 43, 9

Baldea, M., Daoutidis, P., & Kumar, A. (2006). Dynamics and control of integrated networks with purge streams, *AIChE Journal* 52, 1460

Bansal, V., Perkins, J.D., Pistikopoulos, E.N., Ross, R., & van Schijndel, J.M.G. (2000). Simultaneous design and control optimization under uncertainty, *Computers and Chemical Engineering* 24, 261

Bhattacharjee, B., Schwer, D.A., Barton, P.I., & Green, Jr., W.H.G. (2003). Optimally- reduced kinetic models: reaction elimination in large-scale kinetic mechanisms, *Combustion and Flame* 135, 191

Bildea, C.S., & Dimian, A.C. (2003). Fixing flow rates in recycle systems: Luyben's rule revisited *Industrial and Engineering Chemistry Research* 42, 4578

Dimian, A.C., & Bildea, C.S. (2008). Chemical Process Design, Computer-Aided Case Studies, *Weinheim: Wiley-VCH*, 261

Engell, S. (2007). Feedback control for optimal process operation, *Journal of Process Control* 17, 203

Jacobsen, E.W., & Skogestad, S. (1995). Multiple steady-states and instability in distillation. Implications for operation and control, *Industrial and Engineering Chemistry Research* 34, 4395

Larsson, T., & Skogestad, S. (2000). Plantwide control – A review and a new design procedure, *Modelling, identification and control* 21, 209

Mahajanam, R.V., Zheng, A., & Douglas, J.M. (2001). A shortcut method for controlled variable selection and its application to the butane alkylation process, *Industrial and Engineering Chemistry Research* 40, 3208

Mäkilä, P.M. (1991). On identification of stable systems and optimal approximation, *Automatica* 27, 663

Marquardt, W. (2001). Nonlinear model reduction for optimization based control of transient chemical processes, *Proceedings of the 6th international Conference of Chemical Process Control, AIChe Symp. Ser. 326*, Vol. 98, 12

Mullhaupt, A.P., & Riedel, K.S. (2004). Exponential condition number of solutions of the discrete Lyapunov equation, *IEEE Transactions on Signal Processing* 52, 1257

Nafe, J., & Maas, U. (2002). A general algorithm for improving ILDMs, *Combustion Theory and Modelling* 6, 697

Nagy, Z.K., & Braatz, R.D. (2003). Robust nonlinear model predictive control of batch processes, *AIChE Journal* 49, 1776

Nagy, Z.K., & Braatz, R.D. (2007). Distributional uncertainty analysis using power series and polynomial chaos expansions, *Journal of Process Control* 17, 229

Nagy, Z.K., Mahn, B., Franke, R., & Allgöwer, F. (2007). Evaluation study of an efficient output feedback nonlinear model predictive control for temperature tracking in an industrial batch reactor, *Control Engineering Practice* 15, 839

Naka, Y., Lu, M.L., & Takiyama, H. (1997). Operational design for start-up of chemical processes, *Computers and Chemical Engineering* 21, 997

Penzl, T. (2006). Algorithms for model reduction of large dynamical systems, *Linear Algebra and its Applications* 415, 322

Prasad, V., & Wayne Bequette, B. (2003). Nonlinear system identification and model reduction using artificial neural networks, *Computers and Chemical Engineering* 27, 1741

Ranzi, E., Dente, M., Goldaniga, A., Bozzano, G., & Faravelli., T. (2001). Lumping procedures in detailed kinetic modeling of gasification, pyrolysis, partial oxidation and combustion of hydrocarbon mixtures, *Progress in Energy and Combustion Science* 27, 99

Rathinam, M, & Petzold, L. (2003). A new look at proper orthogonal decomposition, *SIAM Journal on Numerical Analysis* 41, 1893

Scherpen, J.M.A. (1994). Balancing for nonlinear systems, *PhD Thesis*, University of Twente, Enschede, The Netherlands

Schweiger, C.A., & Floudas, C.A. (1997). Integration of design and control: Optimization with dynamic models, Optimal Control: Theory, algorithms and applications, Hager, W.W., Pardalso, P.M. (Eds.), *Kluwer Academic Publishers*

Seki, H., & Naka, Y. (2006). A hierarchical controller design for a reactor/separator system with recycle, *Industrial and Engineering Chemistry Research* 45, 6518

Skogestad, S., & Larsson, T. (1998). A review of plantwide control, *Technical report, http://www.nt.ntnu.no/users/skoge/publications/1998/plantwide_review1/plantwide_review 1.pdf* (last visited 29.09.2008)

Skogestad, S., & Postlethwaite, I. (1996). Multivariable feedback control, Chichester:John *Wiley and Sons*, 449

Van den Bergh, J. (2005). Model reduction for dynamic real-time optimization of chemical processes, *PhD Thesis*, Delft University of Technology, The Netherlands

Vasbinder, E.M., & Hoo, K.A. (2003). Decision-Base Approach to Plantwide Control Structure Synthesis, *Industrial and Engineering Chemistry Research* 42, 4586

4

DYNAMIC OPTIMIZATION USING A REDUCED PROCESS MODEL

The chapter explores the application of the structure-retaining model reduction approach, presented in Chapter 3, in the context of dynamic optimization of chemical plants operation. The focus is on the derivation and use of reduced models for the design and implementation of optimal dynamic operation in large-scale chemical plants. A case study is used to show the application of the model reduction approach, similar to the previous chapter.

1. Introduction

As mentioned in Chapter 3, the development of control systems that maintain the steady state of a chemical plant is one approach to achieve the economical performances in today's competitive environment. However, this is not the only answer to the problem. Another approach is responding continuously to the market conditions through dynamic operation. This requires that the control systems are able to implement the optimal dynamic behaviour.

Dynamic optimization problems for chemical processes can be found in a wide variety of applications.

One typical example is the assessment of the trajectories for the optimal operation of batch and semi-batch reactors (Srinivasan, Bonvin & Palanki, 2003; Srinivasan, Bonvin, Visser & Palanki, 2003; Mohan, Rao, Prasad, Krishna, Rao & Sarma, 2005; Arpornwichanop, Kittisupakorn & Mujtaba, 2005; Srinivasan & Bonvin, 2007; Simon, Introvigne, Fischer & Hungerbuehler, 2008).

Other applications include continuous processes in transient regimes, such as

- Start-up (Arellano-Garcia, Carmona & Wozny, 2008; Sonntag, Su, Stursberg & Engell, 2008; Haugwitz, Akesson & Hagander, 2009)
- Shut-down or grade transitions (Chatzidoukas, Perkins, Pistikopoulos & Kiparissides, 2003; Flores-Tlacuahuac, Biegler & Saldivar-Guerra, 2006; Prata, Oldenburg, Kroll & Marquardt, 2008)
- Process scheduling (Nystrom, Harjunkoski & Kroll, 2006; Terrazas-Moreno, Flores-Tlacuahuac & Grossmann, 2007; Li & Ierapetritou, 2007; Chatzidoukas, Pistikopoulos & Kiparissides, 2009).

Another class of applications deals with

- Interaction between process design and the control systems design (Mohideen, Perkins & Pistikopoulos, 1996; Bansal, Perins & Pistikopoulos, 2002; Konda, Rangaiah & Lim, 2006; Malcolm, Polan, Zhang, Ogunnaike & Linninger, 2007; Exler, Antelo, Egea, Alonso & Banga, 2008)
- Model predictive control (Engell, 2007; Nagy, 2007; Grossmann, Erdem, Morari, Amanullah, Mazzotti & Morbidelli, 2008)
- Process safety studies (Abel, Helbig, Marquardt, Zwick & Daszkowski, 2000; Xia, Zhao & Jia, 2008; Miri, Tsoukalas, Bakalis, Pistikopoulos, Rustem & Fryer, 2008; Simon, Kencse & Hungerbuehler, 2009)

An important group of applications includes system identification and estimation (Abu-el-zeet, Roberts & Becerra, 2002; Tsai & Wang, 2005; Nagy, Fujiwara, Woo & Braatz, 2008).

Obtaining a solution for such applications is still a difficult task when taking into account the fact that very often the dynamic optimization problem involves large-scale models. Just like in the case of the plantwide control, the quality of the model is crucial for achieving the objective: the model

must represent the plant behaviour with good accuracy, but the complexity must be limited because both applications require repeated solution during limited time.

The structure-retaining model reduction approach will be used in this chapter for the derivation of the optimal profiles for the dynamic operation of a chemical plant. The chapter is structured in the following way: Section 2 presents an overview of the dynamic optimization problem and the main solution techniques. In Section 3, the reduction procedure is applied for the *iso*-butane alkylation plant for obtaining the reduced model to be used for the solution of the dynamic optimization problem. The results of the dynamic optimization are presented in Section 4. Finally, conclusions are presented in Section 5.

2. Dynamic optimization

In practice, a chemical process is modelled dynamically using differential-algebraic equations (DAE's) as shown in Chapter 2, Section 4 of the thesis. In this formulation, the differential equations are used to describe the dynamic behaviour of the system, for example mass and energy balances, while the algebraic equations describe the physical and thermodynamic relations. The objective of the dynamic optimization is to determine, for a dynamic system, the time profiles for a set of decision variables (pressure, temperature, flowrate, heat duty, etc.) that optimise a given performance criterion, subject to specified constraints (safety, environmental and operating constraints). This task can be performed in time or along a spatial parameter. Both time and the spatial parameter can be considered continuous or discrete.

The dynamic optimization problems can be formulated in many different ways, under different assumptions. For the application in the following section, it will be stated as follows:

$$\min_{u(t),t_f,\alpha} \Phi = \int_0^{t_f} \left[\phi\left(x(t),u(t),z(t),t,\alpha\right) \right] dt \tag{4.1}$$

$$s.t. \qquad f\left(x(t),\dot{x}(t),u(t),z(t),\alpha \right) = 0 \tag{4.2}$$

$$g\left(x(t),u(t),z(t),\alpha\right) = 0 \tag{4.3}$$

$$x_{min}(t) \le x(t) \le x_{min}(t) \tag{4.4}$$

$$u_{min}(t) \le u(t) \le u_{max}(t) \tag{4.5}$$

$$z_{min}(t) \le z(t) \le z_{max}(t) \tag{4.6}$$

$$\alpha_{min} \le \alpha \le \alpha_{max} \tag{4.7}$$

$$x(0) = x_0(\alpha) \tag{4.8}$$

In this formulation, $x(t)$ are the state (dependent) variables, $u(t)$ are the control (independent) variables, $z(t)$ are algebraic variables and α are model parameters. The dynamic model of the process is represented by differential-algebraic equations. The equations (4.2) and (4.3) define such a system. Equations (4.4), (4.5) and (4.6) are the path constraints on the state, control and algebraic variables, respectively, while equation (4.8) represents the initial condition on the state variables. Φ is a scalar objective function at the final time, t_f .

There are three classes of dynamic optimization problems:

(a) Parameter optimization

The goal of the parameter optimization is to find a parameter vector α that minimizes the objective function Φ (Geromel, Bernussou & Peres, 1994; Uhl, 2007). The parameter vector can contain both model parameters and/or initial states of the model.

(b) Parameter estimation

The objective of the parameter estimation problem is to fit a model to existing experimental measurements. Since a perfect fit is not possible to obtain, the problem finds the best fit according to a criterion penalizing the deviation between the model predictions and the measured data (Tholudur & Ramirez, 1996; Banga, Versyck & Van Impe, 2002; Rodriguez-Fernandez, Mendes & Banga, J.R., 2004; Michalik, Hannemann & Marquardt, 2009).

(c) Optimal control

The goal is in this case finding the vector of the control variables $u(t)$ that minimizes the objective function, Φ (Mohideen, Perkins & Pistikopoulos, 1996; Carrasco & Banga, 1997; Esposito & Floudas 2000; Labadie, 2004). For this type of problems, the parameter vector α is fixed.

2.1. Numerical methods for dynamic optimization

Currently, the dynamic optimization problems are solved using a variational approach, by using different strategies that apply non-linear programming (NLP) solvers (Biegler, 2007) or by dynamic programming (Cervantes & Biegler, 2001).

The numerical methods for the solution of the dynamic optimization problems are usually classified in:

(a) Indirect (variational) approaches

The indirect (classical) approaches are based on the transformation of the original problem into a two-point boundary problem using the necessary conditions of Pontryagin (Biegler, 2007). For problems without inequality constraints, the optimality conditions can be formulated as a set of

DAE's (Biegler, Cervantes & Wächter, 2002). The resulting problem is difficult to solve when handling active constraints (Banga, Balsa-Canto, Moles & Alonso, 2005; Biegler, 2007).

(b) Direct approaches

The methods based on direct approaches transform the original dynamic optimization problem into a nonlinear programming problem (NLP). These methods can be separated into two groups:

1) Sequential methods

The techniques in this group are also known as control vector parameterization. They decompose the whole system into the control and state spaces. The strategy is to discretize the control variables, $u(t)$ obtaining a relatively small non-linear programming (NLP) problem. The control variables are represented as piecewise polynomials and the optimization is performed with respect to the polynomial coefficients (Schlegel, Stockmann, Binder & Marquardt, 2005). The process model is integrated with a DAE solver at each iteration (Biegler, Cervantes & Wächter, 2002), and the polynomial coefficients are updated. This process can become time consuming for large-scale problems. Moreover, it is well known that these approaches have properties of single shooting methods and cannot handle open loop instability (Biegler, 2007). For this group of methods it is possible to incorporate path constraints, but these are handled approximately, within the limits of the control parameterization (Kameswaran & Biegler, 2006).

2) Simultaneous methods

These methods are also known as complete parameterization or direct transcription. In this case, both the control $u(t)$ and the state variables $x(t)$ are discretized. The result is that the size of the NLP problem is much larger, and requires special solution strategies (Cervantes, Wächter, Tütüncü & Biegler, 2000; Cervantes, Tonelli, Brandolin, Bandoni & Biegler, 2002). As a result, these methods directly couple the solution of the DAE system with the optimization problem; the DAE system is solved only once, at the optimal point (Biegler, Cervantes & Wächter, 2002). There are mainly two different approaches to discretize the state variables explicitly: multiple shooting and collocation on finite elements (Biegler & Grossmann, 2004; Biegler, 2007).

2.2. The sequential method for dynamic optimization

As mentioned in the previous section, in a sequential method the evolution in time of the control variables is parameterized by a finite number of (numerical) parameters, $\mu = (\mu_1, \mu_2, ..., \mu_N)$ and $\tau = (\tau_1, \tau_2, ..., \tau_N)$:

$$u(t) = \varphi(t, \mu_k) \qquad \text{for} \qquad \tau_{k-1} < t < \tau_k \tag{4.9}$$

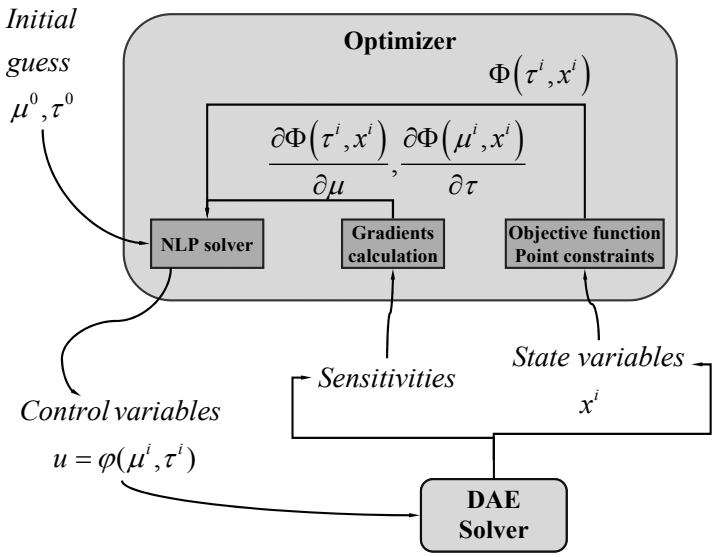

Figure 4.1. Dynamic optimization algorithm

Given fixed values of parameters, the objective function of the dynamic optimization problem is evaluated simply by integrating the dynamic system. The parameters are then updated by the optimization algorithm and the procedure is repeated, as shown in Figure 4.1.

Since the parameters determine the control profiles used to compute the values of the state variables, the objective function can be written as:

$$\Phi\left(x\left(t,u\left(t\right),\mu\right),u\left(t\right),y\left(t,u\left(t\right),\mu\right),t,\mu\right)=\Phi \tag{4.10}$$

This transforms the infinite dimensional optimization problem into a finite dimensional problem.

Often, the objective function Φ can be written as an additional differential equation in the DAE system, by differentiating equation (4.1):

$$\frac{\partial\Phi}{\partial t}=\phi\left(x\left(t\right),u\left(t\right),z\left(t\right),t,\alpha\right) \tag{4.11}$$

3. Model reduction for dynamic optimization

The advantages of the structure-retaining model reduction approach presented in Chapters 2 and 3 of this thesis make it a good candidate for use in the assessment of the optimal dynamic profiles for the operation of a chemical plant. The method uses the knowledge regarding the structure that exists in a chemical plant in the form of units that are connected by material streams. By applying model-order reduction and/or model simplification to individual units, and then coupling these

reduced models to obtain the reduced model of the full plant, several advantages can be envisaged. For example, the physical meaning of the variables is kept when the model is broken into smaller parts, which are connected together. Moreover, due to the flexibility of the procedure, the nonlinearity of the resulting model is kept.

In the following section, the application of this approach will be used for solving a dynamic optimization problem. This will be done by means of a case study: the *iso*-butane alkylation plant. The model reduction is used for modifying the model of the plant in such way that the desired behaviour, set by the objective of the dynamic optimization problem, is obtained. Using this reduced model it will be shown that the dynamic optimization problem can be solved, and the optimum profiles for the control variables can be determined.

3.1. The rigorous model of the *iso*-butane alkylation plant

For the purpose of this research, the same process presented in Chapter 3 will be used. The rigorous model developed in Aspen Dynamics®, consisting of a CSTR and three distillation columns (as shown in the flowsheet in Figure 4.2) will be the basis for the assessment of the optimum dynamic operation profiles.

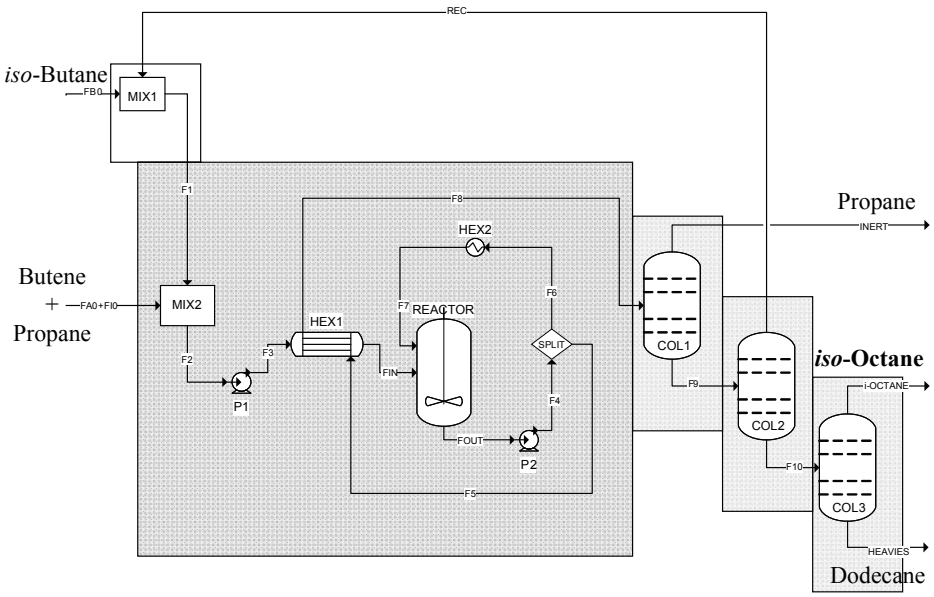

Figure 4.2. The iso - butane – butene alkylation plant flowsheet

For the plantwide control, the option that proved insensitive to disturbances during the assessment of the plantwide control structure is chosen. In this case, the fresh feed of butene is fixed, while the *iso*-butane is brought into the process on flow control, as shown in Figure 4.3. When a

disturbance is applied to one of the fresh feeds, a new steady state is reached in a relatively short time when this plantwide control is used, as demonstrated in Chapter 3 of this thesis. This is an important characteristic when solving the dynamic optimization problem. Local control is also present: the reactor is operated at constant volume and temperature. The reaction temperature is controlled using the coolant flowrate for this purpose.

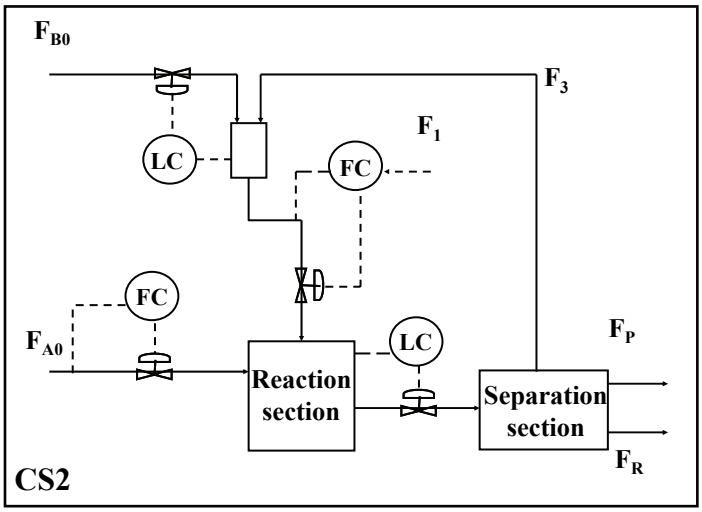

Figure 4.3.Control structure for the alkylation plant

For the distillation columns (Figure 4.4), in addition to the inventory control loops (pressure, levels in the reflux drum and the column sump), top and bottom concentrations are controlled as well.

According to the plantwide control strategy, a new production rate can be achieved by changing the butene feed. Moreover, an increase of the recycle flow is necessary in order to keep the selectivity at a high value. An increase in the flow rates will lead to an increase in the energy consumption for the separation of the different components.

The changes in flow rate can be done step-like, the magnitude of the steps being calculated using the steady state model of the plant, or in a more efficient way, by dynamic optimization.

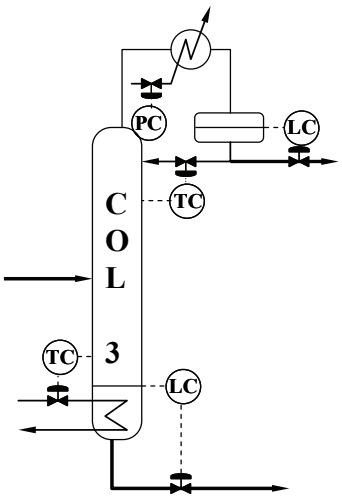

Figure 4.4.Control structure for the distillation columns

The objective of the dynamic optimization problem should be stated before the model reduction is performed, in order to be able to choose the right variables to be kept in the reduced model:

Increase the plant production by 20% while minimizing the energy consumption in the distillation columns during the transient period. Moreover, a new steady state must be ensured.

3.2. The reduced model

As seen in the previous section, the full nonlinear model is developed using Aspen Dynamics®. In order to obtain the reduced model, the same procedure presented in Chapter 3 is used. The plant flowsheet (Figure 4.2) is split into controlled groups of units (CGU's). The following blocks are obtained:

(a) The reactor (CSTR) + the heat exchanger around it;
(b) Three distillation columns (COL1, COL2 and COL3)
(c) Mixing vessels
(d) Pumps

Since the mixers and the pumps are considered instantaneous (no dynamics), they are not interesting for the purpose of the model reduction.

For this particular case, the reduced model will be developed using gProms® instead of MATLAB®. There are two reasons for this choice:

(1) gProms® has already implemented a toolbox for solving steady-state and dynamic optimizations problems. For the dynamic optimization, two methods can be used: (a) the single-shooting and (b) the multiple-shooting method.

(2) The time needed to solve the reduced model using gProms® is much smaller compared to MATLAB®, as it will be shown in Section 3.2.3 of this chapter. This advantage will drastically reduce the computational time needed for solving the dynamic optimization problem.

The reduced model of the iso-butane alkylation plant that will be used for the dynamic optimization application consists of the reduced models of the different CGU's, together with the plantwide control loops shown in Figure 4.3.

In the next sections, the procedure for reducing the individual CGU's is presented, with emphasis on the particularities derived for the type of application considered (dynamic optimization).

3.2.1. The reactor sub-system

As seen in Chapter 3 of the thesis, the reactor has a strong nonlinear behaviour. For this reason, model simplification is used to reduce this unit. The simplified dynamic model presented in Chapter 3, Section 4.4.1, consisting of five component balances, and assuming constant temperature and physical properties is implemented in gProms®.

There is a good agreement between the simplified model developed in gProms® and the AspenDynamics® nonlinear model, as shown in Figure 4.5.

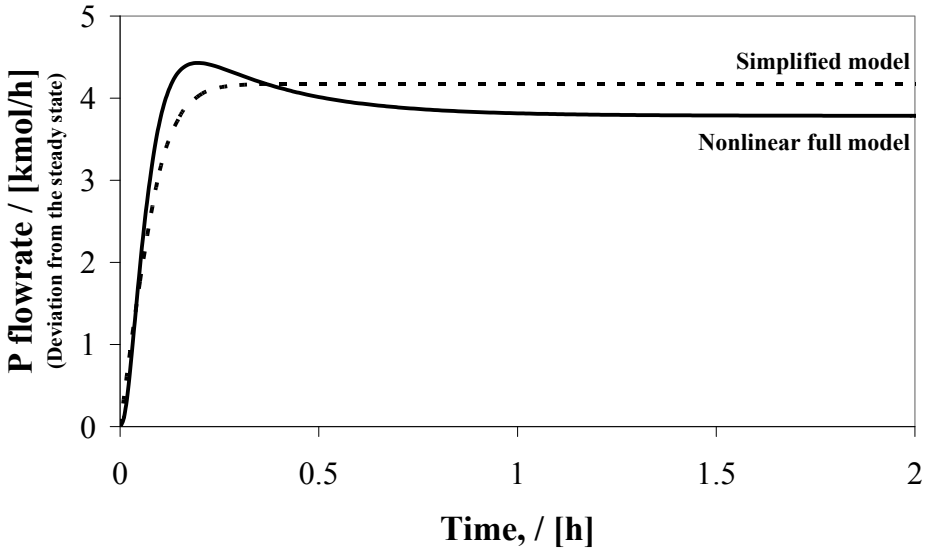

Figure 4.5. Model reduction of the reactor sub-system:
Time response of the nonlinear and simplified model for a step of +20% on the butene in the feed

3.2.2. The distillation columns

For the distillation columns, linear model-order reduction techniques will be used. The linear model is obtained using AspenDynamics®, similarly to the procedure presented in Chapter 3 of the thesis. Some modifications to the previous model are done in order to be able to use the resulting models for the purpose of the dynamic optimization problem. The reboiler duty and the reflux ratio are considered as output variables of the linear model, together with the outlet streams flow rates. These modifications have an effect on the number of states the resulting models have once the reduction procedure is applied, as presented in Table 4.1. The balanced realization of the linear models of the distillation columns is performed in MATLAB® and the resulting balanced models are reduced. The reduced models of the three distillation columns are further implemented in gProms®.

3.2.3. Performance of the reduced model

After all the reduced models of the individual controlled group of units (CGU's) are available, these models are connected in order to obtain the reduced model of the full *iso*-butane alkylation plant. An issue one has to deal while connecting the individual reduced models is the initialization. In gProms®, the model needs good starting points in order to converge. This issue is solved by taking advantage exactly of the decentralization of the control problem. Having separate reduced models for each unit in the plant flowsheet allows the individual models to be run separately in order to get good starting values for the reduced model of the full plant.

Table 4.1. Model reduction results

Unit	Model reduction technique	Full nonlinear model	Reduced model	
			MATLAB®	gProms®
CSTR	Model simplification	15 states	**5** states	**6** states
COL1	Model-order reduction	185 states	**20** states	**25** states
COL2		191 states	**25** states	**29** states
COL3		163 states	**22** states	**17** states
Simulation time, (s)		150	**30**	**2**

The outcome of the model reduction procedure is presented in Table 4.1 together with the time needed for simulating five hours of dynamic behaviour, under similar conditions. These results are compared with the reduced model obtained with MATLAB®.

4. The dynamic optimization

The reduced model for the *iso*-butane alkylation plant has been obtained and implemented in the previous Section. The dynamic optimization problem presented in equations (4.1) – (4.8) is further implemented in gProms® and solved using the single-shooting method.

The objective function to be minimised is the sum of the reboiler duties in the three distillation columns. Two control variables are considered:

(a) The flowrate of the fresh feed of butene (F_{A0})

(b) The flowrate of the first mixer's outlet stream (F_1)

These two variables are on flow control in the plantwide control structure CS2, which is presented in Figure 4.3. A continuous piecewise-constant control is chosen for these two variables in the implementation of the dynamic optimization problem.

The optimizer is required to determine the optimum control profiles that ensure the 20% increase in production, together with the time needed to reach this state. Once this goal is achieved,

the optimizer must ensure that a new steady state is reached and that the production is kept constant for a fixed amount of time.

The two control variables are discretized into twenty-five time intervals. The size of the first twenty intervals is free, while for the last five intervals a fixed length is imposed to a value of one hour each. Moreover, a selectivity constraint is imposed on the process, in order to maintain the formation of the product obtained in the secondary reaction at a low value. The selectivity is constrained to a value above 80%. A list of constraints is presented in Table 4.2.

Table 4.2. Constraints for the dynamic optimization problem

Variable	Type	Unit	Lower bound	Upper bound
Selectivity	Inequality end-point	$[\%]$	80	100
Production rate		$\left[kmole/h\right]$	34.7	35.0
Selectivity	Interior point	$[\%]$	80	100
Production rate		$\left[kmole/h\right]$	25	45
Flowrate of second mixer inlet stream		$\left[kmole/h\right]$	20	100

In a first attempt, the full nonlinear model is implemented in AspenDynamics®. The software offers the possibility to perform dynamic optimization using a specialized toolbox. However, this trial was unsuccessful. The solver stuck shortly after the beginning of the simulation and no solution could be found.

Subsequently, the solution of the problem using gProms® (version 3.01) is attempted. All the constraints mentioned above are introduced as inequality type constraints in the gProms® dynamic optimization toolbox. The different gProms® solvers used for the solution of the dynamic optimization problem are listed in Table 4.3.

Table 4.3. gProms® solvers used for the solution of the dynamic optimization problem

Solver	Type	Algorithm
DOSolver	CVP_SS	Control vector parametrization single-shooting
DASolver	DASOLV	Variable time step/variable order backward differentiation formulae
LASolver	MA48	Direct LU-factorization algorithm for large, sparse, asymmetric systems of linear equations
NLSolver	BDNLSOL	Nonlinear sets of equations rearranged to block triangular form

The optimum control profiles of the control variables, shown in Figure 4.6, are obtained after several time-consuming, trial-and-error iterations. The values of the constrained variables are listed in Table 4.4.

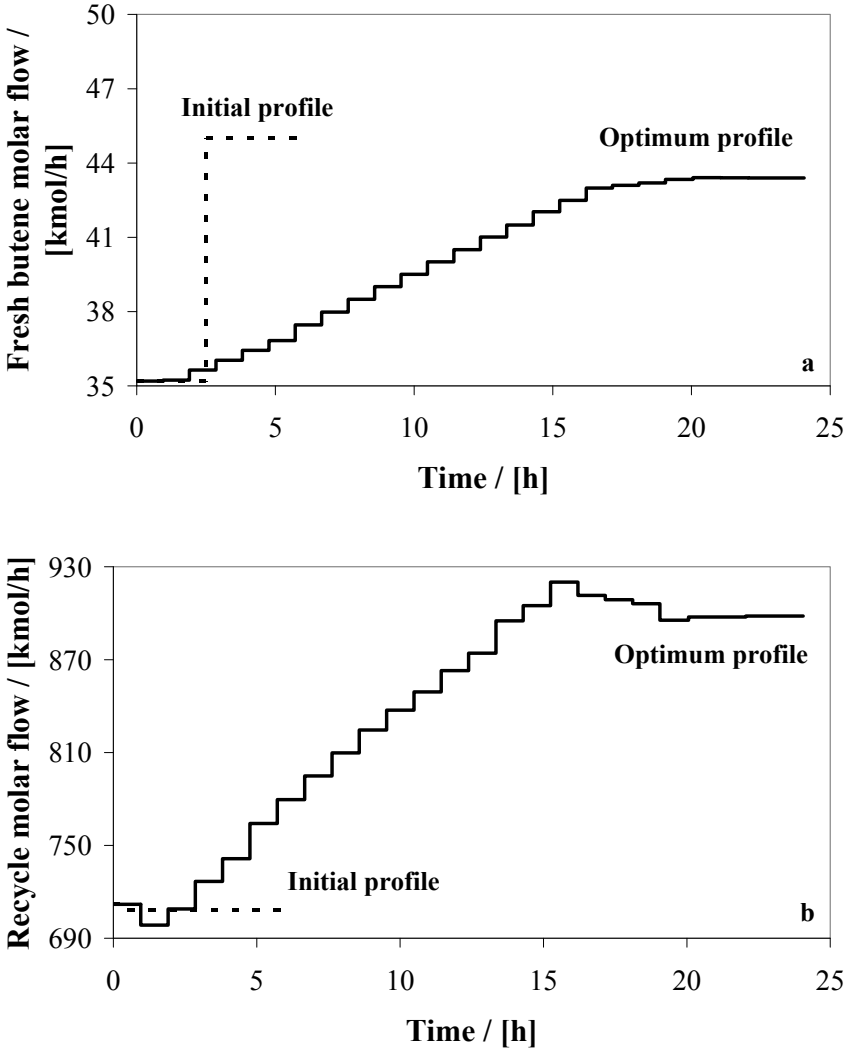

Figure 4.6. Optimum control profile for: (a) the fresh butene flow rate and (b) the recycle flow rate

The solution was obtained after a number of about 150 manual iterations, in which the user inputs initial estimates for the control variables and the time intervals. The initial profiles for the control variables (Figure 4.3) do not satisfy all the constraints, hence the optimizer recalculates them.

Table 4.4. Values of constrained variables

Interval	Time $[h]$	Type	Production rate $\left[kmole/h\right]$	Selectivity $[\%]$	Flowrate inlet second mixer $\left[kmole/h\right]$
0	0	Interior point	29.13	82.76	44.02
1	0.95		29.09	82.56	44.06
2	1.91		29.00	81.37	44.46
3	2.86		29.25	81.17	44.86
4	3.81		29.58	81.18	45.26
5	4.76		29.91	81.21	45.65
6	5.72		30.29	80.84	46.29
7	6.67		30.73	80.90	46.81
8	7.62		31.13	80.86	47.32
9	8.58		31.52	80.81	47.83
10	9.53		31.91	80.75	48.33
11	10.48		32.28	80.67	48.83
12	11.43		32.64	80.57	49.33
13	12.39		33.00	80.48	49.83
14	13.34		33.54	80.37	50.32
15	14.29		33.73	80.30	50.86
16	15.25		34.11	80.28	51.32
17	16.20		34.47	80.17	51.82
18	17.153		34.72	80.54	51.93
19	18.11		34.82	80.61	52.02
20	19.06		34.88	80.47	52.16
21	20.06		34.90	80.41	52.23
22	21.06		34.95	80.52	52.23
23	22.0588		34.96	80.55	52.23
24	23.06		34.96	80.56	52.23

The optimizer is attempting to solve the problem, but eventually stops at a point which is not a solution. The user takes the results of this optimization step, using them as new initial estimates of the dynamic optimization problem and the procedure is repeated until the solution is found. Each manual iteration step required about two hours.

The advantage of having a computationally effective reduced model at this point is obvious, since the model, in its reduced version, does not converge easily. One cause of the increased simulation time is the discretization choice, which introduces discontinuities. Another cause might be in the solver. However, since the gProms® dynamic optimization toolbox is using predefined solvers, this issue cannot be investigated properly.

Further, the optimum profiles of the control variables obtained during the dynamic optimization procedure were implemented intro AspenDynamics®. The agreement between the responses of the nonlinear and the reduced models is excellent, as seen in Figure 4.7.

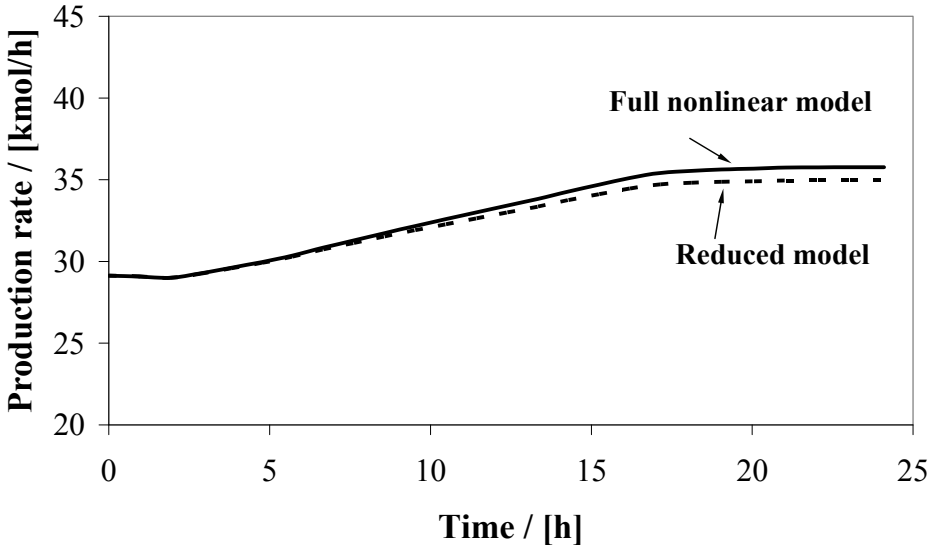

Figure 4.7. Comparison between the response of the full and reduced model after implementation of the optimum control profiles

The results in Figure 4.7 show that the transition time is quite long, as expected when the objective of the dynamic optimization problem was set. From an initial guess of about six hours, the optimum solution led to a transition of about 24 hours. To determine the cause of this behavior a study of the system's time constant should be performed. This study should be done before trying to solve the dynamic optimization problem, in order to get better initial guesses for the control variables, and reduce the optimization time accordingly.

5. Conclusions

The chapter demonstrates the advantage of considering the structure of a process flowsheet when developing reduced-order models to be used during the derivation of the optimum profiles for the dynamic operation of a chemical plant. The structure-retaining model reduction approach acts on the upper levels of the physical structure of the model: process units, compartments, domains. The individual units have been reduced in the following way: linear model-order reduction techniques have been applied for the distillation columns models, while the heat integrated reactor has been reduced by model simplification.

Similar advantages of applying this procedure for the assessment of the plantwide control structures are present for the dynamic optimization of the chemical plant's operation:

- The procedure is flexible. Tailored model reduction techniques are applied to different plant units. In the case presented above, the reactor model was reduced by model simplification, while linear model-order reduction of the balanced realization was used for the distillation columns. The dynamics of the mixers, pumps and the heat exchangers was neglected.
- The solution time is significantly reduced, by factor 75. However, the derivation of the optimal profiles proved to be a time consuming task. This can be improved by determining the time constant of the process a priori or by using a different algorithm/tool to perform the dynamic optimization.

The rigorous dynamic model of the iso-butane alkylation plant could not be used for obtaining a solution of the dynamic optimization problem.

For solving the dynamic optimization problem using the reduced model a "manual" approach must be followed to reach convergence. Several time-consuming optimization steps are performed, in which the solver does not reach a solution. The best available point available is used as initial estimates for the following dynamic optimization step, until a solution is found. Although the use of gProms® did lead to a solution, the difficult procedure required showed that the dynamic optimization was not trivial.

6. References

Abel, O., Helbig, A., Marquardt, W., Zwick, H., & Daszkowski, T. (2000). Productivity optimization of an industrial semi-batch polymerization reactor under safety constraints, *Journal of Process Control* 10, 351

Abu-el-zeet, Z.H., Roberts, P.D., Becerra, V.M. (2002). Enhancing model predictive control using dynamic data reconciliation, *AIChE Journal* 48, 324

Arellano-Garcia, H., Carmona, I., & Wozny, G. (2008). A new operation mode for reactive batch distillation in middle-vessel columns: start-up and operation, *Computers and Chemical Engineering* 32, 161

Arpornwichanop, A., Kittisupakorn, A, & Mujtaba, I.M. (2005). On-line dynamic optimization and control strategy for improving the performance of batch reactors, *Chemical Engineering and Processing* 44, 101

Banga, J.R., Balsa-Canto, E., Moles, C.G., & Alonso, A.A. (2005). Dynamic optimization of bioprocesses: Efficient and robust numerical strategies, *Journal of Biotechnology* 117, 407

Banga, J.R., Versyck, K.J., & Van Impe, J.F. (2002). Computation of optimal identification experiments for nonlinear dynamic process models: a stochastic global optimization approach, *Industrial & Engineering Chemistry Research* 41, 2425

Bansal, V., Perkins, J.D., Pistikopoulos, E.N. (2002). A case study in simultaneous design and control using rigorous, mixed-integer dynamic optimization models, *Industrial and Engineering Chemistry Research* 41, 760

Biegler, L.T. (2007). An overview of simultaneous strategies for dynamic optimization, *Chemical Engineering and Processing* 46, 1043

Biegler, L.T., Cervantes, A.M., Wächter, A. (2002). Advances in simultaneous strategies for dynamic process optimization, *Chemical Engineering Science* 57, 575

Biegler, L.T., Grossmann, I. E. (2004). Retrospective on optimization, *Computers and Chemical Engineering* 28, 1169

Carrrasco, E.F., Banga, J.R. (1997). Dynamic optimization of batch reactors using adaptive stochastic algorithms, *Industrial & Engineering Chemistry Research* 36, 2252

Cervantes, A, Biegler, L.T. (2001). Optimization strategies for dynamic systems, in Encyclopaedia of Optimization, Floudas, C.A. & Pardalos, E.M. (Eds.), *Kluwer Academic Publishers*, Vol. 4, 216

Cervantes, A., Tonelli, S., Brandolin, A., Bandoni, A., Biegler, L.T. (2002). Large-scale dynamic optimization of a low density polyethylene plant, *Computers and Chemical Engineering* 26, 227

Cervantes, A.M., Wächter, A., Tütüncü, R.H., Biegler, L.T. (2000). A reduced space interior point strategi for optimization of differential algebraic systems, *Computers and Chemical Engineering* 24, 39

Chatzidoukas, C., Perkins, J.D., Pistikopoulos, E.N., & Kiparissides, C. (2003). Optimal grade transition and selection of closed-loop controllers in a gas-phase olefin polymerization fluidized be reactor, *Chemical Engineering Science* 58, 3643

Chatzidoukas, C., Pistikopoulos, S., Kiparissides, C. (2009). A hierarchical optimization approach to optimal production scheduling in an industrial continuous olefin polymerization reactor, *Macromolecular Reaction Engineering* 3, 36

Engell, S. (2007). Feedback control for optimal process operation, *Journal of Process Control* 17, 203

Esposito, W.R., Floudas, C.A. (2000). Deterministic global optimization in nonlinear optimal control problems, *Journal of Global Optimization* 17, 97

Exler, O., Antelo, L.T., Egea, J.A., Alonso, A.A., & Banga, J.R. (2008). A tabu search-based algorithm for mixed-integer nonlinear problems and its application to integrated process and control system design, *Computers and Chemical Engineering* 32, 1877

Flores-Tlacuahuac, A., Biegler, L.T., & Saldivar-Guerra, E. (2006). Optimal grade transitions in the high-impact polystyrene polymerization process, *Industrial and Engineering Chemistry Research* 45, 6175

Geromel, J.C., Bernussou, J., & Peres, P.L.D. (1994). Decentralized control through parameter space optimization, *Automatica* 30, 1565

Grosmann, C., Erdem, G., Morari, M., Amanullah, M., Mazzotti, M., & Morbidelli, M. (2008). 'Cycle to cycle' optimizing control of simulated moving beds, *AIChE Journal* 54, 194

Haugwitz, S., Akesson, J., & Hagander, P. (2009). Dynamic start-up optimization of a plate reactor with uncertainties, *Journal of Process Control* 19, 686

Kameswaran, S., & Biegler, L.T. (2006). Simultaneous dynamic optimization strategies: Recent advances and challenges, *Computers and Chemical Engineering* 30, 1560

Konda, N.V.S.N.M., Rangaiah, G.P. Lim, D.K.H. (2006). Optimal process design and effective plantwide control of industrial processes by a simulation-base heuristic approach, *Industrial and Engineering Chemistry Research* 45, 5955

Labadie, J.W. (2004). Optimal operation of multireservoir systems: State-of-the-art review, *Journal of Water Resources Planning and Management-ASCE* 130, 93

Li, Z. & Ierapetritou, M.G. (2007). Process scheduling under uncertainty using multiparametric programming, *AIChE Journal* 53, 3183

Malcolm, A., Polan, J., Zhang, L., Ogunnaike, B.A., & Linninger, A.A. (2007). Integrating systems design and control using dynamic flexibility analysis, *AIChE Journal* 53, 2048

Michalik, C., Hannemann, R., & Marquardt, W. (2009). Incremental single-shooting – A robust method for the estimation of parameters in dynamical systems, *Computers and Chemical Engineering* 33, 1298

Miri, T., Tsoukalas, A., Bakalis, S., Pistikopoulos, E.N., Rustem, B., & Fryer, P.J. (2008). Global optimization of process conditions in batch thermal sterilization of food, *Journal of Food Engineering* 87, 485

Mohan, S.V., Rao, N.C., Prasad, K.K., Krishna, P.M., Rao, R.S., & Sarma, P.N. (2005). Anaerobic treatment of complex chemical wastewater in a sequencing batch biofilm reactor: Process optimization and evaluation of factor interactions using the Taguchi dynamic DOE methodology, *Biotechnology and Bioengineering* 90, 732

Mohideen, M.J., Perkins, J.D., Pistikopoulos, E.N. (1996). Optimal design of dynamic systems under uncertainty, *AIChE Journal* 42, 2251

Nagy, Z.K. (2007). Model based control of a yeast fermentation bioreactor using optimally designed artificial neural networks, *Chemical Engineering Journal* 127, 95

Nagy, Z.K., Fujiwara, M., Woo, X.Y., & Braatz, R.D. (2008). Determination of the kinetic parameters for the crystallization of paracetamol from water using metastable zone width experiments, *Industrial and Engineering Chemistry Research* 47, 1245

Nystrom, R.H., Harjunkoski, & Kroll, A. (2006). Production optimization for continuously operated processes with optimal operation and scheduling of multiple units, *Computers and Chemical Engineering* 30, 392

Prata, A., Oldenburg, J., Kroll, A., & Marquardt, W. (2008). Integrated scheduling and dynamic optimization of grade transitions for a continuous polymerization reactor, *Computers and Chemical Engineering* 32, 463

Rodriguez-Fernandez, M., Mendes, P., & Banga, J.R. (2004). A hybrid approach for efficient and robust parameter estimation in biochemical pathways, *Biosystems* 83, 248

Schlegel, M, Stockmann, K., Binder, T., & Marquardt, W. (2005). Dynamic optimization using adaptive control vector parameterization, *Computers and Chemical Engineering* 29, 1731

Simon, L.L., introvigne, M., Fischer, U., Hungerbuehler, K. (2008). Batch reactor optimization under liquid swelling safety constraint, *Chemical Engineering Science* 63, 770

Simon, L.L., Kencse, H. Hungerbuehler, K. (2009). Optimal rectification column, reboiler vessel, connection pipe selection and optimal control of batch distillation considering hydraulic limitations, *Chemical Engineering and Processing* 48, 938

Sonntag, C., Su, W.J., Stursberg, O., & Engell, S. (2008). Optimized start-up control of an industrial-scale evaporation system with hybrid dynamics, *Control Engineering Practice* 16, 976

Srinivasan, B., Palanki, S., & Bonvin, D. (2003). Dynamic optimizaton of batch processes: I. Characterization of the nominal solution, *Computers and Chemical Engineering* 27, 1

Srinivasan, B., Bonvin, D., Visser, E., Palanki, S. (2003). Dynamic optimizaton of batch processes: II. Role of measurements in handling uncertainty, *Computers and Chemical Engineering* 27, 27

Srinivasan, B. & Bonvin, D. (2007). Real-time optimization of batch processes by tracking the necessary conditions of optimality, *Industrial and Engineering Chemistry Research* 46, 492

Terrazas-Moreno, S., Flores-Tlacuahuac, A., Grossmann, I.E. (2007). Simultaneous cyclic scheduling and optimal control of polymerization reactors, *AIChE Journal* 53, 2301

Tholudur, A., & Ramirez, W.F. (1996). Optimization of fed-batch bioreactors using neural network parameter function models, *Biotechnology Progress* 12, 302

Tsai, K.Y. & Wang, F.S. (2005). Evolutionary optimization with data collocation for reverse engineering of biological networks, *Bioinformatics* 21, 1180

Uhl, T. (2007). The inverse identification problem and its technical application, *Archive of Applied Mechanics* 77, 325

Xia, L., Zhao, Q.C., & Jia, Q.S. (2008). A structure property of optimal policies for maintenance problems with safety-critical components, *IEEE Transactions on Automation Science and Engineering* 5, 519

5

DEVELOPMENT OF A REDUCED MODEL FOR ICE CREAM FREEZING

The focus of this chapter is on the development of a reduced model for a process unit with a complex product: the freezing step in ice cream manufacturing process. Ice cream consists of a liquid matrix in which air bubbles, fat globules and ice crystals are dispersed. The presence of multiple thermodynamic phases with changing size distributions for the dispersed phases and the rotational-axial movement of the ice cream mixture will make the dynamic modelling of the freezing step very complicated. A reduced dynamic model must be suitable to support process design and operation in a computationally effective way. The main physical phenomena accounted for in the model are: (a) the axial convective transport of mass; (b) the radial outflow of heat at the coolant wall to the refrigerant; (c) the growth of the frozen ice layer at the wall; (d) the periodic removal of the ice by scraping and the melting of the ice particle population in the bulk liquid; and (e) the cooling of the ice cream mix.

The development of the reduced model is obtained in two steps. (A) From a conceptually conceivable, truly comprehensive model of the process, a relatively detailed model with five coordinates is developed. This 5-D model is still computationally too intensive for use in inverse problems. (B) Further reductions are performed, primarily aiming at reducing the number of coordinates of the model, going from a 5-D to a 3-D model. The conservation equations for mass, energy and momentum per thermodynamic phase and population balances are complemented with rate equations for the relevant physical phenomena, as well as phase equilibrium conditions and thermodynamic equations of state. The rate laws are kept deliberately simple by coupling a flux to only one dominant driving force and allowing for experimentally adjustable rate parameters. The resulting 3-D model consists of several partial differential equations, with the appropriate number of initial and boundary conditions, and coupled with many nonlinear algebraic equations.

For the use of the reduced model in simulation and optimization applications, it is practical to have a complementary overview of system's input-output. To this end, the model inputs have been classified into feed and operational conditions, design and physical parameters, while the outputs relate to the product quality and process performance.

1. Introduction

1.1. Model reduction for complex units and products

As seen in Chapter 3 and 4 of the thesis, the model reduction in case of the complex processes with simple, single-phase products focuses on the upper levels of the network structure of the process. However, many processes deal with more complex, multiphase products. The complexity of the process lies in these cases in both the structure of the process and the product. Hence the model reduction can be performed at both process (units, compartments, etc.) and product (phases, species, etc.) scales.

In this chapter, the focus will be on developing a reduced model for a single process unit with a complex product. In this way, the characteristics of the model reduction approach when dealing with multiphase products will be highlighted. The influence of the full process flowsheet structure will be neglected at this point.

The main distinction of such a unit with a complex structured product is a reduction in the network-like aspects of the process structure, as it features only the unit possibly having internal distinct compartments and domains, like trays in distillation columns. Moreover, more spatial coordinates inside the unit need to be considered, along which the behaviour and the product structure is distributed. The product structure considers more dispersed phases and populations having internal states and a host of transfer phenomena occur between these component phases and populations.

The model reduction can be performed in two stages:

a) a conceptual reduction in the model development stage
b) a numerical reduction of the mathematical model of the process

This chapter will focus on the options that can be applied for a conceptual model reduction in the development stage.

Similar to the previous chapters a case study will be used to outline the model reduction approach and its advantages. The development of a dynamic model for the freezing step in ice cream manufacture will be presented. The model is intended to be a tool for the design and operation of the freezing of ice cream. For the model to be of a real help in product design and processing studies, the model must be suitable for use in an inverse model, hence the need to ensure the solution of the model is computationally feasible.

1.2. Ice formation in a scraped surface heat exchanger

The freezing of the ice cream mix is one of the most important operations in making the ice cream, for upon it depend the quality, palatability, and yield of the finished product (Arbuckle, 1986). However, understanding the behaviour of the material inside the freezer is still incomplete (Duffy, Wilson & Lee, 2007). Ice cream (Figure 5.1) is a complex colloidal system comprised, in frozen state,

of ice particles, air bubbles, partially coalesced fat globules, all in discrete phases, surrounded by an unfrozen continuous matrix of sugars, proteins, salts, polysaccharides and water.

The freezing process can be divided into two parts: (a) a dynamic freezing step, during which the mix is quickly frozen while under agitation to incorporate air, and (b) a hardening step, that freezes the remaining water, without agitation. The first phase of the freezing accounts for freezing of 33-67% of the water depending on the drawing temperature; the hardening process may account for an additional 23-57%, depending on the drawing temperature (Arbuckle, 1986).

In dynamic freezing, the most important changes in the material streams are the formation of ice particles, incorporation of air (overrun), formation of small air cells, and destabilization of the fat emulsion. Each of these steps is critical to production of high quality ice cream with the desired physical characteristics and must occur whether the freezing is done in a batch or a continuous process. However, differences in formation of these structural elements may occur based on the type of freezer used and the type (and amount) of ingredients used in the mix. The product of the dynamic freezing is soft frozen and flowable, but the degree of stiffness varies with formula, process, freezer design, overrun and temperature.

The air content / air bubble size and the ice particle size affect the texture of ice cream. For this reason, these properties could be used as quality indicators. Since these are distributed properties and direct measurement of these variables inside the freezer barrel is difficult, if not impossible to achieve, are specified in practice. The feed intake, the processing conditions and equipment design parameters are adjustable to meet the target output variables.

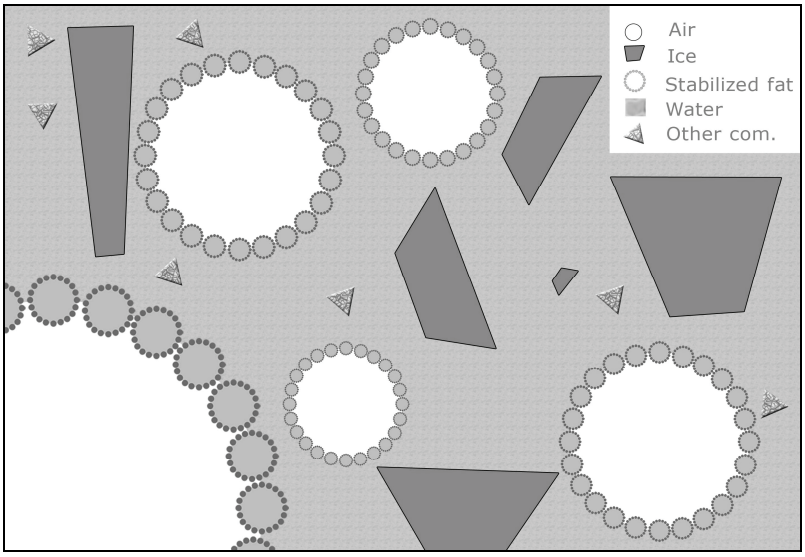

Figure 5.1. Ice cream structure

The steps that need to be followed in order to obtain the model are:

a) A detailed model of the ice cream freezing step is developed. The fundamental phenomena are conceptually considered. Conservation equations for the mass, energy and momentum are considered, taking into account the complexity of the product. Information related to the phase equilibrium conditions, equations of state, and the rate equations are added to the model. Simplifications are introduced in a judicious way, and the variables and the equations are written on a rigorous coordinate set.
b) Having too many coordinates for practical use (computation times and effort) of the model, the coordinate set is reduced. Averaged values are taken for the variables over the domains of the eliminated coordinates. Moreover, reduction of description of phenomena that essentially play out in a 3-D geometric space, like the momentum, is needed. Projection on a lower dimensional space is carried out.
c) Since the knowledge about the mathematical structure and the parameters of the rate equations is limited, these rate equations need to be determined with insight from non-equilibrium thermodynamics (NET) and using experimental data. In a first attempt, each rate equation is made dependent on a single driving force in a linear way, while most of the rate parameters are obtained from literature data. The resulting parameters are not representing the reality in full measure, but the model is able to predict the right "trends" (for example the order of magnitude).

The obtained reduced model is more sophisticated than any preceding model, yet it is reduced with the conceptually conceivable rigorous model of the ice cream freezing unit.

The chapter is structured in the following way: Section 2 introduces the physical phenomena that take place inside the freezer. The detailed (5-D) model, with respect to the conservation equations, is introduced in Section 3. Section 4 presents the reduced (3-D) model, while the equations for the rate laws are presented in Section 5. The 3-D reduced model of the freezing unit is summarized in Section 6. The numerical implementation of the model is presented in Section 7. Section 9 discusses some applications for future model use with some numerical results, while conclusions are presented in Section 10 of this chapter.

2. Physical aspects and modelling approach

In the following section, the ice cream ingredients and structure are discussed in more detail. The features of the freezing equipment, as well as the mechanism are presented in order to create the perspective for the development of the conceptual model of the freezer unit. The end of this section discusses the objective and the approach of the model reduction for the ice cream freezing.

2.1. Ice cream structure

The ice cream microstructure (Figure 5.1) has a strong effect on the sensory manifestation. A typical ice cream consists of about 30% ice, 50% air, 5% fat and 15% matrix (sugar solution) by volume.

This means that all three states of matter are contained in its microstructure: solid ice and fat, liquid sugar solution and gas (Clarke, 2004). These main ingredients provide the sensory properties of the final product: ice gives cooling, fat provides creaminess, air gives lightness and softness, sugar provides sweetness, while the flavours enhance the taste.

However, not only the right amount of components gives the desired properties of the ice cream, but also the way these elements are brought together in the microstructure.

In the following section, the influence of the ice particles, the liquid matrix, the fat droplets and the air bubbles on the ice cream structure will be discussed in more detail.

2.1.1. Ice particles

Ice particles form a discrete phase inside the ice cream structure. The amount and size of the particles have a strong effect on the quality of the product. Formulations that lead to numerous, small, discrete ice particles also lead to enhanced smoothness in texture. Ice crystal formation in ice cream is generally by secondary nucleation in the scraped surface freezer (Goff, 2002). The freezer is the only place in the entire ice cream manufacturing and distribution chain where ice is nucleated. In all other stages of the manufacturing and distribution process any change in temperature results in an increase (colder temperatures) or decrease (warmer temperatures) in the size of existing particles, or possibly the complete disappearance of smaller, less thermodynamically stable particles. This implies that the number of particles in the product after storage and distribution will always be less than the number formed in the freezer. As the tendency is always for the larger particles to grow at the expense of smaller ones, it is important to form a large number of small particles in the freezer.

2.1.2. Liquid matrix

The matrix is a concentrated solution of sugars, stabilizers and milk proteins in water. As the premix becomes freeze-concentrated, components that are either dissolved or dispersed in water are increasingly brought together as temperature decreases and water is removed from solution. Two of the important hydrocolloid components include the polysaccharides and the casein micelles. Typically, at the end of the freezing process, 50% of the water in the ice cream mix is frozen.

2.1.3. Fat droplets

The fat phase exists in the form of tiny globules that have been formed in the homogenizer. The proteins act as emulsifiers and give the fat emulsion its needed stability. When the mix is subject to the whipping action of the freezing barrel, the fat emulsion begins to break down partially and the

fat globules begin to flocculate or destabilize. The air bubbles beaten into the mix are being stabilized by this partially coalesced fat. If emulsifiers were not added, the fat globules would have so much ability to resist the coalescing, that the air bubbles would not be properly stabilized and the ice cream would not have the same smooth texture (Eisner, Wildmoser & Windhab, 2005; Koxholt, Eisenmann & Hinrichs, 2001).

2.1.4. Air bubbles

The air content in the ice cream structure is defined as overrun. The overrun, expressed as percentage, is generally defined as the volume of gas to the volume of liquid (Clarke, 2004)

The main role of the air is to make the ice cream soft. Air is distributed in the form of numerous small air bubbles of size range 20-50 μm (Goff, 1997). The gas phase volume varies greatly from a high of more than 50% to a low of 10-15%. Air is incorporated either through a lengthy whipping process (batch freezers) or as it is drawn into the mix by vacuum (older continuous freezers) or is injected under pressure (modern continuous freezers). The incorporation of air alone, or the shearing action alone, independent of freezing, are not sufficient to cause the high degree of fat destabilization that occurs when ice crystallization and air incorporation occur simultaneously (Marshall, Goff & Hartel, 2003).

2.2. Scraped-surface heat exchanger

The dynamic freezing of ice cream is performed in a scraped surface heat exchanger (SSHE). Ice cream freezers consist of a cylindrical barrel typically 0.2 m in diameter and 1m long. However, the size may vary for the freezers designed for different production rates (Clarke, 2004). The mix is pumped along with air into the SSHE (Figure 5.2) and the action of the rotor inside the tube blends the air into the matrix. The freezing medium in the jacket, typically ammonia, freezes the water into a thin layer of ice on the barrel wall from which finely dispersed ice particles are continuously scraped and incorporated into the ice cream (Russell, Burmester, & Winch, 1997).

The operation of the freezer is controlled by several variables. The pressure of the refrigerant sets the temperature at which it evaporates, hence the wall temperature (typically -30 ^{0}C). The mix and air inflow and the ice cream outflow rates determine the residence times, which can vary from 0.4 to 2 minutes, the overrun, the pressure inside the barrel (typically 5 atm) and the throughput (which can be as much as 3000 l/h in an industrial freezer). All of these factors, together with the rotation speed of the rotor, which is typically 200 rpm, determine the outlet temperature of the ice cream, as well as the size distribution of the air bubbles and ice particles.

The greatest advantage of using SSHE is the constant removal of the stagnant film near the exchanger wall and the subsequent increase in the heat transfer coefficients, and reduction in fouling at the wall (Rao & Hartel, 2006).

The time between scrapes is typically 0.1 s (Clarke, 2004), thus a very thin layer of ice can form before it is removed by the movement of the scraper blades. The number of scraper blades may

vary and is typically in the range of 1 to 4. A typical SSHE cross-sectional configuration is shown in Figure 5.3.

The small ice particles that are scraped off the freezer's wall are dispersed into the liquid mix by the beating of the dasher. There are large temperature gradients inside the barrel, both radial (colder at the wall to warmer at the centre) and axial (warmer at the inlet to colder towards the outlet).

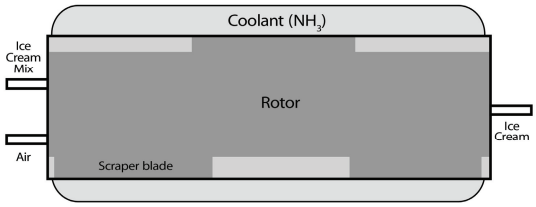

Figure 5.2. Scraped-surface heat exchanger for ice cream freezing

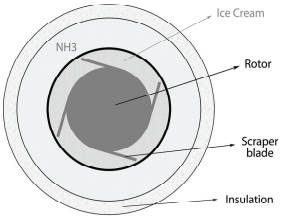

Figure 5.3. Cross-sectional diagram of a typical scraped-surface heat exchanger

Therefore, the dispersed ice particles into the warmer mix at the centre of the barrel, they melt and cool it down; near the inlet the particles all melt, but one-third of the way through the barrel the mix becomes cold enough for the ice particles to survive (Clarke, 2004). The freezing rates inside the barrel can vary from 5 to 27 ^{0}C/min, respectively.

The two primary flow directions of the fluid are flow in the angular direction due to rotation and flow in the axial direction due to the imposed pressure gradient. The velocity components of the two flows form a helical path for the product through the SSHE. A complete mixing in the angular direction is desired to maximize the efficiency of heat transfer and ensure uniform thermal treatment. At the same time, the mixing in the axial direction should be minimized because the axial mixing increases the residence time distribution of the product in the SSHE (Wang, Walton & McCarthy, 1998).

Ice cream behaves as a non-Newtonian material. Moreover, both convection and dissipation of heat can be significant inside the SSHE. Due to these many interacting physical phenomena, coupled with the fact that the geometry is complicated, the overall behaviour inside the SSHE becomes very complex.

2.3. Freezing mechanism

In a recent study, (Qin, Chen, & Farid, 2004) shows that, during the ice formation on a subcooled surface, the ice appears primarily at some spots and forms separate ice 'islands'. These 'islands' grow larger until the subcooled surface was frozen-over by a thin film of ice. During this period, the thickness of these ice patches was almost unchanged. For this reason, (Qin, Chen, & Farid, 2004) concluded that this is an indication of the fact that the growth of ice along the cooling surface is much faster than the growth rate in the normal direction. It was also concluded that the formation of this film characterizes an intermediate, transitional stage between the ice nucleation and the normal

growth of the ice layer. After this transitional stage, the growth of the ice layer starts. For ice layers growing from aqueous solutions, concentration gradients of solutes are formed near the growing front. In this case, the coupling between the heat and the mass transfer should be taken into account (Qin, Chen, Ramachandra & Free, 2005).

In (Marshall, Goff & Hartel, 2003) the following mechanism of describing the ice formation and development in a scraped-surface heat exchanger is presented:

(a) Because of the low temperatures and the rapid freezing process, the ice layer forms at the cylinder wall. This layer is not fully crystallized, but is a slush layer. This slush contains abundant small ice particles, in addition to a concentrated solute (sugars, salts, etc.) and probably has a slightly higher density than the original mix.

(b) The scraper blade removes this slush layer from the barrel wall and mixes it with the warmer mix remaining in the centre of the barrel.

(c) The cold slush melts as it cools the warmer mix. In a continuous freezer, this occurs near the entry point of the mix into the freezer barrel as the freezing process begins.

(d) Once the bulk of the mix is cooled sufficiently, some of the ice particles from the slush begin to survive. These ice particles grow into rounded disk-shaped particles based on the conditions (heat transfer and mixing) in the barrel.

(e) As ice content increases during the freezing process (or along the length of the freezer in a continuous process), the new ice layer scraped from the wall primarily contributes to the growth of the ice particles formed earlier in the process, although some nuclei from the slush layer survive and grow ending up in the product.

(f) As more and more water is turned into ice, the remaining fluid becomes increasingly viscous since the formation ice is taking up essentially pure water (other molecules are excluded from ice as particles form).

2.4. Scope and approach to modelling of the ice cream freezing unit

The modelling of the freezing unit is at its beginnings. Only recently, a transition from a trial-and-error approach for the development of the unit to a more rigorous approach, where in the centre of the design is a model based on fundamental knowledge, has been started. However, the changes are done in small steps.

In (Bongers, 2006) the freezer unit was modelled in a simplified way. The barrel was considered as a series of well-mixed stages. Heat, mass and momentum equations were developed considering the phases as pseudo-continuous. Details regarding the distribution of the air bubbles and ice particles within the ice cream structure were not taken into account.

In other models, the distribution of ice particles or air bubbles is present only partially. For example, in (Aldazabal, Martin-Meizoso, Martinez-Esnaola & Farr, 2006) only the ice particles distribution is considered and the growth of these particles is modelled, while in (Duffy, Wilson & Lee, 2007) the modelling of the isothermal fluid flow inside the freezer unit is attempted.

Other models focused on the heat (Sun, Pyle, Fitt, Please, Baines & Hall-Taylor, 2004) or momentum (Yataghene, Pruvost, Fayoll & Legrand, 2008) inside a scraped surface heat exchanger, using a generic non-Newtonian fluid.

Table 5.1. Models of the ice cream freezing step

Model attributes		Sun et al, 2004	Aldazabal et al, 2006	Bongers, 2006	Duffy et al, 2007	Yataghene et al, 2008
Scope of model		Heat transfer in SSHE	**Ice growth in SSHE**	**Heat transfer in SSHE**	Fluid flow in SSHE	CFD analysis of flow pattern
Distributed		No	Yes (Ice)	No	No	No
Domains		2	2	3	2	2
Phases	*Continuous*	Fluid	Liquid	Fluid	Fluid	Fluid
	Dispersed	-	Ice	Ice + Air + Fat	-	-
Components		1	3+	6	1	1
Dynamic		No	No	Yes	No	No
Coordinates	*Spatial*	2	3	1	2	2
	Internal	0	0	0	0	0
	Total	2	3	2	2	2
Differential (conservation) equations	*Mass*	Yes	Partial	Yes	Yes	Yes
	Population	No	Partial	No	No	No
	Energy	Fluid domain	No	Yes	No	No
	Momentum	Yes	No	Yes	Yes	Yes
Algebraic equations	*Rate laws*	Yes	Growth only	Yes	Yes	Yes
	Physical properties	Yes	Yes	Yes	Yes	Yes

An overview of the main characteristics of these models is presented in Table 5.1. The models which refer to the modelling of the ice cream freezing have the scope in bold, while the rest refer to models of non-Newtonian fluids in a scraped surface heat exchanger.

To conclude, there is not yet available a model of the freezing unit that combines all the physical effects present:

- axial mass transport with spiralling flow and mixing
- mass, heat and momentum transfers between phases
- non-Newtonian flow behaviour
- evolution of size distributions of the dispersed phases, such as ice crystals and air bubbles
- scrapping of the solid ice layer from the inner heat exchanger surface, etc

The ambition of this research is to combine some main effects into a new, more comprehensive model. Yet, the resulted model remains a reduced model with respect to the conceptually conceivable complete model, covering in principle all relevant coordinates, phases, species and phenomena.

In the previous sections, information regarding the physical aspects of the ice cream freezing has been presented. The focus in the following is on the conceptual phase of the model formulation and reduction for ice cream freezing in a SSHE.

Applying the modelling and model reduction procedure (summarized in Table 2.1 and Figure 2.13, respectively, in Chapter 2 of this thesis) for the ice cream freezing will result in several models. An overview of the different types of models and in which component of the model the simplifications were implemented, for each case, is presented in Figure 5.4.

Firstly, there is the "conceptual model" of the ice cream freezing, as the scientist's perception of physics of the process. This contains all the available information regarding the phenomena and their interactions in the unit. This model is the mental model reference from which reductions are going to be made.

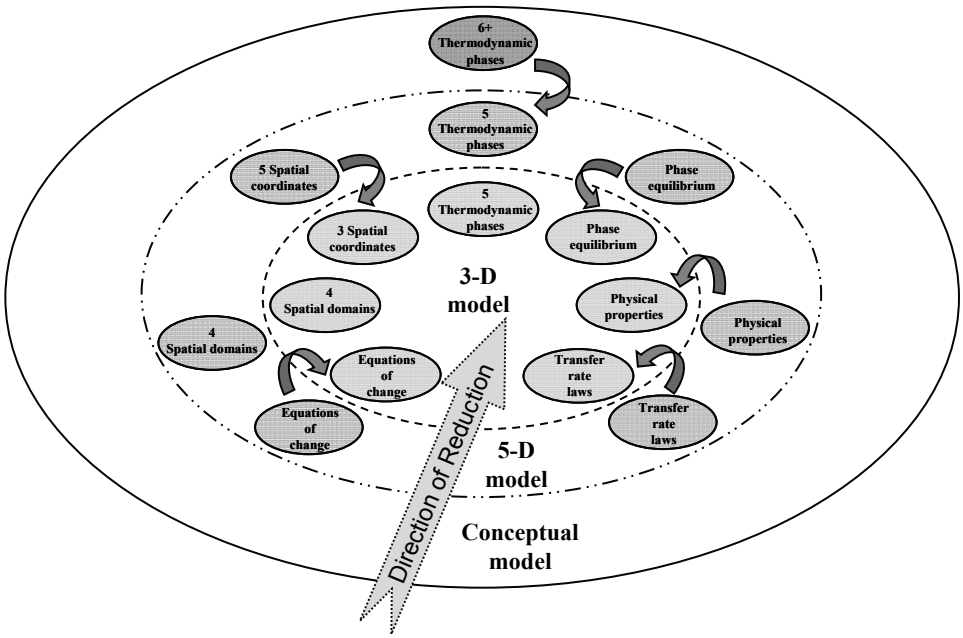

Figure 5.4. Ice cream modelling approach

Secondly, there is the "5-D model". This model considers five coordinates (the time and four spatial coordinates), four spatial domains (as shown in Figure 5.5) and five thermodynamic phases inside the freezer. The conservation equations are written in a rigorous way. This model includes also

rigorous information regarding the phase equilibrium and all the rate law equations. Solving a model with five coordinates (time and spatial) requires a huge computational effort. Moreover, the knowledge about the mathematical structure and the parameters of the detailed, distributed rate equations is limited.

For these reasons, a simplification is required in order to make the solving of the model possible. Firstly, the number of coordinates is reduced by "averaging" over one or more coordinates. The "averaging" procedure is explained later. Moreover, simplifications are introduced in the fluid flow equations, in the rate laws, as well as in the physical properties models. The result of this procedure is the "3-D" model.

The 5-D and the 3-D models are further detailed in the following sections.

3. Specification of the 5-D model of the ice cream freezing unit

Once the process system to be modelled has been defined, the suitable network structure, as well as the mathematical relationships for the behaviour of the different entities should be specified. The following sections discuss the 5-D model of the ice cream freezing unit, which is derived from the conceptual model.

The first step in developing a chemical engineering model is to set the conservation equations. For this, all the fundamental physical resources and phenomena are conceptually considered. Thus, the model includes equations for the mass, energy and momentum for all the phases and domains considered.

The conservation equations are based on five coordinates are considered: the time, t, the axial coordinate, z, the radial coordinate, r, the angular coordinate, θ, and the internal coordinate of the distributed phase, s. For this reason, this version of the model of the ice cream freezing step will be called the *5-D model*.

This 5-D model is not developed in full detail in this section. Only the conservation equations are covered. Understanding these conservation equations is a pre-requisite for developing the more practical reduced 3-D model. In the description of the conservation equations of the 5-D model in this section, the emphasis is on making proper physical assumptions. To avoid pages of extensive mathematical equations, the resulting mathematical equations are presented in the Appendices.

3.1. Spatial domains with thermodynamic phases

Taking into account the physical aspects presented in Section 2 and considering the intermediate stage in ice formation instantaneous, the phases at the process side are assumed split between two domains (see Figure 5.5). The two domains at the process side are forming the "barrel" compartment, although in reality, the barrel is separated by the blades in a number of domains, which are not considered at this point:

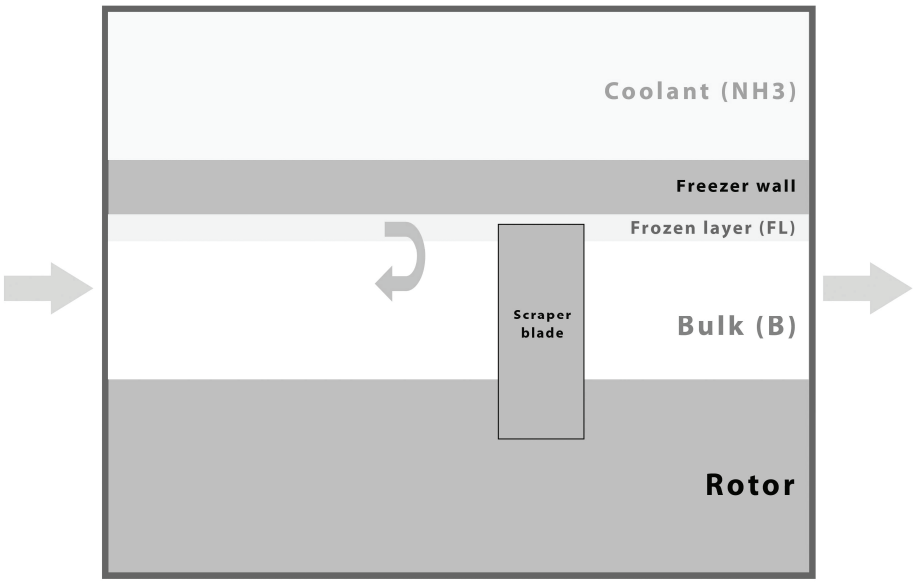

Figure 5.5. Model domains

1) The frozen layer domain

The water that is exposed to the freezer wall crystallizes instantaneously and forms a frozen layer (FL) of immobile (solid) ice. In this layer, the ice crystallizes only by primary nucleation due to fast freezing. The ice is subsequently removed from this layer by the scraper blades. The rate of ice formation is determined by the cooling rate and the heat transfer. The rate of change for the frozen layer is determined by the movement of the scraper blades. In reality, all the components are present in this layer. However, for the purpose of this research, we will assume that only water and ice are predominant in this layer.

2) The bulk domain

This domain is represented by the moving fluid ice cream. The ice scraped from the frozen layer – as a size distributed population of small crystalline particles - is transported into this domain by the movement of the scraper blades. In the same time, a part of the ice coming from the frozen layer is melting into the bulk (B). The ice can crystallize in this compartment by secondary nucleation. However, this is not considered in our research, because the bulk fluid is assumed too warm for that purpose. The bulk consists of ice particles, air bubbles and fat globules dispersed in a pseudo-continuous and pseudo-homogeneous fluid matrix of unfrozen water, sugars, proteins, etc. In order not to make the model much too complex, the following phases will be considered as pseudo-components of the fluid matrix in the next chapters: ‘water’, ‘sugar’, ‘fat’ and ‘other components’.

Table 5.2. Thermodynamic phases considered in the model

Phases	Domains				
	Process side		Equipment related		
	Bulk layer	Frozen layer	Wall	Coolant	Rotor
Ice	✓◘	✓■			
Air	✓◘				
Matrix	✓■				
Solid metal			✓■		✓■
Boiling liquid				✓■	

◘ = dispersed phase; ■ = continuous phase

The model will consider two types of phases: the phases at the process side and the equipment related phases, which are shown in Table 5.2. Each phase contains at least one component. The phases at process side are: (a) the ice particles, as a size distributed population, (b) the fluid matrix, and (c) the air phase in the bulk domain and (c) the solid layer of ice in the frozen layer domain. Although the fat is a separate phase inside the ice cream structure, in the following it will be assumed as being lumped inside the liquid matrix phase. In addition to these process related phases, some equipment related phases must be accounted for the energy and momentum balance: the solid phases (not deformable) – the freezer wall and the rotor, and the fluid coolant medium – boiling ammonia.

3.2. The generic equation of conservation for the physical resources

A pseudo-continuous approach is taken in which the entire space between the barrel wall and the rotor space is assigned to the bulk fluid and the frozen layer. The rotating scraper blades are ignored in the modelling. The effects of these rotating blades are accounted for the equations of change for mass, energy and momentum. A correction for the effective volume available to the fluid phases must be made, after subtracting the volume taken by the blades from the void volume.

The coordinates for the domains considered in the model are presented in Table 5.3.

The conservation equations of a physical resource can be written in differential form, in the following general way (adapted from Hangos & Cameron, 2001):

$$\frac{\partial}{\partial t}\Phi^{(R)} + \nabla \cdot J^{(R)} = q^{(R)} + \theta^{(R)}_{(\varphi\rightarrow)} \tag{5.1}$$

The divergence of $J^{(R)}$ is given by equation (7.5) in Appendix 1.

Table 5.3. Coordinates considered in the model

Coordinate		Domains				
		Process side		Equipment related		
		Bulk layer	Frozen layer	Wall	Coolant	Rotor
Time		$0 < t$				
Spatial	**Axial**	$0 < z < L$				
	Radial	$R_0 < r < R - \delta_{FL}$	$R - \delta_{FL} < r < R$	$R < r < R + \delta_{wall}$	$R + \delta_{wall} < r < R_c$	$0 < R_0$
	Angular	$0 < \theta < 2\pi$				
Internal		$0 < s^{(i)} < s^{(i)}_{max}$	*NA*			

Initial conditions and a number of boundary conditions for each coordinate considered must be specified (Hoffman, 2001) together with equation (5.1).

List of symbols

$\Phi^{(R)}$ = specific quantity of resource

$J^{(R)}$ = flux of resource

$q^{(R)}$ = terms related to the sources and sinks of property

$\theta^{(R)}_{(\varphi\rightarrow)}$ = terms related to the transfer terms from other phases

L = freezer length, $[m]$

R_0 = internal radius of the freezer, $[m]$

R = external radius of the freezer, $[m]$

δ_{FL} = the thickness of the frozen layer, $[m]$

$s^{(i)}_{max}$ = upper bound for the internal coordinate, $[m]$ or $[kg]$

δ_{wall} = wall thickness, $[m]$

3.3. Mass

The conservation equations for the mass are written taking into account the complexity of the processing. Information related to the phase equilibrium conditions, equations of state, and the rate equations are considered. Simplifications are introduced in a judicious way, and the variables and the equations are written on a rigorous coordinate set.

The following assumptions are considered when writing the conservation equations for the mass:

1. In the bulk domain, only two phases are considered: the “ice” (particles) phase and an aggregated liquid “matrix” phase. This liquid matrix phase is assumed pseudo-continuous. The mixture of the “matrix” phase, the solid “ice” particles and the “air” phase is known as “ice cream”.
2. The “ice” phase is considered as a size distributed population of particles, dispersed in the “matrix” phase. The state of a particle is characterized by internal state variables. Only one internal state variable will be considered: the diameter or equivalently, the mass of a particle. The age and the temperature of a particle could be considered as the second and the third internal state variable, respectively, but will not be taken into account (e.g., for the purpose of calculating the residence time distribution of the ice particles leaving the freezer).
3. The “aerated liquid” phase is an aggregated one, containing the continuous liquid “matrix” and dispersed “air” bubbles.
4. The “air” phase is normally dispersed as a population of bubbles of different sizes inside this liquid phase in a real physical system. In this model, the “air” phase will represented as a separate, lumped phase, being treated as a pseudo-component inside the liquid “matrix”.
5. The liquid “matrix” contains water and some dissoluted organic components, such as fat, sugar, proteins, etc. Only the following components are considered in the model: “water”, “fat”, and “sugar”. The rest of the components, depending on the ice cream recipe, will be lumped into one single component known as “other”. In total, the model assumes a number of five (pseudo)-components.
6. The “frozen layer” domain contains only solid ice. The ice in the “frozen layer” it is assumed immobile in axial and angular direction. The thickness of the “frozen layer” in radial direction varies periodically due to growth by freezing in between two successive scrapings.
7. The temperature of the “frozen layer” is considered lower than the temperature inside the bulk domain at the same axial position.
8. Ice crystallization does not occur inside the bulk domain. Only the melting of particles is considered. No nucleation, attrition or agglomeration is considered.
9. There are some mass-related transfers between the “frozen layer” and the “bulk” domain. The removal of the ice from the frozen layer and its transfer into the bulk is due to the scraping action. Water from the “matrix” phase and dispersed ice particles in the bulk domain are (radially) transferred to the frozen layer.
10. Though the coolant exerts its action by (partial) evaporation, the total flow remains constant along the axial direction and the mass balance is not of interest.

In the previous assumptions, different phases were presented, which will also be used in the development of the models equations. An overview of their composition is presented in Table 5.4.

3.3.1. The bulk domain

The mass conservation equations for the bulk domain are written for the dispersed phases (ice particles), as well as for the pseudo-continuous phases (liquid matrix, air).

Table 5.4. Nomenclature and composition of the phases considered in the model

Phases	Components					
	Ice	*Water*	*Air*	*Sugar*	*Fat*	*Other*
***Ice*◘**	✓					
***Matrix*■**		✓		✓	✓	✓
***Air*◘**			✓			
***Aerated liquid*■**		✓	✓	✓	✓	✓
***Ice cream*■**	✓	✓	✓	✓	✓	✓
***Frozen layer*■**	✓					

◘ = dispersed phase; ■ = continuous phase

(a) The conservation equations for the *dispersed phases* for the bulk domain are written in the form (Ramkrishna, 2000) of the *population balance equation* (7.9), in Appendix 2.

(b) The conservation equations for the mass of the *pseudo-continuous phases* in the bulk domain are written in the form of the *mass balance equation* (7.16), in Appendix 2.

3.3.2. The frozen layer domain

The starting point for the derivation of the mass conservation equations for the frozen layer is the mass balance equation (7.21), in Appendix 2. Since the frozen layer consists practically of a solid layer of pure ice, the concentration of ice inside this layer is constant.

The only thing changing during the freezing is the position of the boundary of the frozen layer, through the layer's thickness. The thickness of the frozen layer modifies periodically through two actions, shown in Figure 5.6:

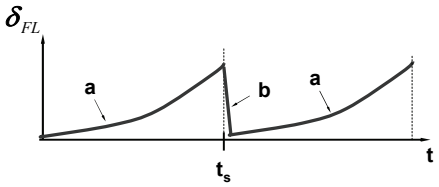

Figure 5.6. Periodical modification of the thickness of the frozen layer

(a) the crystallization of water on the freezer's wall during the time between two successive scrapes, t_s

(b) the removal of the thin layer of ice obtained by the movement of the scraper blades at t_s

3.3.3. The equipment related domains and phases

The mass conservation equations for the equipment related domains phases (rotor, wall and coolant) are not required, since no transformation of this resource is considered by the model in these phases.

3.4. Momentum

In a similar way to the mass conservation equations, the momentum conservation is written on the same rigorous coordinate set. It is assumed that the momentum of the phases inside the ice cream mixture are added up and lumped into the momentum of the ice cream mixture as a whole. The momentum equations are written in the compact form of a substantial derivative balance equation for the 3-D vectorial momentum, shown in equation (7.26), in Appendix 3.

The consequence of this lumping is that information on the momentum of the individual phases is lost. To remedy for this loss the following assumption is made:

11. The “ice” and “aerated liquid” phases in the bulk layer are assumed to have locally equal velocities for each of the directions (axial, radial, and angular).

3.5. Energy

Some additional assumptions need to be taken into account when writing the energy conservation equations:

12. The “aerated liquid” and the “ice” phases are in thermodynamic equilibrium for the given composition of the “matrix” phase at an ‘equilibrium’ temperature. Below this temperature the ice particles form. Above this temperature they melt.
13. The liquid – ice equilibrium temperature is lower than the “aerated liquid” temperature due to a melting point depression due to the sugars in the liquid.
14. Due to external cooling, the frozen ice layer has internally lower temperature than the “aerated liquid” in the bulk domain.
15. After breaking away from the frozen layer, the ice particles in the bulk domain heat up rapidly to the temperature of the particles existing in the bulk domain. This assumption of rapid heating of the ice particles is justified by the relatively high thermal conductivity inside the ice crystal, relative to the heat conductivity in the bulk fluid and the heat transfer rate to the crystals.
16. The temperature of the inner part of the ice particle is uniform.
17. The ice particles floating in the bulk will all have the same temperature, which is lower than the “aerated liquid” phase temperature. This temperature is taken equal to the ice-water-sugar phase equilibrium.
18. The heat transfer from the “aerated liquid” phase to ice particles is used for the supply of energy for a phase change between solid (ice) and liquid water.

19. The temperature at the interface between the frozen layer and the bulk will be equal to the equilibrium temperature of the ice in the bulk domain. From there, a (small) temperature gradient over the frozen layer exists towards a lower temperature at the interface with the inner side of the metal wall due to cooling by the coolant at the outer side of the freezer wall.
20. The metal wall will have inside lower temperatures than the frozen layer, while they have equal temperature at their interface.
21. Fast dynamic storage effects in the metal wall will be ignored by virtue of high thermal conductivity, in such way that a thermal pseudo-steady state flux is maintained in radial direction.
22. At the interface with the coolant, the metal wall takes the (lower) temperature of the coolant.
23. The coolant has a constant temperature all over the entire external surface of the metal wall, which is assumed to be maintained by phase equilibrium between liquid and vapour phase of the coolant.
24. A pseudo-steady state assumption is applied to the energy balance of the rotor. Dynamic storage effects are ignored. The rotor has internally a uniform temperature in radial and angular directions due to a high conductivity. The rotor temperature can vary in axial direction.
25. The axial rotor temperature is set locally equal to the temperature of the "aerated liquid" phase at the interface, with no heat transfer between rotor and fluid. This latter condition is physically a simplification, but thought to have a minor effect to the amount of work done by the rotor on the fluid.
26. The energy content is expressed by means of enthalpy, accounting for volume work.

Under these assumptions of non-equilibrium between some of the domains and phases, five energy balances will be required. These energy balances are coupled by heat transfer terms, expressing the heat content of mass being transferred between phases as well as the direct conductive thermal heat transfer. The energy balances will be written for:

(a) The aerated liquid phase (assumed to have the same temperature).
(b) The (melting of) ice particles in the fluid bulk
(c) The frozen layer, applying the average thickness over the periodic scraper rotation
(d) The metal wall (pseudo steady state assumption leading to a flux expression)
(e) The coolant (to get the cumulative cooling duty)

The coupling between these balances is done in the following way:

a) 0/1: Work done by the rotor/scraper is absorbed by the fluid in the bulk
b) 1/2: Heat flux by heat transfer from the fluid phase to the colder floating ice particles and the energy flux of melt water flow from the melting ice particles into the fluid bulk
c) 2/3: Heat flux from the relatively warm bulk fluid to the frozen layer and, in opposite direction, the energy flux of the scraped ice particles from frozen layer to the bulk
d) 3/4: Heat transfer flux from the frozen layer to the metal wall

e) 4/5: Heat transfer flux from the metal wall to the axially flowing coolant

The driving forces considered for the heat transfer are presented in Table 5.5. The energy transfers between the frozen layer and the floating ice particles and from the floating ice particles to the fluid in the bulk are both coupled with mass transfer processes.

Table 5.5. Type of transfers between the phases

Phase 1	Phase 2	Conduction	Convection	Work
B	***Rotor***	✓		✓
B	***Ice***	✓	✓	
B	***Air***	(equilibrium)		
B	***FL***	✓	✓	
FL	***Ice***		✓	
FL	***Wall***	✓		
Wall	***Coolant***	✓		

The scraping rate and the cooling rate co-determine the (averaged) flux of ice particles from the frozen layer into the bulk. The heat flux through the frozen layer extracts heat by freezing water into ice at the interface of the frozen layer and the bulk between two successive scrapings.

The heat transfer from the bulk fluid to the ice particles determines the rate of melting of the ice particles and the flux of cold water into the bulk.

The energy balances are written in the following sections in terms of enthalpy. Relations to link the enthalpy and the temperature (typical quantity used in practical applications) are described in Section 5 of this chapter.

3.5.1. The bulk domain

The matrix phase and the air phase are assumed to be a pseudo-continuous phase, the "aerated liquid" phase.

The conservation equation for the energy of the "aerated liquid" bulk domain is written in the form of the energy balance equation (7.34), in Appendix 4.

3.5.2. The ice particles in the bulk domain

It should be mentioned the fact that there are two types of ice particles in the bulk: the fresh particles coming from the frozen layer by scraping, and the ice particles already present in the bulk. It is assumed that the heating of the ice particles coming from the frozen layer inside the bulk domain is very rapid. Once in bulk, the ice particles temperature starts to change due to the difference in temperature between the particles and the liquid bulk, and eventually melt. Since the ice particles have different sizes, the heating and the melting will take place with different rates depending on the sizes and internal temperature of the particles. This means that the temperature should be considered as a new internal state of an ice particle. When modelling the ice particle population as a whole a new

internal coordinate should be considered while writing the population balance equations for the ice particles: the thermal coordinate, $\Theta^{(i)}$.

The introduction of one extra coordinate $\Theta^{(i)}$ will increase the dimensionality of the population balance equations to 6-D. This will increase the model complexity beyond the possibility to validate experimentally such an extension. For this reason, the inner temperature of a particle will not be considered as an additional inner state variable.

In the following, it is assumed that all ice particles have the same temperature while they are melting. The temperature has a value between the temperature of the frozen layer, which is the temperature of the fresh particles scraped from the wall, and the temperature of the ice-matrix equilibrium. The ice particles do not warm up inside.

Moreover, we assume that the ice particles in the bulk are one pseudo-continuous phase. The mass conservation equation is derived in this case from the population balance for the ice particles, by integrating over all the particle sizes. The energy conservation equation can be written in a similar way with equation (7.43) in Appendix 4.

3.5.3. The rotor

The energy conservation equation for the rotor is not required since it is assumed no heat transfer interaction with the aerated liquid phase. The mechanical work term has been transferred to the energy balance of the liquid phase.

3.5.4. The frozen layer domain

The energy conservation equation for the frozen layer is written in the form of the energy balance equation (7.48) in Appendix 4.

3.5.5. The freezer's wall

The energy conservation equation for the freezer's wall is written in the form of the energy balance equation (7.53) in Appendix 4.

3.5.6. The coolant

The energy conservation equation for the coolant is written in the form of the energy balance equation (7.57) in Appendix 4.

3.6. Overview of the reductions in the 5-D model

The following main reductions have been performed with respect to the mass balances in the 5-D model:

1) lumping of distributed phase: “air” phase, normally a population of bubbles, is treated as a pseudo-continuous phase
2) lumping of phases: “air” with the “liquid” phase; “fat” with the “liquid” phase
3) lumping of components in one pseudo-component: all the other components of the ice cream mix, such as proteins, stabilizers, emulsifiers, etc. in “others”; different types of sweeteners present in the mix, in “sugar”
4) lumping of components in the “liquid” phase into “water”, “fat”, “sugar”, “air”, “other”
5) single component (ice) in the frozen layer
6) no crystallization phenomena considered in the ice cream fluid, except for scraping and melting

With respect to the momentum balance:

7) lumped momentum balance over liquid and ice phases in the bulk domain

The reductions with respect to the energy balance in the 5-D model consist of:

8) eliminating the rotor energy balance
9) ignoring the internal energy distribution in the ice particles by assuming uniform temperature
10) applying steady state assumption to the energy balance of the metal wall
11) assuming constant temperature for the coolant

While even this 5-D model of the ice cream freezing unit is the result of some significant reductions, it is computationally too demanding for routine use in inverse problems. Therefore, further reductions will take place, primarily aiming at reducing the number of coordinates of the model, going from a 5-D to a 3-D model.

4. Specification of the 3-D model of the ice cream freezing unit

In the previous section, the conservation equations are written on a rigorous coordinate set and are able to accommodate rate terms for any fundamental phenomena. However, having five coordinates is not practical for solving the model in a repetitive mode in inverse problems. For this reason, the set of coordinates will be reduced. This is done by:

- Eliminating the angular and radial coordinates. The reason for eliminating these coordinates is that it offers major gains in model reduction, while fair approximations can be made for the flow and mixing events in the domains of these coordinates. Radial and angular flows and mixing are very fast due to the rapid rotation of the scraping blades and thought to be instantaneous
- Integrating out of the derivative terms with respect to each eliminated variable over its respective domains
- Averaging the variables over the domains of the eliminated coordinates. The averaging procedure is detailed in Appendix 5.

The resulting reduced model will have only three coordinates: the time t , the axial position z , and the internal coordinate of the particles $s^{(i)}$. For this reason, this reduced model will be called the *3-D model*.

The chosen elimination of the radial and angular coordinates induces the following additional modelling assumptions. The counting of the assumptions is continued from Section 3.

27. Cylinder symmetry is imposed on the freezer, covering the external metal wall, the frozen layer of ice against the inner surface of this wall, and the bulk domain in which the aerated liquid phase is moving forward.

28. Drastic simplification of hydrodynamics of the ice cream is considered. The rotation time of the scraper is very short relatively to the time the "aerated liquid" phase is transported through the freezer in axial direction. Due to the fast rotation of the scraper, the ice cream will exhibit complex spiralling movements and mixing in radial and angular directions with slow net transport in axial direction. This complex hydrodynamics will be simplified, knowing the effective mixing time is small. Consequently, the ice cream is practically well mixed within a cross-sectional area, perpendicular to the axial direction. Therefore, all process variables in the bulk domain will be averaged over such a cross-sectional area, while they will vary with axial position and time.

29. The axial convective velocities of the "ice" and "aerated liquid" phases in the bulk are averaged over the cross-sectional area. The velocities are taken proportional to the rotational speed of the scraper, which provides for the momentum.

30. Axial dispersion is not considered for the time being, although in practice the rotational movement by a scraper will induce some dispersion. The mathematical and computational convenience of this assumption lies in avoiding second order spatial derivatives with two-point boundary values, demanding iterative approaches to satisfy such boundary conditions.

31. The effects of change in density of the bulk mixture on the axial velocity can be accounted for by assuming the total ice cream mass flow is considered constant through the freezer. When the density of the mixture reduces with the increased ice content, the axial velocity must go up.

32. The event of scraping of the ice from the frozen layer by a scraping blade happens almost instantaneously; it is very short relative to the time interval for growth of the ice layer by freezing between two successive scrapings.

33. Work done by the rotor/scraper is absorbed by the fluid in the bulk.

34. The temperature and pressure inside the bulk domain are assumed to be radially uniform, but varying in axial direction.

35. In view of the small temperatures in the freezer (-10 to +10 ^{0}C) the temperature dependency of some of the physical properties (density, specific heat, conductivity) of pure components is neglected.

By assuming that the perfect mixing takes place within the time interval of rotation of a scraping blade, it is not relevant to consider dynamics of events on a time scale below this rotation

time within the 3-D model. The rotation time provides for the lower bound on a relevant time difference.

4.1. Mass

In the following sections, the result of the averaging with respect to the radial and angular coordinates of the conservation equation in the bulk and in the frozen layer will be presented. The averaged terms of the conservation equations are based on the lemmas presented in Appendix 5. An overview of the resulting equations is presented in Appendix 6.

4.1.1. The bulk domain

The starting point of the averaging procedure is the equation of change for either a distributed or a pseudo-continuous phase. The conservation equation is multiplied with r and integrated from $r = R_0$ to $r = R - \delta_{FL}$ and $\theta = 0$ to $\theta = 2\pi$, and the averaging procedures presented in Appendix 5 are applied. The resulting conservation equations apply over the radial (cross-sectional) areas of the spatial domains (rotor, bulk, frozen layer, wall) in the freezer.

The complete derivation of the equation for the ice phase can be found in Appendix 7. When assuming the distributed phase as being pseudo-continuous, the terms in the conservation equation of the dispersed phase are related to their pseudo-continuous equivalents. The complete derivation of this equation for the liquid phase can be found in Appendix 8.

Unavoidably, due to the presence of many phases, spatial domains, chemical species, and coordinates, the symbolic notation of the physical variables becomes quite complicated. In the list of symbols below, a superscript (φ) refers to a thermodynamic phase, while a subscript or a string of subscripts refer to a resource (mass, energy), a spatial domain (*B, FL*), a chemical species (j) and a spatial coordinate (z, s).

In case of a resource being transferred between two domains, the direction of transfer is described by an arrow. For example $B \rightarrow FL$ refers to a transfer from the bulk to the frozen layer domain.

The scalar quantities, such as concentrations, do not have a directional index as a subscript, in contrast to the vectorial ones, like fluxes, where a directional index must be added. The time dependency of the variables is assumed implicitly and is not expressed as such. The overhead bar refers to a quantity that has been averaged over a cross-sectional area ("radially averaged").

For example $\bar{j}^{(\varphi)}_{m,B,j,z}$ is a cross-sectional averaged flux (j) of mass (m) of phase (φ) in domain (B) of species j at position z .

The first term on the left-hand side of the conservation equations accounts for the variation in time of the volume-specific quantity of resource (concentration of particles for the dispersed phase,

and concentration of the pseudo-continuous phases). The second and third terms account for the flux of particles (for the dispersed phases) or mass (for the pseudo-continuous phases) in the direction of the principal coordinates considered.

The terms on the right-hand side of the conservation equations account for the different sources and sinks and the transfer to and from different domains or phases. For this particular case, the source term refers to the melting of ice particles in the bulk in the case of the pseudo-continuous matrix, while the transfer terms refer to the transfer of particles and mass to and from the frozen layer.

a) The balance equation for the dispersed and distributed phases

The ice particles in the bulk are treated as a dispersed phase, with size as a distributed phase. The air bubbles could also be treated in this way, but for the purpose of this research, the air is assumed as a pseudo-component inside the continuous phase.

$$\frac{\partial\left(\bar{n}_B^{(\varphi)}\right)}{\partial t}+\frac{\partial\left(\bar{j}_{B,z}^{(\varphi)}\right)}{\partial z}+\frac{\partial\left(\bar{j}_{B,s}^{(\varphi)}\right)}{\partial s^{(\varphi)}}=\bar{B}_B^{(\varphi)}-\bar{D}_B^{(\varphi)}+\bar{R}_{t,FL\to B}^{(\varphi)}\cdot\frac{S_B}{A_B}-\bar{R}_{t,B\to FL}^{(\varphi)}\cdot\frac{S_B}{A_B} \tag{5.2}$$

With the **initial condition**:

The initial distribution of particles is defined by:

$$\bar{n}_B^{(\varphi)}(0,z,s^{(\varphi)})=\bar{n}_{B,0}^{(\varphi)}\left(z,s^{(\varphi)}\right) \tag{5.3}$$

And the **boundary conditions**:

1) In axial direction

At the entrance of the freezer, the flow of particles is defined by a given flow function $\tilde{F}_{B,z}^{(\varphi)}$:

$$\left(\bar{j}_{B,z}^{(\varphi)}\cdot A_B\right)\Big|_{z=0}=\tilde{F}_{B,z}^{(\varphi)}\left(t,s^{(\varphi)}\right) \tag{5.4}$$

2) Along the internal coordinate

For the maximum particle size, it is considered the particle flux vanishes (Ramkrishna, 2000):

$$\bar{j}_{B,s}^{(\varphi)}\Big|_{s_{max}^{(\varphi)}}=0 \tag{5.5}$$

The functions $\bar{n}_{B,0}^{(\varphi)}$ and $\tilde{F}_{B,z}^{(\varphi)}$ must be specified as model inputs by the model user.

The concentration of the particle phase (as a pseudo-continuous phase) is determined using the following equation:

$$\rho^{(\varphi)}\cdot\int_0^{\infty}\left(\bar{n}_B^{(\varphi)}\cdot a^{(\varphi)}\cdot ds^{(\varphi)}\right)=\bar{c}_B^{(\varphi)} \tag{5.6}$$

List of symbols

$\bar{n}_B^{(\varphi)}$ = the radially averaged concentration of dispersed particles in the bulk, $\left[\#/m^3 \right]$

$\bar{j}_{B,z}^{(\varphi)}$ = the radially averaged flux of particles in axial direction z in the bulk, $\left[\#/m^2 \cdot s \right]$

$\bar{j}_{B,s}^{(\varphi)}$ = the radially averaged flux of particles along the internal coordinate s in the bulk, $\left[\#/m^2 \cdot s \right]$

$\bar{u}_z^{(\varphi)}$ = the radially averaged velocity in axial direction, $\left[m/s \right]$

$\bar{r}_s^{(\varphi)}$ = the radially averaged growth/melting rate, $\left[m/s \right]$

$\bar{B}_B^{(\varphi)}$ = the radially averaged birth of particles in the bulk domain term, $\left[\#/m^3 \cdot s \right]$

$\bar{D}_B^{(\varphi)}$ = the radially averaged death of particles in the bulk domain term, $\left[\#/m^3 \cdot s \right]$

$\bar{R}_{t,FL\to B}^{(\varphi)}$ = the radially averaged transfer term (flux) from the frozen layer to the bulk, $\left[\#/m^2 \cdot s \right]$

$\bar{R}_{t,B\to FL}^{(\varphi)}$ = the radially averaged transfer term (flux) from the bulk to the frozen layer, $\left[\#/m^2 \cdot s \right]$

$\tilde{F}_{B,z}^{(\varphi)}$ = flow of particles with size s in phase φ entering the bulk at $z = 0$, $\left[\#/s \right]$

$\bar{n}_{B,0}^{(\varphi)}$ = nucleation rate of particles in phase φ in the bulk, $\left[\#/m^3 \right]$

A_B = cross-sectional area of the bulk, $\left[m^2 \right]$

S_B = circumference of the bulk area, $\left[m \right]$

b) The balance equation for the pseudo-continuous phases

The liquid matrix and the air phase are treated as a pseudo-continuous phase.

$$\frac{\partial\left(\varepsilon_B^{(\varphi)} \cdot \bar{c}_{B,j}^{(\varphi)}\right)}{\partial t} + \frac{\partial\left(\bar{j}_{m,B,j,z}^{(\varphi)}\right)}{\partial z} = \varepsilon_B^{(\varphi)} \cdot \bar{G}_{B,j}^{(\varphi)} - \varepsilon_B^{(\varphi)} \cdot \bar{R}_{t,B\to FL,j}^{(\varphi)} \cdot \frac{S_B}{A_B} \tag{5.7}$$

With the **initial condition**:

The concentration of the pseudo-continuous phase is defined by:

$$\bar{c}_{B,j}^{(\varphi)}(0,z) = \bar{c}_{B,j,0}^{(\varphi)}(z) \tag{5.8}$$

And the **boundary condition**:

At the entrance of the freezer, the flow is defined by a given entrance flow function $\tilde{F}^{(\varphi)}_{B,z,j,0}$:

$$\left(\bar{j}^{(\varphi)}_{m,B,j,z} \cdot A_B\right)\Big|_{z=0} = \tilde{F}^{(\varphi)}_{B,z,j,0}(t) \tag{5.9}$$

List of symbols

$\bar{c}^{(\varphi)}_{B,j}$ = the radially averaged concentration of component j in the bulk, $\left[kg/m^3\right]$

$\varepsilon^{(\varphi)}_B$ = the radially averaged volume fraction of phase φ in the bulk, $[-]$

$\bar{j}^{(\varphi)}_{m,B,j,z}$ = the radially averaged mass flux of component j in axial direction in the bulk, $\left[kg/m^2 \cdot s\right]$

$\bar{R}^{(\varphi)}_{t,B\to FL,j}$ = the radially averaged transfer term (flux) of component j from the bulk to the frozen layer, $\left[kg/m^2 \cdot s\right]$

$\bar{G}^{(\varphi)}_{B,j}$ = the radially averaged rate of change of component j in the bulk, $\left[kg/m^2 \cdot s\right]$

$\tilde{F}^{(\varphi)}_{B,z,j,0}$ = mass flow of component j entering the bulk at location $z = 0$, $\left[kg/s\right]$

4.1.2. The frozen layer domain

The starting point is the equation of change for mass of the ice phase in the frozen layer. The frozen layer contains only ice and this ice is treated as a continuous phase. Any change in the mass of ice per unit area of metal wall is expressed in a change of thickness of the ice layer. It is physically the only degree of freedom because the ice density is more or less a constant (a weak function of temperature).

The frozen layer is subject to a periodic scraping operation, as shown in Figure 5.6. In between two successive scrapings, the growth of the layer by freezing occurs. Due to the thickness of the scraper blades relative to the circumferential length along the freezing wall, the duration of the scraping action at any radial position is very short relative to the time interval between two scrapings. The time interval between two successive scrapings is divided between the "freezing" and the "scraping" intervals.

The assumption that the frozen layer consists only of solid ice leads to the concentration of the ice particles inside the frozen layer being equal to the density of ice:

$$\bar{c}^{(i)}_{FL}(t,z) = \rho^{(i)} \tag{5.10}$$

After the averaging procedure in Appendix 6 is applied, the following equation is obtained for the variation of the ice layer thickness during the freezing interval:

$$\frac{\partial \delta_{FL}(t,z)}{\partial t} = \frac{\bar{R}^{(i)}_{t,m,B\to FL}(t,z) + \bar{R}^{(l)}_{t,B\to FL,w}(t,z)}{\rho^{(i)}_{FL}} \tag{5.11}$$

The right hand side terms represent the ice and water fluxes to the frozen layer. The derivation of this equation can be found in Appendix 9.

With the **initial and final conditions**:

At the beginning of a freezing interval, the thickness of the layer is at its minimum, because a scraping has just been completed:

At $t = 0$ $\delta_{FL} = \delta_{FL,min}(z)$ (5.12)

At the end of a freezing interval, the thickness of the frozen layer is at its maximum:

At $t = t_{s+}$ $\delta_{FL} = \delta_{FL,max}(z)$ (5.13)

The moment of the scrapping is known, co-determining the maximum thickness that can be achieved. The thickness of the frozen layer is an unknown variable.

List of symbols

$\delta_{FL,min}$ = the minimum thickness of the frozen layer, $[m]$

$\delta_{FL,max}$ = the maximum thickness of the frozen layer, $[m]$

$\bar{R}^{(i)}_{t,m,B\to FL}$ = transfer term of ice (mass) from the bulk to the frozen layer, $\left[kg/m^2 \cdot s\right]$

$\bar{R}^{(l)}_{t,B\to FL,w}$ = transfer term of water from the bulk to the frozen layer, $\left[kg/m^2 \cdot s\right]$

A rigorous equation for calculating the fluxes $\bar{R}^{(i)}_{t,m,B\to FL}$ and $\bar{R}^{(l)}_{t,B\to FL,w}$ will be presented in Section 5 of this chapter. Considering the short time intervals between two successive scrapings and the separation of the freezing event and the scraping action, it is fair to assume that the respective fluxes are constant over such short time intervals. Hence, the corresponding dynamic models per sub-interval can be solved analytically.

(A) The dynamic model for the freezing of the frozen layer

Equation shows how the thickness of the frozen layer grows due to the incoming fluxes of water and ice from the bulk. This growth happens over a very short time interval $[0, t_{s-}]$. The value of the time t_s is inversely proportional to the frequency of scraping, ω_r^*:

$$t_s = \frac{1}{\omega_r^*} \tag{5.14}$$

Where this frequency is proportional to the rotational frequency and number of blades:

$$\omega_r^* = \omega_r \cdot N_{blades} \tag{5.15}$$

Invoking that for the time interval $[0, t_{s-}]$ the fluxes of water and ice coming from the frozen layer are constant, equation (5.11) is rewritten:

$$d\delta_{FL}(t,z) = \frac{\bar{R}_{t,m,B\to FL}^{(i)}(z) + \bar{R}_{t,B\to FL,w}^{(l)}(z)}{\rho_{FL}^{(i)}} dt \tag{5.16}$$

Equation (5.16) is integrated analytically to obtain an expression for the maximum thickness of the frozen layer:

$$\int_{\delta_{FL,min}}^{\delta_{FL,max}} d\delta_{FL}(t,z) = \int_{t_0}^{t_{s-}} \frac{\bar{R}_{t,m,B\to FL}^{(i)}(z) + \bar{R}_{t,B\to FL,w}^{(l)}(z)}{\rho_{FL}^{(i)}} dt \tag{5.17}$$

Hence, the maximum thickness of the frozen layer at the end of the freezing sub-interval is:

$$\delta_{FL,max} = \delta_{FL,min} + \frac{\bar{R}_{t,m,B\to FL}^{(i)}(z) + \bar{R}_{t,B\to FL,w}^{(l)}(z)}{\rho_{FL}^{(i)}} \cdot (t_{s-} - t_0) \tag{5.18}$$

(B) The dynamic model for the scraping of the frozen layer

At time t_s, the actual scraping of the frozen layer occurs. This process happens almost instantly, over an amount of time much shorter than the growth time interval. The thickness of the frozen layer is decreased from the maximum thickness up to a minimum thickness, $\delta_{FL,min}$.

For this case, the thickness of the frozen layer varies in the following way:

$$\frac{\partial \delta_{FL}(t,z)}{\partial t} = -\frac{\bar{R}_{t,m,FL\to B}^{(i)}(z)}{\rho_{FL}^{(i)}} \tag{5.19}$$

At the beginning of the scraping interval, the thickness of the layer is at its minimum, because the layer had the time to grow during the freezing interval. At the end of the scraping interval, the thickness is at its minimum, because a scraping has just been completed.

Using the initial thickness just before scraping and the final one, after the scraping, the integration leads to:

$$\int_{\delta_{FL,\max}}^{\delta_{FL,min}} d\delta_{FL}(t,z) = -\int_{t_0}^{t_s} \frac{\bar{R}^{(i)}_{t,m,FL\to B}(z)}{\rho^{(i)}_{FL}} dt \tag{5.20}$$

$$\delta_{FL,max} = \delta_{FL,min} + \frac{\bar{R}^{(i)}_{t,m,FL\to B}(z)}{\rho^{(i)}_{FL}} \cdot (t_s - t_0) \tag{5.21}$$

$\bar{R}^{(i)}_{t,m,FL\to B}$ = transfer term of ice (mass) from the frozen layer to the bulk, $\left[kg/m^2 \cdot s \right]$

This rate of scraping of ice is an unknown flux. In principle, it could be derived from an analysis of the effects of the mechanical forces breaking up the ice layer into fragments. However, this is a very complicated matter. There is an easier way of deriving this rate by making use of the strictly periodic nature of the scraping. The net effect of the growth by freezing is equal to the net effect of the scraping, returning the thickness of the ice layer back to its initial thickness. An expression for the transfer term of ice from the frozen layer to the bulk as the sum of the transfer terms for the water and ice coming from the bulk to the frozen layer by equating (5.18) and (5.21):

$$\bar{R}^{(i)}_{t,m,FL\to B}(t,z) = \left[\bar{R}^{(i)}_{t,m,B\to FL}(z) + \bar{R}^{(l)}_{t,B\to FL,w}(z) \right] \cdot \frac{(t_{s-} - t_0)}{(t_s - t_0)} \tag{5.22}$$

The consequence of this equation is that expressions for these freezing rates must be derived from thermodynamic and kinetic considerations and will be presented in Section 5.

4.2. Momentum

A momentum flux of a mass stream with the velocity u, mass density ρ and pressure P is given by $P + \rho \cdot u^2$. Due to friction losses, the momentum flux will decrease, leading to a relation between pressure and the velocity changes. As the equipment is often designed and operated to keep the mass flux constant, the velocity is considered virtually constant and the pressure change is the key variable of interest in equipment engineering models. The reason for this is that mechanical work is required to overcome this pressure change in attaining a target mass flux. The objective of this sub-section is to deliver a reduced momentum balance that establishes a relation between the mass flux and the pressure drop.

Due to the complex rotational movements in axial direction and the non-Newtonian flow behaviour of the ice cream, a major shortcut is taken in modelling the momentum conservation: radially symmetric axial convective flow of the bulk is driven by a pressure drop over the equipment.

In (Bongers, 2006) the flow is expressed as a function of the pressure drop, $|\Delta P|$ using the theory of (Frederickson & Bird, 1958). This concerns the analytical solution of the equation of motion for the steady state axial flow of and incompressible, non-Newtonian fluid in a long cylindrical annulus.

The following assumptions are considered in this derivation by (Frederickson & Bird, 1958):

36. It is assumed that the flow is isothermal. This assumption would imply that the viscous dissipation term in the energy balance equation is negligible or compensated by heat removal.
37. The fluid is incompressible ($\rho = const.$).
38. Steady state flow is assumed.
39. The flow is laminar.
40. The freezer is sufficiently long to neglect the end effects.
41. It is assumed that the local shear stress depends on the local shear rate by a power law model.

Under the assumptions of incompressible fluid, steady state laminar flow, the z -component of the equation of motion in cylindrical coordinates will be:

$$\frac{\partial P}{\partial z} = -\left[\frac{1}{r}\cdot\frac{\partial\left(r\cdot\tau_{B,rz}\right)}{\partial r}\right] + \rho_B^{(i+l+a)}\cdot g_z \tag{5.23}$$

This equation is valid over the entire annular region for any kind of fluid.

If $\frac{\partial P}{\partial z}$ is assumed constant:

$$\Delta P = P_0 - P_L \tag{5.24}$$

Equation (5.23) becomes:

$$\frac{1}{r}\cdot\frac{d\left(r\cdot\tau_{B,rz}\right)}{dr} = \frac{\Delta P}{L} + \rho_B^{(i+l+a)}\cdot g_z \tag{5.25}$$

For the power law model, the local shear stress depends on the local shear rate by:

$$\tau_{B,rz} = -K_B^{(i+l+a)}\cdot\left|\frac{\partial u_z}{\partial r}\right|^{n-1}\cdot\frac{\partial u_z}{\partial r} \tag{5.26}$$

The volume rate of flow is determined by integrating the velocity distribution over the annular domain:

$$\phi_{v,B}^{(i+l+a)} = 2\pi \cdot R^2 \cdot \int_{\Gamma_0}^{1} u_z \cdot \Gamma d\Gamma \tag{5.27}$$

The resulting equation relating mass flow rate and pressure drop is derived from (Frederickson & Bird, 1958). The derivation is detailed in Appendix 10.

$$\phi^{(i+l+a)} = \rho^{(i+l+a)} \cdot \pi R^3 \cdot \left(\frac{|\Delta P|}{L} \cdot \frac{R}{2 \cdot K_B^{(i+l+a)}} \right)^{\frac{1}{n}} \cdot \frac{n}{2n+1} \cdot \left(1 - \frac{R_0}{R} \right)^{\frac{2n+1}{n}} \tag{5.28}$$

The equation counts two variables: pressure drop and mass flow. In order to be able to solve the equation, the mass flow is specified, while the pressure drop is determined using equation (5.28).

List of symbols

$|\Delta P|$ = the pressure drop, $[Pa]$

P_0 = the static pressure at freezer's inlet, $[Pa]$

P_L = the static pressure at freezer's outlet, $[Pa]$

R_0 = the inner radius of the annulus, $[m]$

R = the outer radius of the annulus, $[m]$

Γ = the dimensionless radial coordinate, $[-]$

$K_B^{(i+l+a)}$ = the consistency of the ice cream (power law), $\left[Pa \cdot s^n \right]$

n = flow behaviour index of the ice cream (power law), $[-]$

$\phi^{(i+l+a)}$ = mass flow, $\left[kg/s \right]$

$\rho^{(i+l+a)}$ = density, $\left[kg/m^3 \right]$

$\bar{u}_z$ = average velocity, $\left[m/s \right]$

$\tau_{B,rz}$ = local shear stress, $[Pa]$

4.3. Energy

Reduced energy balances will be presented for the bulk, the frozen layer, the freezer wall and the coolant. The energy balance for the rotor is ignored on the grounds of assumptions 25 and 26, assuming the rotor is at any axial position in local thermal equilibrium with the "liquid" in the bulk

domain (having the same temperature). The averaging of the energy equations is performed similarly to the averaging of the mass conservation equations: multiply the conservation equation with r and integrate from $r = R_0$ to $r = R - \delta_{FL}$ and $\theta = 0$ to $\theta = 2\pi$, and then apply the averaging procedures presented in Appendix 5.

4.3.1. The bulk domain

In case of the bulk, the energy conservation equations are written for the "aerated liquid" phase and for the "ice" particles in the bulk. As the two phases have different temperature with heat transfer from the liquid to the ice particles, two energy balances will be developed.

a) Single ice particle

The particles melting rate, required for the ice particles population balance, is obtained from the assumption that the melting rate and the conductive heat transfer rate are balanced around a single ice particle, as shown in Figure 5.7.

The incoming heat is used for melting the ice into water and for heating up the inner part of a particle, rising its inner temperature in this way. This heat balance can be turned into a rate of change of the ice particles coordinate by means of some model reductions.

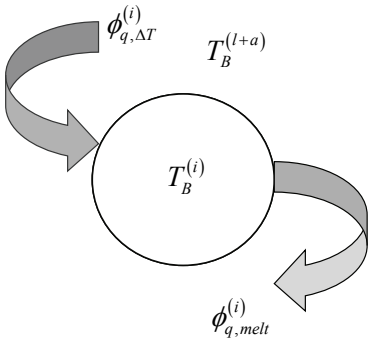

Figure 5.7. Representation of the energy transfer terms around an ice particle

The internal diffusion of heat from the boundaries to the inner part by thermal conductivity is much higher than the transfer rate of heat from the bulk fluid to the crystal. All heat coming into the crystal is first used for heating the crystal to the melting point and then used for the melting of the surface layer. Only a small fraction of the total incoming heat that propagates inwards is needed for heating up the inner core of a crystal to the equilibrium temperature as compared to the required heat of melting. The time it takes to heat up a crystal to its melting point is also very short relative to the melting time itself.

The melting rate of the ice particles is determined by the available heat flow coming from the bulk. It is assumed that the dissolution process of water molecules is almost instantaneous (not limiting) once the heat activation is present.

$$\phi_{q,melt}^{(i)} = \phi_{q,\Delta T}^{(i)} \tag{5.29}$$

List of symbols

$\phi_{q,melt}^{(i)}$ = heat flow due to melting of ice particles, $[W]$

$\phi_{q,\Delta T}^{(i)}$ = heat flow towards the ice particle, due to temperature difference between the ice particle and the liquid bulk, $[W]$

b) The ice phase

The consequence of the thermal modelling assumption 17 is that all the ice particles, fresh and old, have all the same temperature. By summation (integration) over the energy content of all particles, the energy balance over the ice phase in the bulk domain is written in the following form:

$$\frac{\partial\left(\varepsilon_B^{(i)} \cdot \bar{c}_B^{(i)} \cdot \bar{h}_B^{(i)}\left(T_B^{(i)}\right)\right)}{\partial t} + \frac{\partial\left(\bar{e}_{B,z}^{(i)}\right)}{\partial z} = \bar{E}_{B\leftrightarrow FL}^{(i)} + \bar{q}_{\Delta T,B\to i}^{(i)} - \left[\frac{\partial \ln\left(\varepsilon_B^{(i)} \cdot \bar{c}_B^{(i)}\right)}{\partial \ln T_B^{(i)}}\right]_{\bar{P}} \cdot \frac{D\bar{P}}{Dt} \tag{5.30}$$

An expression for determined the energy flux in axial direction, $\bar{e}_{B,z}^{(\varphi)}$ is defined in Section 5.2.3 of this chapter.

With the **initial condition**:

The initial enthalpy profile for the ice phase is defined considering that the initial temperature of the mix is known:

$$T_B^{(i)}\Big|_{t=0} = T_{B,0}^{(i)}(z) \tag{5.31a}$$

This is equivalent to:

$$\bar{h}_B^{(i)}\left(T_B^{(i)}\right)\Big|_{t=0} = \bar{h}_{B,0}^{(i)}(z) \tag{5.28 b}$$

And the **boundary condition**:

At the entrance of the freezer, the temperature of the mix is known:

$$T_B^{(i)}\Big|_{z=0} = T_{B,z=0}^{(i)}(t) \tag{5.32}$$

The relation used to determine the enthalpy from the temperature is defined in Section 5.1.2 of this chapter.

The mass flux related heat transfer effects are determined from the following equation:

$$\bar{E}^{(i)}_{B\leftrightarrow FL} = \frac{S_B}{A_B}\cdot\left(-\bar{R}^{(i)}_{t,m,B\to FL}\cdot\bar{h}^{(i)}_{B} + \bar{R}^{(i)}_{t,m,FL\to B}\cdot\bar{h}^{(i)}_{FL}\right) \tag{5.33}$$

The heat of melting is incorporated in the definition of the enthalpy, as shown in Section 5.1.2 of this chapter. The melting heat of the ice particles and the thermal heat transfer term $\bar{q}^{(i)}_{\Delta T,B\to i}$ in equation (5.30) are much more important than the heat effects associated with the mass transfer between the ice phase in the bulk and the frozen layer, $\bar{E}^{(i)}_{B\leftrightarrow FL}$. Rate laws for these terms will be presented in Section 5.5.2 of this chapter.

c) The liquid phase

$$\frac{\partial\left(\varepsilon_B^{(l+a)}\cdot\bar{c}_B^{(l+a)}\cdot\bar{h}_B^{(l+a)}\left(T_B^{(l+a)}\right)\right)}{\partial t} + \frac{\partial\left(\bar{e}_{B,z}^{(l+a)}\right)}{\partial z} = \bar{E}^{(l)}_{B\leftrightarrow FL,w} - \frac{S_B}{A_B}\cdot\bar{q}^{(l)}_{\Delta T,B\leftrightarrow FL} - \bar{q}^{(i)}_{\Delta T,B\to i}$$
$$+\bar{\dot{Q}}_{v,B} + \bar{\dot{Q}}_{scrap,B} - \left[\frac{\partial\ln\left(\varepsilon_B^{(l+a)}\cdot\bar{c}_B^{(l+a)}\right)}{\partial\ln T_B^{(l+a)}}\right]_{\bar{P}}\cdot\frac{D\bar{P}}{Dt} \tag{5.34}$$

With the **initial condition**:

The initial temperature profile for the liquid is known:

$$T_B^{(l+a)}\Big|_{t=0} = T_{B,0}^{(l+a)}(z) \tag{5.35a}$$

This is equivalent to:

$$\bar{h}_B^{(l+a)}\left(T_B^{(l+a)}\right)\Big|_{t=0} = \bar{h}_{B,0}^{(l+a)}(z) \tag{5.32 b}$$

And the **boundary conditions**:

At the entrance of the freezer, the temperature profile is known:

$$T_B^{(l+a)}\Big|_{z=0} = T_{B,z=0}^{(l+a)}(t) \tag{5.36}$$

The enthalpy profile is determined using the equation defined in Section 5.1.2 of this chapter.

In this case, the heat transfer rate related to mass transfer effects is determined from the following equation:

$$\bar{E}^{(l)}_{B\leftrightarrow FL,w} = \frac{S_B}{A_B}\cdot\left(-\bar{R}^{(l)}_{t,B\to FL,w}\cdot\bar{h}^{(l)}_{B,w}\right) \tag{5.37}$$

Equations for the transfer terms that appear in energy balances (5.30) and (5.34), as well as expressions to relate the enthalpy with the temperature must be added to the model. These are presented in Section 5 of this chapter.

List of symbols

$\bar{h}^{(i)}_B$ = the enthalpy of the ice phase in the bulk, $\left[J/kg\right]$

$T^{(i)}_B$ = the temperature of the ice phase in the bulk, $\left[K\right]$

$\bar{e}^{(\varphi)}_{B,z}$ = the energy flux in axial direction, $\left[W/m^2\right]$

$\bar{E}^{(i)}_{B\leftrightarrow FL}$ = the heat effects associated to the mass transfer between the ice phase in the bulk and the ice phase in the frozen layer, $\left[W/m^3\right]$

$\bar{R}^{(i)}_{t,m,FL\to B}$ = the radially averaged transfer term (flux) from the frozen layer to the bulk, $\left[kg/m^2\cdot s\right]$

$\bar{R}^{(i)}_{t,m,B\to FL}$ = the radially averaged transfer term (flux) from the bulk to the frozen layer, $\left[kg/m^2\cdot s\right]$

$\bar{h}^{(i)}_{FL}$ = the enthalpy of the ice phase in the frozen layer, $\left[J/kg\right]$

$\bar{q}^{(i)}_{melt}$ = the heat generation term due to the melting of the ice particle, $\left[W/m^3\right]$

$\bar{q}^{(i)}_{\Delta T,B\to i}$ = the conductive heat transfer term due to the difference in temperature between the ice particle and the equilibrium temperature, $\left[W/m^3\right]$

$\bar{R}^{(i)}_{m,B}$ = the radially averaged melting term for the ice in the bulk domain $\left[kg/m^3\cdot s\right]$

Δh_{cryst} = the enthalpy of crystallization, $\left[J/kg\right]$

$\bar{h}^{(i+a)}_B$ = the enthalpy of the liquid phase in the bulk, $\left[J/kg\right]$

$T_B^{(l+a)}$ = the temperature of the liquid phase in the bulk, $[K]$

$\bar{E}_{B\leftrightarrow FL,w}^{(l)}$ = the heat effects associated to the heat transfer between the liquid phase in the bulk and the ice phase in the frozen layer, $\left[W/m^3\right]$

$\bar{q}_{\Delta T,B\leftrightarrow FL}^{(l)}$ = the conductive heat transfer term due to the difference in temperature between the liquid phase in the bulk and the frozen layer, $\left[W/m^3\right]$

$\bar{\dot{Q}}_{scrap,B}$ = averaged work done by scraping the ice layer into the bulk domain, $\left[W/m^3\right]$

$\bar{P}$ = radially averaged pressure in the bulk, $[Pa]$

The energy balances for the two phases in the bulk domain, represented by equations (5.30) and (5.34) include several heat exchange rates on which there is an uncertainty on the actual form of the exchange equations defining them. To eliminate these terms for the solution of the energy balance, these balances are added to form the overall energy balance per unit volume of the bulk domain:

$$\frac{\partial\left(\bar{H}_B^{(i+l+a)}\right)}{\partial t}+\frac{\partial\left(\bar{e}_{B,z}^{(i+l+a)}\right)}{\partial z}=\bar{E}_{B\leftrightarrow FL}^{(i)}+\bar{E}_{B\leftrightarrow FL,w}^{(l)}-\frac{S_B}{A_B}\cdot\bar{q}_{\Delta T,B\leftrightarrow FL}^{(l)}+\bar{\dot{W}}_B \tag{5.38}$$

With:

$$\bar{H}_B^{(i+l+a)}=\bar{H}_B^{(i)}\left(T_B^{(i)}\right)+\bar{H}_B^{(l+a)}\left(T_B^{(l+a)}\right) \tag{5.39}$$

The ice particles in the bulk and the liquid phase have different temperatures, one for each phase.

$$\bar{H}_B^{(i)}=\varepsilon_B^{(i)}\cdot\bar{c}_B^{(i)}\cdot\bar{h}_B^{(i)}\left(T_B^{(i)}\right) \tag{5.40}$$

$$\bar{H}_B^{(l+a)}=\varepsilon_B^{(l+a)}\cdot\bar{c}_B^{(l+a)}\cdot\bar{h}_B^{(l+a)}\left(T_B^{(l+a)}\right) \tag{5.41}$$

Having one energy balance for two phases, in order to obtain two temperatures another condition must be imposed. The temperature of the ice particles is taken to the ice-water-sugar phase equilibrium temperature in the bulk domain, according to assumption 17:

$$T_B^{(i)}=T_{B,e} \tag{5.42}$$

The temperature of the liquid phase can be determined in this case from the overall energy balance over the bulk domain in equation (5.38).

List of symbols

$\bar{H}_B^{(i+l+a)}$ = the total enthalpy of the phases in the bulk domain, $\left[J/kg \right]$

$e_{B,z}^{(i+l+a)}$ = energy flux in axial direction, $\left[W/m^2 \right]$

$T_{B,e}$ = the equilibrium temperature in the bulk domain, $\left[K \right]$

$\bar{W}_B$ = the work done in the bulk, $\left[W/m^3 \right]$

4.3.2. The frozen layer domain

While the radial coordinate has been eliminated for the bulk region, it cannot be directly removed in the frozen layer, as radial heat conduction from bulk to the freezer wall through the frozen layer is essential for heat removal. The objective of this sub-section is to provide an analytical equation for the heat flux by conduction in axial direction as function of temperature at both interfaces of the frozen layer for the time-averaged thickness of the ice layer (time average over growth and scraping intervals). This heat flux expression is obtained by analytically solving a pseudo-steady state energy balance in the radial direction.

The averaging procedures presented in Appendix 5, applied for the frozen layer have to take into account the periodical modification of the frozen layer's thickness.

In the following, the frozen layer will be treated as a cylindrical wall, with a thickness equal to the average thickness of the frozen layer. The terms containing the velocity in the axial direction can be discarded, since the only relevant contribution is the contribution of the heat conduction in radial direction.

$$\frac{\partial\left(\rho_{FL}^{(i)} \cdot \bar{h}_{FL}^{(i)}\right)}{\partial t} + \frac{\partial\left(r \cdot \bar{q}_{r,FL}\right)}{\partial r} = 0 \tag{5.43}$$

With the **initial condition**:

The initial temperature profile is known:

$$T_{FL}^{(i)}\Big|_{t=0} = T_{FL,0}^{(i)}(z) \tag{5.44}$$

The enthalpy profile is determined using the equation defined in Section 5.1.2 of this chapter.

And the **boundary conditions**:

The cumulative heat flux at the inner boundary with the bulk is defined as the sum of the mass flux related energy streams and a conductive heat transfer term from the bulk liquid to the frozen layer:

$$\bar{q}_{r,FL}\Big|_{R-\bar{\delta}_{FL}} = \bar{E}^{(i)}_{B\leftrightarrow FL} + \bar{E}^{(l)}_{B\leftrightarrow FL,w} + \bar{q}^{(l)}_{\Delta T,B\leftrightarrow FL} \tag{5.45}$$

Assuming a pseudo-steady state energy balance over the frozen layer, the heat flux at the freezer wall is given by integration of:

$$\frac{\partial\left(r\cdot\bar{q}_{r,FL}\right)}{\partial r} = 0 \tag{5.46}$$

In addition:

$$\bar{q}_{r,FL} = -\lambda^{(i)}\cdot\frac{dT}{dr} \tag{5.47}$$

With the **boundary conditions**:

At $r = R - \delta_{FL}$ $\qquad T = T^{(i)}_{FL}$ (5.48)

At $r = R$ $\qquad T = T_{wall}$ (5.49)

When assuming that the thermal conductivity of the frozen layer is constant, the following expression is obtained:

$$T^{(i)}_{FL} - T_{wall} = \left(R-\delta_{FL}\right)\cdot\bar{q}_{r,FL}\Big|_{R-\bar{\delta}_{FL}}\cdot\frac{ln\left(R/R-\delta_{FL}\right)}{\lambda^{(i)}} \tag{5.50}$$

List of symbols

$T^{(i)}_{FL}$ = the temperature of ice in the frozen layer, $[K]$

T_{wall} = the temperature of the wall at the product side, $[K]$

$\lambda^{(i)}$ = the thermal conductivity of the ice, $\left[W/m\cdot K\right]$

δ_{FL} = the thickness of the frozen layer, $[m]$

R = the radius of the freezer, $[m]$

4.3.3. The freezer wall

The objective of this sub-section is to provide an analytical equation for the heat conduction in axial direction as function of temperature at both interfaces of the freezer wall, using a pseudo-steady state energy balance in radial direction over the wall. The terms containing the velocity in the axial direction can be discarded, since the only relevant contribution is the contribution of the heat conduction in radial direction.

$$\frac{\partial\left(\rho_{wall}^{(metal)}\cdot\bar{h}_{wall}^{(metal)}\right)}{\partial t}+\frac{\partial\left(r\cdot\bar{q}_{r,wall}\right)}{\partial r}=0 \tag{5.51}$$

The temperature difference over the freezer wall $T_{wall}-T_{wall,coolant}$ is determined from solving the energy balance over the freezer wall in radial direction:

$$q_{r,wall}=-\lambda^{(wall)}\cdot\frac{dT_{wall}}{dr} \tag{5.52}$$

With the **boundary conditions**:

At $r=R$ $\qquad T_{domain}=T_{wall}$ (5.53)

At $r=R+\delta_{wall}$ $\qquad T_{domain}=T_{wall,coolant}$ (5.54)

When assuming that the thermal conductivity of the wall is constant:

$$T_{wall}-T_{wall,coolant}=\left(R-\delta_{FL}\right)\cdot\bar{q}_{r,FL}\Big|_{R-\bar{\delta}_{FL}}\cdot\frac{ln\left(R+\delta_{wall}/R\right)}{\lambda^{(wall)}} \tag{5.55}$$

List of symbols

$T_{wall,coolant}$ = the temperature of the wall at the coolant side, $[K]$

$\lambda^{(wall)}$ = the thermal conductivity of the metal wall, $\left[W/m\cdot K\right]$

δ_{FL} = the thickness of the metal wall, $[m]$

4.3.4. The coolant

The conservation equation for the coolant is written in the following way:

$$\frac{\partial\left(\rho^{(NH_3)}\cdot\bar{h}_c\left(T_c\right)\right)}{\partial t}+\frac{\partial\left(F_c\cdot\bar{h}_c\left(T_c\right)\right)}{\partial z}=\bar{q}_{\Delta T,wall\leftrightarrow coolant} \tag{5.56}$$

The enthalpy of the boiling coolant is determined from the enthalpies of the liquid and vapours phases from the following equation:

$$\bar{h}_c(T_c) = x_c \cdot h_c^{(v)}(T_c) + (1 - x_c) \cdot h_c^{(l)}(T_c) \tag{5.57}$$

Assuming that the temperature of the coolant is constant and pseudo-steady state, the conservation is rewritten as:

$$F_c \cdot \Delta \bar{h}_c(T_c) \cdot \frac{\partial x_c}{\partial z} = \bar{q}_{\Delta T, wall \leftrightarrow coolant} \tag{5.58}$$

With the **boundary condition**:

At $z = 0$ $\qquad x_c = x_{c,0}$ (5.59)

List of symbols

T_c = temperature of the coolant, $[K]$

$\rho^{(NH_3)}$ = density of ammonia, $\left[kg/m^3 \right]$

$\bar{h}_c$ = enthalpy of the coolant, $\left[J/kg \right]$

F_c = coolant flow rate, $\left[kg/s \right]$

x_c = mass fraction of vapours, $[-]$

$h_c^{(v)}$, $h_c^{(l)}$ = enthalpy of the vapour and liquid coolant, $\left[J/kg \right]$

$\Delta \bar{h}_c$ = enthalpy of vaporization for the coolant, $\left[J/kg \right]$

4.4. Overview of the model reduction for the conservation equations in the 3-D model

A first reduction of conservation equations of the 5-D model was the reduction of the number of coordinates from five to three by averaging with respect to the radial and angular coordinates for the mass, population and energy balances, using the averaging procedures defined in Appendix 5 of this thesis.

The axial velocities of all the phases inside the ice cream mix are equal. The effects of change in density of the mixture are accounted in the axial velocity.

All process variables are constant over the cross-sectional area, while varying with the axial position and time. Axial dispersion is not considered.

The fluxes to and from the frozen layer are assumed to be constant during the time between two successive scrapings, but varying with axial position and time.

The momentum balance is written in a reduced form, as a relationship between the mass flux and the pressure drop.

The ice particles in the bulk have the same temperature, equal to the phase equilibrium temperature of the ice-water-sugar.

The energy balance for the phases in the bulk domain is written for the liquid ice cream, consisting of matrix, air and ice particles.

When writing the energy balance for the frozen layer, this layer is considered as a solid wall, with a thickness equal to the average thickness of the layer.

Pseudo-steady state is assumed when writing the energy balance over the frozen layer, freezer wall and the coolant.

5. Constitutive equations for the 3-D model

The differential equations defining the conservation of resources during the ice cream freezing process, presented in the previous sections, contain variables within the various terms that have not yet been specified or related to each other. The number of variables present in the conservation equations exceeds the number of these equations; hence, some additional equations are required to close the mathematical model of the process. These are the so-called constitutive equations.

These relations are presented in the order of their relationship to the various terms in the conservation equations:

(a) Dynamic derivative terms: the *hold-u*p of a resource (mass, energy, ...)

(b) Convective derivative term with a *flux*

(c) *Rates* of the various kinetic phenomena, such as ice particle melting rate, mass and heat transfer effects, scraping rate, work done by the rotor, viscous dissipation etc.

The following constitutive equations will be presented:

1) thermodynamic equations of state to obtain the density, the specific heat and the enthalpy
2) the fluxes of convective transport of mass, energy and momentum
3) the rate laws for conductive phenomena, with associated transport coefficients (diffusion coefficients, thermal conductivity and viscosity) per phase and the associated transfer coefficients (heat transfer, momentum) over boundary layers in a fluid phase; the solid phases have no boundary layer effects
4) rate laws for transfer of mass, energy and momentum between phases and for sources and sinks within a phase

The laws defining these terms will be presented in the following sections, together with the thermodynamic equations of state. An overview of all the constitutive equations is presented in Table

5.6. For the simplicity of notation, for the radially averaged terms in the conservation equations the "dash" will be dropped.

5.1. Thermodynamic equations of state

The thermodynamic equations of state will be presented for the mass, energy, transport.

5.1.1. Density of phases

a) Density of the liquid phase

The density of the air and liquid mix (the "aerated liquid" phase) is determined as a function of the densities of the components in the following way:

$$\frac{1}{\rho_{domain}^{(mix)}} = \sum_{j} \left(\frac{x_{domain,j}^{(\varphi)}}{\rho_{j}^{(\varphi)}} \right) \tag{5.60}$$

The density of the components of the matrix is assumed to have a constant value during the freezing process. The values of the densities are presented in Table 7.2, in Appendix 11.

The density of the air is determined using the ideal gas law, at the initial temperature and pressure of the ice cream mix:

$$\rho_{domain}^{(a)} = \frac{M_a \cdot P_{domain}}{R \cdot T_{domain}} \tag{5.61}$$

List of symbols

$\rho_{domain}^{(mix)}$ = density of the mix, $\left[kg/m^3 \right]$

$x_{domain,j}^{(\varphi)}$ = mass fraction of component j , $[-]$

$\rho_{j}^{(\varphi)}$ = density of component j , $\left[kg/m^3 \right]$

P_{domain} = pressure inside the domain, $[Pa]$

T_{domain} = temperature inside the domain, $[K]$

R = specific gas constant, $\left[J/kg \cdot K \right]$

M_a = molecular weight of air, $\left[kg/kmole \right]$

Table 5.6. Constitutive equations for the ice cream freezing model

Type of law	Reference phase	Counter phase	Mass		Momentum		Energy			
Thermodynamic equation of state	***Ice***		*Density*	constant			*Specific heat*	constant	*Enthalpy*	Eq. (5.63)
	Liquid			constant				constant		
	Air			Eq. (5.61)				constant		Eq. (5.65)
	Metal			constant				constant		
	Coolant			constant						
	Mixing rule			Eq. (5.60)						Eq. (5.66)
Flux	***Ice (particle)***		Eq. (5.70) & (5.72)				Eq. (5.73)			
	Liquid		Eq. (5.71)							
	Air		Eq. (5.71)							
	Solid ice (FL)						Eq. (5.74)			
	Metal									
	Coolant		constant							
Conductive transport	***Ice***		*Diffusivity*	constant	*Viscosity*		*Conductivity*	constant		
	Liquid			constant				constant		
	Air							constant		
	Metal							constant		
	Coolant							constant		
	Mixing rule					Eq. (5.133)		Eq (5.135) & (5.137)		
Transfer coefficient	***Ice (particle)***		Eq. (5.125)				Eq. (5.139)			
	Liquid		Eq. (5.129)							
	Ice cream mix						Eq. (5.138)			
	Solid ice (FL)						Eq. (5.140)			
	Freezer wall						Eq. (5.140)			
	Coolant						Eq. (5.142)			
Phase transfer rate	***Ice (particle)***	***Aerated liquid***	Eq. (5.109)				Eq. (5.116)			
		Solid ice (FL)	Eq. (5.81)				Eq. (5.116)			
	Aerated liquid	***Solid ice (FL)***	Eq. (5.90)				Eq. (5.116)			
		Rotor					Eq. (5.120) & Eq. (5.124)			
	Solid ice (FL)	***Ice (particle)***	Eq. (5.95)				Eq. (5.116)			
		Rotor								
	Metal	***Coolant***								

5.1.2. Specific heat and enthalpy

The specific heat for the various components and phases is assumed constant. The values for the components of the ice cream mix are presented in Table 7.2 in Appendix 11.

The enthalpy of a specific phase is determined using an arbitrary zero reference for the enthalpy. This zero reference enthalpy is determined for a reference temperature equal to 298 K and liquid phase:

$$T_{ref} = 298 \tag{5.62}$$

The relationship between the enthalpy and the temperature, when a phase transition is present:

$$h_{domain}^{(\varphi_2)}(T) = h_{domain}^{(\varphi_1)}\left(T_{ref}\right) + \int_{T_{ref}}^{T^{(\varphi_1 \to \varphi_2)}} c_{p,j}^{(\varphi_1)}(T)\,dT + \Delta h^{(\varphi_1 \to \varphi_2)}\left(T^{(\varphi_1 \to \varphi_2)}\right) + \int_{T^{(\varphi_1 \to \varphi_2)}}^{T} c_{p,j}^{(\varphi_2)}(T)\,dT \tag{5.63}$$

For the case of the phase transition between the liquid water and ice, the enthalpy of the phase change (enthalpy of crystallization) is taken at the normal melting temperature at 1 bar:

$$T^{(\varphi_1 \to \varphi_2)} = 273.15 \tag{5.64}$$

The value of this enthalpy is presented in Table 7.2, in Appendix 11.

For the species for which the phase transition is not present, the enthalpy is determined from the following equation:

$$h_{domain,j}^{(\varphi)}(T) = h_{domain,j}^{(\varphi)}\left(T_{ref}\right) + \int_{T_{ref}}^{T} c_{p,j}^{(\varphi)}(T)\,dT \tag{5.65}$$

The enthalpy of a mixture is determined using a weight additive model, by adding the enthalpy contribution of each pure component:

$$h_{domain}^{(mix)} = \sum_j \left(x_{domain,j}^{(\varphi)} \cdot h_{domain,j}^{(\varphi)} \right) \tag{5.66}$$

In equation (5.66), any non-ideal interactions have been ignored.

List of symbols

T_{ref} = the reference temperature, $[K]$

$c_{p,j}^{(\varphi)}$ = intrinsic heat capacity of component j in phase φ, $\left[J/kg \cdot K \right]$

φ_1, φ_2 = phases

$T^{(\varphi_1 \to \varphi_2)}$ = temperature of the phase change, $[K]$

$\Delta h^{(\varphi_1 \to \varphi_2)}$ = enthalpy of the phase change, $\left[J/kg \right]$

$h_{domain,j}^{(\varphi)}$ = enthalpy of a pure component j in phase φ, $\left[J/kg \right]$

a) Enthalpy of the dispersed phase

In case of the *dispersed phases*, the averaged enthalpy is determined considering the contribution of each particle, $h_{n,domain}^{(\varphi)}$, at the temperature of a single particle, $T_{n,domain}^{(\varphi)}$. The use of a single particle's temperature is not practical from a computational point of view. This implies the introduction of a new coordinate in the population balance for the dispersed phase, as discussed in Section 3.5.2 of this chapter.

According to assumption 17, the ice particles have all the same temperature. For this reason, the averaged enthalpy of the dispersed phase will be determined using the enthalpy calculated at the average temperature of the particles, $\bar{T}_{domain}^{(\varphi)}$:

$$h_{domain}^{(\varphi)} = \frac{h_{n,domain}^{(\varphi)}\left(\bar{T}_{domain}^{(\varphi)} \right)}{\varepsilon_{domain}^{(\varphi)} \cdot \rho^{(\varphi)}} \cdot \int_{m_{min}^{(\varphi)}}^{m_{max}^{(\varphi)}} \left[n_{domain}^{(\varphi)}\left(m^{(\varphi)} \right) \right] dm \tag{5.67}$$

List of symbols

$h_{n,domain}^{(\varphi)}$ = enthalpy of a single ice particle, $\left[J/kg \right]$

$T_{n,domain}^{(\varphi)}$ = temperature of a single ice particle, $\left[K \right]$

$\bar{T}_{domain}^{(\varphi)}$ = average temperature of ice particles, $\left[K \right]$

$h_{domain}^{(\varphi)}$ = enthalpy of the ice phase, $\left[J/kg\ phase \right]$

$n_{domain}^{(\varphi)}$ = the ice particle density, $\left[\#/m^3 \right]$

$m^{(\varphi)}$ = particle's mass, $\left[kg/\# \right]$

$\varepsilon_{domain}^{(\varphi)}$ = volume fraction of phase φ, $\left[- \right]$

$\rho^{(\varphi)}$ = density of phase φ, $\left[kg/m^3 \right]$

5.1.3. Ice-water-sugar phase equilibrium

The particles melt as long as the following condition is respected:

$$T_B(z) > T_{B,e} \tag{5.68}$$

The value of the equilibrium temperature of the bulk is determined using:

$$T_{B,e} = T_m^{(i)} - \frac{1860 \cdot x_{s,B}}{M_s \cdot (1 - x_{s,B})} \tag{5.69}$$

42. The sucrose is chosen to represent the different types of sugars present in the ice cream mix.

From the look of the freezing curve for most of the mix compositions, it can be concluded that in the temperature range where the SSHE operates, only about one third to one-half of the water is present in solid state. A good source for calculating initial freezing temperatures and freezing curves of mixes can be found in (Leighton, 1926), (Bradley & Smith, 1983) and (Bradley, 1986).

List of symbols

T_B = the temperature of the bulk phases, $[K]$

$T_{B,e}$ = the equilibrium temperature of the liquid phase inside the bulk, $[K]$

$T_m^{(i)}$ = the melting point of ice, $[K]$

M_s = molecular weight of sugar, $\left[{}^{kg}/_{kmole} \right]$

$x_{s,B}$ = sugar mass fraction in the bulk, $[-]$

5.2. Fluxes in a spatial direction

A flux involves an intra phase transport of resources.

5.2.1. Mass flux in axial direction

The mass and population balance equations contain convective derivative terms with a flux. In the following, relations for computing these fluxes are defined.

a) *The population balance equation* for the dispersed and distributed phases (ice particles in the bulk)

The flux of particles along the axial coordinate is calculated using:

$$j_{B,z}^{(\varphi)} = u_{B,z} \cdot n_B^{(\varphi)} \tag{5.70}$$

b) *The mass balance equation* for the pseudo-continuous phases (liquid matrix in the bulk, air)

The mass flux of component along the axial coordinate is calculated from the following equation:

$$j_{m,B,j,z}^{(\varphi)} = u_{B,z} \cdot \varepsilon_B^{(\varphi)} \cdot c_{B,j}^{(\varphi)} \tag{5.71}$$

5.2.2. Mass flux along the internal coordinate

The population balance equation contains a flux along the internal coordinate, which is determined from the following equation:

$$j_{B,s}^{(\varphi)} = r_{s,B}^{(\varphi)} \cdot n_B^{(\varphi)} \tag{5.72}$$

5.2.3. Energy flux in axial direction

The mass flux in axial direction and the energy flux can be easily related using the following equation:

$$e_{B,z}^{(\varphi)} = j_{m,B,z}^{(\varphi)} \cdot h_B^{(\varphi)} \tag{5.73}$$

List of symbols

$u_{B,z}$ = velocity in the bulk domain, $\left[m/s \right]$

$r_{s,B}^{(\varphi)}$ = growth/melting rate of ice particles in the bulk domain, $\left[m/s \right]$

$e_{B,z}^{(\varphi)}$ = energy flux in axial direction, $\left[W/m^2 \right]$

5.2.4. Energy flux in radial direction

For two of the domains (the frozen layer and the freezer wall), the radial coordinate is still important from the point of view of the energy balance. These two domains are treated as composite cylindrical walls (Bird, Stewart & Lightfoot, 2002). The conductive flux in radial direction is determined using Fourier's law:

$$q_{r,domain} = -\lambda^{(\varphi)} \cdot \frac{dT_{domain}}{dr} \tag{5.74}$$

The **boundary conditions** must be defined for both the frozen layer and the freezer wall:

a) The frozen layer

At $r = R - \delta_{FL}$ $\qquad T_{domain} = T_{FL}^{(i)}$ (5.75)

At $r = R$ $T_{domain} = T_{wall}$ (5.76)

b) The freezer wall

At $r = R$ $T_{domain} = T_{wall}$ (5.77)

At $r = R + \delta_{wall}$ $T_{domain} = T_{wall,coolant}$ (5.78)

List of symbols

$q_{r,domain}$ = radial energy flux in the domain, $\left[W/m^2 \right]$

$\lambda^{(\varphi)}$ = heat conductivity of the phase φ, $\left[W/m \cdot K \right]$

$T_{FL}^{(i)}$ = temperature of the frozen layer, $\left[K \right]$

T_{wall} = temperature of the wall at the product side, $\left[K \right]$

$T_{wall,coolant}$ = temperature of the wall at the coolant side, $\left[K \right]$

5.2.5. Energy flux in radial direction over the frozen layer and the metal wall

An equation for the temperature drop $T_B^{(i)} - T_{coolant}$ is the outcome of solving the energy balance over the frozen layer and the metal wall in radial direction.

The heat transfer coefficient for these 'walls' is determined assuming that this layer behaves like a cylindrical solid wall.

The heat flux in radial direction will be determined from the following equation:

$$q_0 = U_0 \cdot \left(T_B^{(i)} - T_{coolant} \right) \tag{5.79}$$

The expression for the overall heat transfer coefficient for cylindrical solid walls is presented in Section 5.4.4 of this chapter.

List of symbols

q_0 = heat flux in radial direction, based on the inner surface of the freezer, $\left[W/m^2 \right]$

U_0 = overall heat transfer coefficient based on the inner surface of the freezer, $\left[W/m^2 \cdot K \right]$

$T_{coolant}$ = temperature of the coolant, $\left[K \right]$

5.3. Rate laws

A rate law involves a transfer of a physical resource between phases or domains, as well as "point" processes, such as sources and sinks within a phase. The knowledge about the mathematical

structure and the parameters of the rate equations presented in the previous sections is limited. Rigorous equations can be written for few of these rates. Even if rigorous equations could be written, the imposed drastic simplification of the fluid flow behaviour requires approximations of the laws. In the next sections, a pragmatic, linear structure of the rate laws is proposed. This structure must be consistent with insights from non-equilibrium thermodynamics (NET) and needs to be validated using experimental data.

The rate laws for melting, mass and heat transfer are all structured in the same fundamental way: the rate is proportional to a single thermodynamic driving force. This driving force is mechanically enhanced or diminished by the scraper rotation. The transfer coefficient is built up from a nominal transfer coefficient and an empirical adjustment parameter ("fudge factor"). The nominal transfer rate coefficient represents a theoretical, state-of-the-art estimate. The empirical adjustment factor is needed for fine-tuning to experimental data.

$$Rate = C_{rate} \cdot f\left(\omega_r\right) \cdot k_{rate} \cdot F_d \tag{5.80}$$

List of symbols

C_{rate} = the empirical adjustment parameter ("fudge factor")

$f\left(\omega_r\right)$ = the effect of the scraper rotation on the transfer rate

ω_r = rotor speed, $\left[rps\right]$

k_{rate} = the nominal transfer rate coefficient (a 'state-of-the-art' estimate from the literature)

F_d = the thermodynamic driving force, e.g., arising from differences between phases

In the next sections, the specific rate laws are introduced, covering changes in mass, particle distributions, momentum and energy, in that order. After completing the description of the rate laws the determination of the nominal transfer rate coefficients is discussed.

5.3.1. Mass transfer and ice melting processes

The mass transfer events involve exchanges of water and ice between two phases and domains: water in the bulk domain, ice particles in the bulk domain and solid ice in the frozen layer.

The rate laws for the mass transfer terms will be detailed in the following order:

- ice particles transported from the bulk domain to the frozen layer
- components in the liquid phase of the bulk domain transported to the frozen layer
- scraping of ice from the frozen layer into the bulk domain

The different mass transfer terms for ice and water are shown in Figure 5.8. An overview of all the mass related transfer terms is presented in Table 5.7, at the end of this section.

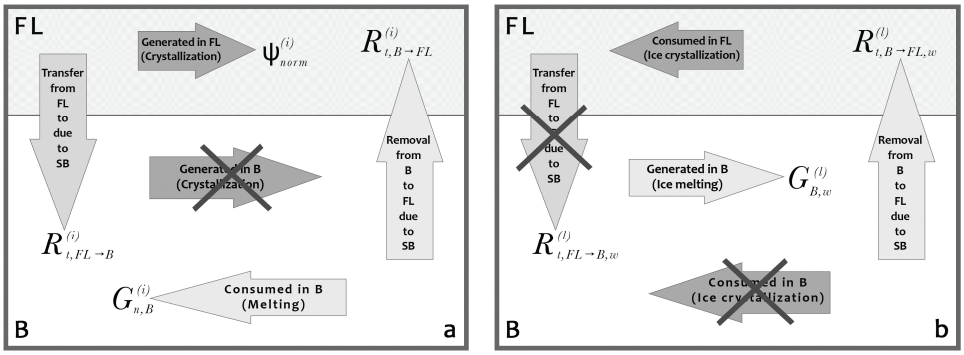

Figure 5.8. Transfer terms for the: (a) ice and (b) water

a) Transfer of ice particles from the bulk to the frozen layer

It is possible that a small fraction of the ice particles from the bulk is transferred to the frozen layer and is integrated into the frozen layer. This process of ice particle transfer will happen only if there are enough particles in the bulk and a favourable temperature difference between the ice particles in the bulk and the colder surface of the (growing) frozen layer to which particles may stick and freeze.

The flux in this case will be proportional to the concentration of ice particles in the bulk domain:

$$R^{(i)}_{t,B\to FL}\left(t,z,s^{(i)}\right) = C_a \cdot k_B^{(i)} \cdot f_1\left(\omega_r\right) \cdot n_B^{(i)}\left(t,z,s^{(i)}\right) \tag{5.81}$$

This easily measurable 'force', number of particles, is chosen over the fundamental thermodynamic driving force, the chemical potential difference between the ice particles and the frozen layer. An additional assumption is that the ice particles, irrespective of their size, will have an equal chance of being frozen into the frozen layer. For this reason, the transfer coefficients are independent of the size $s^{(i)}$ in the rate equation. Hence, the total mass transfer rate is obtained by integration over all sizes and is written as:

$$R^{(i)}_{t,m,B\to FL}\left(t,z\right) = C_a \cdot k_B^{(i)} \cdot f_1\left(\omega_r\right) \cdot \varepsilon_B^{(i)} \cdot c_B^{(i)}\left(t,z\right) \tag{5.82}$$

Where the concentration of the ice particles in the bulk domain, $c_B^{(i)}$ is given by

$$c_B^{(i)} = \rho^{(i)} \cdot \int_0^{\infty}\left(n_B^{(i)} \cdot a^{(i)}\right) \cdot ds^{(i)} \tag{5.83}$$

In addition, the action of the rotating scraper will have an influence on the rate of transfer. The rotor action is accounted for in the term $f_1\left(\omega_r\right)$. This term has the following qualitative properties:

- When the rotor speed is zero, the spontaneous transfer of ice particles from the bulk to the frozen layer is extremely unlikely and will be ignored
- When the rotor speed is very high, the ice has too high a momentum to stick on the wall
- There is a value of the rotor speed, $\omega_{r,max} \in (0,\infty)$ for which the transfer rate of ice from the frozen layer to the bulk is a maximum

The conditions for maximum are stated as follows:

$$\left.\frac{\partial f_1}{\partial \omega_r}\right|_{\omega_r < \omega_{r,max}} \geq 0 \qquad \text{(Ascending slope)}$$
$$\left.\frac{\partial f_1}{\partial \omega_r}\right|_{\omega_r > \omega_{r,max}} \leq 0 \qquad \text{(Descending slope)} \tag{5.84}$$

The function meeting the conditions above is pragmatically postulated as a Weibull distribution-type of function, due to the flexible properties of this distribution:

$$f_1(\omega_r) = \begin{cases} \Sigma_\omega \cdot \Lambda_\omega^{-\Sigma_\omega} \cdot (\omega_r)^{\Sigma_\omega - 1} \cdot e^{-\left(\frac{\omega_r}{\Lambda_\omega}\right)^{\Sigma_\omega}} & for\ \omega_r \geq 0 \\ 0 & for\ \omega_r < 0 \end{cases} \tag{5.85}$$

Λ_ω and Σ_ω are adjustable parameters. However, they must be chosen such that the function is positive and that there is a maximum in this function.

$$\Lambda_\omega > 0$$
$$\Sigma_\omega > 1 \tag{5.86}$$

It is noted that under these parametric conditions, the Weibull function (5.85) satisfies the boundary conditions (5.84). The maximum rotational speed is determined from:

$$\omega_{r,max} = \Lambda_\omega \cdot (\Sigma_\omega - 1)^{1/\Sigma_\omega} \qquad for\ \Sigma_\omega > 1 \tag{5.87}$$

b) Transfer of component j from the bulk to the frozen layer

Since it is assumed that the frozen layer contains only ice, the transfer of "sugar", "fat", "Air" and "other" components from the bulk to the frozen layer is not possible. For this reason, for these components, the rate vanishes:

$$R^{(l)}_{t,B\to FL,j} = C_b \cdot k_B^{(l)} \cdot f_2(\omega_r) \cdot \varepsilon_B^{(l)} \cdot c^{(l)}_{B,j}(t,z) = 0 \tag{5.88}$$

due to the fact that: $k^{(l)}_{L,j} = 0$ (5.89)

For the transfer of water, the driving force is a difference between its actual local concentration in the bulk and the phase equilibrium concentration.

$$R^{(l)}_{t,B\to FL,w}(t,z) = C_b \cdot k^{(l)}_{B,w} \cdot f_2(\omega_r) \cdot \left[c^{(l)}_{B,w}(t,z) - c^{(l)}_{B,w,e}\left(T_{B,e}\right) \right] \tag{5.90}$$

The term $f_2(\omega_r)$ takes into account the rotor action. It is assumed that when there is no rotor action at all, the transfer rate of water to the frozen layer surface is negligible. For sufficiently high rotor action, the mass transfer limitation at the bulk side completely vanishes. Therefore, this term has the following properties:

For $\omega_r \to 0$ $f_2(\omega_r) \to 0$ (5.91)

For $\omega_r \to \infty$ $f_2(\omega_r) \to 1$ (5.92)

Several equations can be postulated for the $f_2(\omega_r)$ term. For the purpose of this research, the following function will be used:

$$f_2(\omega_r) = \left(\frac{k_\omega \cdot \omega_r}{1 + k_\omega \cdot \omega_r} \right)^{n_\omega} \tag{5.93}$$

$$n_\omega \geq 1 \tag{5.94}$$

List of symbols

C_b = the fudge factor, $[-]$

$k^{(l)}_{B,w}$ = mass transfer coefficient for water, $\left[m/s \right]$

$c^{(l)}_{B,w,e}$ = equilibrium concentration of water at the interface between the frozen layer and the bulk, $\left[kg/m^3 \right]$

c) Transfer of ice from the frozen layer to the bulk by scraping action

For the transfer term of ice particles coming from the frozen layer the following two cases are considered:

(1) The distribution of the ice particles coming from the frozen layer is physically the result of a merger of two size distributions: (a) one of the ice crystals coming from the bulk into the frozen layer, and (b) one of the fresh ice formed by crystallization of the water coming into the frozen layer from the bulk. In this case, complex phenomena need to be taken into account: within the frozen layer, the nucleation, growth, agglomeration of the newly formed ice particles resulted from the water crystallization, as well as growth, agglomeration of the ice particles that come from the bulk.

Covering this implies the set-up of a new population balance equation for the 'ice' phase in the frozen layer. Moreover, the history – as reflected by their attained states - of the ice particles must be considered: the particles coming from the bulk have a different history and states than the ones that are newly formed. This will complicate the frozen layer model even more.

For this reason, a second, simpler approach will be considered:

(2) Any ice formed by crystallization of either the water or the ice coming from the bulk forms a compact uniform layer. Upon scraping, where the movements of the blades crack the solid ice layer, a completely new distribution of ice crystal sizes is formed. This implies that any information on the origin of the ice in the frozen layer is erased. Moreover, local processes such as nucleation, growth and agglomeration of ice particles in the frozen layer can be neglected. By the scraping of the blades, a new distribution of ice particles is formed, entering the bulk domain. This approach is captured in the following assumption:

43. The thickness of the frozen layer and the rotational speed of the scraper determine the particle size distribution of the ice particles being scraped away. This distribution removed from the frozen layer is independent of the size distribution of the ice particles inside the bulk. Due to the lack of detailed fundamental information, a qualitatively suitable empirical distribution function is postulated for the size of the scraped ice particles coming from the frozen layer.

Knowing a size distribution function one can relate that to the mass transfer rate. When specifying a mass transfer rate a time-averaged value will be taken over the time interval of the growth of the frozen layer and the scraping, smoothing the periodic dynamic character. The mass transfer term of ice from the frozen layer to the bulk (assuming the ice particle population is a pseudo-continuous phase in the size coordinate) is defined as:

$$R^{(i)}_{t,m,FL\to B}(t,z) = \rho^{(i)} \cdot \int_0^\infty \left(R^{(i)}_{t,FL\to B}\left(t,z,s^{(i)}\right) \cdot a^{(i)}(s) \right) ds \tag{5.95}$$

When assuming that the frozen layer is in short term stationary state, the sum of the incoming and outgoing mass fluxes over the scrapping period must vanish.

$$R^{(i)}_{t,m,FL\to B}(t,z) = \left[R^{(i)}_{t,m,B\to FL}(t,z) + R^{(l)}_{t,B\to FL,w}(t,z) \right] \cdot \frac{(t_{s-} - t_0)}{(t_s - t_{s-})} \tag{5.96}$$

The (number) flux of ice particles with size $s^{(i)}$ from the frozen layer to the bulk is determined as a fraction of the total mass flux in the following way:

$$R^{(i)}_{t,FL\to B}\left(t,z,s^{(i)}\right)=\frac{R^{(i)}_{t,m,FL\to B}\left(t,z\right)\cdot\psi^{(i)}_{norm}\left(s^{(i)}\right)}{m^{(i)}\left(s^{(i)}\right)} \tag{5.97}$$

$$m^{(i)}\left(s^{(i)}\right)=\rho^{(i)}\cdot v^{(i)}\left(s^{(i)}\right) \tag{5.98}$$

44. The ice particles are assumed to have a spherical shape. Since the real shape of the ice crystal is very irregular, the use of a shape factor could be considered to calculate the volume of the ice particle, $v^{(i)}$.

It is necessary to know this number flux, $R^{(i)}_{t,FL\to B}\left(t,z,s^{(i)}\right)$ because it alters the size distribution of the ice particles in the bulk. The function $\psi^{(i)}_{norm}\left(s^{(i)}\right)$ is the normalised size distribution of the ice particles removed by the scraping blades. This latter function is unknown and it is very difficult to get a theoretical prediction on basis of the mechanics of the scraping process. Therefore, an empirical function will be used:

45. The normalised distribution function $\psi^{(i)}_{norm}\left(s^{(i)}\right)$ for the size of scraped away ice particles is chosen to be a probabilistic Weibull-type of distribution, with the scale parameter equal to Λ and the shape parameter equal to Σ.

The probability density function of the Weibull distribution for the independent coordinate x is given by:

$$\psi^{(i)}_{norm}\left(s\right)=\begin{cases}\Sigma\cdot\Lambda^{-\Sigma}\cdot\left(x\left(s\right)\right)^{\Sigma-1}\cdot e^{-\left(\frac{x(s)}{\Lambda}\right)^{\Sigma}} & for\ x\left(s\right)\geq 0\\ 0 & for\ x\left(s\right)<0\end{cases} \tag{5.99}$$

$$\begin{aligned}&\Lambda>0\\&\Sigma>0\end{aligned} \tag{5.100}$$

This independent coordinate x is related to the size coordinate s. There is a normalisation condition in the size coordinate:

$$\int_0^{\infty}\psi^{(i)}_{norm}\left(s\right)ds=1 \tag{5.101}$$

$$s^{(i)}<s^{(i)}_{max} \tag{5.102}$$

The relation between x and s must be specified. The independent coordinate x runs from $[0,\infty)$. It is a function of the particle size, $s^{(i)}$, which may cover a smaller finite range $(0, s_{max}^{(i)}]$ in physical reality. For this reason, $x \to \infty$ must correspond to $s^{(i)} \to s_{max}^{(i)}$. The precise relationship between x and $s^{(i)}$ is open to choice and will depend on the actual physical situation.

List of symbols

Λ = scale parameter of the Weibull distribution $[-]$

Σ = shape parameter of the Weibull distribution $[-]$

$x(s)$ = the normalised coordinate of the particle size distribution leaving the frozen layer

$m^{(i)}$ = the ice particle mass, $\left[kg/\# \right]$

$v^{(i)}$ = the volume of the ice particle, $\left[m^3/\# \right]$

$a^{(i)}$ = the surface area of an ice particle, $\left[m^2/\# \right]$

d) Transfer of component j from the frozen layer to the bulk

Only ice is transferred from the frozen layer to the bulk. The value of the transfer term for all other components j from the frozen layer to the bulk is zero, because of a zero concentration in the frozen layer:

$$c_{FL,j}(t,z) = 0 \tag{5.103}$$

$$R_{t,FL\to B,j}^{(l)} = C_f \cdot k_{FL,j} \cdot f_2(\omega_r) \cdot c_{FL,j}(t,z) = 0 \qquad \forall j \tag{5.104}$$

e) Rate of change of ice particle population by generation ($B_B^{(i)}$) and removal ($D_B^{(i)}$)

According to assumption 8, there is no crystallization or nucleation of the ice particles inside the bulk domain. Moreover, due to the same assumption, the death of particles due to agglomeration or attrition is ignored. For this reason, the rates of change of ice particles by generation and removal in the bulk are zero:

$$B_B^{(i)} = 0 \tag{5.105}$$

$$D_B^{(i)} = 0 \tag{5.106}$$

f) Rate of change of ice particles due to melting in the bulk domain

The rate of change of the ice particles size coordinate is expressed by $r_s^{(i)}$. This rate of change determines the flux of melting particles along the size coordinate:

$$j_{B,s}^{(\varphi)} = r_{s,B}^{(\varphi)} \cdot n_B^{(\varphi)} \tag{5.107}$$

The derivative term of this flux with respect to the particle's coordinate $s^{(i)}$ is represented in the population balance by a new algebraic variable:

$$g_{n,B}^{(i)} = -\frac{\partial j_{B,s}^{(i)}\left(t,z,s^{(i)}\right)}{\partial s^{(i)}} \tag{5.108}$$

By integrating of this local rate of change over the particle coordinate one can obtain the mass transfer rate due to the joint effect of all melting ice particles, $G_{m,B}^{(i)}$, which is equal to the mass transfer of liquid water due to melting of ice particles in the bulk, $G_{B,w}^{(l)}$.

The specification of the internal coordinate of an ice particle will lead to determining the transfer rate due to the melting of the ice particles:

The mass transfer rate due to the joint effect of all melting ice particles in the bulk is determined as follows:

$$G_{B,w}^{(l)} = \rho^{(i)} \cdot \int_0^{\infty} \left(g_{n,B}^{(i)} \cdot a^{(i)}\right) ds = \rho^{(i)} \cdot \int_0^{\infty} \left(\frac{\partial j_{B,s}^{(i)}\left(t,z,s^{(i)}\right)}{\partial s^{(i)}} \cdot a^{(i)} \right) ds \tag{5.109}$$

List of symbols

$g_{n,B}^{(i)}$ = number rate of local change of ice due to melting of the ice particles, $\left[{}^{\#}/_{m^3 \cdot s} \right]$

$G_{m,B}^{(i)}$ = mass rate of local change of ice due to melting of ice particles, $\left[{}^{kg}/_{m^3 \cdot s} \right]$

$G_{B,w}^{(l)}$ = mass rate of local change of water due to melting of ice particles, $\left[{}^{kg}/_{m^3 \cdot s} \right]$

The mass transfer rate due to melting can be determined from the sequence: $r_s^{(i)}$, $j_{B,s}^{(i)}$, $G_{n,B}^{(i)}$, $G_{B,w}^{(l)}$. A constitutive equation must be specified for the rate of change of the ice particle's coordinate, $r_s^{(i)}$.

The starting point for the derivation of such a constitutive equation is the heat balance around an ice particle, shown in Figure 5.7.

The heat flow towards the ice particle is calculated from the following equation, determined using the shrinking core model described in Appendix 12:

$$\phi_{q,\Delta T}^{(i)} = -8 \cdot \pi \cdot \lambda^{(i)} \cdot s^{(i)} \cdot \left(T_B - T_B^{(i)} \right) \tag{5.110}$$

The heat flux through the particle surface is determined using:

$$q_{\Delta T}^{(i)} = \frac{\phi_{q,\Delta T}^{(i)}}{a^{(i)}} \tag{5.111}$$

The energy supply to all the ice particles the following relation is used:

$$q_{melt}^{(i)} = \int_0^{\infty} \left(q_{\Delta T}^{(i)} \cdot n_B^{(i)} \right) ds \tag{5.112}$$

The melting rate for a single ice particle can be written as:

$$r_s^{(i)} \left(t, z, s^{(i)} \right) = \frac{q_{\Delta T}^{(i)}}{\Delta h_{cryst}} \tag{5.113}$$

Table 5.7. Overview of the rate laws for the mass related events

Rate	Fudge factor	Rotor action effect	Nominal transfer coefficient	Driving force
Transfer of ice from the FL to the B	-	$f_1(\omega_r)$	-	ω_r^*
Transfer of ice from the B to the FL	C_a	$f_2(\omega_r)$	$k_B^{(i)}$	$n_B^{(i)}$
Transfer of water from the B to the FL	C_b	$f_3(\omega_r)$	$k_{B,w}^{(l)}$	$c_{B,w}^{(l)} - c_{B,w,e}^{(l)}$
Ice melting in the B	C_c	*1*	$k_r^{(i)}$	$T_B - T_{B,e}$
Water production by ice melting in the B	C_c	*1*	$k_r^{(i)}$	$T_B - T_{B,e}$

The rate of local change of ice due to melting is determined from the following expression:

$$G_{m,B}^{(i)} = -\rho^{(i)} \cdot \int_0^{\infty} \left(g_{n,B}^{(i)} \cdot a^{(i)} \right) ds = -\rho^{(i)} \cdot \int_0^{\infty} \left(\frac{\partial j_{B,s}^{(i)} \left(t, z, s^{(i)} \right)}{\partial s^{(i)}} \cdot a^{(i)} \right) ds \tag{5.114}$$

The rate of local change of water due to ice melting is:

$$G_{B,w}^{(l)} = -G_{m,B}^{(i)} \tag{5.115}$$

List of symbols

$q_{\Delta T}^{(i)}$ = heat flux due to temperature difference between the ice particles and the liquid bulk, $\left[W/m^2 \right]$

$q_{melt}^{(i)}$ =heat flux due to melting of ice particles in the bulk, $\left[W/m^2 \right]$

Δh_{cryst} = the enthalpy of crystallization, $\left[J/kg \right]$

g) Rate of change of water due to ice melting in the bulk

The mass transfer rate of water due to the ice melting in the bulk domain is determined from the expression for $G_{B,w}^{(l)}$ in equation (5.109).

5.3.2. Energy transfer processes

Energy is expressed by means of enthalpy in this model. In the following sections, the rate laws for the energy transfer terms are detailed. The different energy transfer terms are shown in Figure 5.9.

a) Transfer due to a transfer of mass, q_j

The enthalpy flux transferred between two phases or domains due to a transfer of mass is determined by its enthalpy content:

$$q_{(j,D_1 \to D_2)}^{(\varphi)}(t,z) = R_{t,m,D_1 \to D_2}^{(\varphi)} \cdot h_{D_1}^{(\varphi)} \tag{5.116}$$

List of symbols

$q_{(j,D_1 \to D_2)}^{(\varphi)}$ = the enthalpy flux due to mass transfer of phase φ between the domains D_1 and D_2, $\left[W/m^2 \right]$

$R_{t,m,D_1 \to D_2}^{(\varphi)}$ = the mass flux of phase φ transferred between the domains D_1 and D_2, $\left[kg/m^2 \cdot s \right]$

$h_D^{(\varphi)}$ = the enthalpy of phase φ in the domain D, $\left[J/kg \right]$

b) Heat term due to melting of the ice particles, $q_{melt}^{(i)}$

The heat term due to the melting of ice particles in the bulk is determined from the mass flux of ice from melting and the heat of crystallization in the following way:

$$q_{melt}^{(i)} = G_{m,B}^{(i)} \cdot \Delta h_{cryst} \tag{5.117}$$

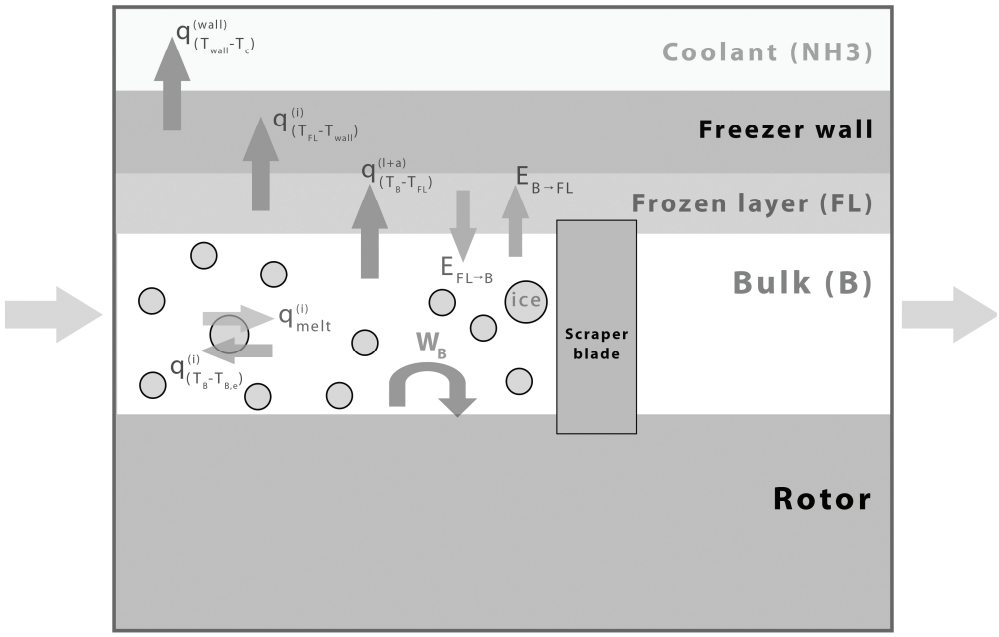

Figure 5.9. Energy transfer terms

It has to be noted that this term does not show up explicitly in the enthalpy balance for the bulk phase. This is because the phase change effects have been accounted for in the definition of the enthalpy per phase, sharing a common reference point for the definition of the enthalpy (Section 5.1.2 of this chapter).

c) Transfer due to temperature difference, $q_{\Delta T}$

The heat flux due to a temperature difference is determined using the heat transfer coefficient as the nominal transfer coefficient and the temperature difference as driving force:

$$q^{(\varphi)}_{(\Delta T)}(t,z) = U^{(\varphi)}_{domain} \cdot \Delta T \tag{5.118}$$

Equation (5.118) is applied for calculating the heat transfer terms presented in the first column of Table 5.8.

List of symbols

$U^{(\varphi)}_{domain}$ = total heat transfer coefficient, $\left[W/m^2 \cdot K \right]$

$U^{(l+a)}_{B}$ = total heat transfer coefficient from the aerated fluid bulk phase to frozen layer, $\left[W/m^2 \cdot K \right]$

$U_{B,i}$ = total heat transfer coefficient between the ice particles and the fluid bulk, $\left[W/m^2 \cdot K \right]$

$U_{FL}^{(i)}$ = total heat transfer coefficient between the frozen layer and the freezer wall, $\left[W/m^2 \cdot K \right]$

U_0 = total heat transfer coefficient between the bulk and the coolant, $\left[W/m^2 \cdot K \right]$

Table 5.8. Transfer terms due to temperature differences

Transfer term	Nominal transfer coefficient	Driving force
$q^{(l+a)}_{(T_B - T_{FL})}$	$U_B^{(l+a)}(\delta_{FL})$	$T_B - T_{FL}^{(i)}$
$q^{(i)}_{(T_{FL} - T_{wall})}$	$U_{FL}^{(i)}$	$T_{FL}^{(i)} - T_{wall}$
$q^{(i)}_{(T_B - T_{B,e})}$	$U_{B,i}$	$T_B - T_{B,e}$
$q_{(T_{wall} - T_c)}$	U_0	$T_{wall} - T_{coolant}$

d) Heat generation due to mechanical work in the bulk

The heat generation due to mechanical work in the bulk W_B it is assumed to come from two main sources (Bongers, 2006): (1) the viscous dissipation, due to the fluid flow around the rotor $Q_{v,B}$; and (2) the scraping friction between the blades and the barrel wall $Q_{scrap,B}$:

$$W_B(t,z) = Q_{v,B}(t,z) + Q_{scrap,B}(t,z) \tag{5.119}$$

According to (Bongers, 2006), this dissipation of mechanical energy accounts for as much as 50% of the heat removed by the refrigerant.

In the following, rate laws for these two terms will be postulated.

d1) Heat generation due to the viscous generation in the bulk domain

The energy balance over the ice cream mixture in the bulk domain accounts for viscous dissipation. In (Bongers, 2006) the viscous dissipation term is equal to the product of the shear stress and the shear rate.

$$Q_{v,B}(t,z) = -C_v \cdot \tau_B(t,z) \cdot \dot{\gamma}_B(t,z) \tag{5.120}$$

The shear stress is calculated using a power law-type equation (Bird, Stewart & Lightfoot, 2002), considering steady-state shear flow:

$$\tau_{B,rz} = -\eta_B^{(i+l+a)} \cdot \dot{\gamma}_B \tag{5.121}$$

Where:

$$\dot{\gamma}_B = \frac{\partial u_z}{\partial r} \tag{5.122}$$

An averaged shear rate for the barrel domain is used as an approximation:

$$\dot{\gamma}_B = C_\gamma \cdot \pi \cdot \omega_r \cdot \frac{2 \cdot D}{D - D_0} \tag{5.123}$$

List of symbols

W_B = the heat generation due to mechanical work, per unit volume in the barrel, $\left[W/m^3 \right]$

$Q_{v,B}$ = the viscous dissipation term, $\left[W/m^3 \right]$

$\tau_{B,rz}$ = the shear stress, $\left[Pa \right]$

$\eta_B^{(i+l+a)}$ = the viscosity of the ice cream, $\left[Pa \cdot s \right]$

$\dot{\gamma}_B$ = the shear rate, $\left[1/s \right]$

C_v, C_γ = fudge factor

D = outer diameter of the freezer, $\left[m \right]$

D_0 = inner diameter of the freezer, $\left[m \right]$

d2) Heat due to the scraping of the ice layer at the freezer wall

For the scraping friction, the work done by the scraper is a function of the flux of ice being scraped from the frozen layer at the wall and the energy it takes to brake solid ice into particles. The following equation will be used to determine this term:

$$Q_{scrap,B} = c_1 \cdot \frac{S_B}{A_B} \cdot R_{i,m,FL \to B}^{(i)} \cdot \mathrm{E}_{mech}^{(i)} \tag{5.124}$$

The intrinsic ice breaking energy $\mathrm{E}_{mech}^{(i)}$ represents the energy required to break one kilogram of ice into particles. The factor $\frac{S_B}{A_B}$ is needed to convert from area (of incoming ice flux) to unit volume in the barrel.

List of symbols

c_1 = fudge factor, $\left[- \right]$

$E_{mech}^{(i)}$ = intrinsic ice breaking energy, $\left[J/kg \right]$

$R_{t,m,FL\to B}^{(i)}$ = flux of ice being scraped from the frozen layer at the wall, $\left[kg/m^2 \cdot s \right]$

5.4. Conductivities and transfer coefficients

A warning is in order before discussing the way the conductivities and the transfer coefficients are determined. By neglecting in the model reduction effort the details of the fluid flow, the price to pay is a severe sacrifice with respect to the rigour of estimation of the transfer coefficients. The classical way of estimating transfer coefficients by means of dimensionless numbers between various forces and the use of physical engineering correlations, has become nearly impossible due to lack of information on local flow fields and Reynolds numbers. In addition, the multiphase nature of the ice cream in the bulk domain and its non-Newtonian behaviour are hampering factors in finding good predictions.

Therefore, the equations for transfer coefficients to be presented in the following must be seen as tentative ones, representing tendencies. Care has been taken to have the proper physical asymptotes for extreme conditions.

5.4.1. Mass transfer coefficients

a) Ice particles from the bulk to the frozen layer

The overall mass transfer coefficient for the ice particles in the bulk is determined from two resistances to transfer in series: a resistance in the liquid phase side ($1/k_L^{(i)}$) and one for the integration at the surface of the frozen layer ($1/k_T^{(i)}$):

$$k_B^{(i)} = \frac{k_S^{(i)} \cdot k_T^{(i)}}{k_S^{(i)} + k_T^{(i)}} \tag{5.125}$$

The mass transfer coefficient of the ice particles is taken constant, with the value presented in Table 7.2, in Appendix 11.

The resistance at the surface gets smaller if the “freezing potential” is bigger. Therefore, the transfer coefficient at the side of the frozen layer surface is taken proportional to a freezing potential expressed as a scaled temperature difference ($\sigma_T^{(i)}$):

$$k_T^{(i)} = k_{T,0}^{(i)} \cdot \left[\sigma_T^{(i)} \right]^a \tag{5.126}$$

Moreover, the “freezing potential” is expressed as a scaled temperature difference:

$$\sigma_T^{(i)} = \frac{T_{FL}^{(i)} - T_{B,e}^{(i)}}{T_{B,e}^{(i)}} \tag{5.127}$$

$$a \geq 1 \tag{5.128}$$

In view of the principle of considering linear driving forces dependency, it is recommended to take the exponent a equal to one.

List of symbols

$k_B^{(i)}$ = overall mass transfer coefficient for the ice particles in the bulk, $\left[m/s \right]$

$k_S^{(i)}$ = mass transfer coefficient of the ice particles, $\left[m/s \right]$

$k_T^{(i)}$ = transfer coefficient due to temperature difference between the frozen layer and the bulk, $\left[m/s \right]$

$\sigma_T^{(i)}$ = the freezing potential, $\left[- \right]$

b) Water from the bulk to the frozen layer

A similar mechanism as for the ice particles is put in place for the transfer of water. The overall transfer coefficient for the water from the bulk to the frozen layer is determined from two resistances to transfer in series: a resistance at the liquid phase side ($1/k_{L,w}^{(l)}$) and one at the frozen layer surface ($1/k_{T,w}^{(l)}$). The latter resistance gets smaller if the "freezing potential" is bigger. Therefore, the transfer coefficient at the side of the frozen layer surface is taken proportional to a freezing potential expressed as a scaled temperature difference ($\sigma_{T,w}^{(l)}$).

$$k_{B,w}^{(l)} = \frac{k_{L,w}^{(l)} \cdot k_{T,w}^{(l)}}{k_{L,w}^{(l)} + k_{T,w}^{(l)}} \tag{5.129}$$

As there is plenty of water at the bulk side, if there is enough rotor action, the mass transfer coefficient $k_{L,w}^{(l)}$ becomes very large relative to $k_{T,w}^{(l)}$ and it cancels out. At the surface of the frozen layer, the water must turn into ice with a certain rate coefficient:

$$k_{B,w}^{(l)} = k_{T,FL,w}^{(l)} = k_{T,FL,w,0}^{(l)} \cdot \left[\sigma_T^{(i)} \right]^{a_w} \tag{5.130}$$

Similarly, the freezing potential is expressed as a scaled temperature difference:

$$\sigma_T^{(i)} = \frac{T_{FL}^{(i)} - T_{B,e}^{(i)}}{T_{B,e}^{(i)}} \tag{5.131}$$

$$a_w \geq 1 \tag{5.132}$$

In view of the principle to consider linear driving force dependency, it is recommended to take the exponent a_w equal to one.

List of symbols

$k_{B,w}^{(l)}$ = overall mass transfer coefficient for the water in the bulk, $\left[m/s \right]$

$k_{L,w}^{(l)}$ = mass transfer coefficient of the water, $\left[m/s \right]$

$k_{T,w}^{(l)}$ = transfer coefficient due to temperature difference between the frozen layer and the bulk, $\left[m/s \right]$

$\sigma_T^{(i)}$ = the freezing potential, $\left[- \right]$

5.4.2. Viscosity

The rheology of ice cream is very complex: it depends on the number, size and shape of the suspended ice, fat and air particles, the concentration of the sugars, protein and polysaccharides, and the temperature. Most of these factors are changing significantly during the manufacturing process. The ice, fat and air particles are forming, the concentration of the solution is increasing and the temperature decreases. As a result, the viscosity of ice cream increases by several orders of magnitude (Clarke, 2004).

The ice cream mix, which is a solution of sugars and stabilizers and a suspension of fat droplets, is a shear-thinning liquid, obeying a power-law type equation. As the mix freezes and air is inserted inside the structure, its viscosity increases both because the temperature is decreased and because ice particles and air bubbles are formed as well. At -5 ^{0}C (the temperature at which it normally leaves the factory freezer) ice cream is a viscoelastic, shear-thinning fluid. Like the mix, it obeys the power-law equation, but with different values of the rate law parameters. As its temperature is lowered, it becomes more solid-like.

The following power-law type equation will be used for determining the viscosity of the aerated ice cream mix:

$$\eta_B^{(i+l+a)} = K_B^{(i+l+a)}(T) \cdot \left(\dot{\gamma} \right)^{n-1} \tag{5.133}$$

The terms $K_B^{(i+l+a)}$ and n in equation (5.133) are rheological constants, characterizing the fluid. Newtonian fluids are a special case of equation (5.133) in which $K_B^{(i+l+a)} = \eta_B^{(i+l+a)}$ and $n = 1$. The consistency $K_B^{(i+l+a)}$ is calculated as a function of the temperature from the following equation:

$$K_B^{(i+l+a)} = e^{A+\frac{B}{T}+C\cdot\left(1-x_v^{(a)}\right)} \tag{5.134}$$

List of symbols

$\eta_B^{(i+l+a)}$ = non-Newtonian viscosity of the ice cream mix, $\left[Pa\cdot s\right]$

$x_v^{(a)}$ = volume fraction of air, $\left[-\right]$

A, B, C = constants, determined experimentally

The values for the parameters used to calculate the viscosity are presented in Table 7.1, in Appendix 11.

5.4.3. Thermal conductivity

The values for the thermal conductivities of the pure components and phases are assumed constant and the values considered are presented in Table 7.2 in Appendix 11.

Two main factors affect the apparent thermal conductivity of the frozen ice cream: temperature due to its strong influence on the ice fraction and the ice cream apparent density due to the greater influence of the air insulation effect (Cogné, Andrieu, Laurent, Besson & Nocquet, 2003).

1) Thermal conductivity of the un-aerated mix

The thermal conductivity of the liquid phase is modelled using the intrinsic thermal conductivity values of each pure component and their volume fractions. The thermal conductivity of the mix is determined as a function of the thermal conductivity of the pure components, using the parallel model (Renaud, Briery, Andrieu & Laurent, 1992):

$$\lambda_{domain}^{(mix)} = \sum_j \left(x_{v,domain,j}^{(\varphi)} \cdot \lambda_j^{(\varphi)} \right) \tag{5.135}$$

$$x_{v,domain,j}^{(\varphi)} = x_{domain,j}^{(\varphi)} \cdot \frac{\rho_{domain}^{(mix)}}{\rho_j^{(\varphi)}} \tag{5.136}$$

List of symbols

$\lambda_{domain}^{(mix)}$ = thermal conductivity of the un-aerated mix, $\left[W/m\cdot K\right]$

$x_{v,domain,j}^{(\varphi)}$ = volume fraction of component j , $\left[-\right]$

$x_{domain,j}^{(\varphi)}$ = mass fraction of component j , $\left[-\right]$

$\lambda_j^{(\varphi)}$ = thermal conductivity of component j , $\left[W/m\cdot K\right]$

2) Thermal conductivity of the aerated mix

As the air intrinsic thermal conductivity is very low, the air induced porosity has a large influence on the apparent thermal conductivity of commercial frozen ice creams. Since the experimental observations show that the air phase was dispersed as quite spherical bubbles inside the structure (Goff, 1997; Caillet, Cogné, Andrieu, Laurent & Rivoire, 2003), the thermal conductivity is modelled using the Maxwell's relationship (Cogné, Andrieu, Laurent, Besson & Nocquet, 2003):

$$\lambda_{domain}^{(mix,a)} = \lambda_{domain}^{(mix)} \cdot \frac{2\lambda_{domain}^{(mix)} + \lambda^{(a)} - 2\varepsilon^{(a)} \cdot \left(\lambda_{domain}^{(mix)} - \lambda^{(a)}\right)}{2\lambda_{domain}^{(mix)} + \lambda^{(a)} + \varepsilon^{(a)} \cdot \left(\lambda_{domain}^{(mix)} - \lambda^{(a)}\right)} \tag{5.137}$$

List of symbols

$\lambda_{domain}^{(mix,a)}$ = thermal conductivity of the aerated mix, $\left[W/_{m \cdot K}\right]$

$\varepsilon^{(a)}$ = the air volume fraction, $[-]$

$\lambda^{(a)}$ = thermal conductivity of air, $\left[W/_{m \cdot K}\right]$

5.4.4. Heat transfer coefficients

1) Heat transfer coefficient of the ice cream mix

It is assumed that the heat transfer coefficient is based on the properties of the overall (multi-phase) ice cream mixture, without taking into account the contributions of the individual phases in the mixture.

The heat transfer coefficient of the ice cream mix is estimated using an empirical correlation, based on the penetration theory (Bongers, 2006):

$$\alpha_B^{(l+a)} = \Phi \cdot 2\sqrt{\rho^{(l+a)} \cdot c_p^{(l+a)} \cdot N_{blades} \cdot D \cdot \lambda_B^{(l+a)}} \tag{5.138}$$

This expression for the heat transfer coefficient is valid for laminar flow or for the transition region between laminar and turbulent flow.

In equation (5.138) Φ is a correction factor accounting for the axial dispersion and the incomplete temperature equalization and mixing. The correction factor is a function of the Péclet number (Trommelen, Beek & Van de Westelaken, 1971).

List of symbols

Φ = empirical correction factor, $[-]$

$\rho^{(i+l+a)}$ = density of the fluid bulk, $\left[kg/_{m^3}\right]$

$\lambda_B^{(i+l+a)}$ = thermal conductivity of the fluid bulk, $\left[W/_{m \cdot K} \right]$

2) Heat transfer coefficient at the liquid side of the ice particles

The expression for the heat transfer coefficient for an ice particle is determined by applying the shrinking core model for the melting of the ice particle:

$$\alpha_{ice} = \frac{8 \cdot \pi \cdot \lambda^{(B)}}{s^{(i)}} \tag{5.139}$$

The derivation of equation (5.139) is described in Appendix 12.

3) Heat transfer coefficient of the walls

For determining the heat transfer coefficient of the freezer wall and the frozen layer, the following equation will be used:

$$\alpha_{wall} = \frac{1}{r_{in}} \cdot \frac{\lambda_{wall}}{\ln\left(r_{out} / r_{\text{in}}\right)} \tag{5.140}$$

4) Overall heat transfer coefficient of cylindrical walls

For determining the overall heat transfer coefficient of cylindrical walls the following expression is defined, based on the inner surface (Bird, Stewart & Lightfoot, 2002):

$$\frac{1}{r_0 \cdot U_0} = \frac{1}{r_0 \cdot \alpha_0} + \sum_{i=1}^{n} \frac{\ln\left(r_i / r_{i-1}\right)}{\lambda_{i-1,i}} + \frac{1}{r_n \cdot \alpha_n} \tag{5.141}$$

The equation is defined for heat conduction through a laminated tube with a fluid at temperature T_a inside the tube and temperature T_b outside, and a number of n regions.

5) Heat transfer coefficient of the coolant

The coolant is assumed to have a high, constant heat transfer coefficient, corresponding to the boiling regime.

$$\alpha_c = 12000 \tag{5.142}$$

List of symbol

λ_{wall} = heat conductivity of the wall, $\left[W/_{m \cdot K} \right]$

r_{in} , r_{out} = inner and outer radius of the wall, $[m]$

α_c = heat transfer coefficient for the coolant, $\left[W/_{m^2 \cdot K} \right]$

U_0 = overall heat transfer coefficient based on the inner surface, $\left[W/m^2 \cdot K \right]$

α_0 = heat transfer coefficient of the fluid with the temperature T_a , $\left[W/m^2 \cdot K \right]$

α_n = heat transfer coefficient of the fluid with the temperature T_b , $\left[W/m^2 \cdot K \right]$

$\lambda_{i-1,i}$ = thermal conductivity of the region $i-1, i$, $\left[W/m \cdot K \right]$

r_0 = inner radius of the tube, $\left[m \right]$

r_n = outer radius of the tube, $\left[m \right]$

r_i = the radius of the region i , $\left[m \right]$

5.5. Overview of the reductions for the constitutive equations in the 3-D model

At the constitutive equations level, the following reductions were considered:

1. The density of air is calculated using the ideal gas law.
2. The sucrose is chosen to represent the different types of sugars present in the ice cream mix.
3. The enthalpy of the ice particles dispersed in the bulk is determined considering the contribution of every particle at the temperature of the ice phase in the bulk.
4. The viscosity of the aerated ice cream mix is determined using a power-law type of equation.
5. The properties (density, specific heat, viscosity) of the other pure components are considered constant along the freezer.
6. The ice particles are assumed to have a spherical shape.
7. The transfer coefficients at the side of the frozen layer surface are taken proportional to a freezing potential expressed as a scaled temperature difference ($\sigma_T^{(i)}$).
8. The heat transfer coefficient of the ice cream mix is estimated using an empirical correlation, based on the penetration theory.
9. The frozen layer and the freezer wall are treated as composite cylindrical walls for the heat balance equations.
10. The heat transfer coefficient of the coolant is considered constant along the freezer length.
11. The rate laws for melting, mass and heat transfer are all structured in the same fundamental way: the rate is proportional to a single thermodynamic driving force. This driving force is mechanically enhanced or diminished by the scraper rotation. The transfer coefficient is built up from a nominal transfer coefficient and an empirical adjustment parameter.
12. The distribution of the ice particles removed from the frozen layer is independent of the size distribution of the ice particles inside the bulk. Due to the lack of detailed empirical information, a Weibull-type distribution is assumed for the scraped ice particles removed from the frozen layer.

13. The rate of change of ice particles due to melting in the bulk is determined assuming that the incoming heat from the aerated bulk liquid is used only for the melting.
14. The heat generation due to the viscous dissipation is determined using a power-law type of equation for the shear stress, under steady state shear flow assumptions.
15. The scraping friction is determined using a power-law type of function based on the amount of ice being scraped from the frozen layer at the wall.

6. Summary of the mathematical structure of the 3-D model

An overview of the physical structure of the reduced model for the ice cream freezing is presented in Table 5.9. Based on this physical structure, the mathematical model consists of a number of seven partial differential equations (PDE's):

a) Five mass conservation equations for the five species in the pseudo-continuous matrix phase
b) One population conservation equation for the ice particle in the bulk
c) One energy conservation equation for the fluid in the bulk, consisting of matrix, ice particles and air

To this set of partial differential equations, a number of seven initial conditions and nine boundary conditions are added.

Moreover, a number of eleven nonlinear algebraic equations (NLAE's) are related to the various transfer terms in the balance equations:

a) One algebraic equation to determine the thickness of the frozen layer
b) One algebraic equation for the transfer rate of water from the bulk to the frozen layer
c) Two algebraic equations for the transfer rate of ice from and to the frozen layer
d) One algebraic equation for the melting rate of ice particles in the bulk
e) One algebraic equation for the generation of water due to ice melting in the bulk
f) One algebraic equation for the heat transfer rate from the bulk to the coolant
g) Two algebraic equations for the viscous dissipation and work in the bulk
h) One algebraic equations for the thermodynamic equilibrium ice-water-sugar
i) One algebraic equation to determine the pressure drop

Finally, some more algebraic equations are present to determine:

j) Physical properties of the different pure species considered in the model: six species x three properties (density, specific heat, conductivity) = eighteen equations for the pure component
k) Mixing rules for the three physical properties above – three equations
l) The viscosity of the ice cream mix – one equation
m) Enthalpy of the different phases: two phases (aerated liquid and ice phase in the bulk) x one equation = two equations
n) Mass fluxes in axial direction – one equation x six species = six equations

o) Mass fluxes along the radial coordinate – one equation x one species = one equation

p) Energy flux in axial direction – one equation x one pseudo-component = one equation

q) Mass transfer coefficients for the liquid and the ice particles in the bulk = two equations

r) Heat transfer coefficients for the ice cream mix, liquid side of the ice particles, frozen layer, freezer wall and the coolant – five equations

Table 5.9. Overview of the ice cream freezing model

3-D (time, axial and internal coordinate)								
Conservation	***Mass*** *(differential)*	**Bulk (B)**		Water	Sugar	Fat	Other	Air
		Mechanism	Convection	✓	✓	✓	✓	✓
			Transfer	FL				
			Generation	✓				
		BC	Continuity of fluxes					
		Frozen layer (FL)		**Ice**				
		Mechanism	Transfer	B				
		IC	Known initial thickness of layer					
	Population *(differential)*	**Bulk (B)**		**Ice**				
		Mechanism	Convection	✓				
			Transfer	B & FL				
			Consumption	✓				
		IC	Known inlet distribution of particles					
		BC	Known distribution of maximum size particles					
	Momentum *(algebraic)*	Pressure drop driven radially symmetric axial convective flow						
	Energy	**Bulk (B)** *(differential)*						
		Mechanism	Convection	✓				
			Generation	Viscous dissipation, scraping friction, melting				
			Transfer	FL				
			Work	✓				
		BC	Known inlet temperature					
		Frozen layer (FL) *(algebraic)*						
		Freezer wall *(algebraic)*						
		Coolant *(algebraic)*						

<table>
<tr><td colspan="6">3-D (time, axial and internal coordinate)</td></tr>
<tr><td rowspan="15">Constitutive equations (algebraic)</td><td colspan="2" rowspan="4">Physical property variations</td><td colspan="2">Density</td></tr>
<tr><td colspan="2">Enthalpy</td></tr>
<tr><td colspan="2">Viscosity</td></tr>
<tr><td colspan="2">Conductivity</td></tr>
<tr><td colspan="2" rowspan="4">Heat transfer coefficients</td><td colspan="2">Ice cream mix</td></tr>
<tr><td colspan="2">Frozen layer</td></tr>
<tr><td colspan="2">Freezer wall</td></tr>
<tr><td colspan="2">Coolant</td></tr>
<tr><td colspan="2" rowspan="2">Mass transfer coefficients</td><td colspan="2">Ice particles</td></tr>
<tr><td colspan="2">Water</td></tr>
<tr><td rowspan="11">Rates of transfer</td><td rowspan="2">Mass</td><td colspan="2">Water from B to FL</td></tr>
<tr><td colspan="2">Water due to melting of ice in B</td></tr>
<tr><td rowspan="3">Population</td><td colspan="2">Ice from B to FL</td></tr>
<tr><td colspan="2">Ice from FL to B</td></tr>
<tr><td colspan="2">Melting of ice in B</td></tr>
<tr><td rowspan="7">Energy</td><td colspan="2">Heat transfer due to transfer of mass</td></tr>
<tr><td rowspan="3">Heat transfer due to a temperature difference</td><td>B to FL</td></tr>
<tr><td>FL to Wall</td></tr>
<tr><td>Wall to Coolant</td></tr>
<tr><td colspan="2">Heat transfer due to melting of ice particles</td></tr>
<tr><td rowspan="2">Heat generation due to mechanical work</td><td>Viscous dissipation</td></tr>
<tr><td>Scraping friction</td></tr>
<tr><td colspan="5">Thermodynamic equilibrium ice-water-sugar</td></tr>
</table>

s) Rotor contribution function – two equations

t) Distribution of the ice particles being scraped from the frozen layer – one equation

The total number of equations in the nonlinear set is seven differential equations, with seven initial and nine boundary conditions, and fifty-four nonlinear algebraic equations. The initial and boundary conditions are actually degrees of freedom in the use of the model and must be specified when solving the model.

There are also numerous parameters in the model, which can be classified as:

- Physical parameters (e.g., in physical correlations)
- Design parameters (e.g., diameters, length of the freezer)
- Operational parameters (e.g, rotational speed)

The reduced model does not contain uncertainty descriptions of the model parameters or the constitutive equations.

Table 5.10. Conservation equations for the 3-D model

Resource	Phase	Conservation equations	Initial condition	Boundary conditions
Mass & Population	***Ice particles in the bulk***	$\frac{\partial\left(n_B^{(\varphi)}\right)}{\partial t}+\frac{\partial\left(j_{B,z}^{(\varphi)}\right)}{\partial z}+\frac{\partial\left(j_{B,s}^{(\varphi)}\right)}{\partial s^{(\varphi)}}=$ $B_B^{(\varphi)}-D_B^{(\varphi)}+R_{t,FL\to B}^{(\varphi)}\cdot\frac{S_B}{A_B}-R_{t,B\to FL}^{(\varphi)}\cdot\frac{S_B}{A_B}$	$n_B^{(\varphi)}(0,z,s^{(\varphi)})$ $=\bar{n}_{B,0}^{(\varphi)}\left(z,s^{(\varphi)}\right)$	1) $\left(j_{B,z}^{(\varphi)}\right\|_{z=0}=\frac{\tilde{F}_{B,z}^{(\varphi)}\left(t,s^{(\varphi)}\right)}{A_B}$ 2) $j_{B,s}^{(\varphi)}\Big\|_{s_{max}^{(\varphi)}}=0$
	Matrix	$\frac{\partial\left(\varepsilon_B^{(\varphi)}\cdot c_{B,j}^{(\varphi)}\right)}{\partial t}+\frac{\partial\left(j_{m,B,j,z}^{(\varphi)}\right)}{\partial z}$ $=\varepsilon_B^{(\varphi)}\cdot G_{B,j}^{(\varphi)}-\varepsilon_B^{(\varphi)}\cdot R_{t,B\to FL,j}^{(\varphi)}\cdot\frac{S_B}{A_B}$	$c_{B,j}^{(\varphi)}(0,z)$ $=c_{B,j}^{(\varphi)}(z)$	$\left(j_{m,B,j,z}^{(\varphi)}\right\|_{z=0}=\frac{\tilde{F}_{B,z,j,0}^{(\varphi)}(t)}{A_B}$
	Frozen layer	End of freezing interval	$\delta_{FL,max}=\delta_{FL,min}+\frac{R_{t,m,B\to FL}^{(i)}(t,z,s)+R_{t,B\to FL,w}^{(l)}(z)}{\rho_{FL}^{(i)}(z)}\cdot(t_{s-}-t_0)$	
		End of scraping interval	$\delta_{FL,max}=\delta_{FL,min}+\frac{R_{t,m,FL\to B}^{(i)}(t,z)}{\rho_{FL}^{(i)}(z)}\cdot(t_s-t_0)$	
Momentum	***Bulk domain***	$\phi^{(i+l+a)}=\rho^{(i+l+a)}\cdot\pi R^3\cdot\left(\frac{\lvert\Delta P\rvert}{L}\cdot\frac{R}{2\cdot K_B^{(i+l+a)}}\right)^{\frac{1}{n}}\cdot\frac{n}{2n+1}\cdot\left(1-\frac{R_0}{R}\right)^{\frac{2n+1}{n}}$		
Energy	***Ice cream in bulk***	$\frac{\partial\left(H_B^{(i+l+a)}\right)}{\partial t}+\frac{\partial\left(e_B^{(i+l+a)}\right)}{\partial z}=E_{B\leftrightarrow FL}^{(i)}+$ $E_{B\leftrightarrow FL,w}^{(l)}-\frac{S_B}{A_B}\cdot q_{\Delta T,B\leftrightarrow FL}^{(l)}+W_B$	$T_B^{(i+l+a)}(0,z)=$ $T_{B,0,z}^{(i+l+a)}$	$T_B^{(i+l+a)}(t,0)=T_{B,0}^{(i+l+a)}$
	Frozen layer	$T_{FL}^{(i)}-T_{wall}=(R-\delta_{FL})\cdot q_{r,FL}\Big\|_{R-\bar{\delta}_{FL}}\cdot\frac{ln\left(R/R-\delta_{FL}\right)}{\lambda^{(i)}}$		
	Freezer wall	$T_{wall}-T_{wall,coolant}=(R-\delta_{FL})\cdot q_{r,FL}\Big\|_{R-\bar{\delta}_{FL}}\cdot\frac{ln\left(R+\delta_{wall}/R\right)}{\lambda^{(wall)}}$		
	Coolant	$F_c\cdot\Delta h_c(T_c)\cdot\frac{\partial x_c}{\partial z}=q_{\Delta T,wall\leftrightarrow coolant}$	PSSA	$x_c\Big\|_{z=0}=x_{c,0}$

PSSA = pseudo-steady state assumption

A remark is in order on the wellposedness and solvability of the model. The model is well posed in the sense that the number of variables, derivatives of variables and equations match and form a closed system (no rigorous proof offered on paper; the hard empirical verification is in the implementation of the model for numerical solution).

An overview of the most important equations in the mathematical structure of the reduced model for the ice cream freezing step is presented in Table 5.10.

Furthermore, it is noticed that the model equations are continuous in the variables and at least once differentiable, which favours the existence of a solution. Whether there can be multiple solutions

cannot be a priori excluded due to some non-linearity in the algebraic equations for the rate laws. Multiplicity of solutions and the possible occurrence of a high differential index (>1) in this PDAE set are points of attention when developing the numerical solution procedure.

7. Input-output structure of the reduced model for model use

The previous sections presented the physical and behavioural structure of a reduced model according to the outline in Chapter 2 of this thesis. In spite of the reduction efforts, the ice cream freezer model is still very complex with respect to its internal structure.

When using a model of a process unit for computations, having this view on the internal structure can be rather hampering by its richness of details. Therefore, it is systems engineering practice to develop a complementary view at a higher level of abstraction for the use of the model. This view is presented as an *information input-output diagram* (Figure 5.10).

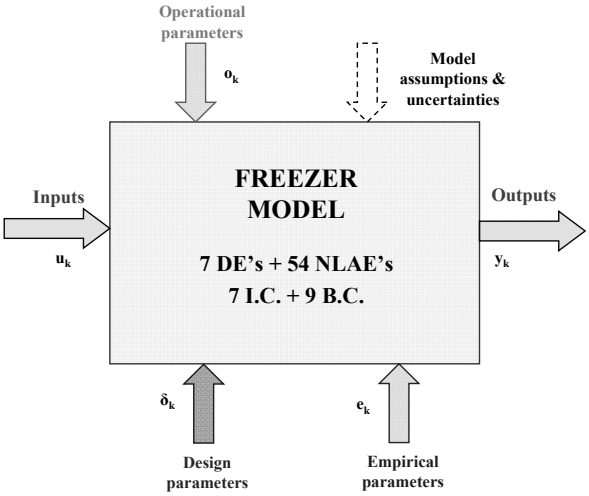

Figure 5.10. Input-output structure of the model

Depending on the objectives of the model, the variables in the input-output structure may play a different role, as detailed in the following sections. The choice for the different groups of parameters and variables for the ice cream freezing model is detailed in Chapter 6 of the thesis.

a) Validation of the model

The freezer model contains many unknown adjustable parameters, which, in a model parameter estimation and validation effort, can be statistically estimated from experimental data on inputs and outputs. Figure 5.11 shows this information flow.

After having done parameter estimation based on one set of experimental data, a model validation step can be done by means of predictions using another set of independent measured data.

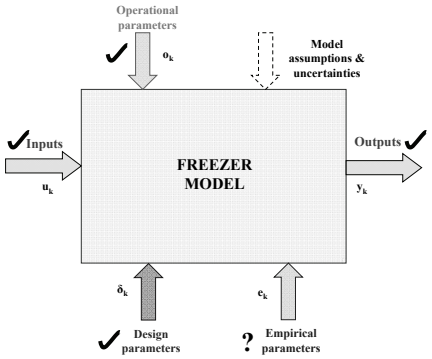

Figure 5.11. Specifications for model parameter estimation and validation

b) Analysis of the freezer performance

The analysis of the freezer performance signifies the simulation of the model outputs given the inputs, operational conditions, and design parameters. This application is depicted in Figure 5.12. The output variables are connected with quality criteria of the final product and with the process performance. Examples of product quality variables are softness, creaminess and cooling sensation. Relations that link the output variables to the product quality exist (Bongers, 2008; 2009), but are beyond the purpose of this thesis.

c) Optimization of the freezer operation

For this application, depicted in Figure 5.13, the model is able to determine the optimal operating conditions given the outputs, the inputs and the design parameters. Depending on the objectives of the model, the variables in the input-output structure may play a different role, as detailed in the following sections.

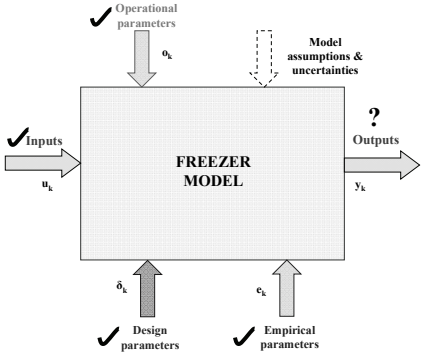

Figure 5.12. Specifications for analysis of the freezer performance

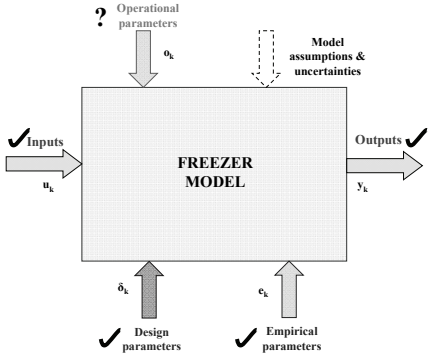

Figure 5.13. Specifications for the optimization of the freezer operation

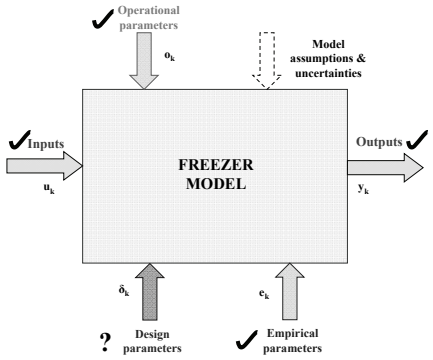

Figure 5.14. Specifications for improvement of freezer design

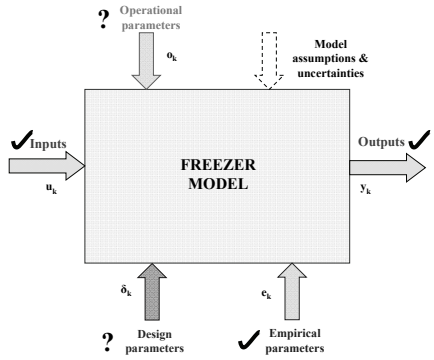

Figure 5.15. Specifications for product design

d) Improvement of the freezer design

The improvement of the freezer design signifies that the model is able to calculate the optimal design parameters given the outputs, the inputs and the operating conditions, as shown in Figure 5.14.

e) Product design

This application implies that the model is able to predict the optimal design parameters and the optimal operating conditions of the freezer, given the outputs and the inputs, as shown in Figure 5.15.

It should be noted that the use of the freezer model for optimization purposes require some additional modelling by specifying:

- A proper objective function, fit for its goal
- Inequality constraints specifying the operational window, equipment integrity window
- "Knowledge" constraints which bound the domain of validity of the empirical rate laws, and which must avoid the improper use of such rate laws outside tested areas

The optimization studies with the freezer model are kept beyond the scope of this thesis for a practical reason of time constraints on the thesis research effort.

8. Conclusions

The development of a reduced 3-D model of the ice cream freezing step has been presented in this chapter. The structure-retaining model reduction approach acts more on the contextual and the lower levels of the physical structure of the model (domains, phases, species, etc.), and less on the

numerical level of the process model. The starting point for the model reduction procedure is not an existing complete, rigorous model of the freezing unit, but a conceptual one under design.

The model considers six species: (a) liquid water, (b) ice, (c) sugar, (d) fat, (e) air, and (f) other components. The ice is assumed distributed inside a fluid matrix composed of the other species; hence, two phases are present in the unit. The unit is decomposed in the following compartments: (a) the barrel, with two domains, the bulk and the frozen layer, (b) the freezer wall and (c) the coolant.

The equations of conservation are written for the following resources: (a) mass, for the continuous phases, (b) population, for the distributed ice phase, (c) energy, and (d) momentum; three coordinates are considered: time, axial position and internal coordinate of the ice particles.

Regarding the phenomena that take place in the unit:

a) *Mass*: transport along the freezer, transfer between the barrel domains for the water

b) *Population*: transport along the freezer, transfer between the barrel domains, and melting for the ice particles in the bulk

c) *Energy*: transport along the freezer, transfer from the fluid bulk to the scraped ice particles and to the coolant through the barrel wall

d) *Momentum*: pressure drop driven radially symmetric axial convective flow

Having formulated the model equations, and presented an input-output view of the use of the reduced model, the next step is the numerical implementation of the model in a suitable software environment and its use for practical computational applications. The numerical implementation does not consist only in writing the model equations in the format required by the software, but also in a verification of the correctness of the equations and their implementation. This is done in Chapter 6 of this thesis. The numerical solution method, as well as the application of the ice cream freezing model for a parametric sensitivity type of analysis will be discussed in Chapter 6 as well.

9. References

Aldazabal, J., Martin-Meizoso, A., Martinez-Esnaola, J.M., & Farr, R. (2006). Deterministic model for ice cream solidification, *Computational Materials Science* 38, 9

Arbuckle, W.S. (1986). Ice cream, *AVI Publishing*, 4th edition

Bird, B.R., Stewart, W.E., & Lightfoot, E.N. (2002). Transport phenomena, *John Wiley & Sons*

Bongers, P.M.M. (2006). A heat transfer model of a scraped surface heat exchanger for ice cream, *Proceedings of the 16th European Symposium on Computer Aided Process Engineering and 9th International Symposium on Process Systems Engineering,* 539

Bongers, P.M.M. (2008). Model of the product properties for process synthesis, *Proceedings of the 18th European Symposium on Computer Aided Process Engineering,* 55

Bongers, P.M.M. (2009). Process and equipment design optimising product properties and attributes, *Proceedings of the 19th European Symposium on Computer Aided Process Engineering,* 225

Bradley, R.L. Jr. and Smith, K. (1983). Finding the freezing point of frozen desserts, *Dairy Record* 84, 114

Bradley, R.L. Jr. (1986). Plotting freezing curves of frozen desserts, *Dairy Record* 85, 86

Caillet, A., Cogné, C., Andrieu, J., Laurent, P., Rivoire. (2003). A. Characterization of ice cream structure by direct microscopy. Influence of freezing paramters, *Lebensmittel-Wissenschaft und-Technologie* 36, 743

Clarke, C. (2004). The science of ice cream, *Royal Society of Chemistry*

Cogné, C., Andrieu, J., Laurent, P., Besson, P., Nocquet, J. (2003). Experimental data and modelling of thermal properties of ice cream, *Journal of Food Engineering* 58, 331

Duffy, B.R., Wilson, S.K., Lee, M.E.M. (2007). A mathematical model of fluid flow in a scraped-surface heat exchanger, *Journal of Engineering Mathematics* 57, 381

Eisner, M.D., Wildmoser, H., Windhab, E.J. (2005) Air cell microstructuring in a high viscous ice cream matrix, *Colloids and Surfaces A: Physicochem. Eng. Aspects* 263, 390

Fredrickson, A.G., Bird, R. B. (1958). Non-Newtonian Flow in Annuli, *Industrial and Engineering Chemistry* 50, 347

De Goede, R., and de Jong, E.J. (1993). Heat transfer properties of a scraped-surface heat exchanger in the turbulent flow regime, *Chemical Engineering Science* 48, 1393

Goff, H.D. (1997). Colloidal aspects of ice cream – A review, *Int. Dairy Journal* 7, 363

Goff, H.D. (2002). Formation and stabilization of structure in ice-cream and related products, *Current Opinion in Colloid and Interface Science* 7, 432

Goff,H.D. Theoretical aspects of the freezing process, (*http:// www.foodsci.uoguelph.ca/dairyedu/freeztheor.html*)

Hangos, K.M., Cameron, I.T. (2001). Process modelling and model analysis, *Academic Press*

Hoffman, J. D. (2001). Numerical methods for engineers and scientists, 2nd Edition, *Marcel Dekker, Inc.*, New York

Koxholt, M.M.R., Eisenmann, B., Hinrichs, J. (2001). Effect of the fat globule sizes on the meltdown of ice cream, *Journal of Dairy Science* 84, 31

Leighton, A. (1926). On the calculation of the freezing point of ice-cream mixes and of the quantities of ice separated during the freezing process, *Journal of Dairy Science* 10, 300

Marshall, R.T., Goff, H.D., Hartel, R.W. (2003). Ice Cream, 6th Edition, *Kluywer Academic/Plenum Publishers*, New York

Qin, F.G.F., Chen, X.D., Farid, M.M. (2004). Growth kinetics of ice films spreading on a subcooled solid surface, *Separation and Purification Technology* 39, 109

Qin, F., Chen, X.D., Ramachandra, S., Free, K. (2005). Heat transfer and power consumption in a scraped-surface heat exchanger while freezing aqueous solutions, *Separation and Purification Technology* 48, 150

Ramkrishna, D. (2000). Population balances: Theory and applications to particulate systems in engineering, *Academic Press*

Rao, C.S., Hartel, R.W. (2006). Scraped surface heat exchangers, *Critical Review in Food Science and Nutrition* 46, 207

Renaud, T., Briery, P., Andrieu, J., & Laurent, M. (1992). Thermal properties of model foods in the frozen state, *Journal of Food Engineering* 51, 83

Russell, A. B., Burmester, S.S.H., & Winch, P.J. (1997). Characterization of shear thinning flow within a scraped surface heat exchanger, *Trans IChemE* 75, 191

Sun, K.H., Pyle, D.L., Fitt, A.D., Please, C.P., Baines, M.J., & Hall-Taylor, N. (2004). Numerical study of 2D heat transfer in a scraped surface heat exchanger, *Computers & Fluids* 33, 869

Trommelen, A.M., Beek, W.J., & Van de Westelaken, H.C. (1971). A mechanism for heat transfer in a Votator-type scraped-surface heat exchanger, *Chemical Engineering Science* 26, 1987

Wang, W., Walton, J.W., McCarthy, K.L. (1998). Flow profiles of power law fluids in scraped surface heat exchanger geometry using MRI, *Journal of Food Process Engineering* 22, 11

Yataghene, M., Pruvost, J., Fayolle, F., & Legrand, J. (2008). CFD analysis of the flow pattern and local shear rate in a scraped surface heat exchanger, *Chemical Engineering and Processing* 47, 1550

6

NUMERICAL APPLICATION OF THE REDUCED MODEL FOR ICE CREAM FREEZING

This chapter deals with a numerical implementation and application of the ice cream freezing model. The 3-D model is reduced to its steady state version (2-D). The numerical implementation and verification of this model in MATLAB® is presented. The nonlinear set of differential and algebraic equations is discretized using a finite volume numerical approach, which offers a good trade-off between accuracy and speed. The predictive capabilities of the model are assessed on basis of a base case scenario, which is further used as a starting point for the generation of parametric sensitivity information for identifying and screening of parameters having a dominant effect on the model outputs.

1. Introduction

The model development procedure presented in Chapter 1 of this thesis (summarised in Figure 1.4) consists of four main steps: (a) the model specification and design; (b) the model implementation; (c) the model validation and (d) the model application.

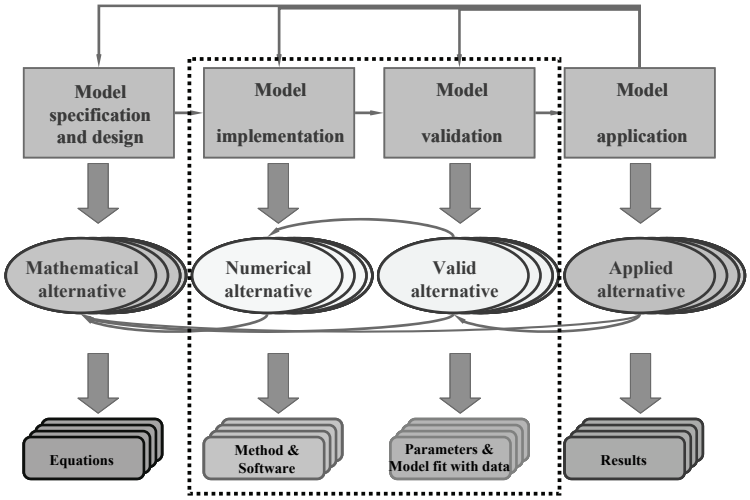

Figure 6.1. Model development cycle

In the following sections, the model development procedure is continued with an application of model implementation and verification, as shown in Figure 6.1, to the ice cream freezing model. These steps are continued with the model validation. This step consists of: a) the design and execution of an experimental programme for collecting informative data; b) model parameter estimation; and c) validation of these estimates by means of model predictions of process outputs against measured data, independent from the model fitting data set. Due to the significant effort required, this step will not be treated fully. Only the analysis of the parametric sensitivity of the model will be treated in this chapter.

A reduced dynamic model of the freezing unit has been developed in Chapter 5 of this thesis. Based on this physical structure, the mathematical model consists of a number of seven hyperbolic partial differential equations (PDE's) and ten coupled nonlinear algebraic equations (NLAE's), written for three coordinates: time, axial position and internal coordinate of the ice particles in the bulk. To this set of partial and differential equations (PDAE's), algebraic equations to determine the physical properties of the different species considered in the model, as well for the matrix are taken into account as well. An overview of the physical structure of the ice cream freezing model is presented in Table 5.9, in Chapter 5, while the conservation equations are summarised in Table 5.10. The resulting input-output structure of the model is presented in Figure 6.2.

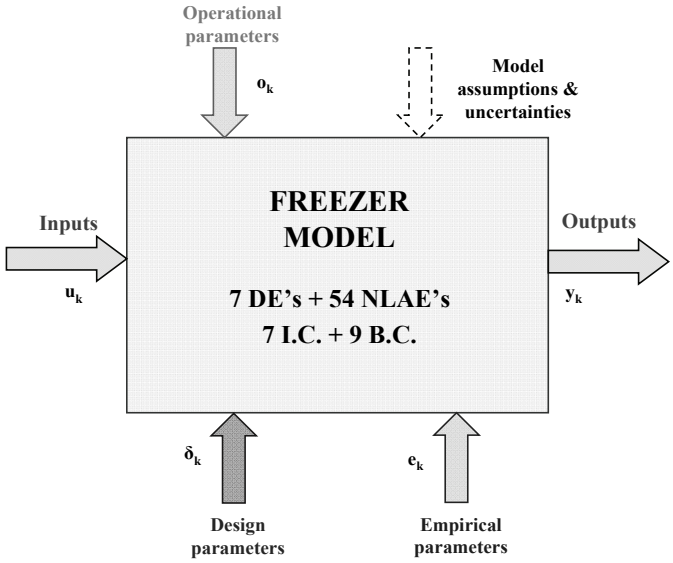

Figure 6.2. Input-output structure of the model

$3-D$ *model* $\{time(t); position(z); particle\ size(s)\}$

Variables: x *states*; v *algebraic*; p *parameters*

Equations:
$$F_{PDE}\left(\partial x/\partial t, x, \nabla_z x, \nabla_s x, v; p\right) = 0$$
$$F_{NAE}\left(x, v; p\right) = 0 \qquad (6.1)$$

Boundary conditions: $BC\left(x, v; u(t)\right) = 0$

Initial conditions: $IC\left(x; x_0(z,s)\right) = 0$

Obtaining and interpreting the numerical solutions of the 3-D model summarised in equations (6.1) offers a significant challenge. For this reason, it is preferred to start in a simpler way, by considering the steady state version of the model first. The result is a 2-D model, for which a numerical solution scheme will be developed in the following sections. The viability of this scheme will be shown by means of a single case study. A more extensive application of the model for further improvement of the design and operation of the freezer is, as interesting as it may be, beyond the scope of this thesis.

Section 2 of this chapter presents the numerical implementation of the steady state version of the reduced (3-D) model. The selection of the numerical methods and the software environment used for solving the model are briefly introduced, together with the discretization of the model equations.

Moreover, a verification of the model implementation, for asserting the correct behaviour of the numerical implementation for some extreme cases (all rate parameters are assumed zero, the bulk domain consists of only liquid water, etc.) is described in this section as well. Pilot results for solving the steady state model are presented. The use of the model for inverse problems is not considered yet, just its direct use in simulations. In Section 3, the first stage of the model validation step is discussed: the analysis of the parametric sensitivity of the model. A sensitivity analysis based on a singular value decomposition approach is used. The conclusions are presented in Section 4.

2. Development of a numerical scheme and implementation

Having formulated all the model equations, the next step is the implementation of the steady state model in a software environment. It is clear that an analytical solution is beyond practical reach; hence, a numerical solution of the steady state model is attempted.

Within the set of model equations, the population balance for the ice particles is the toughest to solve. There are several numerical techniques available for solving population balance equations. Recently, comparative studies have been published on the accuracy of these models (Qamar, Elsner, Angelov, Warnecke & Seidel-Morgenstern, 2006; Mesbah, Kramer, Huesman & Van den Hof, 2009). It has been shown that high order finite volume methods are well capable of dealing with population balances. These schemes are simple to implement and have relatively low computational requirements, as compared to other methods.

The total number of equations in the nonlinear set is seven differential equations, with seven initial and nine boundary conditions, and fifty-four nonlinear algebraic equations. The initial and boundary conditions are actually degrees of freedom in the use of the model and must be specified when solving the model. These nonlinear partial differential and algebraic equations (PDAE's) are approximated in MATLAB® by a set of ordinary differential (ODE's) and algebraic equations (AE's), as explained in Section 3.1.3 in Chapter 2 of this thesis. This set of ODE's is solved using ODE solvers available in MATLAB®.

Although a state-of-the-art dynamic PDAE solver, such as gProms® or Jacobian®, might have been more efficient for the solution, the potential transferability of the model to industrial partners who do not have access to such solvers lead to the decision to use MATLAB® as the software environment for the numerical implementation.

2.1. Discretization of coordinates and mathematical operators

Three coordinates are considered in the domain of the original 3-D model of the ice cream freezer:

(a) the time coordinate, t

(b) the spatial coordinate, z

(c) the internal coordinate of the ice particles, $s^{(i)}$

The discretization of the coordinates in the domain involves a few aspects:

(a) the lower bound of the domain
(b) the upper bound of the domain
(c) the discretization resolution
(d) direction of the discretization

The discretization resolution has a strong effect on the accuracy of the solution. The smaller the spacing, the more accurate the solution becomes. However, a high number of intervals will have an effect on the increase of the computational time. The direction of the discretization has an effect on the stability of the solution.

The span of the coordinates is determined in the following, being defined as the ratio between the upper and the lower bounds of the coordinates. These bounds are estimated for the required domain of operation and design. Time will also be considered for comparison with spatial position and particle size.

For the time coordinate, t :

The ratio between the maximum and the minimum value of the time variable is calculated. The maximum value is considered the operation time, which usually has values of the order of weeks. The minimum value of the time is the time the particles grow.

$$\frac{\tau_{max}}{\tau_{min}} = \frac{operation\ \ time}{time\ \ particle\ grows} = \frac{10^{6}}{10^{-2}} = 10^{8} \tag{6.2}$$

For the spatial coordinate, z :

Similarly, a ratio is calculated for the spatial coordinate. The maximum value is the freezer length, which is in the order of meters. The minimum value considered is the maximum particle size, since no distinction is desired between the ice crystals.

$$\frac{z_{max}}{z_{min}} = \frac{freezer\ \ length}{biggest\ \ crystal\ \ size} = \frac{10}{10^{-4}} = 10^{5} \tag{6.3}$$

For the internal coordinate, $s^{(i)}$:

$$\frac{s^{(i)}_{max}}{s^{(i)}_{min}} = \frac{biggest\ \ crystal\ \ size}{smallest\ \ crystal\ \ size} = \frac{10^{-4}}{10^{-7}} = 10^{3} \tag{6.4}$$

Since the ratio of the time coordinate is the highest of these three, it is concluded that this coordinate is preferred as the continuous coordinate, when a numerical integrator for differential equations is used. The other two coordinates can be discretized over their domain. If time drops out,

the spatial coordinate comes next into consideration as the continuous coordinate for a numerical integrator for differential equations.

a) The time coordinate, t

Under the steady state assumption, the time coordinate does not appear in the model.

b) The spatial coordinate, z

In the case of the spatial coordinate, the lower bound is equal to zero, while the upper bound is equal to the length of the freezer, L.

$$z_{min} = 0 \tag{6.5}$$

$$z_{max} = L \tag{6.6}$$

For given lower and upper bounds, the simplest spacing is equidistant, but sometimes it may be more convenient to have a smaller spacing (higher resolution) in certain parts of the domain, and a larger spacing in other parts. The spacing should not go below $10^{-5} \cdot L$. Under the steady state assumption, the spatial coordinate is not discretized and kept as a continuous coordinate.

c) The internal coordinate, $s^{(i)}$

The lower bound should be equal to or smaller than the critical nucleus size and equal to or larger than zero. The upper bound should be chosen such that the concentration of particles at this point is assumed zero. Since it is assumed that the ice is being formed only in the frozen layer, the upper bound for the internal coordinate is:

$$s_{max}^{(i)} = (2 \div 5) \cdot \delta_{FL} \tag{6.7}$$

For given lower and upper bounds, the simplest spacing is equidistant, but sometimes it may be more convenient to have a smaller spacing (higher resolution) in certain parts of the domain, and a larger spacing in other parts. Depending on the employed crystallization kinetics, the use of a crystal size domain with non-equidistant node spacing is favourable.

Moreover, whether a numerical method is appropriate for the reduction of the population balance equations (PBE's) to a set of differential and algebraic equations (DAE's) is foremost determined by the dominant crystallization mechanisms (Bermingham, 2003).

If crystal growth occurs, the PBE has a convective character. In this case, the PBE is classified as a hyperbolic PDE. Hyperbolic PDE's are best solved with an upwind finite difference method or a finite volume method (Bermingham, 2003). For crystal melt, a similar procedure is used, except that the convective character in now directed downwind along the internal (size) coordinate.

Although first order upwind finite difference and finite volume methods do not suffer from numerical instabilities when used correctly, they do invariably exhibit numerical diffusion. As a result, acceptable solutions require relatively fine grids (Bermingham, 2003).

Additional assumptions on the numerics are considered:

1. The size distributed population balance of the ice phase is discretized for nc classes of particles (from $s_{min}^{(i)}$ to $s_{max}^{(i)}$)
2. The ice particles in class $k+1$ are melting into particles in class k and water (Figure 6.3).

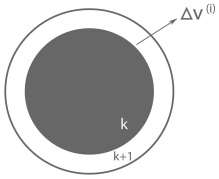

Figure 6.3. The melting of the particles in class k

For the ice particles size, discretization is performed in the following way:

$$s_k^{(i)} = s_{k-1} + \Delta s_k^{(i)} \tag{6.8}$$

In the following study, the discretization is assumed equidistant. The discretization step is calculated in the following way:

$$\Delta s_k^{(i)} = \frac{s_{max}^{(i)} - s_{min}^{(i)}}{nc - 1} \tag{6.9}$$

nc = the number of classes of particles considered, $[-]$

2.2. Discretization of model equations for the steady state model

Considering the discretization of the ice particles size, and assuming steady state, the conservation equations for the mass are re-written in the form presented in Table 6.1.

When going from the continuous to the discerte coordinate, one needs only to show how it affects the mathematical operators, such as partial derivative and integral. The algebraic operations $(+, -, \cdot, /,$ etc.) are not affected as these take place in a single point, independent of the discretization.

The transfer terms for the mass related are calculated using the equations in Table 6.2. The discretization of the rate of change of the ice particles in the bulk will be discussed in more detail in the following section.

Table 6.1. Mass conservation equations for the bulk – continuous and discrete form

Phase	Continuous & dynamic	Discrete + Steady state
Ice	$\frac{\partial\left(j_{B,z}^{(\varphi)}\right)}{\partial z}=-g_{n,B}^{(i)}+R_{t,FL\to B}^{(\varphi)}\cdot\frac{S_B}{A_B}$ $-R_{t,B\to FL}^{(\varphi)}\cdot\frac{S_B}{A_B}$	$\frac{\partial\left(j_{B,k}^{(i)}\right)}{\partial z}=-g_{n,B,k}^{(i)}+R_{t,FL\to B,k}^{(i)}\cdot\frac{S_B}{A_B}-R_{t,B\to FL,k}^{(i)}\cdot\frac{S_B}{A_B}$
Water in Matrix	$\frac{\partial\left(j_{m,B,w,z}^{(l)}\right)}{\partial z}=\varepsilon_B^{(l)}\cdot G_{B,w}^{(l)}-$ $\varepsilon_B^{(l)}\cdot R_{t,B\to FL,w}^{(l)}\cdot\frac{S_B}{A_B}$	$\frac{\partial\left(j_{B,z,w}^{(l)}\right)}{\partial z}=G_{B,w}^{(l)}-R_{t,B\to FL,w}^{(l)}\cdot\frac{S_B}{A_B}$
Component j in Matrix	$\nabla_z\left(j_{B,j,z}^{(l)}\right)=0$	$\frac{\partial\left(j_{B,j,z}^{(l)}\right)}{\partial z}=0$

Table 6.2. Overview of the rate laws for the mass related events – continuous and discrete form

Rate	Continuous equation	Discrete equation
Transfer of ice fromFL to B, $R_{t,FL\to B}^{(i)}$	$\frac{R_{t,m,FL\to B}^{(i)}\cdot\psi_{norm}^{(i)}}{m^{(i)}}$	$\frac{R_{t,m,FL\to B}^{(i)}\cdot\psi_{norm,k}^{(i)}}{m_k^{(i)}}$
Transfer of ice from B to FL, $R_{t,B\to FL}^{(i)}$	$C_a\cdot k_B^{(i)}\cdot f_1\left(\omega_r\right)\cdot n_B^{(i)}$	$C_a\cdot k_B^{(i)}\cdot f_1\left(\omega_r\right)\cdot n_{B,k}^{(i)}$
Transfer of water from B to FL, $R_{t,B\to FL,w}^{(l)}$	$C_b\cdot k_{B,w}^{(l)}\cdot f_2\left(\omega_r\right)\cdot\left[c_{B,w}^{(l)}-c_{B,w,e}^{(l)}\right]$	
Rate of melting of ice in the B, $G_{m,B}^{(i)}$	$-\rho^{(i)}\cdot\int_0^{\infty}\left(g_{n,B}^{(i)}\cdot a^{(i)}\right)ds$	$-\frac{\pi}{6}\cdot\rho^{(i)}\cdot\sum_k\left(g_{n,B,k}^{(i)}\cdot\left(s_k^{(i)}\right)^3\right)$
Rate of change of water due to ice melting in the B, $G_{B,w}^{(l)}$	$\rho^{(i)}\cdot\int_0^{\infty}\left(g_{n,B}^{(i)}\cdot a^{(i)}\right)ds$	$\frac{\pi}{6}\cdot\rho^{(i)}\cdot\sum_k\left(g_{n,B,k}^{(i)}\cdot\left(s_k^{(i)}\right)^3\right)$

2.3. Discretization of the population balance equation for the ice particles

The model is solved numerically considering a steady-state assumption. This assumption transforms the mass and energy conservation partial differential equations in a set of ordinary differential equations (ODE's) with respect to the spatial coordinate. However, the population balance equation for the ice particles in the bulk remains a partial differential equation. In order to transform it into an ODE with respect to the spatial coordinate, the finite volume method will be used for the gridding of the size coordinate. The population balance will be solved under the assumption of persistent melting of the ice particles, giving rise to a hyperbolic PDE, where the characteristic is incoming at the upper side of the internal coordinate domain.

2.3.1. Finite volume method

The first step in applying the finite volume method (FVM) is the definition of a grid for the size domain. The grid is shown in Figure 6.4. The space between the grid points forms the so-called control volumes. The number densities are computed at the geometric centres of these control volumes, which are the computational nodes.

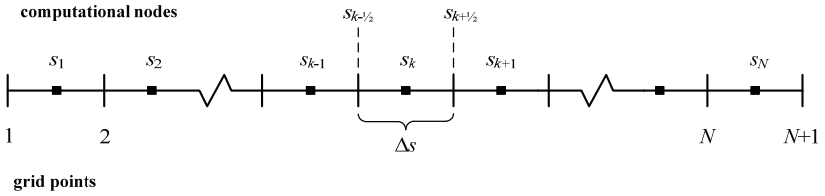

Figure 6.4. Grid for the finite volume method

Hence, the discretized number density corresponds to the average number density in each control volume, for example:

$$n_{B,k}^{(i)}(z) = \frac{1}{\Delta s^{(i)}} \cdot \int_{s_{k-½}^{(i)}}^{s_{k+½}^{(i)}} n_B^{(i)}\left(s^{(i)}, z\right) \cdot ds^{(i)} \tag{6.10}$$

The partial derivative with respect to the particle size must be evaluated at the computational nodes. The calculation of the derivative requires the values for the number densities and the melting rates at the grid points. The derivative is calculated using:

$$g_{n,B}^{(i)}\Big|_{s_k^{(i)}} = \frac{\partial j_{B,s}^{(i)}}{\partial s^{(i)}}\Bigg|_{s_k^{(i)}} = \frac{\partial\left(r_s^{(i)} \cdot n_B^{(i)}\right)}{\partial s^{(i)}}\Bigg|_{s_k^{(i)}} = \frac{\left(r_s^{(i)} \cdot n_B^{(i)}\right)\Big|_{k+½} - \left(r_s^{(i)} \cdot n_B^{(i)}\right)\Big|_{k-½}}{s_{k+½}^{(i)} - s_{k-½}^{(i)}} \tag{6.11}$$

The melting rate at the grid point is obtained directly from the kinetic rate expressions. However, the number densities cannot be evaluated at these grid points. The values for the number densities can estimated by several interpolation techniques (Mesbah, Kramer, Huesman & Van den Hof, 2009) such as the first-order upwind or higher-order interpolation schemes.

2.3.1.1. First-order upwind interpolation

The values of the number density at the grid points are simply approximated by the values at the computational nodes. The sign of the melting term determines which point to choose. The computational nodes for the interpolation need to be “upstream” of the grid points:

$$n_{B,k-1/2}^{(i)} = \begin{cases} n_{B,k-1}^{(i)} & \text{for } r_{s,B,k-1/2}^{(i)} > 0 \quad k = 2...N \\ n_{B,k}^{(i)} & \text{for } r_{s,B,k-1/2}^{(i)} \le 0 \quad k = 2...N \end{cases} \tag{6.12}$$

$$n_{B,k+1/2}^{(i)} = \begin{cases} n_{B,k}^{(i)} & \text{for } r_{s,B,k+1/2}^{(i)} \ge 0 \quad k = 1...N \\ n_{B,k+1}^{(i)} & \text{for } r_{s,B,k-1/2}^{(i)} < 0 \quad k = 1...N-1 \end{cases} \tag{6.13}$$

For melting of the ice particles, equation (6.11) is approximated as follows:

$$g_{n,B}^{(i)}\Big|_{s_k^{(i)}} = \frac{\partial j_{B,s}^{(i)}}{\partial s^{(i)}}\bigg|_{s_k^{(i)}} = \frac{\partial\left(r_s^{(i)} \cdot n_B^{(i)}\right)}{\partial s^{(i)}}\bigg|_{s_k^{(i)}} = \frac{r_s^{(i)}\Big|_{k+1/2} \cdot n_{B,k+1}^{(i)} - r_s^{(i)}\Big|_{k-1/2} \cdot n_{B,k}^{(i)}}{\Delta s^{(i)}} \qquad k = 1...N-1 \tag{6.14}$$

The boundary condition must be implemented as well. A hypothetical computational node located at $N+1$ accounts for the upper limit in the particle size domain. The number density is put to zero at this nonexistent point, therefore the derivative at the computational node N becomes:

$$g_{n,B}^{(i)}\Big|_{s_k^{(i)}} = \frac{\partial\left(r_s^{(i)} \cdot n_B^{(i)}\right)}{\partial s^{(i)}}\bigg|_{s_N^{(i)}} = \frac{0 - r_s^{(i)}\Big|_{N-1/2} \cdot n_{B,N}^{(i)}}{\Delta s^{(i)}} \tag{6.15}$$

The implementation of the first order approximation of the finite volume method is outlined in more detail in (Bermingham, 2003). It has been shown that the first order upwind interpolation schemes suffer from numerical diffusion. This effect can be surpassed by using a larger number of grid points or by implementing higher order interpolation formulae.

2.3.1.2. Higher order interpolation

A higher order scheme is obtained by piecewise polynomial interpolation of the space between the computational nodes.

The approximation at the grid point $s_{k+1/2}^{(i)}$ is written as:

$$n_{B,k+1/2}^{(i)} = n_{B,k}^{(i)} + \frac{1+\kappa}{4} \cdot \left(n_{B,k+1}^{(i)} - n_{B,k}^{(i)}\right) + \frac{1-\kappa}{4} \cdot \left(n_{B,k}^{(i)} - n_{B,k-1}^{(i)}\right) \tag{6.16}$$

where κ is a parameter in the range $[-1,1]$

For $\kappa = -1$ a second-order, accurate fully one-sided upwind scheme is obtained; while for $\kappa = 1$ a standard, second accurate central scheme is obtained. For other values of the parameter, κ a combination of the two schemes is obtained (Mesbah, Kramer, Huesman & Van den Hof, 2009).

Equation (6.16) is valid for the situation of growth. For melting, the expression should be mirrored at the particular grid points $s^{(i)}_{k+1/2}$ with $k = 1...N$:

$$n^{(i)}_{B,k+1/2} = n^{(i)}_{B,k+1} + \frac{1+\kappa}{4}\cdot\left(n^{(i)}_{B,k} - n^{(i)}_{B,k+1}\right) + \frac{1-\kappa}{4}\cdot\left(n^{(i)}_{B,k+1} - n^{(i)}_{B,k+2}\right) \tag{6.17}$$

$$n^{(i)}_{B,k-1/2} = n^{(i)}_{B,k} + \frac{1+\kappa}{4}\cdot\left(n^{(i)}_{B,k-1} - n^{(i)}_{B,k}\right) + \frac{1-\kappa}{4}\cdot\left(n^{(i)}_{B,k} - n^{(i)}_{B,k+1}\right) \tag{6.18}$$

Two choices for the parameter κ are often encountered in literature: $\kappa = 1/3$ and $\kappa = -1$ (Qamar, Elsner, Angelov, Warnecke, & Seidel-Morgenstern, 2006). It has been shown that for $\kappa = 1/3$ schemes linear equations become third order accurate, while for other cases the equations become second order accurate.

Moreover, a flux limiter is implemented into equations (6.17) – (6.18), which is able to limit the spatial derivatives near sharp changes in the solution domain, therefore avoiding oscillatory behaviour of the solution (Qamar, Elsner, Angelov, Warnecke & Seidel-Morgenstern, 2006).

2.4. Software environment

The differential equations of the ice cream freezer model have been discretized using the procedure presented in Section 2.2 and 2.3 of this chapter, under the steady state assumption. In this way, the PDAE system has been transformed into a set of nonlinear ODE's. It appears that the algebraic equations can be rewritten in an explicit form, with the exception of the equations for calculating the temperature difference between the frozen layer and the wall, and the wall and the coolant.

$$2-D \;\; model \;\; \left\{position\,(z);\; particle\ size\,(s)\right\}$$

$$Variables: \;\; x_s \;\; states;\;\; v_s \;\; algebraic;\;\; p \;\; parameters$$

$$\begin{aligned} Equations: \quad & ODE's: && \partial x_s/\partial z = \mathbb{F}_{ODE}\left(x_s, v_s; p\right) \quad for \quad s \in S-grid \\ & NLAE's: && v_s \;\; = \mathbb{F}_{NAE}\left(x, v; p\right) \end{aligned} \tag{6.19}$$

$$Input\ as\ Boundary\ condition: \;\; x_s\left(z_0\right) = u\left(z_0, s\right)$$

$$Output\ variables: \qquad y\left(z_L\right) = \mathbb{F}_{output}\left(x_s\left(L\right)\right)$$

The numerical solution of the discretized steady state ice cream freezing model presented in equations (6.19) is performed using MATLAB®.

The resulting set of ODE's is solved using the built-in MATLAB® ode solver "*ode15s*", which is a multistep, variable order solver based on the numerical differentiation formulas. At each step, the solver estimates the local error ε in the $i-$th component of the solution. This error must satisfy the following condition (Matlab, 2008):

$$\left|\varepsilon(i)\right| \le max\left(RelTol \cdot abs\left(y(i)\right), AbsTol(i)\right) \tag{6.20}$$

List of symbols

$\varepsilon(i)$ = local error in the $i-$th component of the solution

$RelTol$ = specified relative tolerance of the solver

$AbsTol$ = specified absolute tolerance of the solver

$y(i)$ = the $i-$th component of the solution

The relative tolerance of the solver, *RelTol* is set to $1.0e-05$, while the absolute tolerance is set to $1.0e-06$ for all the variables, with the exception of the frozen layer's thickness (δ_{FL}), for which the tolerance is $1.0e-09$. In this way, it is ensured that the tolerances are small compared to the values of the state variables.

2.5. Verification of the model implementation

Before proceeding with the model applications, the correctness of the numerical implementation of the model is verified.

A first verification is performed by checking the conservation property of the overall amount of water. In this way, the correctness of the mass conservation equations is assessed. This step is performed in Appendix 14.

The second verification relates to the model implementation and it is done by testing the behaviour of the steady state model in an extreme case: all the rate parameters are zero. The values for the rest of the model parameters used in this step are shown in Tables 6.3 - 6.5 and in Appendix 11. The results for the verification step when all the mass transfer rates parameters are considered zero are presented in Figure 6.5. The results show, obviously, that there is no transfer of mass between the liquid bulk and the frozen layer. No water is being frozen, and no ice is being scraped from the wall. The composition of the ice cream mix remains unchanged along the freezer.

Figure 6.6 presents the temperature profiles for the case when all the mass transfer rates parameters are assumed zero, as well as the parameters for all the heat transfer terms. In this case, all the temperatures remained unchanged along the freezer, as expected. Similarly, the pressure drop vanishes when friction losses disappear by zero viscosity.

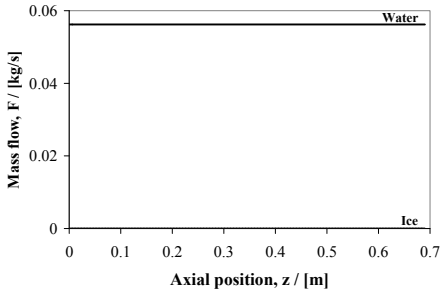

Figure 6.5. Verification of the model implementation: Mass flows in the bulk domain

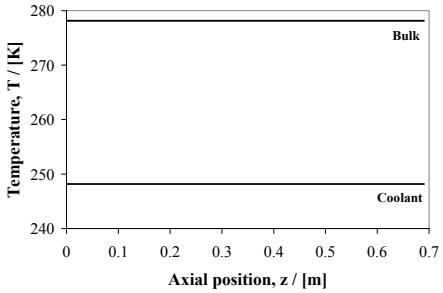

Figure 6.6. Verification of the model implementation: Temperatures

To prove rigorously that each of the rate laws has been implemented correctly by means of comparisons with analytical solutions for simplified cases is a rather cumbersome effort and has been skipped. Consequently, this has to be checked later against physical meaningfulness of the simulated cases, such as correct physical trends and steady states.

3. Model applications

In the following sections, a procedure for using the steady state model of the ice cream freezing for simulation and validation purposes will be presented.

3.1. Model simulation

Once the model equations are available and implemented in a software environment, and the numerical implementation is verified, the model can be used for different types of applications such as simulation or validation. During this step, the capability of the model to represent the physical system must be assessed. This is done by model simulation and comparing model predictions with actual experimental data.

3.1.1. Simulation scenario

The model is used as a simulation tool for reproducing physically plausible scenarios by means of case based simulations. In the following section, the base case scenario, which will be used to analyze the parameric sensitivity of the model, is defined.

Given the operating conditions (Table 6.3), the inputs (Table 6.4), the physical properties (Appendix 11), the design parameters (Table 6.5), the empirical parameters (Table 6.6), the outputs of the model are analysed.

Table 6.3. Overview of the operating conditions variables for the base case

Name	Symbol	Unit	Value
Inlet temperature	$T_{B,0}$	$[K]$	278.15
Inlet pressure	P_0	$[Pa]$	$5 \cdot 10^5$
Feed flow rate of the mix	$F_{in}^{(ic)}$	$\left[l/h \right]$	280
Temperature of the coolant	T_c	$[K]$	248.15
Rotor speed	ω_r	$[rpm]$	240

Table 6.4. Overview of the input variables for the base case

Name		Symbol	Unit	Value
Inlet mass fraction	Ice	$x_{B,0}^{(i)}$	$[-]$	0.000
	Water	$x_{B,w,0}^{(l)}$	$[-]$	0.645
	Sugar	$x_{B,s,0}^{(l)}$	$[-]$	0.170
	Fat	$x_{B,f,0}^{(l)}$	$[-]$	0.080
	Other	$x_{B,o,0}^{(l)}$	$[-]$	0.105
Overrun		Ovr	$[\%]$	100
Type of sugar (molar weight)		M_s	$\left[kg/kmole \right]$	342.3

Table 6.5. Overview of design parameters for the base case

Name	Symbol	Unit	Value
Freezer length	L	$[m]$	0.690
Inner freezer diameter	D	$[m]$	0.204
Rotor diameter	D_0	$[m]$	0.180
Freezer wall thickness	δ_{wall}	$[m]$	0.01
Scraper blades thickness	δ_{blade}	$[m]$	10^{-4}
Number of scraping blades	N_{blades}	$[-]$	2

Table 6.6. Overview of the empirical parameters for the base case

Name		Symbol	Unit	Value
Fudge factors for mass transfer terms	Transfer of ice from B to FL	C_a	$[-]$	1
	Transfer of water from B to FL	C_b	$[-]$	1
	Ice melting in B	C_c	$[-]$	1
Parameter for the Nusselt number		Φ	$[-]$	2.5
Parameters for the work done by the scraper		c_1	$[-]$	5.0
		c_2	$\left[J/kg \right]$	$\Delta h_{cryst}/4$
Parameter for the viscous dissipation		C_γ	$[-]$	3.5
Parameters of the Weibull distribution	Scale	Λ	$[-]$	$40 \cdot 10^{-6}$
	Shape	Σ	$[-]$	4.0
Power law parameters		A	$[-]$	−107.57
		B	$[-]$	29565
		C	$[-]$	3.0
		n	$[-]$	0.65
Rotor action function parameters		k_ω	$[-]$	10^{-3}
		n_ω	$[-]$	3.0
Minimum thickness of the frozen layer		$\delta_{FL,min}$	$[m]$	10^{-5}

Table 6.7. Overview of the numerical control parameters for the base case

Name	Symbol	Unit	Value
Number of discretization points	nc	$[-]$	200
Maximum particle size considered	$s_{max}^{(i)}$	$[m]$	$100 \cdot 10^{-6}$

The output variables are given in Table 6.8.

Table 6.8. Overview of the output variables for the base case

Name	Symbol	Unit
Outlet temperature of the mix	$T_{out}^{(ic)}$	$[K]$
Mass fraction of water in the product	$x_{out,w}^{(ic)}$	$[-]$
Mass fraction of ice in the product	$x_{out,i}^{(ic)}$	$[-]$
Mean diameter of the volume weighted distribution of ice particles	$d_{4,3}^{(i)}$	$[m]$
Mean diameter of the surface area weighted distribution of ice particles	$d_{3,2}^{(i)}$	$[m]$
Pressure drop	ΔP	$[Pa]$
Total amount of heat removed	Q_{tot}	$[kW]$
Production rate	$F_{out}^{(ic)}$	$[l/h]$

3.1.2. Simulation results and discussion

The results are obtained for the steady state model of the ice cream freezing process, by using the first order upwind approximation technique described in Section 6.2.1. This method is not as accurate as the higher-order methods, but has the advantage of being fast. For the purpose of this study, the results are not required to be very accurate, since the model is required to follow only the expected trends of the variables. For applications where the behaviour of the freezer must be followed closely by the model, an increase in accuracy will be required.

Table 6.9. Simulation times for different levels of accuracy for the first order upwind approximation for particle size

Number of discretization points, nc	Simulation time, t [s]
100	6
200	15
500	96
1000	555

An option to increase the accuracy of the first order upwind approximation is to use a higher number of discretization points for the ice particle size. This will have an effect on time required for the model solution, as seen from the results in Table 6.9.

Figure 6.7 presents the simulation results of the size distribution of the ice particles in the bulk domain, for different numbers of discretization points.

The use of a higher number of points will have an effect on the solution, but in the same time, there is an increase in the simulation time. The relative error between the simulation with 100 and

1000 discretization points for the internal coordinate of the ice particles is less than 1.5%, while the increase in computation time is of factor 100.

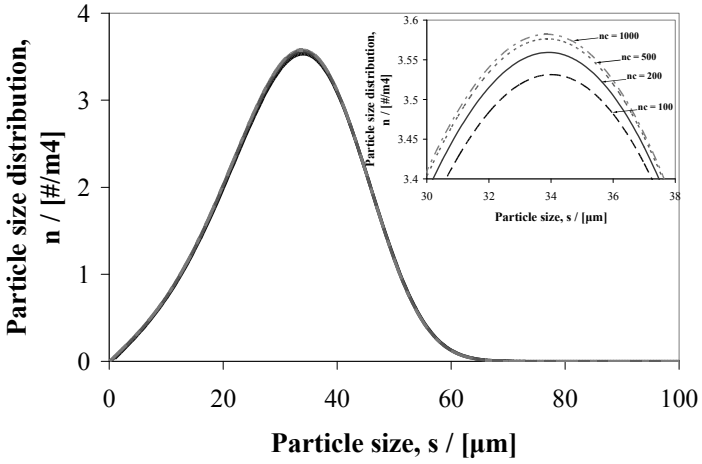

Figure 6.7. Simulation results for different levels of accuracy of the first order upwind approximation: Particle size distribution of the ice particles in the bulk domain

For this reason, a number of 200 discretization points for the size coordinate are used in obtaining the results presented in the following sections. The simulation results are displayed for 120 integrator stepping points in the axial direction. The computation time is ~ 15 seconds.

The size distribution of the ice particles coming from the frozen layer to the bulk has an influence on the final size distribution of the ice particles, as shown in Figure 6.8 and Table 6.10.

For the application presented in the following sections, a "normal" distribution of the ice particles coming from the frozen layer to the bulk is considered, with the value of the shape parameter for the Weibull distribution, $\Sigma = 4$.

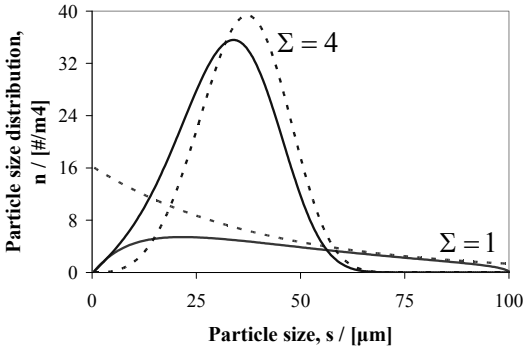

Figure 6.8. Simulation results for different size distributions of the ice particles coming from the frozen layer in the bulk: Particle size distribution of ice particles in the bulk at the freezer's exit (a) no particle melting (dashed line); (b) particle melting (solid line). Σ represents the shape parameter of the Weibull distribution

The flow and temperature profiles are plotted along the axial direction of the heat exchanger in Figures 6.9 and 6.10 respectively. The results obtained for the output variables are presented in Table 6.10. The mass flow profiles in Figure 6.9 show that the ice does not survive inside the aerated liquid bulk at the beginning of the freezer. It takes some time until the aerated liquid phase in the bulk, which is warm upon entrance, cools down and reaches the equilibrium temperature of the ice-water-sugar phase equilibrium.

This signifies that all the ice coming from the frozen layer during this period melts completely, and the temperature of the bulk liquid is decreased until the equilibrium temperature. Once this temperature is reached, the ice particles coming from the frozen layer survive inside the aerated liquid phase, and the concentration of ice inside the bulk domain increases.

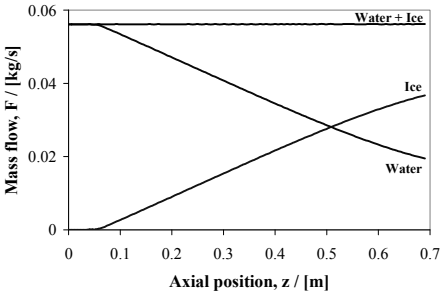

Figure 6.9. Mass flow profiles along the freezer (axial direction): ice and water

Table 6.10. Overview of the output variables for the ice cream freezing model for different size distributions of the ice particles coming from the frozen layer to the bulk

Output	Symbol	Unit	Size distribution of ice particles from the FL to the B	
			Exponential, $\Sigma = 1$	"Normal", $\Sigma = 4$
Outlet temperature of the mix	$T_{out}^{(ic)}$	$[K]$	269.1	269.02
Mass fraction of water in the product	$x_{out,w}^{(ic)}$	$[-]$	0.2218	0.2222
Mass fraction of ice in the product	$x_{out,i}^{(ic)}$	$[-]$	0.4196	0.4192
Mean diameter of the volume weighted distribution of ice particles	$d_{4,3}^{(i)}$	$[m]$	$71.1 \cdot 10^{-6}$	$41.6 \cdot 10^{-6}$
Mean diameter of the surface area weighted distribution of ice particles	$d_{3,2}^{(i)}$	$[m]$	$64.5 \cdot 10^{-6}$	$39.2 \cdot 10^{-6}$
Pressure drop	ΔP	$[Pa]$	$2.79 \cdot 10^{4}$	$2.79 \cdot 10^{4}$
Total amount of heat removed	Q_{tot}	$[kW]$	14.50	14.50

This behaviour is better visible in the temperature profiles shown in Figure 6.10. At the beginning of the freezer, the aerated liquid phase in the bulk temperature decreases fast until the temperature of the ice-water-sugar phase equilibrium.

Figure 6.11 presents the concentration profiles of the ice cream mix along the freezer. Since for all the components of the mix, with the exception of the ice and water, no transfer is considered, the concentration profiles of these components remain constant along the tube. Moreover, the sum of the mass fractions is equal to one, as expected, as seen in Figure 6.11.

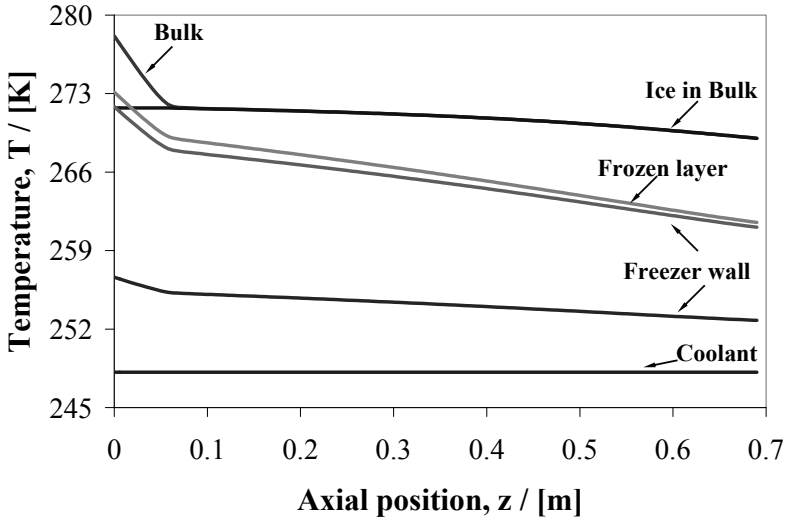

Figure 6.10. Temperature profiles along the freezer (axial direction)

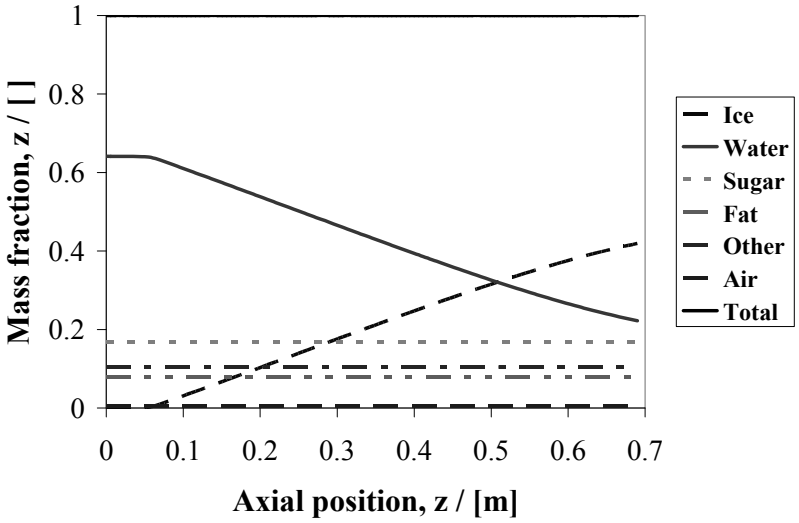

Figure 6.11. Mass fraction profiles along the freezer (axial direction)

The meltdown of the ice particles is visualised using the particles size distribution plots, shown in Figures 6.12 and 6.13. In this figures, two types of processes are presented:

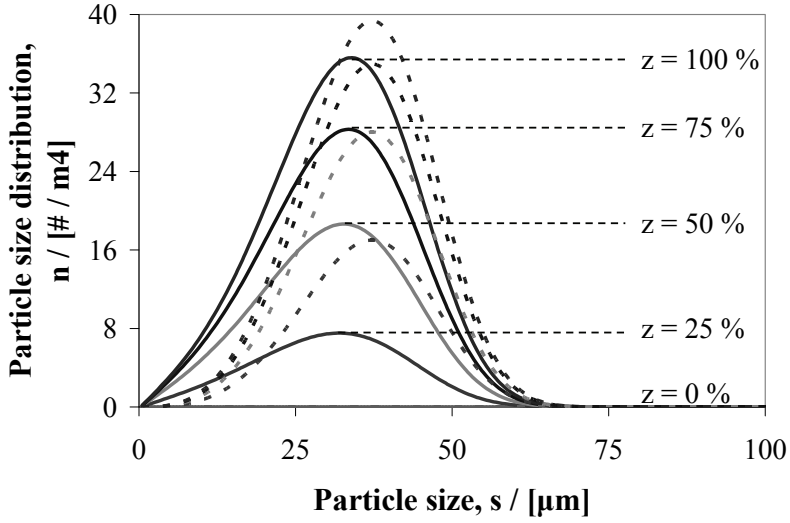

Figure 6.12. Ice particle size distribution along the freezer axial direction, z (a) with no particle melting (dashed line) and (b) with particle melting (solid line)

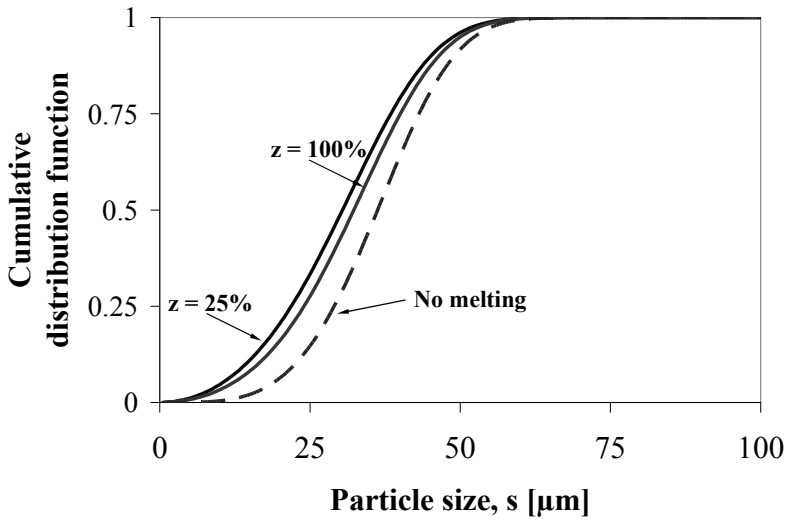

Figure 6.13. Ice particle cumulative distribution along the freezer axial direction, z (a) with no particle melting (dashed line) and (b) with particle melting (solid lines)

Firstly, the melting of the ice particles is neglected (the dashed lines). The ice particle distribution grows along the axial direction of the freezer and the shape remains unaffected. The only phenomenon that changes the magnitude of the ice distribution is the transfer to and from the frozen

layer. The number of ice particles steadily increases, while the shape corresponds with the size distribution of the scraped away ice particles.

Secondly, the melting of the ice particles during axial transport is considered (the solid lines). In this case, both effects are visible: there is an increase of the total amount of ice particles as the fluid moves along the tube, due to the transfer from the frozen layer, and, in the same time, the size distribution shifts towards smaller sizes, due to melting.

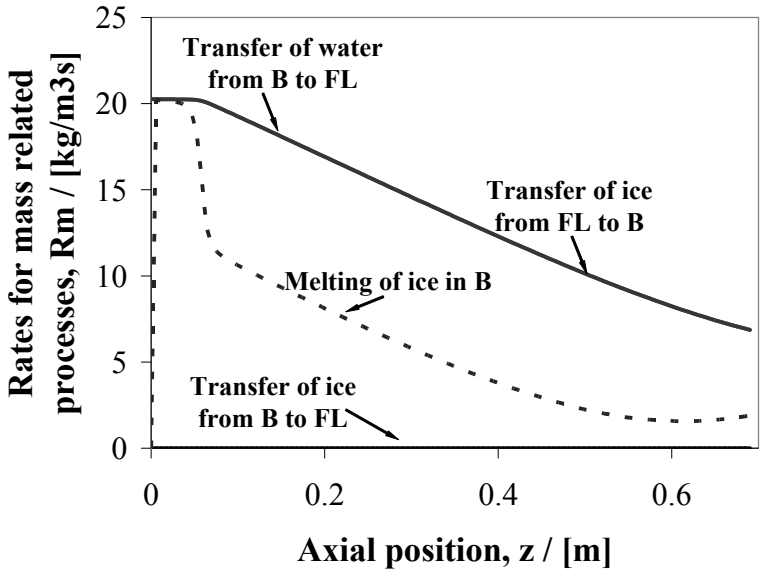

Figure 6.14. Rates for the mass transfer related processes along the freezer axial direction, z
Water and ice phases in the bulk domain

In Figures 6.14 and 6.15, the variation of some of the mass and energy related processes are presented.

From Figure 6.14 it can be seen that the amount of ice transferred from the bulk to the frozen layer is practically negligible compared to the amount of water in the same direction. Due to the steady state assumption, the amount of ice coming from the frozen layer into the bulk domain is equal to the sum of the water and ice being transferred from the bulk.

In the same time, it can be noticed that at the beginning of the freezer, all the ice coming from the frozen layer melts completely. Only once the equilibrium temperature is reached the ice particles start to survive, and the rate of melting decreases.

Concerning Figure 6.15, it is interesting to note that the heat due to scraping diminishes when moving along the axial coordinate, because the frozen layer diminishes in thickness due to decreasing liquid water content available for freezing.

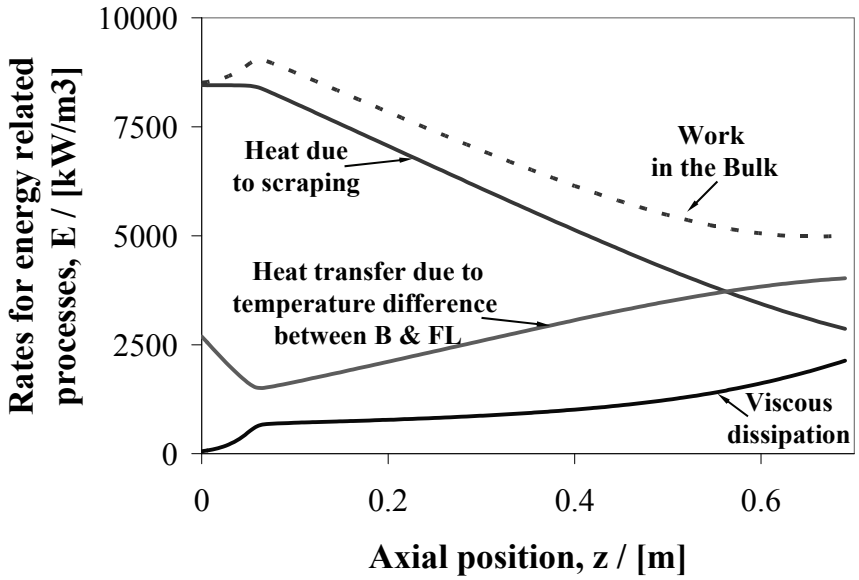

Figure 6.15. Rates for the energy transfer related processes along the freezer axial direction, z
Aerated liquid phase in the bulk domain

3.2. Parametric sensitivity analysis for validation purposes

Collecting the data required to validate the model can be resource intensive. Furthermore, poorly planned experiments will cause a greater loss of time and resources and will yield to little useful information. For this reason, it is important to develop a strategy to perform the model validation in a systematic way in order to maximise the information obtained from each experiment and to minimise the number of analyses, the cost of materials and the required time. This is achieved by design of experiments.

The *design of experiments* is a technique that aims to obtain the maximum information from an experimental apparatus. There are different ways of making a design of experiments. When models of an experimentally investigated system exist, these can be used in devising experiments that will yield the most informative data, in a statistical sense, for use in parameter estimation and model validation (Franceschini & Macchietto, 2008). For example, a priori information on system behaviour (as captured by the model) is used before an experiment takes place. The experimental results will hopefully offer new information for updating the model. Thus, before designing the experiments it is important to determine how the behaviour of the system depends on the values of the different parameters that characterize the system. The analysis of how a system responds to changes in the parameters us called *parametric sensitivity* (Varma, Morbidelli & Wu, 1999).

A sensitivity analysis is useful for understanding the relationships between the different parameters of the model and the model performance. This relationship is quantified by a sensitivity value. If a small change in a parameter value causes a large change in the output variables then these outputs are said to be sensitive to that parameter. For this reason, the parameter will have to be determined very accurately.

Two types of sensitivities can be defined (Varma, Morbidelli & Wu, 1999):

a) *Local sensitivity* – provide information on the effect of a small change in each input parameter, around a fixed nominal value, on each output or performance (dependent) variable. In this way, the directionality of the parameters impact on the performance will be determined.

b) *Global sensitivity* – provide information on the effect of large (real-life) variations of all parameters on the output or performance (dependent) variables. In this way, the magnitude of the parameters impact on the performance will be determined.

The (local) sensitivity is defined in the following way:

$$S_{jm} = \frac{\partial y_j}{\partial w_m} \tag{6.21}$$

These sensitivities are scale dependent.

List of symbols

y = output (performance) variable

w = parameter

3.2.1. Sensitivity analysis by singular value decomposition

When the dependency of multiple outputs with respect to multiple parameters is considered, one obtains a matrix filled with local sensitivities. Several questions arise at this point. What should be done with such a matrix? What is the dominant pattern of influence? A tool for analysing a sensitivity matrix of the model parameters is the *singular value decomposition (SVD)*. It is used for the identification of the dominant parameters, for example those parameters whose modifications cause the largest changes into the system. Moreover, this approach offers information related to the direction of the model outputs as well (Seferlis & Grievink, 2001).

The principle is to apply a SVD to the local sensitivity matrix. The local sensitivity matrix S_L is calculated by applying small variations on the model parameters:

$$S_L = \begin{bmatrix} \frac{\partial y_1}{\partial w_1} & \cdots & \frac{\partial y_1}{\partial w_m} \\ \vdots & \ddots & \vdots \\ \frac{\partial y_j}{\partial w_1} & \cdots & \frac{\partial y_j}{\partial w_m} \end{bmatrix} \tag{6.22}$$

The calculation of the singular values is scale-dependent (Seferlis & Grievink, 2001), therefore a scaling is needed in order to be able to compare the perturbations:

$$\frac{\partial y_j}{\partial w_m} = \frac{w^s}{y^s} \cdot \frac{\partial y_j}{\partial w_m} \tag{6.23}$$

The SVD rewrites the scaled sensitivity matrix in the following form:

$$S_L^s = U \cdot \Sigma \cdot V^T \tag{6.24}$$

with

$$U^T \cdot U = V^T \cdot V = I_r \tag{6.25}$$

$$\Sigma = diag\left(\sigma_1^2, \sigma_2^2, ..., \sigma_r^2\right) \tag{6.26}$$

where

$$r = min\left(j, m\right) \tag{6.27}$$

List of symbols

y^s = scaling factor on the model performance variables

w^s = scaling factor on the model parameters

S_L^s = scaled sensitivity matrix

Σ = singular values matrix

U = matrix of the orthonormal "input" basis vector directions for S_L^s

V = matrix of the orthonormal "output" basis vector directions for S_L^s

σ_r^2 = singular values

An algorithm is defined for performing the singular value decomposition. The following steps need to be followed:

1. Select the relevant parameters, w for which an analysis should be performed. They can be grouped in categories such as operational, process design, physical, numerical control parameters, etc.

2. Select the relevant performance variables, y .
3. Define a base case with fixed parameters values, w_0 and calculate the values of the performance variables, y_0 . For the ice cream model, the base case is defined in Section 6.2.2.
4. Perform sensitivity analysis by making small local (linear) variations (0.5-1.0%) in the parameters of the model. The components of the sensitivities matrix are scaled with the nominal values of the performance variables and the parameters for the base case scenario (y_0 and w_0 , respectively).
5. Apply SVD to the local sensitivity matrix and determine the number of dominant singular values. Find the directionality of impact (matrices U and V for the dominant singular values) on the performance variables.
6. Find the magnitude of the impact on the performance variables by making global, directional variations (10-20%) in the parameters of the model. The dominant directions determined during Step 5 will be chosen for this global study.

In the following section, the focus is on the generation of local parametric sensitivity information for identifying and screening the dominant parameters. Accurate values of these dominant parameters must be determined from experimental data obtained from a model-based design of experiments.

3.2.2. Results of the parametric sensitivity analysis and discussion

A perturbation of 0.5% is applied on the model parameters and the effects are analyzed for each category of parameters separately. The results of the SVD and the dominant effects are presented in the following sections, for a number of four groups of parameters: (a) the operational parameters; (b) the input parameters; (c) the freezer design parameters; and (d) the empirical parameters.

Table 6.11. Output variables for the parametric sensitivity analysis of the ice cream freezing model

Output	Symbol
Outlet temperature of the mix	$T_{out}^{(ic)}$
Mass fraction of water in the product	$x_{out,w}^{(ic)}$
Mass fraction of ice in the product	$x_{out,i}^{(ic)}$
Mean diameter of the volume weighted distribution of ice particles	$d_{4,3}^{(i)}$
Mean diameter of the surface area weighted distribution of ice particles	$d_{3,2}^{(i)}$
Pressure drop	ΔP
Total amount of heat removed	Q_{tot}

The results will be presented in the form of the singular vectors for each group of parameters. The input singular vector u corresponds to the largest singular value and indicates the input direction that causes the largest modification in the performance. The corresponding output singular vector v indicates the output direction in which the inputs are most effective.

Table 6.11 shows the output variables that are considered for the sensitivity analysis.

3.2.2.1. Operational parameters

The operational parameters considered for this study are presented in Table 6.12.

From the singular values presented in Figure 6.16 it is concluded that there is one dominant direction for the operational parameters group. The computation time is ~ 60 seconds.

Table 6.12. Operational parameters for the parametric sensitivity analysis of the ice cream freezing model

Input	Symbol
Inlet temperature of the mix	$T_{B,0}$
Coolant temperature	T_c
Inlet mass flow of the mix	$F_{in}^{(ic)}$
Rotational speed	ω_r

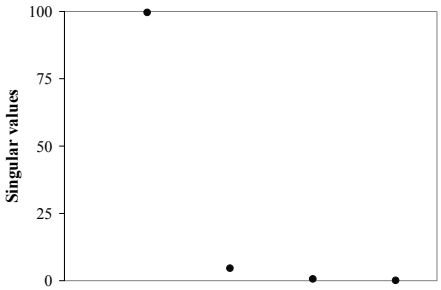

Figure 6.16. The singular values for SVD on the operational parameters of the model

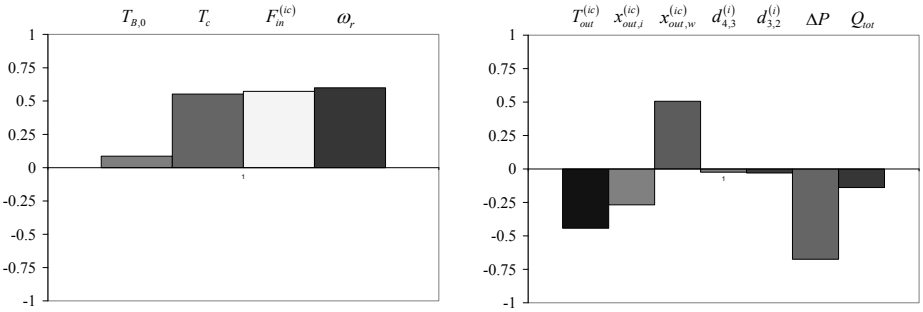

Figure 6.17. The singular vectors for the operational parameters group: a) Input singular vector; b) Output singular vector

The singular vectors are presented in Figure 6.17. These singular vectors for the dominant directions are listed in Table 7.4, in Appendix 15. From the results in Figure 6.17, it can be concluded that the most sensitive perturbation of parameter combinations is an increase in the coolant

temperature, coupled with an increase of the inlet mass flow of ice cream mix and rotational speed. This will determine a decrease of the outlet temperature of the product and the pressure drop along the freezer, as well as an increase of the water concentration in the final product.

It can be concluded that the set of dominant parameters to be considered in the validation experiments for the operational parameters group are the coolant temperature, the inlet mass flow of ice cream mix and the rotational speed.

3.2.2.2. Input parameters

The input parameters considered for this study are listed in Table 6.13.

The singular value decomposition reveals two dominant directions (Figure 6.18) for the input parameters group. The singular vectors are presented in Figures 6.19 - 6.20 and listed in Table 7.5 in Appendix 15. The computation time is ~ 95 seconds.

Table 6.13. Input parameters for the parametric sensitivity analysis of the ice cream freezing model

Input	Symbol
Inlet water mass fraction	$x_{B,w,0}^{(l)}$
Inlet sugar mass fraction	$x_{B,s,0}^{(l)}$
Inlet fat mass fraction	$x_{B,f,0}^{(l)}$
Inlet mass fraction of other components	$x_{B,o,0}^{(l)}$
Overrun	Ovr
Type of sugar (molar weight)	M_s

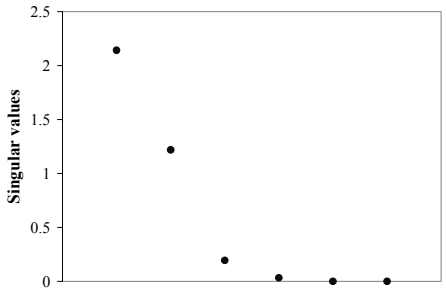

Figure 6.18. The singular values for SVD on the input parameters of the model

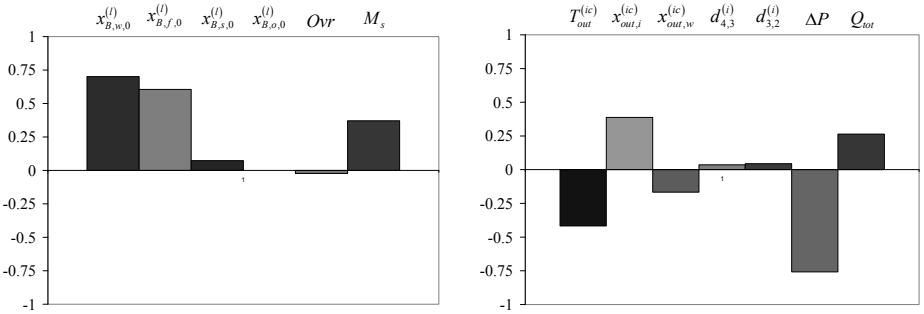

Figure 6.19. The first set of singular vectors for the operational parameters group: a) Input singular vector; b) Output singular vector

The first direction of change shown in Figure 6.19 indicates that the most sensitive perturbation in the input parameters is an increase of the concentrations of water and fat in the inlet mix will have an effect on the decrease of the output temperature of the product and an increase of the ice formation. Moreover, a decrease of the pressure drop along the freezer and of the total amount of heat removed is also predicted.

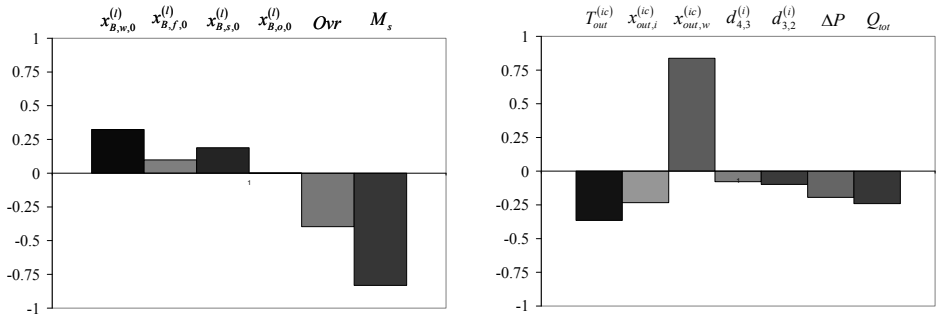

Figure 6.20. The second set of singular vectors for the operational parameters group: a) Input singular vector; b) Output singular vector

The second direction of change in Figure 6.20 indicates that an increase of the amount of water, coupled with decrease of the amount of air in the inlet mix will decrease the outlet temperature and the ice content in the final product. The type of sugar will also have a strong effect on these variables as well, as shown in Figure 6.20.

The validation experiments for the input parameters group must be performed in two directions. Firstly, a set of parameters consisting of the inlet mass fractions of water and fat, as well as the type of sugars should be considered. Secondly, to the inlet mass fraction of water and the type of sugars, the overrun must be added to get the most significant results.

3.2.2.3. Freezer design parameters

Table 6.14 lists the freezer design parameters considered for the sensitivity analysis.

The singular values (Figure 6.21) reveal two dominant directions for the freezer design parameters group. The singular vectors are shown in Figures 6.22 - 6.23 and listed in Table 7.6 in Appendix 15. The computation time is ~ 85 seconds.

The first set of singular vectors in Figure 6.22 indicate that an increase of the freezer diameter will lead to an increase of the outlet temperature, a decrease of the water concentration coupled with an increase of the ice concentration in the final product and a decrease of the pressure drop along the freezer. Moreover, an increase of the total amount of heat removed is indicated as well.

The second set of singular vectors, in Figure 6.23, indicate that the decrease of the freezer length, coupled with a decrease of the rotor diameter and an increase of the freezer wall thickness will

have an effect of decreasing the outlet temperature of the mix. The ice formation, the pressure drop along the freezer and the total amount of heat removed inside the freezer are reduced as well under these conditions.

Table 6.14. Freezer design parameters for the parametric sensitivity analysis of the ice cream freezing model

Input	Symbol
Freezer length	L
Inner freezer diameter	D
Rotor diameter	D_0
Freezer wall thickness	δ_{wall}
Scraper blades thickness	δ_{blade}

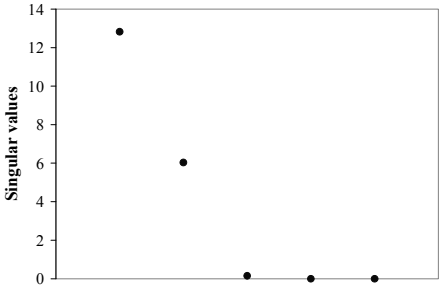

Figure 6.21. The singular values for SVD on the freezer design parameters of the model

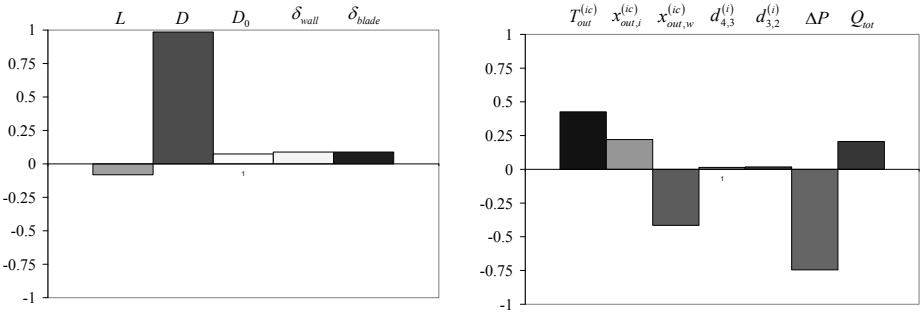

Figure 6.22. The first set of singular vectors for the freezer design parameter group: a) Input singular vector; b) Output singular vector

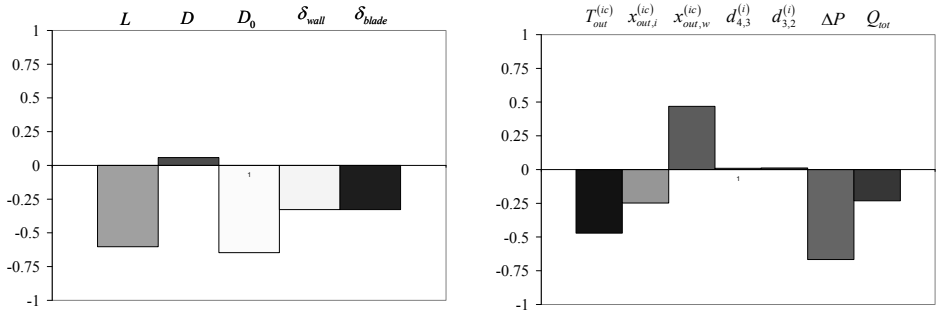

Figure 6.23. The second set of singular vectors for the freezer design parameter group: a) Input singular vector; b) Output singular vector

Similarly, to the input parameters group, the freezer design parameters group validation experiments should be focused on two directions. Firstly, the change in freezer diameter, indicated by the first set of singular vectors must be analyzed. Secondly, validation experiments must be performed considering as set of dominant parameters the freezer length, the rotor diameter, the freezer's wall and the blade thickness.

3.2.2.4. Empirical parameters

Finally, the empirical parameters used for this study are listed in Table 6.15.

It appears from the singular values presented in Figure 6.24 that there are two dominant directions. The singular vectors for the dominant directions are shown in Figures 6.25 - 6.26 and listed in Table 7.7 in Appendix 15. The computation time is ~ 190 seconds.

Table 6.15. Empirical parameters for the parametric sensitivity analysis of the ice cream freezing model

Input		Symbol
Fudge factors for mass transfer terms	Transfer of ice from B to FL	C_a
	Transfer of water from B to FL	C_b
	Ice melting in B	C_c
Parameter for the Nusselt number		Φ
Parameter for the viscous dissipation		C_γ
Parameters for the work done by the scraper		c_1
		c_2
Parameters of the Weibull distribution	Scale	Λ
	Shape	Σ
Rotor action function parameters		k_ω
		n_ω
Minimum thickness of the frozen layer		$\delta_{FL,min}$

The first set of singular vectors indicates that the increase of the mass transfer processes between the frozen layer and the bulk domain (C_a and C_b) will have an effect of decreasing the outlet temperature of the mix and the pressure drop along the freezer. A decrease of the ice formation is also predicted, due to the increase in the rotor speed action (ω_r).

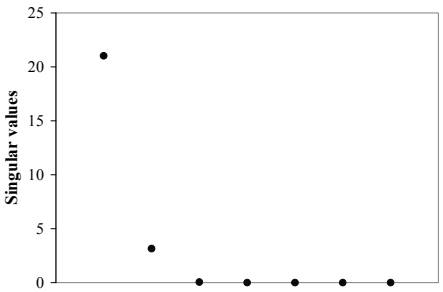

Figure 6.24. The singular values for SVD on the empirical parameters of the model

The second set of singular vectors shows that an increase of the ice particle size coming from the frozen layer (Σ), coupled with the increase of the rotor action will have a strong effect on the increase of the size of the ice particles in the final product.

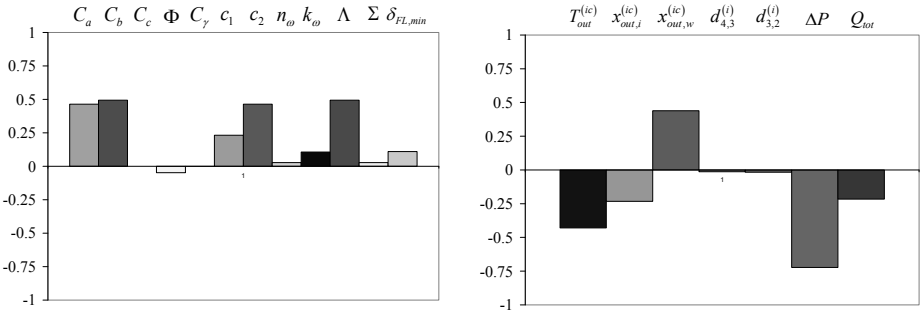

Figure 6.25. The first set of singular vectors for the empirical parameter group: a) Input singular vector; b) Output singular vector

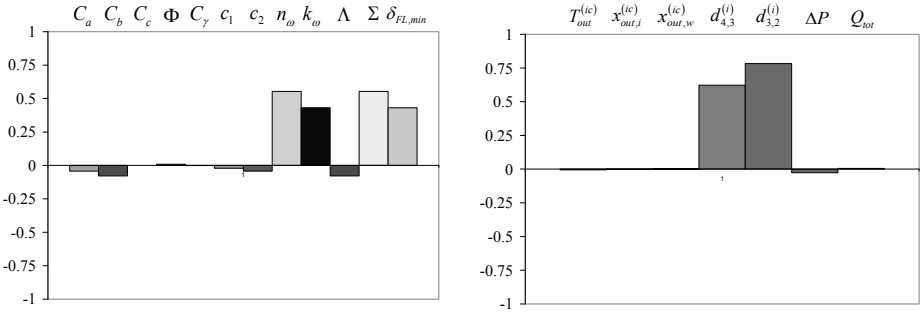

Figure 6.26. The second set of singular vectors for the empirical parameter group: a) Input singular vector; b) Output singular vector

The singular vectors obtained for the empirical parameters group show that the validation experiments must be performed in two directions as well. The first direction consists of the parameters related to the mass transfer of ice and water to the frozen layer, the parameters of the rotor action function, the parameters of the viscous dissipation term, and the scale of the Weibull distribution function. The second direction relates to the parameters of the rotor action function as well, together with the shape of the Weibull distribution function, and the minimum thickness of the frozen layer.

4. Conclusions

The steady state version (2-D) of the reduced 3-D model of the ice cream freezing step developed in Chapter 5 of this thesis has been implemented numerically in MATLAB®. The model reduction acted in this case at numerical level of the process model, more specifically on the approximation of the functions and operators. The equations were discretized along the internal coordinate of the ice particles using a first order upwind approximation. A verification of the correctness of the numerical implementation of the model has been performed using extreme cases with analytical solutions (the transfer rates were set to zero).

Moreover, the model has been used for some simulation scenarios for predicting the correct trends of the outputs. These results have been also used successfully for generating parametric sensitivity data for the identification and screening of dominant parameters of the model. Accurate values of the dominant parameters must be determined from experimental data obtained from a model-based design of experiments. The computation times for the solution of this steady state model are short enough, certainly when compared to the time it takes to analyse and interpret the results.

5. References

Bermingham, S.K. (2003). A Design Procedure and Predictive Models for Solution Crystallization Processes, *PhD Thesis*, *Delft University of Technology*, The Netherlands

Franceschini, G. & Macchietto, S. (2008). Model-based design of experiments for parameter precision: State of the art, *Chemical Engineering Science* 63, 4846,

Matlab (2008), User Manual, version 7.7.0.471 (R2008b)

Mesbah, A., Kramer, H.J.M., Huesman, A.E.M., & Van den Hof, P.M.J. (2009). A control oriented study on the numerical solution of the population balance equation for crystallization processes, *Chemical Engineering Science* 64, 4262

Qamar, S., Elsner, M.P., Angelov, I.A., Warnecke, G., & Seidel-Morgenstern, A. (2006). A comparative study of high-resolution schemes for solving population balances in crystallization, *Computers and Chemical Engineering* 30, 1119

Seferlis, P. & Grievink, J. (2001). Optimal design and sensitivity analysis of reactive distillation units using collocation models, *Industrial and Engineering Chemistry Research* 40, 1673

Varma, A., Morbidelli, M. & Wu, H. (1999). Parameteric sensitivity in chemical systems, *Cambridge University Press*

7

CONCLUSIONS AND RECOMMENDATIONS

This thesis covers the formulation and testing of an approach for the reduction of process models used for chemical engineering applications. In this concluding chapter, the key contributions of this research are highlighted being (partial) answers to the research questions posed at the beginning of this thesis. These key contributions are the formulation of a reduction procedure, which is able to preserve the essential structural features of a process, and the testing of this procedure on two realistic process modelling case studies. Additionally, various paths for further research are discussed, together with some recommendations for future study. These recommendations refer to the application of the model reduction procedure in a consistent and generic way, and to the further development of the reduced models developed during the case studies.

1. Research questions and approach

Modelling is an important tool in understanding the behaviour of a given system, as well as for making decisions during the product and process lifecycle. For many applications, the model has to be able to predict the behaviour of the system with sufficient accuracy, in a computationally fast way to meet demands of an efficient work process. For this latter reason, reduction of the model complexity is often required. Although a technique used in many areas of engineering, modelling and model reduction is still based on the expertise of individuals (Cameron & Ingram, 2009), obtained by experience. The need for a more systematic approach remains.

Existent model reduction techniques from the system and control area in chemical and process engineering can be applied to a complete process (unit) model, but often achieve only modest results. For example, the gain achieved in computing time is not as large as needed and this gain is offset by loss of structural process information in the reduced model. On the other hand, specific existent chemical engineering approaches to model simplification often select one critical model attribute, such as lumping of species of reactions, but leave the remainder of a model as it is. Would it be possible to find a more balanced approach between the systemic reduction without paying much regard for the underlying (physical) structure and the chemical engineering approach of focusing on a single model attribute and ignoring the systems view?

Therefore, the following questions are addressed in this thesis:

1. What are the main structural features of chemical process models that co-determine the model size and the computational efforts? Where is the structure being addressed in the modelling procedures?
2. How does the model structure reflect in the reduction approaches?
3. Is it possible to exploit efficiently these structural features when reducing the complexity of the process model?
4. Are the reduced models fit for purpose?

These research questions have been tackled by:

(a) Formulating a *structure-retaining model reduction approach*, which acts as an integrating framework for selectively applying existent reduction techniques to a process to be modelled;
(b) This approach is tested on two realistic *process modelling case studies*.

The main conclusions of this research are presented in Section 2, while recommendations for further work are given in Section 3.

2. Conclusions on model reduction approach with test results

2.1. Generation of model reduction options by a decomposition approach

The most common way of approaching the modelling for chemical engineering applications is to decompose the system into individual entities that perform a transformation of resources, using the network concept with nodes and edges. The process nodes are connected by material or information edges, depending on the type of resources they transport. The following levels of decomposition for the modelling procedure have been identified:

(a) *Contextual* level, which includes all the decisions related to the specification of the model and the applications it will be used for

(b) S*tructure* level, consisting of all the information referring to the physical entities composing the system, the phenomena that take place inside the individual entities, as well as the connections between them

(c) *Mathematical* level, composed of information related to the mathematical relations defining the behaviour of the process

(d) *Numerical* level, which contains the decisions for the numerical solution method and algorithm

(e) *Software implementation* level, which contains the decisions for the way of implementation of the model and numerical algorithm

At each level of decomposition, a series of attributes have been identified that have an effect on the model complexity. These attributes range from physical and behavioural entities composing the process system (units, domains, phases, etc.) to numerical schemes that are used to solve the process model. All have an effect on the complexity of the final software-implemented model. The model complexity depends on the number of equations that need to be solved, the number of terms in the model equations, as well as on the mathematical operations these equations contain and the coupling between the equations. For these reasons, each of the attributes offers handles for performing model reduction.

A *structure-retaining model reduction* is proposed. This approach has two stages: *decomposition* and *aggregation*. *Decomposition* is applied in the first stage to: (i) the nodes in the process network, (ii) the resources flowing through the edges and being processed in the node according to the behavioural model for each node. The model reduction within a node can be performed at all respective levels of the modelling procedure:

(1) Conceptual: by changing model functions and goals

(2) Structure: by simplifying the physical (compartments, domains, phases, phenomena, etc.) and behavioural (rate equations) structure of the model

(3) Mathematical: by reducing the number and the complexity of the model equations
(4) Numerical: by reducing the numerical accuracy and order of approximations of the mathematical operations
(5) Software: by efficient coding of model equations for fast execution

In the second stage, *aggregation* takes place: the overall process model is constructed from the reduced models of the nodes using the network structure. Starting from a network-based decomposition the reduction procedure is able to preserve the essential structural features of the process. Moreover, the physical meaning of the variables and equations is preserved as much as possible.

This approach has both conceptual and numerical elements, which makes it hard to assess its fitness for purpose on theoretical grounds only. Therefore, making test applications with this approach is seen as a practical way to evaluate its performance. The pragmatic criteria for success of the structure-retaining model reduction approach are that one is able to develop a model that:

- is solved successfully in an acceptable amount of time
- retains sufficient predictive accuracy for practical applications
- retains the topological and physical structure of the process to a sufficient level of detail

2.2. Applications of the structure-retaining model reduction approach

The application of the method has been investigated for two types of processes:

(A) A complex (multi-unit) process with simple (single phase) product: an *iso*-butane alkylation plant
(B) A simple (single unit) process with complex (multiphase) product: the freezing step in an ice cream manufacture process

2.2.1. Model reduction for complex processes with simple products

For the *iso*-butane alkylation plant, a rigorous dynamic model of the process is possible to develop, since the laws of conservation describing the model are not too difficult to implement and solve. In the same time, information regarding all the process rate phenomena is available. Moreover, the solution of the rigorous model is obtained in a satisfactory amount of time for off-line simulation applications, using Aspen Dynamics®. The complexity of this rigorous model lies in its nonlinear behaviour, determined by the reactor-separation-recycle structure in the plant flowsheet.

The use of this rigorous model for two practical applications is tried. These two applications are: (i) the assessment of the plantwide control structures and (ii) the dynamic optimization of the plant's operation. When the solution of these two problems is attempted, the rigorous model, works for the plantwide control problem, but fails when the solution of the dynamic optimization problem is sought. This requires the development of a reduced model of the plant.

Two model reduction approaches are applied and their results are compared with outcomes of the rigorous model:

(a) A reduced model is obtained using the *traditional model reduction approach*. Model order-reduction is attempted on the full rigorous model. Indeed, a reduced model is obtained which, however, wrongly approximates the rigorous model's behaviour.

(b) The *structure-retaining model reduction approach* has been applied for obtaining the reduced model of the process. The conceptual stage of the model reduction acts at the systemic and the higher levels of the physical structure (units) of the chemical plant, for this type of processes. The process model is decomposed in smaller models of each unit in the process flowsheet. Then, numerical model reduction is performed for each unit or groups of units individually. The distillation columns are reduced by balanced linear model-order reduction, eliminating the states for which the Hankel singular values are small. The model of the reactor is reduced by model simplification, considering only the component balances and constant temperature and physical properties. The obtained reduced models are connected according to the flowsheet in the next stage, to obtain the reduced model of the full process.

The reduced model has been implemented in MATLAB® / SIMULINK® for the assessment of the plantwide control structures, and in gProms® for the dynamic optimization of the plant's operation. The simulation results of the reduced models were accurately approximating the behaviour of the rigorous nonlinear model of the *iso*-butane alkylation plant.

Due to the differences in handling the models, improvement of the solution time of the reduced model has been observed in gProms®, when compared to MATLAB® / SIMULINK®. The two reduced models have been solving considering the same operating scenario and using the same hardware capabilities.

The two applications using the structure-retaining reduced model of the alkylation plant were successful: the reduced model reflected the process flowsheet structure, and it could be solved at the expense of a small sacrifice in predictive accuracy. The result is not yet 100% satisfactory as the dynamic optimization problem took a (too) long time to solve. The cause of this slow convergence can be due to an inadequate model structure and inherent to the nature of the optimization problem.

2.2.2. Model reduction for simple processes with complex products

Ice cream is a complex product and its formation by freezing was the second test problem. The development of a rigorous model for the freezer is conceptually conceivable, but practically infeasible. The model will become very complex, because the formation of the very involved internal structural features of the ice cream has to be properly included in the model. However, it is currently impossible to formulate such a comprehensive model because of the limited quantitative knowledge

regarding the rate phenomena that occur inside the system, let alone to solve it when having to deal with laws of conservation of an exceptional high dimensionality (≥ 5 coordinates).

For these reasons, an essential reduction is performed in this case both conceptually and numerically, during the stages of the modelling procedure, yielding a reduced 3-D model. The purpose of this reduced model is the application to parameter estimation, simulation of operational scenarios and design optimizations.

For this type of processes, the conceptual stage of the *structure-retaining model reduction approach* acts on the lower levels of the physical structure (species, phases, domains, compartments, coordinates), as well as on the behavioural level (phenomena) of the process model. The numerical stage focused less on reducing the number of model equations, and more on simplifying the different terms in these equations.

The model considers mass, momentum and energy as resources that are transformed inside the unit. Five coordinates are considered initially, which are further reduced to three. Moreover, the actual product structure consists of five different phases, with six species. The ice particles are modelled as a population with a distributed size, while all other phases (including air bubble and fat globules) are assumed pseudo-continuous and homogeneous. The momentum conservation has been simplified to an expression relating the mass flow with the pressure drop. The model assumes that all the ice particles in the bulk have the same temperature and the energy conservation equation for the bulk is written for the liquid ice cream phase (matrix, air, ice particles). The frozen layer is treated as a solid wall and pseudo-steady state is assumed when writing the energy balances over the frozen layer, the freezer wall and the coolant. Further simplification has been introduced in the expression of the rate laws, which are assumed dependent only of a single driving force. The obtained reduced model has seven partial differential equations, with seven initial conditions and nine boundary conditions, and fifty-four nonlinear algebraic equations.

The steady state version of this model was successfully implemented in MATLAB®, and verified. The numerical implementation of the model equations approximates the population balance for the ice particles in the bulk using a first order finite volume method. The verification implied the testing of the conservation properties of the model and of proper physical limits for extreme conditions. The accuracy of the verified reduced model prediction could not be fully tested since data from an experimental programme was not ready and its acquisition was beyond the purpose of the thesis. However, it has been ascertained for a base case scenario that the model predicts the right trends for the output variables, using the order-of-magnitude estimates for the value of the empirical parameters present in the model.

Being able to predict proper trends, the model has been used to determine the relative importance of the model parameters and their influence on the model outputs. This parametric sensitivity is a first stage of the model validation step in preparation to a design of experiments for parameter estimation and validation.

To conclude, the resulting reduced model of the ice cream freezer retains important features of the physical structure of the process and its steady state version is solved fast enough for simulation and parametric sensitivity-type of applications. Since the accuracy of the reduced model has not been verified against experimental data, this criterion for the success of the model reduction procedure still remains to be checked.

3. Recommendations

The following section is structured in an inverse order relative to the conclusion section. First, the recommendations for the particular cases are discussed, to offer some perspective on the specific cases. Since for the process of type A, the rigorous model is available, the recommendations will focus mainly on aspects of the structure-retaining model reduction approach, while for the process of type B, a second group of recommendations will focus on model development and refinement for the ice cream freezing step. The decomposition of the process modelling for model reduction is discussed next, for improvements towards a more generic structure-retaining model reduction approach.

3.1. Model reduction for complex processes with simple products

The application of the model reduction strategy that accounts for the internal structure of the process in the case of the *iso*-butane alkylation plant demonstrated the advantages of the approach, and, in the same time, it raised some more questions.

The dynamic optimization of the plant operation has been solved with some difficulty, requiring trial-and-error iterations for the initial values of the initial profiles of the control variables. One reason might be that the structure decomposition is application dependent and, for this particular case, was not done up to a satisfactory level. The optimality of the decomposition strategy needs to be investigated further. The relation to the formulation of an optimization problem is also part of this effort. For example, which parts of the model have significant impact on the objective function should be investigated. Another reason for the difficulty of solving the dynamic optimization problem might not be in the model, but in the solvers used in the gProms® or Aspen Dynamics® optimization toolbox. The investigation of this issue cannot be easily performed because access to the code is not always possible. Moreover, it could be that a combination of both the model and the numerical solvers is behind the difficult solution of the dynamic optimization problem, which would make the investigation even harder.

Another issue that needs to be investigated further is how to ensure that the decomposition of the different individual units is performed in a consistent way. The cut-off criteria for the model decomposition focused on eliminating the least important states in an individual unit, without accounting explicitly for the effects at the significant scale of the full process. It should be ensured that the decomposition of the different individual entities in the model structure is done in such way to maintain the significant (time) scales of the full process.

Moreover, the case discussed in Chapters 3 and 4 of the thesis has a relatively simple flowsheet structure, although meaningful for the purpose of the research. The application of the procedure for more complex process (with more recycle loops, for example) could offer extra insight into the benefits of the structure-retaining model reduction approach.

3.2. Model reduction for a single unit with complex products

3.2.1. Application of the structure-retaining approach

Similar to the processes with a complicated flowsheet structure, in the case of the ice cream freezing model the issue of setting a consistent criteria for cut-off when applying model decomposition must be further investigated. The significant time and spatial scales of the important phenomena that take place inside the freezer must be kept in the reduced model, and the decomposition should be done accordingly.

3.2.2. Selective model refinement

Several selective refinements are recommended in order to make the reduced model of the freezing step more meaningful as a tool for product design type of applications.

Firstly, the complex movement of the ice cream mix inside the freezer barrel resembles a helical flow. Redefining the spatial coordinate of the unit accordingly would allow for a more rigorous approach. The axial coordinate can be replaced by the introduction of a helical coordinate, often used for modelling of extruders (Yu & Hu, 1997). The simplification of the momentum conservation in the form of the pressure drop – mass flow dependency does not fully account for the complex movements that take place inside the freezer.

Secondly, it is possible that, in some of the cases, the dependence of the rate laws on a single driving force is not sufficient to describe effectively the processes that take place inside the freezer. The dependence of the rate laws on more driving forces must be investigated further. In the same time, the possibility that a specific rate does not depend in a linear way on the dominant driving force must be considered as well. Rather than inserting up-front all generic dependencies on driving forces in the model, dedicated experiments on lab-scale must reveal which dependencies are the dominant ones and only these are included in the model. The structure-retaining model reduction approach allows for the different phenomena that take part in the process to be kept separated and distinct. In this way, the change in the dependence of the rate laws on one or more driving forces, due to ongoing experimental testing, can be done without having to repeat previous steps in the model development.

Thirdly, the final product qualities are dependent not only on the distribution of ice particles inside the microstructure, but also on the distribution of the air bubbles and fat droplets. Adding such distributions with corresponding internal coordinates to the model will lead to an increase in model complexity, since more phases will be considered, with corresponding conservation equations, rate laws for the relevant physical phenomena, physical properties, etc. However, it may be possible to use

only one generic internal size coordinate for all distributed phases (ice, air, fat) by use of proper scaling factors per phase, thus limiting the increase in complexity.

3.2.3. Preparing for model validation and applications

In order to have a powerful tool for applications, and extension from a steady state to the dynamic version of this reduced model has to be developed, verified and validated. Once the validated dynamic model is available, it can be used for applications such as simulations of operating scenarios, control studies, dynamic optimizations, etc.

Another important point is that the accuracy of the model predictions depends on the numerical methods and tools that are used for its solution. For solving the partial differential equations, more sophisticated methods such as higher order finite volume methods or orthogonal collocation could be used if deemed necessary. The accuracy of the solutions will increase, but together with that, the computation time of the model solution will go up as well. This can be surpassed to some extent by use of state-of-the-art (dynamic) PDAE solvers such as gProms®, which behave better than MATLAB®.

A first step towards the model validation has been performed and described in Chapter 6 of this thesis: identification of parameter sets with a high impact on the model outputs. The next step in the model development procedure is to develop and perform experiments in order to generate data for validation. Based on the importance and influence of the parameters on the model outputs, as determined from the parametric sensitivity analysis, a design of experiments must be performed in order to get suitable data for parameter estimation. Once the model parameters are obtained, the model can be validated against a second independent set of experimental data. This validation will allow the model to be used further for practical applications, such as product design, optimization of process operation, etc.

The experimental procedure requires further research as well. In the past experimental set-ups, it is common to have quantitative information on the product structure at the end of the freezer, hence the final product composition, including information on the population distribution. This was because past models did not account for the entire range of phenomena that take place inside the unit. Dedicated experiments for measuring specific product structure variables along the freezing process will improve the quality of the final validated model, by offering information on the phenomena accounted for in the reduced 3-D model.

3.3. Decomposition of the process for model reduction

From the discussion in the previous sections, it can be concluded that the decomposition of the process for model reduction depends on the intended model application. For different types of applications and processes, the decomposition and the model reduction approach acts at different levels of detail.

Although the case studies presented in this thesis offered options on how to perform the reduction for particular processes, there is still an issue on how to decompose the model in an optimum way for generic applications and to set criteria for cut-off of time and spatial scales in a consistent way over all the individual units. The break down of the model structure (Figure 7.1) can be done at different levels of detail, as shown in Chapter 2 of the thesis. The performance of the model clearly depends on the cut level in this line of exploration for the model structure. The choice of this level is critical: too high involves the modelling of many useless features; too low may lead to useless results. The focus in this thesis was on attributes of the structure. Further, features of the dynamic behaviour, or of the control system should be investigated as well.

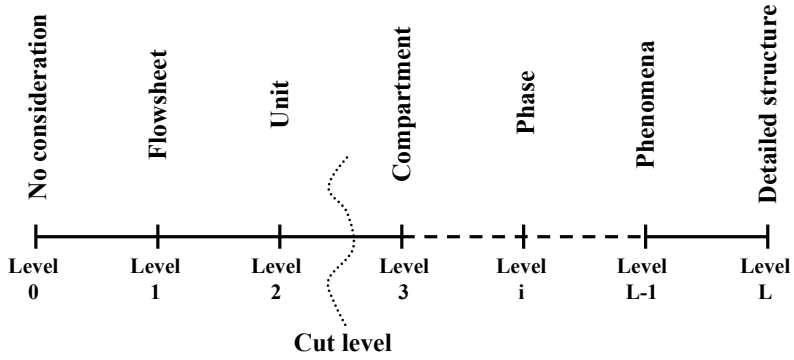

Figure 7.1. Line of exploration for the model structure

The approach used in the development of the models presented in this thesis proved to be a challenge in itself. The two extremes that were considered were:

(a) The rigorous modelling approach. In this case, the model is developed in full detail, taking into account all the structure and behaviour components present in the system, right from the beginning of the model development. Often, this may prove to be time consuming, since the initial level of complexity can lead to difficulties in model solving from an early stage.

(b) The "simple to complex" approach. The models developed using this approach are considering initially only partial and relevant structure and behaviour components of the system, in order to gain knowledge on the various internals of the process. Once this goal is achieved, more detail is added to the initial case, in order to reach a desired level of model complexity.

There should always be a trade-off between these two approaches in order to be able to develop a model, which is suitable for practical use.

The success of the structure-retaining approach depends largely on two factors. First, the *experience of the model developer* has an effect on the different choices during the model development. Based on the user skills, and the clarity of the model goals, the reduced model takes into account all the important phenomena, without being too complex for solving. Second, it is important that *adequate tools* (numerical methods, software, and hardware) are available for solving the model. The reduced model should be accurate enough to be used in practical applications, but sometimes the available tools are not sufficient to ensure it due to the high complexity still present in the models.

Taking into account all these factors, a testing programme has to be developed for the decomposition of process for modelling in an optimum way. A similar procedure to the design of experiments could be followed, in order to choose meaningful processes and applications that will offer maximum of information on the reduction approach. This information should include how detailed the physical structure will be to achieve the modelling goal for a generic application. Moreover, consistent treatment of the different individual nodes in the process network should be ensured, such that the overall time and spatial scales retain their significance.

In many cases, the different software environments available offer several model reduction options that can be used when implementing process models. Aspen Dynamics®, for example has a linearization toolbox, while MATLAB® offers order model reduction for the balanced realization of linear models. The implementation of automated model reduction tools in such software environments, with options of the most common existent (order-) reduction techniques available (linearization, model-order reduction, etc.), will be beneficial for the development time of future reduced process models, as well as for the use of the structure-retaining model reduction approach.

Once these model reduction options are available in various software environments, new techniques of model synthesis can be investigated. The model can be formulated as a superstructure over a field of (reduced) model building blocks and this superstructure offers options on how to connect the different blocks in a way that satisfies constraints on behaviour and meets targets of an objective function for model performance.

The application of the structure-retaining model reduction approach to processes with smaller scales (such as nanoclusters, molecular scale, etc.), where the behaviour is different from the processes at macroscales, or for networks in other engineering areas (electrical, mechanical, etc.), where the structure is different from a chemical process, could be investigated as well.

4. References

Cameron, I.T. & Ingram, G.D. (2009). A survey of industrial process modelling across the product and process lifecycle, *Computers and Chemical Engineering* 32, 420

Yu, Q., Hu, G.H. (1997). Development of a helical coordinate system and its application to analysis of polymer flow in screw extruders. Part I. The balance equations in a helical coordinate system, *Journal of Non-Newtonian Fluid Mechanics* 69, 155

8

APPENDIX

1. Summary of differential operations involving the mathematical operators in cylindrical coordinates

For writing the different conservation equations in this thesis, as well as in the following sections of this appendix, different mathematical operators were used. Using a cylindrical system of coordinates, the mathematical operators have the following form (Bird, Stewart & Lightfoot, 2002):

$$\nabla_z = \frac{\partial}{\partial z} \tag{8.1}$$

$$\nabla_r = \frac{1}{r} \cdot \frac{\partial}{\partial r} r \tag{8.2}$$

$$\nabla_\theta = \frac{1}{r} \cdot \frac{\partial}{\partial \theta} \tag{8.3}$$

$$\nabla_{s^{(\varphi)}} = \frac{\partial}{\partial s^{(\varphi)}} \tag{8.4}$$

$$\left(\nabla \cdot \Upsilon\right) = \frac{1}{r} \cdot \frac{\partial\left(r \cdot \Upsilon_r\right)}{\partial r} + \frac{1}{r} \cdot \frac{\partial\left(\Upsilon_\theta\right)}{\partial \theta} + \frac{\partial \Upsilon_z}{\partial z} + \frac{\partial \Upsilon_z}{\partial s^{(\varphi)}} \tag{8.5}$$

$$\begin{aligned}\left[\tau : \nabla u\right] = {} & \tau_{rr} \cdot \left(\frac{\partial u_r}{\partial r}\right) + \tau_{r\theta} \cdot \left(\frac{1}{r} \cdot \frac{\partial u_r}{\partial \theta} - \frac{u_\theta}{r}\right) + \tau_{rz} \cdot \left(\frac{\partial u_r}{\partial z}\right) \\ & + \tau_{\theta r} \cdot \left(\frac{\partial u_\theta}{\partial r}\right) + \tau_{\theta\theta} \cdot \left(\frac{1}{r} \cdot \frac{\partial u_\theta}{\partial \theta} + \frac{u_r}{r}\right) + \tau_{\theta z} \cdot \left(\frac{\partial u_\theta}{\partial z}\right) \\ & + \tau_{zr} \cdot \left(\frac{\partial u_z}{\partial r}\right) + \tau_{z\theta} \cdot \left(\frac{1}{r} \cdot \frac{\partial u_z}{\partial \theta}\right) + \tau_{zz} \cdot \left(\frac{\partial u_z}{\partial z}\right)\end{aligned} \tag{8.6}$$

The substantial derivative for a scalar field:

$$\frac{Dx}{Dt} = \frac{\partial x}{\partial t} + u_r \cdot \frac{\partial x}{\partial r} + \frac{u_\theta}{r} \cdot \frac{\partial x}{\partial \theta} + u_z \cdot \frac{\partial x}{\partial z} \tag{8.7}$$

The substantial derivative for a vector field:

$$\begin{aligned}\frac{D\Upsilon_z}{Dt} &= \frac{\partial \Upsilon_z}{\partial t} + u_r \cdot \frac{\partial \Upsilon_z}{\partial r} + \frac{u_\theta}{r} \cdot \frac{\partial \Upsilon_z}{\partial \theta} + u_z \cdot \frac{\partial \Upsilon_z}{\partial z} \\ \frac{D\Upsilon_r}{Dt} &= \frac{\partial \Upsilon_r}{\partial t} + u_r \cdot \frac{\partial \Upsilon_r}{\partial r} + \frac{u_\theta}{r} \cdot \frac{\partial \Upsilon_r}{\partial \theta} + u_z \cdot \frac{\partial \Upsilon_r}{\partial z} - \frac{\Upsilon_\theta^2}{r} \\ \frac{D\Upsilon_\theta}{Dt} &= \frac{\partial \Upsilon_\theta}{\partial t} + u_r \cdot \frac{\partial \Upsilon_z}{\partial r} + \frac{u_\theta}{r} \cdot \frac{\partial \Upsilon_\theta}{\partial \theta} + u_z \cdot \frac{\partial \Upsilon_\theta}{\partial z} + \frac{\Upsilon_r \cdot \Upsilon_\theta}{r}\end{aligned} \tag{8.8}$$

2. Mass and population conservation equations

a. The population balance equations for the dispersed phase

The equations written in this form are used for the ice particles in the bulk. They could be used for the air bubbles if they would be considered as a dispersed phase. The conservation equations in the bulk domain for the *dispersed phases* are written in the form of the population balance equation, in phase φ :

$$\frac{\partial}{\partial t} n_B^{(\varphi)} + \nabla_z \cdot \left(u_z^{(\varphi)} \cdot n_B^{(\varphi)} \right) + \nabla_r \cdot \left(u_r^{(\varphi)} \cdot n_B^{(\varphi)} \right) + \nabla_\theta \cdot \left(u_\theta^{(\varphi)} \cdot n_B^{(\varphi)} \right) + \nabla_{s^{(\varphi)}} \cdot \left(r_s^{(\varphi)} \cdot n_B^{(\varphi)} \right) = B_B^{(\varphi)} - D_B^{(\varphi)} \quad (8.9)$$

With the **initial condition**:

Initially, there is an initial concentration of dispersed particles inside the bulk domain:

At $t = 0$ $\qquad n_B^{(\varphi)} = n_{B,0}^{(\varphi)} \left(z, r, \theta, s^{(\varphi)} \right)$ (8.10)

The **boundary conditions**:

For each one of the coordinates, one boundary condition is sufficient, since the partial differential equations are of hyperbolic-type and first order (Hoffman, 2001). The boundary conditions should be defined upstream of the flow direction.

a) In axial direction

Continuity of flows:

At $z = 0$ $\qquad \left[u_z^{(\varphi)} \cdot n_B^{(\varphi)} \left(t, z, r, \theta, s^{(\varphi)} \right) \right]_{z=0} = j_{B,z,0}^{(\varphi)} \left(t, r, \theta, s^{(\varphi)} \right)$ (8.11)

b) In radial direction

The radial inflow is assumed non-zero at $r = R$.

At $r = R$ $\qquad \left[u_r^{(\varphi)} \cdot n_B^{(\varphi)} \left(t, z, r, \theta, s^{(\varphi)} \right) \right]_{r=0} = j_{B,r,0}^{(\varphi)} \left(t, z, \theta, s^{(\varphi)} \right)$ (8.12)

c) In angular direction

Periodic continuity:

At $\theta = 2\pi$ $\qquad u_\theta^{(\varphi)} (t, r)\big|_{\theta=2\pi} = u_\theta^{(\varphi)} (t, r)\big|_{\theta=0}$ (8.13)

d) Along the internal coordinate

The boundary condition for the particle size is put at the upper range of the particle size due to the size reduction by melting of the particles.

At $s^{(\varphi)} = s_{max}^{(\varphi)}$ $\qquad n_B^{(\varphi)} \left(t, z, r, \theta, s^{(\varphi)} \right)\Big|_{s^{(\varphi)} = s_{max}^{(\varphi)}} = n_{B, s_{max}^{(\varphi)}}^{(\varphi)} (t, z, r, \theta)$ (8.14)

In case of particle growth, the boundary condition for the particle size is put at the lower range of the particle size.

List of symbols

$n_B^{(\varphi)}$ = concentration of particles, $\left[{}^{\#}/_{m^3 \cdot s} \right]$

φ = phase

t = time, $[s]$

$u^{(\varphi)}$ = phase velocity, $\left[{}^{m}/_{s} \right]$

z = axial coordinate, $[m]$

r = radial coordinate, $[m]$

θ = angular coordinate, $[rad]$

$s^{(\varphi)}$ = internal coordinate, $[m]$ or $[kg]$

$r_s^{(\varphi)}$ = the rate of growth/melting along the internal coordinate $s^{(\varphi)}$, $\left[{}^{m}/_{s} \right]$ or $\left[{}^{kg}/_{s} \right]$

$n_{B,0}^{(\varphi)}$ = initial concentration of ice particles, $\left[{}^{\#}/_{m^3} \right]$

$j_{B,z,0}^{(\varphi)}$ = initial flux of particles in axial direction, $\left[{}^{\#}/_{m^2 \cdot s} \right]$

$j_{B,r,0}^{(\varphi)}$ = initial flux of particles in radial direction, $\left[{}^{\#}/_{m^2 \cdot s} \right]$

$B_B^{(\varphi)}$ = birth rate of particles in the bulk, $\left[{}^{\#}/_{m^3 \cdot s} \right]$

$D_B^{(\varphi)}$ = "death" rate of particles, $\left[{}^{\#}/_{m^3 \cdot s} \right]$

b. The mass conservation equations for the pseudo-continuous phase

The equations written in this form are used for the components of the matrix phase, as well as for the air phase in the bulk domain. They could be used for the ice particles in the bulk if they would be considered as a pseudo-continuous phase. The equations of change for the mass of the *pseudo-continuous phases* in the bulk domain are written in the following form, per specie j in phase φ:

$$\frac{\partial\left(\varepsilon_B^{(\varphi)} \cdot c_{B,j}^{(\varphi)}\right)}{\partial t} + \nabla_z \cdot \left(u_z^{(\varphi)} \cdot \varepsilon_B^{(\varphi)} \cdot c_{B,j}^{(\varphi)}\right) + \nabla_r \cdot \left(u_r^{(\varphi)} \cdot \varepsilon_B^{(\varphi)} \cdot c_{B,j}^{(\varphi)}\right) + \nabla_\theta \cdot \left(u_\theta^{(\varphi)} \cdot \varepsilon_B^{(\varphi)} \cdot c_{B,j}^{(\varphi)}\right) = \varepsilon_B^{(\varphi)} \cdot R_{B,j}^{(\varphi)} \quad (8.15)$$

With the **initial condition**:

An initial concentration of component j in phase φ is considered:

$$\text{At} \quad t = 0 \qquad c_{B,j}^{(\varphi)} = c_{B,j,0}^{(\varphi)}\left(z, r, \theta\right) \tag{8.16}$$

The **boundary conditions**:

a) In axial direction

Continuity of fluxes:

$$\text{At} \quad z = 0 \qquad \left[u_z^{(\varphi)} \cdot \varepsilon_B^{(\varphi)} \cdot c_{B,j}^{(\varphi)}\right]\Big|_{z=0} = j_{m,B,z,j,0}^{(\varphi)}\left(t, r, \theta\right) \tag{8.17}$$

b) In radial direction

Radial inflow is non-zero at $r = R$.

$$\text{At} \quad r = R \qquad \left[u_r^{(\varphi)} \cdot \varepsilon_B^{(\varphi)} \cdot c_{B,j}^{(\varphi)}\right]\Big|_{r=R} = j_{m,B,r,j,0}^{(\varphi)}\left(t, z, \theta\right) \tag{8.18}$$

c) In angular direction

Periodic continuity:

$$\text{At} \quad \theta = 2\pi \qquad u_\theta^{(\varphi)}\Big|_{\theta=2\pi} = u_\theta^{(\varphi)}\Big|_{\theta=0} \tag{8.19}$$

It is assumed that the density of the continuous phase is calculated as:

$$\rho_{B,j}^{(\varphi)} = \varepsilon_B^{(\varphi)} \cdot c_{B,j}^{(\varphi)} \tag{8.20}$$

List of symbols

$c_{B,j}^{(\varphi)}$ = concentration of component j in the bulk, $\left[kg\ phase \,/\, m^3\ phase\right]$

$\varepsilon_B^{(\varphi)}$ = the volume fraction occupied by phase φ in the space between the rotor axis and the freezer wall, $[-]$

$u^{(\varphi)}$ = bulk phase velocity, $\left[m/s\right]$

$R_{B,j}^{(\varphi)}$ = rate of change of component j in the bulk, $\left[kg/m^3 \cdot s\right]$

$c_{B,j,0}^{(\varphi)}$ = initial concentration of component j in the bulk, $\left[kg/m^3\right]$

$j_{m,B,z,j,0}^{(\varphi)}$ = initial mass flux of component j in axial direction, $\left[kg/m^2 \cdot s\right]$

$j_{m,B,r,j,0}^{(\varphi)}$ = initial mass flux of component in radial direction, $\left[kg/m^2 \cdot s\right]$

j = component of the phase

c. The mass conservation equations for the frozen layer domain

The conservation equation for the frozen layer is written in the following way:

$$\frac{\partial\left(c_{FL}^{(i)}\right)}{\partial t}+\nabla_z\cdot\left(u_z^{(i)}\cdot c_{FL}^{(i)}\right)+\nabla_r\cdot\left(u_r^{(i)}\cdot c_{FL}^{(i)}\right)+\nabla_\theta\cdot\left(u_\theta^{(i)}\cdot c_{FL}^{(i)}\right)=R_{FL}^{(i)} \tag{8.21}$$

With the **initial condition**:

An initial concentration of ice is considered inside the frozen layer:

At $t=0$ $\quad c_{FL}^{(i)}=c_{FL,0}^{(i)}\left(z,r,\theta\right)$ (8.22)

The **boundary conditions**:

a) In axial direction

Continuity of fluxes

At $z=0$ $\quad \left[u_z^{(i)}\cdot c_{FL}^{(i)}\right]\Big|_{z=0}=j_{m,FL,z,0}^{(i)}\left(t,r,\theta\right)$ (8.23)

b) In radial direction

The radial inflow is non-zero at $r=R-\delta_{FL}$.

At $r=R-\delta_{FL}$ $\quad \left[u_r^{(i)}\cdot c_{FL}^{(i)}\right]\Big|_{r=R+\delta_{FL}}=j_{FL,r,0}^{(i)}\left(t,z,\theta\right)$ (8.24)

c) In angular direction

Periodic continuity:

At $\theta=2\pi$ $\quad u_\theta^{(i)}\Big|_{\theta=2\pi}=u_\theta^{(i)}\Big|_{\theta=0}$ (8.25)

List of symbols

$c_{FL}^{(i)}$ = concentration of ice in the frozen layer, $\left[kg/m^3\right]$

$R_{FL}^{(i)}$ = rate of change of the ice in the frozen layer, $\left[kg/m^3\cdot s\right]$

$c_{FL,0}^{(i)}$ = initial concentration of ice in the frozen layer, $\left[kg/m^3\right]$

$j_{m,FL,z,0}^{(i)}$ = initial mass flux of ice in axial direction, $\left[kg/m^2\cdot s\right]$

$j_{m,FL,r,0}^{(i)}$ = initial mass flux of ice in radial direction, $\left[kg/m^2\cdot s\right]$

3. Momentum conservation equations

In a similar way with the mass conservation equations, the momentum conservation is written on the rigorous coordinate set. It is assumed that all the phases inside the bulk domain are lumped into a single phase, the "ice cream".

From (Bird, Stewart & Lightfoot, 2002), the equations of motion in terms of τ, applied to the bulk domain have the following form:

$$\frac{D\left(\rho_B^{(i+l+a)} \cdot u\right)}{Dt} = -\nabla P - \left[\nabla \cdot \tau_B\right] + \rho_B^{(i+l+a)} \cdot g \tag{8.26}$$

The equations are written without assuming that τ_B is symmetric.

With the **initial condition**:

An initial velocity profile is assumed inside the bulk:

At $t = 0$ $u\big|_{t=0} = u_0$ (8.27)

The **boundary conditions**:

a) In axial direction

The outlet pressure of the product is known:

At $z = L$ $P = P_L$ (8.28)

b) In radial direction

At $r = R - \delta_{FL}$ $u_r = 0$ (8.29)

At $r = 0$ $u_r = 0$ (8.30)

c) In angular direction

Periodic continuity:

At $\theta = 2\pi$ $u_\theta\big|_{\theta=2\pi} = u_\theta\big|_{\theta=0}$ (8.31)

List of symbols

P = pressure, $[Pa]$

P_L = the pressure at freezer's outlet, $[Pa]$

$\rho_B^{(i+l+a)}$ = the density of the bulk phase, $\left[kg/m^3\right]$

u = velocity, $\left[m/s\right]$

τ_B = the shear stress, $[Pa]$

g = gravitational acceleration, $\left[m/s^2\right]$

4. Energy conservation equations

The energy conservation equation has the general form:

$$\frac{D(\rho \cdot h)}{Dt} = -(\nabla \cdot q) - \left(\frac{\partial \ln \rho}{\partial \ln T}\right)_P \cdot \frac{Dp}{Dt} - [\tau : \nabla u] \tag{8.32}$$

Equation (8.32) represents the equation of energy written in terms of flux, q (Bird, Stewart & Lightfoot, 2002). This equation will be detailed for each of the phases considered in the following sections, for cylindrical coordinates.

a. The energy conservation equations for the fluid bulk

The liquid phase and the air phase are assumed to be a pseudo-continuous phase, the 'aerated fluid bulk' phase. It is assumed that the density of the 'aerated fluid" is calculated in the following form:

$$\rho_B^{(l+a)} = \varepsilon_B^{(l+a)} \cdot c_B^{(l+a)} \tag{8.33}$$

The equation of change for the energy of the 'aerated fluid bulk' phase becomes:

$$\frac{D\left(\varepsilon_B^{(l+a)} \cdot c_B^{(l+a)} \cdot h_B^{(l+a)}\right)}{Dt} = -(\nabla \cdot q_B) - \left(\frac{\partial \ln \varepsilon_B^{(l+a)} \cdot c_B^{(l+a)}}{\partial \ln T_B}\right)_P \cdot \frac{DP}{Dt} - [\tau : \nabla u] + \sum Q_{\Delta T,B} + W_B \tag{8.34}$$

With the **initial condition**:

An initial enthalpy profile is assumed inside the bulk:

At $t = 0$ $\qquad h_B^{(l+a)}\Big|_{t=0} = h_{B,0}^{(l+a)}(z, r, \theta)$ (8.35)

The **boundary conditions**:

a) In axial direction

At $z = 0$ $\qquad \left[u_z \cdot h_B^{(l+a)}\right]_{z=0-} = \left[u_z \cdot h_B^{(l+a)}\right]_{z=0+}$ (8.36)

At $z = L$ $\qquad \left[\frac{\partial T_B}{\partial z}\right]_{z=L} = 0$ (8.37)

b) In radial direction

The energy at the interface goes entirely to the frozen layer:

At $r = R - \delta_{FL}$ $\qquad \left[-\lambda_B^{(l+a)} \cdot \frac{\partial T_B}{\partial r}\right]_{r=R-\delta_{FL}} = Q_{\Delta T,B}$ (8.38)

At $r = 0$ $\qquad \left.\frac{\partial h_B^{(l+a)}}{\partial r}\right|_{r=0} = 0$ (8.39)

c) In angular direction

Periodic continuity:

$$\text{At} \quad \theta = 2\pi \qquad \left.\frac{\partial h_B^{(l+a)}}{\partial \theta}\right|_\theta = 0 \qquad \left.\frac{\partial q_{\theta,B}}{\partial \theta}\right|_\theta = 0 \tag{8.40}$$

List of symbols

$\varepsilon_B^{(l+a)}$ = the volume fraction occupied by the aerated fluid phase in the space between the rotor axis and the freezer wall, $[-]$

$c_B^{(l+a)}$ = concentration of the aerated fluid phase in the bulk, $\left[kg\ phase \middle/ m^3\ phase\right]$

$\rho_B^{(l+a)}$ = the density of the aerated fluid phase in the bulk, $\left[kg \middle/ m^3\right]$

$h_B^{(l+a)}$ = the specific enthalpy of the aerated fluid phase, $\left[J \middle/ kg\right]$

q_B = the conductive heat flux vector, $\left[W \middle/ m^2\right]$

T_B = the temperature inside the bulk, $[K]$

$[\tau : \nabla u]$ = the viscous dissipation term, $\left[W \middle/ m^3\right]$

u = the velocity, $\left[m \middle/ s\right]$

$Q_{\Delta T,B}$ = energy flow due to a difference in temperature between the bulk and the other phases, $\left[W \middle/ m^3\right]$

$W_B(t,z)$ = work done in the bulk layer, $\left[W \middle/ m^3\right]$

$\frac{DP}{Dt}$ = the substantial time derivative of the pressure

$\lambda_B^{(l+a)}$ = the thermal conductivity, $\left[W \middle/ m \cdot K\right]$

b. The energy conservation equations for the ice particles in the bulk domain

It is assumed that the heating of the ice particles coming from the frozen layer inside the bulk domain is very rapid. The temperature changes in axial direction and in time. Once in bulk, the ice particles temperature starts to change due to the difference in temperature between the particles and

the liquid bulk, and eventually melt. Since the ice particles have different sizes, the heating and the melting will take place with different velocities for each type of particles. This means that a new internal coordinate should be considered while writing the population balance equations for the ice particles: the thermal coordinate, $\Theta^{(i)}$.

The population balance for the ice particles in the bulk will be rewritten in such way that the concentration of the particles is a function of two internal variables: the internal coordinate, $s^{(i)}$ and a thermal coordinate, $\Theta^{(i)}$:

$$\frac{\partial}{\partial t} n_B^{(i)} + \nabla_z \cdot \left(u_z^{(i)} \cdot n_B^{(i)} \right) + \nabla_r \cdot \left(u_r^{(i)} \cdot n_B^{(i)} \right) + \nabla_\theta \cdot \left(u_\theta^{(i)} \cdot n_B^{(i)} \right) + \nabla_{s^{(i)}} \cdot \left(r_s^{(i)} \cdot n_B^{(i)} \right) + \nabla_{\Theta^{(i)}} \cdot \left(r_\Theta^{(i)} \cdot n_B^{(i)} \right) = B_B^{(i)} - D_B^{(i)} \tag{8.41}$$

When the particle diameter is assumed as internal coordinate, the thermal coordinate is the particle's temperature. For the case of the particle's mass considered as internal coordinate, the particle's specific enthalpy is taken as thermal coordinate. The introduction of one extra variable $\Theta^{(i)}$ will increase the model's complexity. For this reason, the inner temperature of a particle will not be considered as an additional inner state variable.

It is assumed that all the ice particles have the same temperature until they completely melt. This temperature is the equilibrium temperature. The energy coming from the bulk is used only for the warming of the surface and the melting. The ice particles do not warm up inside. Moreover, the ice particles in the bulk are assumed as one pseudo-continuous phase. The mass conservation equation is derived in this case from the population balance for the ice particles, by integrating over all the particle sizes. The energy conservation equation can be written in a similar way with equation (8.34):

$$\frac{D\left(\varepsilon_B^{(i)} \cdot c_B^{(i)} \cdot h_B^{(i)} \right)}{Dt} = -Q_{\Delta T, B}^{(i)} \tag{8.42}$$

With the **initial condition**:

An initial enthalpy profile is assumed inside the bulk:

At $t = 0$ $$h_B^{(i)}\Big|_{t=0} = h_{B,0}^{(i)}(z, r, \theta) \tag{8.43}$$

The **boundary conditions**:

a) In axial direction

At $z = 0$ $$\left[u_z \cdot h_B^{(i)} \right]_{z=0-} = \left[u_z \cdot h_B^{(i)} \right]_{z=0+} \tag{8.44}$$

b) In angular direction

Periodic continuity:

$$\text{At} \quad \theta = 2\pi \qquad \left.\frac{\partial h_B^{(i)}}{\partial \theta}\right|_{\theta} = 0 \qquad \left.\frac{\partial q_{\theta,B}}{\partial \theta}\right|_{\theta} = 0 \tag{8.45}$$

List of symbols

$Q_{\Delta T,B}^{(i)}$ = heat term due to difference in temperature between the ice particles and the bulk, $\left[W/m^3\right]$

$h_B^{(i)}$ = the specific enthalpy of the ice particles in the bulk, $\left[J/kg\right]$

c. The energy conservation equations for the frozen layer domain

The energy conservation equation in terms of q (8.32) written for the frozen layer:

$$\frac{D\left(\rho_{FL}^{(i)} \cdot h_{FL}^{(i)}\right)}{Dt} = -\left(\nabla \cdot q_{FL}\right) \tag{8.46}$$

With the **initial condition**:

An initial enthalpy profile is assumed inside the bulk:

$$\text{At} \quad t = 0 \qquad h_{FL}^{(i)}\Big|_{t=0} = h_{FL,0}^{(i)}(z,r,\theta) \tag{8.47}$$

The **boundary conditions**:

a) In axial direction

$$\text{At} \quad z = 0 \qquad \left[-\lambda_{FL}^{(i)} \cdot \frac{\partial T_{FL}^{(i)}}{\partial z}\right]_{z=0} = Q_{in} \tag{8.48}$$

b) In radial direction

The energy at the interface goes entirely to the frozen layer:

$$\text{At} \quad r = R - \delta_{FL} \qquad \left[-\lambda_{FL}^{(i)} \cdot \frac{\partial T_{FL}^{(i)}}{\partial r}\right]_{r=R-\delta_{FL}} = Q_{\Delta T,B} \tag{8.49}$$

$$\text{At} \quad r = R \qquad \left[-\lambda_{FL}^{(i)} \cdot \frac{\partial T_{FL}^{(i)}}{\partial r}\right]_{r=R} = Q_{\Delta T,wall} \tag{8.50}$$

List of symbols

$\varepsilon_{FL}^{(i)}$ = the volume fraction occupied by the ice phase, $[-]$

$c_{FL}^{(i)}$ = concentration of the ice phase in the frozen layer, $\left[kg\ phase/m^3\ phase\right]$

$h_{FL}^{(i)}$ = the specific enthalpy of the ice phase in the frozen layer, $\left[J/kg \right]$

$Q_{\Delta T,B}$ = energy due to a difference in temperature between the bulk and the other phases, $\left[W/m^3 \right]$

$Q_{\Delta T,FL}^{(i)}$ = heat term due to difference in temperature between the frozen layer and the wall, $\left[W/m^3 \right]$

$\lambda_{FL}^{(i)}$ = the thermal conductivity of the ice phase inside the frozen layer, $\left[W/m \cdot K \right]$

d. The energy conservation equations for the freezer wall

The energy conservation for the freezer's wall is written under pseudo steady state assumption, leading to a flux expression.

$$\frac{\partial\left(r \cdot q_{r,wall}\right)}{\partial r} = 0 \tag{8.51}$$

With the **initial condition**:

An initial enthalpy profile is assumed inside the bulk:

At $r = R$ $\qquad q_{r,wall}\Big|_{r=R} = Q_{\Delta T,wall}$ (8.52)

The **boundary conditions**:

At $r = R + \delta_{wall}$ $\qquad q_{r,wall}\Big|_{r=R+\delta_{wall}} = Q_{\Delta T,c}$ (8.53)

The heat flux is evaluated using Fourier's law of heat conduction:

$$q_{r,wall} = -\lambda_{wall} \cdot r \cdot \frac{dT_{wall}}{dr} \tag{8.54}$$

List of symbols

$q_{r,wall}$ = heat flux through the freezer wall, $\left[W/m^2 \right]$

λ_{wall} = the heat conductivity of the wall, $\left[W/m \cdot K \right]$

e. The energy conservation equations for the coolant

The coolant is assumed to have a high heat transfer coefficient. Newton's law of cooling is used to relate the normal heat flux component to the temperature difference between the freezer wall and the coolant:

$$q_{coolant} = U_{wall,coolant} \cdot \left(T_{wall,coolant} - T_{coolant}\right) \tag{8.55}$$

List of symbols

$U_{wall,coolant}$ = heat transfer coefficient at the coolant side, $\left[W/m^2 \cdot K \right]$

$T_{wall,coolant}$ = temperature of the freezer wall at the coolant side, $\left[K \right]$

$T_{coolant}$ = temperature of the coolant, $\left[K \right]$

5. Averaging procedure along the radial and angular coordinates

The following lemmas are introduced for performing the averaging along the radial and angular coordinates:

a) Averaging with respect to θ

For a function $f(r,\theta)$, the averaging over the angular coordinate is performed in the following way:

$$\frac{1}{2\pi} \cdot \int_0^{2\pi} f(r,\theta) d\theta = \bar{f}_\theta(r) \tag{8.56}$$

List of symbols

$f(r,\theta)$ =function

$\bar{f}_\theta$ = angularly averaged function

b) Averaging with respect to r

For a function $f(r,\theta)$, the averaging over the radial coordinate is performed in the following way:

$$\frac{2}{R_1^2 - R_0^2} \cdot \int_{R_0}^{R_1} r \cdot f(r,\theta) dr = \bar{f}_r(\theta) \tag{8.57}$$

List of symbols

$\bar{f}_r$ = radially averaged function

R_0 = lower bound of the radius, $\left[m \right]$

R_1 = upper bound of the radius, $\left[m \right]$

c) Averaging with respect to r and θ

For a function $f(r,\theta)$, the averaging over the radial and angular coordinate is performed in the following way:

$$\pi \cdot \left(R_1^2 - R_0^2\right) \cdot \bar{f}_{\theta r} = \int_{R_0}^{R_1} \int_{0}^{2\pi} \left[r \cdot f(r,\theta)\right] d\theta dr \tag{8.58}$$

When looking at the PBE-ice in equation (8.9) one can see:

(a) Terms in which there is no derivative operation with respect to the radial and angular coordinates (e.g., in the derivative terms with respect to time, axial position and size and the algebraic source and sink expressions). The averaging procedure over radial and angular coordinates is essentially identical for all cases.
(b) Terms in which there is a derivative operation with respect to the radial coordinate.
(c) Terms in which there is a derivative operation with respect to the angular coordinate.

For each of the cases above, the averaging will be performed as follows:

(a) No derivative operation with respect to the radial and angular coordinates

In this case, equation (8.57) is applied.

$$\pi \cdot \left(R_1^2 - R_0^2\right) \cdot \bar{T}_{\theta r} = \int_{R_0}^{R_1} \int_{0}^{2\pi} \left[r \cdot T(r,\theta)\right] d\theta dr \tag{8.59}$$

(b) Derivative operation with respect to the radial coordinate

In this case, the integration with respect to the radial coordinate is performed first, followed by the averaging with respect to the angular coordinate. The resulting averaged term is:

$$2\pi \cdot \left(R_1 \cdot \bar{j}_{R_1,\theta} - R_0 \cdot \bar{j}_{R_0,\theta} \right) = \int_{0}^{2\pi} \left(\int_{R_0}^{R_1} r \cdot \left[\frac{1}{r} \cdot \frac{\partial (r \cdot j)}{\partial r} \right] dr \right) d\theta \tag{8.60}$$

Often, there is no transport at the boundary with the rotor ($r = R_0$):

$$\bar{j}_{R_0,\theta} = 0 \tag{8.61}$$

Hence, the averaged term:

$$2\pi \cdot R_1 \cdot \bar{j}_{R_1,\theta} = \int_{0}^{2\pi} \left(\int_{R_0}^{R_1} r \cdot \left[\frac{1}{r} \cdot \frac{\partial (r \cdot j)}{\partial r} \right] dr \right) d\theta \tag{8.62}$$

List of symbols

T = transfer term, $\left[unit/m^3 \cdot s \right]$

j = flux of component, $\left[unit/m^2 \cdot s \right]$

(c) Derivative operation with respect to the angular coordinate

In this case, the integration with respect to the angular coordinate is performed first:

$$\int_0^{2\pi} \left[\frac{\partial (j)}{\partial \theta} \right] d\theta = j(r,\theta)\Big|_0^{2\pi} = j(r,2\pi) - j(r,0) \tag{8.63}$$

If periodic continuity is assumed, the two terms in equation (8.63) cancel each other:

$$\int_0^{2\pi} \left[\frac{\partial (j)}{\partial \theta} \right] d\theta = 0 \tag{8.64}$$

6. Overview of coordinate-averaged mass conservation equations

a. The averaged conservation equations for the bulk domain

The averaging reduced the number of coordinates for the bulk domain to the following:

(1) Time: $0 < t$

(2) Axial coordinate: $0 < z < L$

(3) Crystal size coordinate: $0 < s^{(i)} < s_{\max}^{(i)} < \min\left\{ L, (R - R_0) \right\}$

The resulting conservation equations inside the bulk become, written considering the average terms:

$$\frac{\partial \left(\bar{n}_B^{(i)} \cdot A_B \right)}{\partial t} + \nabla_z \left(\bar{j}_{B,z}^{(i)} \cdot A_B \right) + \nabla_{s^{(i)}} \left(\bar{j}_{B,s}^{(i)} \cdot A_B \right) = \tag{8.65}$$

$$\bar{B}_B^{(i)} \cdot A_B + \bar{R}_{t,FL \to B}^{(i)} \cdot S_B - \bar{D}_B^{(i)} \cdot A_B - \bar{R}_{t,B \to FL}^{(i)} \cdot S_B$$

$$\frac{\partial \left(\bar{\varepsilon}_B^{(l)} \cdot \bar{c}_{B,j}^{(l)} \cdot A_B \right)}{\partial t} + \nabla_z \left(\bar{j}_{m,B,j,z}^{(l)} \cdot A_B \right) = -\bar{R}_{t,B \to FL,j}^{(l)} \cdot S_B + \bar{R}_{B,j}^{(l)} \cdot A_B \tag{8.66}$$

$$\frac{\partial \left(\bar{\varepsilon}_B^{(a)} \cdot \bar{c}_B^{(a)} \cdot A_B \right)}{\partial t} + \nabla_z \left(\bar{j}_{m,B,z}^{(a)} \cdot A_B \right) = 0 \tag{8.67}$$

With the **initial conditions**:

At $t = 0$, $$\bar{n}_B^{(i)}(0, z, s^{(i)}) = \bar{n}_{B,0}^{(i)}\left(z, s^{(i)}\right) \tag{8.68}$$

$$\bar{c}_{B,j}^{(l)}(0, z) = \bar{c}_{B,j}^{(l)}(z) \tag{8.69}$$

$$\bar{c}_B^{(a)}(0, z) = \bar{c}_{B,0}^{(a)}(z) \tag{8.70}$$

The **boundary conditions**:

a) In axial direction

Continuity of flows:

At $z = 0$ $$\left(\bar{j}_{B,z}^{(i)} \cdot A_B\right)\Big|_r\Big|_{z=0} = \tilde{F}_B^{(i)}\left(t, s^{(i)}\right) \tag{8.71}$$

$$\left(\bar{j}_{m,B,j,z}^{(l)} \cdot A_B\right)\Big|_r\Big|_{z=0} = \tilde{F}_B^{(i)}\left(t, s^{(i)}\right) \tag{8.72}$$

$$\left(\bar{j}_{m,B,z}^{(a)} \cdot A_B\right)\Big|_{z=0} = F_{B,0}^{(a)}(t) \tag{8.73}$$

b) Along the internal coordinate

The boundary condition for the crystal size is put at the upper range of ice crystal size due to the size reduction by the melting of the particles

At $s^{(i)} = s_{max}^{(i)}$ $$\bar{n}_B^{(i)}\left(t, z, s_{max}^{(i)}\right) = n_{B,s_{max}^{(i)}}^{(i)}(t, z) \tag{8.74}$$

For the following sections, the averaged terms will be denoted without the dash.

b. The averaged conservation equation for the frozen layer

The averaging reduced the number of coordinates for the frozen layer domain to the following:

(1) Time: $0 < t$

The resulting conservation equations inside the frozen layer become, written considering the average terms is a differential equation showing the variation of the thickness of the frozen layer:

$$\frac{\partial \delta_{FL}(t, z)}{\partial t} = \frac{\bar{R}_{t,m,B\to FL}^{(i)}(t, z, s) + \bar{R}_{t,B\to FL,w}^{(l)}(t, z)}{c_{FL}^{(i)}(t, z)} \tag{8.75}$$

With the **initial condition**:

An initial concentration of ice is considered inside the frozen layer:

At $t = 0$ $\delta_{FL} = \delta_{FL,0}(z)$ (8.76)

At $t = t_{s+}$ $\delta_{FL} = \delta_{FL,0}(z)$ (8.77)

7. Coordinate-averaged conservation equation for dispersed phases

The starting point is the equation of change for *dispersed phases* in equation (8.9). This equation is multiplied with r and integrated from $r = R_0$ to $r = R - \delta_{FL}$ and $\theta = 0$ to $\theta = 2\pi$. For each term of equation (8.9), the averaging procedures presented in Appendix 5 are then applied.

a) The accumulation term $\dfrac{\partial\left(n_B^{(\varphi)}\right)}{\partial t}$

$$\int_0^{2\pi}\int_{R_0}^{R_1} \frac{\partial\left(n_B^{(\varphi)}\right)}{\partial t}\cdot r\cdot dr\cdot d\theta = \frac{\partial}{\partial t}\left[\int_0^{2\pi}\int_{R_0}^{R_1}\left(n_B^{(\varphi)}\cdot r\cdot dr\cdot d\theta\right)\right] \tag{8.78}$$

The upper bound is defined as:

$$R_1 = R - \delta_{FL} \tag{8.79}$$

Applying the lemma (8.57):

$$\frac{\partial}{\partial t}\left[\int_0^{2\pi}\int_{R_0}^{R_1}\left(n_B^{(\varphi)}\cdot r\cdot dr\cdot d\theta\right)\right] = \frac{\partial}{\partial t}\left[\bar{n}_B^{(\varphi)}\cdot\pi\left(\left(R-\delta_{FL}\right)^2 - R_0^2\right)\right] \tag{8.80}$$

It is defined that:

$$N_B^{(\varphi)}(z,s) = \bar{n}_B^{(\varphi)}(z,s)\cdot\pi\cdot\left(\left(R-\delta_{FL}\right)^2 - R_0^2\right) = A_B\cdot\bar{n}_B^{(\varphi)} \tag{8.81}$$

The cross-sectional area of the bulk domain is calculated using:

$$A_B = \pi\cdot\left(\left(R-\delta_{FL}\right)^2 - R_0^2\right) \tag{8.82}$$

Taking into account the definitions above, equation (8.78) is rewritten in the following way:

$$\int_0^{2\pi}\int_{R_0}^{R_1} \frac{\partial\left(n_B^{(\varphi)}\right)}{\partial t}\cdot r\cdot dr\cdot d\theta = \frac{\partial\left(\bar{n}_B^{(\varphi)}\cdot A_B\right)}{\partial t} = \frac{\partial\left(N_B^{(\varphi)}\right)}{\partial t} \tag{8.83}$$

b) The convective term in axial direction $\nabla_z\left(u_z^{(\varphi)}\cdot n_B^{(\varphi)}\right)$

$$\int_0^{2\pi}\int_{R_0}^{R_1}\frac{\partial\left(u_z^{(\varphi)}\cdot n_B^{(\varphi)}\right)}{\partial z}\cdot r\cdot dr\cdot d\theta=\int_0^{2\pi}\int_{R_0}^{R_1}\frac{\partial\left(j_{B,z}^{(\varphi)}\right)}{\partial z}\cdot r\cdot dr\cdot d\theta=$$
$$=\frac{\partial}{\partial z}\int_0^{2\pi}\int_{R_0}^{R_1}j_{B,z}^{(\varphi)}\cdot r\cdot dr\cdot d\theta \tag{8.84}$$

When applying the lemma (8.57):

$$\frac{\partial}{\partial z}\left[\int_0^{2\pi}\int_{R_0}^{R_1}\left(j_{B,z}^{(\varphi)}\cdot r\cdot dr\cdot d\theta\right)\right]=\frac{\partial}{\partial z}\left[\bar{j}_{B,z}^{(\varphi)}\cdot\pi\left(\left(R-\delta_{FL}\right)^2-R_0^2\right)\right] \tag{8.85}$$

The radially and angularly averaged flux of particles should be written in the following form:

$$\bar{j}_{B,z}^{(\varphi)}=\bar{u}_z^{(\varphi)}\cdot\bar{n}_B^{(\varphi)} \tag{8.86}$$

In this case, two possibilities are considered:

i) The radially averaged number of particles, $\bar{n}_{B,1}^{(\varphi)}$, is defined in the following way:

$$\bar{n}_{B,1}^{(\varphi)}=\frac{1}{A_B}\cdot\int_{R_0}^{R_1}n_B^{(\varphi)}(r)\cdot r\cdot dr \tag{8.87}$$

An averaged velocity is defined as:

$$\bar{u}_{z,1}^{(\varphi)}=\frac{\bar{j}_{B,z}^{(\varphi)}}{\bar{n}_{B,1}^{(\varphi)}} \tag{8.88}$$

List of symbols

$N_B^{(\varphi)}$ = number of dispersed particles, $\left[\#/m\right]$

$\bar{j}_{B,z}^{(\varphi)}$ = radially and angularly averaged flux of particles, $\left[\#/m^2\cdot s\right]$

$\bar{n}_{B,1}^{(\varphi)}$ = radially averaged number of particles, $\left[\#/m^3\right]$

$\bar{u}_{z,1}^{(\varphi)}$ = radially averaged velocity, $\left[m/s\right]$

ii) The radially averaged velocity, $\bar{u}_{z,2}^{(\varphi)}$, is defined in the following way:

$$\bar{u}_{z,2}^{(\varphi)} = \frac{1}{A_B} \cdot \int_{R_0}^{R_1} u_z^{(\varphi)}(r) \cdot r \cdot dr \tag{8.89}$$

It is defined that:

$$\bar{n}_{B,2}^{(\varphi)} = \frac{\bar{j}_{B,z}^{(\varphi)}}{\bar{u}_{z,2}^{(\varphi)}} \tag{8.90}$$

List of symbols

$\bar{n}_{B,2}^{(\varphi)}$ = radially averaged number of particles, $\left[\#/m^3 \right]$

$\bar{u}_{z,2}^{(\varphi)}$ = radially averaged velocity, $\left[m/s \right]$

Note: The radially averaged flux of particles in axial direction, $\bar{j}_{B,z}^{(\varphi)}$, cannot be calculated using :

$$\bar{j}_{B,z}^{(i)} \neq \bar{n}_{B,1}^{(i)} \cdot \bar{u}_{z,2}^{(i)} \neq \bar{n}_{B,2}^{(i)} \cdot \bar{u}_{z,1}^{(i)} \tag{8.91}$$

c) The convective term in radial direction $\nabla_r \left(u_r^{(\varphi)} \cdot n_B^{(\varphi)} \right)$

$$\int_0^{2\pi} \int_{R_0}^{R_1} \frac{1}{r} \cdot \frac{\partial \left(r \cdot u_r^{(\varphi)} \cdot n_B^{(\varphi)} \right)}{\partial r} \cdot r \cdot dr \cdot d\theta = \int_0^{2\pi} \int_{R_0}^{R_1} \frac{1}{r} \cdot \frac{\partial \left(r \cdot j_{B,r}^{(\varphi)} \right)}{\partial r} \cdot r \cdot dr \cdot d\theta \tag{8.92}$$

When applying equation ((8.60):

$$\int_0^{2\pi} \int_{R_0}^{R_1} \frac{1}{r} \cdot \frac{\partial \left(r \cdot j_{B,r}^{(\varphi)} \right)}{\partial r} \cdot r \cdot dr \cdot d\theta = 2\pi \cdot \left[\left(R - \delta_{FL} \right) \cdot \bar{j}_{B,R-\delta_{FL},\theta}^{(\varphi)} - R_0 \cdot \bar{j}_{B,R_0,\theta}^{(\varphi)} \right] \tag{8.93}$$

$$\int_0^{2\pi} \int_{R_0}^{R_1} \frac{1}{r} \cdot \frac{\partial \left(r \cdot j_{B,r}^{(R_0,\theta)} \right)}{\partial r} \cdot r \cdot dr \cdot d\theta = \left[S_B \cdot \bar{j}_{B,R-\delta_{FL},\theta}^{(\varphi)} - S_0 \cdot \bar{j}_{B,R_0,\theta}^{(\varphi)} \right] \tag{8.94}$$

The circumference of the freezer is determined in the following way:

$$S_B = 2\pi \cdot \left(R - \delta_{FL} \right) \tag{8.95}$$

$$S_0 = 2\pi \cdot R_0 \tag{8.96}$$

d) The convective term in angular direction $\nabla_{\theta}\left(u_{\theta}^{(\varphi)} \cdot n_B^{(\varphi)}\right)$

$$\int_0^{2\pi}\int_{R_0}^{R} \frac{1}{r} \cdot \frac{\partial\left(u_{\theta}^{(\varphi)} \cdot n_B^{(\varphi)}\right)}{\partial\theta} \cdot r \cdot dr \cdot d\theta = \int_0^{2\pi}\int_{R_0}^{R} \frac{1}{r} \cdot \frac{\partial\left(j_{B,\theta}^{(\varphi)}\right)}{\partial\theta} \cdot r \cdot dr \cdot d\theta \tag{8.97}$$

There are complex and fast exchanges between flows in the ice cream in radial and angular directions. This happens due to the rapid rotations of the scraper. These exchanges are assumed to lead to strong mixing in a cross-sectional plane, perpendicular to the axial transport direction. This results into a uniform process condition within this plane. Therefore, the averaging is done over both directions simultaneously, while accounting for the exchanges with the frozen layer and the no-flux condition at the inner surface with the rotator.

For the convective term in radial and angular direction, the following simplification will be used:

$$\int_0^{2\pi}\int_{R_0}^{R} \frac{1}{r} \cdot \frac{\partial\left(r \cdot u_r^{(\varphi)} \cdot n_B^{(\varphi)}\right)}{\partial r} \cdot r \cdot dr \cdot d\theta + \int_0^{2\pi}\int_{R_0}^{R} \frac{1}{r} \cdot \frac{\partial\left(u_{\theta}^{(\varphi)} \cdot n_B^{(\varphi)}\right)}{\partial\theta} \cdot r \cdot dr \cdot d\theta = \tag{8.98}$$
$$= R_{t,FL\to B}^{(\varphi)} \cdot S_B - R_{t,B\to FL}^{(\varphi)} \cdot S_B$$

e) The generation term $\nabla_{s^{(i)}}\left(r_s^{(\varphi)} \cdot n_B^{(\varphi)}\right)$

$$\int_0^{2\pi}\int_{R_0}^{R} \frac{\partial\left(r_s^{(\varphi)} \cdot n_B^{(\varphi)}\right)}{\partial s^{(\varphi)}} \cdot r \cdot dr \cdot d\theta = \frac{\partial}{\partial s^{(\varphi)}} \int_0^{2\pi}\int_{R_0}^{R} r_s^{(\varphi)} \cdot n_B^{(\varphi)} \cdot r \cdot dr \cdot d\theta = \tag{8.99}$$
$$= \frac{\partial}{\partial s^{(\varphi)}} \int_0^{2\pi}\int_{R_0}^{R} j_{B,s}^{(\varphi)} \cdot r \cdot dr \cdot d\theta$$

When applying the lemma (8.57):

$$\frac{\partial}{\partial s^{(i)}} \int_0^{2\pi}\int_{R_0}^{R_1} j_{B,s}^{(\varphi)} \cdot r \cdot dr \cdot d\theta = \frac{\partial}{\partial s^{(\varphi)}}\left[\bar{j}_{B,s}^{(\varphi)} \cdot \pi\left(\left(R - \delta_{FL}\right)^2 - R_0^2\right)\right] \tag{8.100}$$

The radially and angularly averaged flux of particles along the internal coordinate should be written in the following form:

$$\bar{j}_{B,s}^{(\varphi)} = \bar{r}_s^{(\varphi)} \cdot \bar{n}_B^{(\varphi)} \tag{8.101}$$

List of symbols

$\bar{r}_s^{(\varphi)}$ = radially averaged growth rate, $\left[m/s \right]$ or $\left[kg/s \right]$

The radially averaged number of particles $\bar{n}_B^{(\varphi)}$ is defined as:

$$\bar{n}_B^{(\varphi)} = \frac{1}{A_B} \cdot \int_{R_0}^{R_1} n_B^{(\varphi)}(r) \cdot r \cdot dr \tag{8.102}$$

It is defined that:

$$\bar{r}_s^{(\varphi)} = \frac{\bar{j}_{B,s}^{(\varphi)}}{\bar{n}_B^{(\varphi)}} \tag{8.103}$$

Hence, the convective term in the axial direction is calculated as follows:

$$\int_0^{2\pi} \int_{R_0}^{R_1} \frac{\partial\left(r_s^{(\varphi)} \cdot n_B^{(\varphi)} \right)}{\partial z} \cdot r \cdot dr \cdot d\theta = \frac{\partial\left(\bar{j}_{B,s}^{(\varphi)} \cdot A_B \right)}{\partial z} \tag{8.104}$$

f) The transfer terms $B_B^{(\varphi)}$ and $D_B^{(\varphi)}$

Applying the lemma (8.57):

$$\int_0^{2\pi} \int_{R_0}^{R_1} R_B^{(\varphi)} \cdot r \cdot dr \cdot d\theta = \bar{R}_B^{(\varphi)} \cdot A_B \tag{8.105}$$

$$R_B^{(\varphi)} = B_B^{(\varphi)},\ D_B^{(\varphi)} \tag{8.106}$$

Taking into account these changes, the conservation equation for the dispersed phase in the bulk is rewritten using the radially and angularly averaged terms in the following way:

$$\frac{\partial\left(\bar{n}_B^{(\varphi)} \cdot A_B \right)}{\partial t} + \nabla_z \left(\bar{j}_{B,z}^{(\varphi)} \cdot A_B \right) + \nabla_{s^{(i)}} \left(\bar{j}_{B,s}^{(\varphi)} \cdot A_B \right) = \tag{8.107}$$

$$\bar{B}_B^{(\varphi)} \cdot A_B + \bar{R}_{t,FL\to B}^{(\varphi)} \cdot S_B - \bar{D}_B^{(\varphi)} \cdot A_B - \bar{R}_{t,B\to FL}^{(\varphi)} \cdot S_B$$

Where the fluxes are calculated using:

$$\bar{j}_{B,z}^{(\varphi)} = \bar{u}_z^{(\varphi)} \cdot \bar{n}_B^{(\varphi)} \tag{8.108}$$

$$\bar{j}_{B,s}^{(\varphi)} = \bar{r}_s^{(\varphi)} \cdot \bar{n}_B^{(\varphi)} \tag{8.109}$$

This is the outcome of the averaging procedure for the **dispersed phase** in the bulk domain.

8. Coordinate-averaged conservation equation for the pseudo-continuous phase

The starting point is the equation of change for mass of the *pseudo-continuous phase* in the bulk domain in equation (8.15). This equation is multiplied with r and integrated from $r = R_0$ to $r = R - \delta_{FL}$ and $\theta = 0$ to $\theta = 2\pi$. For each term of equation (8.15), the averaging procedures presented in Appendix 5 are then applied.

a) The accumulation term $\dfrac{\partial\left(\varepsilon_B^{(\varphi)} \cdot c_{B,j}^{(\varphi)}\right)}{\partial t}$

$$\int_0^{2\pi}\int_{R_0}^{R_1} \frac{\partial\left(\varepsilon_B^{(\varphi)} \cdot c_{B,j}^{(\varphi)}\right)}{\partial t} \cdot r \cdot dr \cdot d\theta = \frac{\partial}{\partial t}\left[\int_0^{2\pi}\int_{R_0}^{R_1}\left(\varepsilon_B^{(\varphi)} \cdot c_{B,j}^{(\varphi)} \cdot r \cdot dr \cdot d\theta\right)\right] \tag{8.110}$$

Applying the lemma (8.57):

$$\frac{\partial}{\partial t}\left[\int_0^{2\pi}\int_{R_0}^{R_1}\left(\varepsilon_B^{(\varphi)} \cdot c_{B,j}^{(\varphi)} \cdot r \cdot dr \cdot d\theta\right)\right] = \frac{\partial}{\partial t}\left[\bar{\varepsilon}_B^{(\varphi)} \cdot \bar{c}_{B,j}^{(\varphi)} \cdot \pi\left(\left(R - \delta_{FL}\right)^2 - R_0^2\right)\right] \tag{8.111}$$

b) The convective term in axial direction $\nabla_z\left(u_z^{(\varphi)} \cdot \varepsilon_B^{(\varphi)} \cdot c_{B,j}^{(\varphi)}\right)$

$$\int_0^{2\pi}\int_{R_0}^{R_1} \frac{\partial\left(u_z^{(\varphi)} \cdot \varepsilon_B^{(\varphi)} \cdot c_{B,j}^{(\varphi)}\right)}{\partial z} \cdot r \cdot dr \cdot d\theta = \int_0^{2\pi}\int_{R_0}^{R_1} \frac{\partial \varepsilon_B^{(\varphi)} \cdot j_{m,B,z,j}^{(\varphi)}}{\partial z} \cdot r \cdot dr \cdot d\theta =$$
$$= \frac{\partial}{\partial z}\int_0^{2\pi}\int_{R_0}^{R_1} \varepsilon_B^{(\varphi)} \cdot j_{m,B,z,j}^{(\varphi)} \cdot r \cdot dr \cdot d\theta \tag{8.112}$$

$$j_{m,B,z,j}^{(\varphi)} = u_z^{(\varphi)} \cdot c_{B,j}^{(\varphi)} \tag{8.113}$$

When applying the lemma (8.57):

$$\frac{\partial}{\partial z}\left[\int_0^{2\pi}\int_{R_0}^{R_1}\left(\varepsilon_B^{(\varphi)} \cdot j_{m,B,z,j}^{(\varphi)} \cdot r \cdot dr \cdot d\theta\right)\right] = \frac{\partial}{\partial z}\left[\bar{\varepsilon}_B^{(\varphi)} \cdot \bar{j}_{m,B,z,j}^{(\varphi)} \cdot \pi\left(\left(R - \delta_{FL}\right)^2 - R_0^2\right)\right] \tag{8.114}$$

The radially and angularly averaged flux of component j should be written in the following form:

$$\bar{j}^{(\varphi)}_{m,B,z,j} = \bar{u}^{(\varphi)}_{z} \cdot \bar{c}^{(\varphi)}_{B,j} \tag{8.115}$$

i) The radially averaged concentration for the component j in the bulk, $c^{(\bar{\varphi})}_{B,j}$ is defined as:

$$c^{(\bar{\varphi})}_{B,j,1} = \frac{1}{A_B} \cdot \int_{R_0}^{R_1} c^{(\varphi)}_{B,j}(r) \cdot r \cdot dr \tag{8.116}$$

The velocity is defined as:

$$\bar{u}^{(\varphi)}_{z,1} = \frac{\bar{j}^{(\varphi)}_{m,B,z,j}}{c^{(\bar{\varphi})}_{B,j,1}} \tag{8.117}$$

List of symbols

$\bar{j}^{(\varphi)}_{m,B,z,j}$ = radially and angularly averaged flux of component j, $\left[kg/m^2 \cdot s \right]$

$c^{(\bar{\varphi})}_{B,j,1}$ = radially averaged concentration for component j, $\left[kg/m^3 \right]$

$\bar{u}^{(\varphi)}_{z,1}$ = radially averaged velocity, $\left[m/s \right]$

ii) The radially averaged velocity, $\bar{u}^{(\varphi)}_{z,2}$ is defined in the following way:

$$\bar{u}^{(\varphi)}_{z,2} = \frac{1}{A_B} \cdot \int_{R_0}^{R} u^{(\varphi)}_{z}(r) \cdot r \cdot dr \tag{8.118}$$

The concentration is defined as:

$$c^{(\bar{\varphi})}_{B,j,2} = \frac{\bar{j}^{(\varphi)}_{m,B,z,j}}{\bar{u}^{(\varphi)}_{z,2}} \tag{8.119}$$

List of symbols

$c^{(\bar{\varphi})}_{B,j,2}$ = radially averaged concentration for component j, $\left[kg/m^3 \right]$

$\bar{u}_{z,2}^{(\varphi)}$ = radially averaged velocity, $\left[m/s \right]$

Note: The radially averaged mass flux of component j in axial direction, $\bar{j}_{m,B,z,j}^{(\varphi)}$ cannot be calculated using:

$$\bar{j}_{m,B,z,j}^{(\varphi)} \neq \bar{c}_{B,j,1}^{(\varphi)} \cdot \bar{u}_{z,2}^{(\varphi)} \neq \bar{c}_{B,j,2}^{(\varphi)} \cdot \bar{u}_{z,1}^{(\varphi)} \tag{8.120}$$

c) The convective term in radial direction $\nabla_r \left(u_r^{(\varphi)} \cdot \varepsilon_B^{(\varphi)} \cdot c_{B,j}^{(\varphi)} \right)$

$$\begin{aligned} &\int_0^{2\pi} \int_{R_0}^{R_1} \frac{1}{r} \cdot \frac{\partial \left(r \cdot u_r^{(\varphi)} \cdot \varepsilon_B^{(\varphi)} \cdot c_{B,j}^{(\varphi)} \right)}{\partial r} \cdot r \cdot dr \cdot d\theta = \\ &\int_0^{2\pi} \int_{R_0}^{R_1} \frac{1}{r} \cdot \frac{\partial \left(r \cdot \varepsilon_B^{(\varphi)} \cdot j_{m,B,r,j}^{(\varphi)} \right)}{\partial r} \cdot r \cdot dr \cdot d\theta \end{aligned} \tag{8.121}$$

When applying equation ((8.60):

$$\begin{aligned} &\int_0^{2\pi} \int_{R_0}^{R_1} \frac{1}{r} \cdot \frac{\partial \left(r \cdot \varepsilon_B^{(\varphi)} \cdot j_{m,B,r,j}^{(\varphi)} \right)}{\partial r} \cdot r \cdot dr \cdot d\theta = \\ &2\pi \cdot \left[\left(R - \delta_{FL} \right) \cdot \bar{\varepsilon}_B^{(\varphi)} \cdot \bar{j}_{m,B,R-\delta_{FL},\theta,j}^{(\varphi)} - R_0 \cdot \bar{\varepsilon}_B^{(\varphi)} \cdot \bar{j}_{m,B,R_0,\theta,j}^{(\varphi)} \right] \end{aligned} \tag{8.122}$$

$$\begin{aligned} &\int_0^{2\pi} \int_{R_0}^{R_1} \frac{1}{r} \cdot \frac{\partial \left(r \cdot \varepsilon_B^{(\varphi)} \cdot j_{m,B,r,j}^{(\varphi)} \right)}{\partial r} \cdot r \cdot dr \cdot d\theta = \\ &\left[S_B \cdot \bar{\varepsilon}_B^{(\varphi)} \cdot \bar{j}_{m,B,R-\delta_{FL},\theta,j}^{(\varphi)} - S_0 \cdot \bar{\varepsilon}_B^{(\varphi)} \cdot \bar{j}_{m,B,R_0,\theta,j}^{(\varphi)} \right] \end{aligned} \tag{8.123}$$

d) The convective term in angular direction $\nabla_\theta \left(u_\theta^{(\varphi)} \cdot \varepsilon_B^{(\varphi)} \cdot c_{B,j}^{(\varphi)} \right)$

$$\int_0^{2\pi} \int_{R_0}^{R_1} \frac{1}{r} \cdot \frac{\partial \left(u_\theta^{(\varphi)} \cdot \varepsilon_B^{(\varphi)} \cdot c_{B,j}^{(\varphi)} \right)}{\partial \theta} \cdot r \cdot dr \cdot d\theta = \int_0^{2\pi} \int_{R_0}^{R_1} \frac{1}{r} \cdot \frac{\partial \left(\varepsilon_B^{(\varphi)} \cdot j_{m,B,\theta,j}^{(\varphi)} \right)}{\partial \theta} \cdot r \cdot dr \cdot d\theta \tag{8.124}$$

In a similar way with the “ice” phase, the averaging in both radial and angular direction for the “liquid” phase is done simultaneously. The exchanges with the frozen layer and the no-flux condition at the inner surface with the rotator are taken into account.

For the convective terms in radial and angular direction the following simplification will be used:

$$\int_0^{2\pi}\int_{R_0}^{R_1}\frac{1}{r}\cdot\frac{\partial\left(r\cdot u_r^{(\varphi)}\cdot\varepsilon_B^{(\varphi)}\cdot c_{B,j}^{(\varphi)}\right)}{\partial r}\cdot r\cdot dr\cdot d\theta=-\bar{R}_{t,B\to FL,j}^{(\varphi)}\cdot S_B \tag{8.125}$$

e) The generation term, $R_{B,j}^{(\varphi)}$

Applying the lemma (8.57):

$$\int_0^{2\pi}\int_{R_0}^{R_1}R_{B,j}^{(\varphi)}\cdot r\cdot dr\cdot d\theta=\bar{R}_{B,j}^{(\varphi)}\cdot A_B \tag{8.126}$$

Taking into account the changes, the conservation equation for the pseudo-continuous phase in the bulk will be:

$$\frac{\partial\left(A_B\cdot\bar{\varepsilon}_B^{(l)}\cdot\bar{c}_{B,j}^{(l)}\right)}{\partial t}+\nabla_z\left(\bar{u}_z^{(l)}\cdot\bar{\varepsilon}_B^{(l)}\cdot\bar{c}_{B,j}^{(l)}\cdot A_B\right)=-\bar{R}_{t,B\to FL,j}^{(l)}\cdot S_B+\bar{R}_{B,j}^{(l)}\cdot A_B \tag{8.127}$$

This is the outcome of the averaging procedure for the **pseudo-continuous phase** in the bulk domain.

9. Averaging of the conservation equation for the ice phase in the frozen layer

The starting point is the equation of change for mass of the "ice" phase in the frozen layer domain in equation (8.21). Since the frozen layer contains only ice, the following procedure is proposed for averaging out r and θ :

The mass of the frozen layer per unit length of freezer is calculated in the following way:

$$m_{FL}^{(i)}\left(\delta_{FL}\right)=\pi\left[R^2-\left(R-\delta_{FL}\left(t,z\right)\right)^2\right]\cdot c_{FL}^{(i)} \tag{8.128}$$

Hence, the concentration of ice inside the frozen layer is determined from the following equation:

$$c_{FL}^{(i)}=\frac{m_{FL}^{(i)}\left(\delta_{FL}\right)}{\pi\left[R^2-\left(R-\delta_{FL}\left(t,z\right)\right)^2\right]} \tag{8.129}$$

The first term of equation (8.21) is rewritten as $\frac{\partial\left[m_{FL}^{(i)}\left(\delta_{FL}\right)\right]}{\partial t}$.

It is assumed there is no movement along the axial coordinate:

$$j_{m,FL,z}^{(i)} = 0 \tag{8.130}$$

The boundary of the frozen layer is moving along the radial coordinate.

The convective term in radial direction $\nabla_r\left(u_r^{(i)} \cdot c_{FL}^{(i)}\right)$

$$\int_0^{2\pi}\int_{R-\delta_{FL}}^{R} \frac{1}{r} \cdot \frac{\partial\left(r \cdot u_r^{(i)} \cdot c_{FL}^{(i)}\right)}{\partial r} \cdot r \cdot dr \cdot d\theta = 2\pi \cdot \left[R \cdot u_R^{(i)} \cdot c_{FL}^{(i)} - \left(R-\delta_{FL}\right) \cdot u_{R-\delta_{FL}}^{(i)} \cdot c_{FL}^{(i)}\right] \tag{8.131}$$

The velocity at the freezer wall is zero:

$$u_R^{(i)} = 0 \tag{8.132}$$

When applying equation (8.60):

$$\int_0^{2\pi}\int_{R-\delta_{FL}}^{R} \frac{1}{r} \cdot \frac{\partial\left(r \cdot u_r^{(i)} \cdot c_{FL}^{(i)}\right)}{\partial r} \cdot r \cdot dr \cdot d\theta = 2\pi \cdot \left(R-\delta_{FL}\right) \cdot \bar{R}_{t,m,B\to FL}^{(i)} \tag{8.133}$$

The convective term in radial direction $\nabla_\theta\left(j_{m,FL,\theta}^{(i)}\right)$:

$$\int_0^{2\pi}\int_{R-\delta_{FL}}^{R} \frac{1}{r} \cdot \frac{\partial\left(u_\theta^{(i)} \cdot c_{FL}^{(i)}\right)}{\partial \theta} \cdot r \cdot dr \cdot d\theta = \int_{R-\delta_{FL}}^{R} \left[\left(u_\theta^{(i)} \cdot c_{FL}^{(i)}\right)\Big|_{\theta=2\pi} - \left(u_\theta^{(i)} \cdot c_{FL}^{(i)}\right)\Big|_{\theta=0}\right] dr \tag{8.134}$$

The variation in time of the mass of the frozen layer:

$$\frac{\partial\left[m_{FL}^{(i)}\left(\delta_{FL}\right)\right]}{\partial t} - S_B \cdot \bar{R}_{t,m,B\to FL}^{(i)} - S_B \cdot \bar{R}_{t,B\to FL,w}^{(l)} = 0 \tag{8.135}$$

Or

$$\frac{\partial\left(\pi\left[R^2 - \left(R-\delta_{FL}\left(t,z\right)\right)^2\right] \cdot c_{FL}^{(i)}\right)}{\partial t} = S_B \cdot \bar{R}_{t,m,B\to FL}^{(i)} + S_B \cdot \bar{R}_{t,B\to FL,w}^{(l)} \tag{8.136}$$

The concentration of ice inside the frozen layer $c_{FL}^{(i)}$ is constant.

But:

$$-2\cdot\pi\cdot c_{FL}^{(i)}\cdot\frac{\partial\left(R-\delta_{FL}\right)}{\partial t}=S_B\cdot\bar{R}_{t,m,B\to FL}^{(i)}+S_B\cdot\bar{R}_{t,B\to FL,w}^{(l)} \tag{8.137}$$

From which results the conservation equation for the ice phase inside the frozen layer:

$$\frac{\partial\delta_{FL}\left(t,z\right)}{\partial t}=\frac{\bar{R}_{t,m,B\to FL}^{(i)}\left(t,z,s\right)+\bar{R}_{t,B\to FL,w}^{(l)}\left(t,z\right)}{c_{FL}^{(i)}\left(t,z\right)} \tag{8.138}$$

$m_{FL}^{(i)}$ = the mass of the frozen layer, $\left[kg/m\right]$

With the **initial condition**:

An initial concentration of ice is considered inside the frozen layer:

At $t=0$ $\delta_{FL}=\delta_{FL,0}\left(z\right)$ (8.139)

At $t=t_{s+}$ $\delta_{FL}=\delta_{FL,0}\left(z\right)$ (8.140)

10. Expression of the volume flow rate

Under the assumptions of incompressible fluid, steady state laminar flow, the z-component of the equation of motion in cylindrical coordinates will be:

$$\frac{\partial P}{\partial z}=-\left[\frac{1}{r}\cdot\frac{\partial\left(r\cdot\tau_{B,rz}\right)}{\partial r}\right]+\rho_B^{(i+l+a)}\cdot g_z \tag{8.141}$$

This equation is valid over the entire annular region for any kind of fluid.

If $\frac{\partial P}{\partial z}$ is assumed constant:

$$\Delta P=P_0-P_L \tag{8.142}$$

Equation (8.141) becomes:

$$\frac{1}{r}\cdot\frac{d\left(r\cdot\tau_{B,rz}\right)}{dr}=\frac{\Delta P}{L}+\rho_B^{(i+l+a)}\cdot g_z \tag{8.143}$$

(Fredrickson & Bird, 1958) integrate equation (8.143) to:

$$\tau_{B,rz} = \frac{F}{2} \cdot \left[r - \frac{\left(C_1 \cdot R\right)^2}{r} \right] \tag{8.144}$$

Where:

$$F = \frac{\Delta P}{L} + \rho_B^{(i+l+a)} \cdot g_z \tag{8.145}$$

List of symbols

F = the sum of forces per unit volume

C_1 = the constant of integration

R = the outer radius of the annulus

The radial distance $C_1 \cdot R$ represents the position at which $\tau_{B,rz} = 0$.

Equation (8.144) is the starting point for the derivation of an expression relating the flow rate to the pressure drop for laminar flow in an annulus.

For the power law model, the local shear stress depends on the local shear rate by:

$$\tau_{B,rz} = -K_B^{(i+l+a)} \cdot \left| \frac{\partial u_z}{\partial r} \right|^{n-1} \cdot \frac{\partial u_z}{\partial r} \tag{8.146}$$

Equations (8.144) and (8.146) are combined and integrated to give the velocity distribution:

$$u_z = R \cdot \left(\frac{F \cdot R}{2 \cdot K_B^{(i+l+a)}} \right)^{\frac{1}{n}} \cdot \int_{\Gamma_0}^{\Gamma} \left(\frac{C_1^2}{\Gamma} - \Gamma \right)^{\frac{1}{n}} d\Gamma \qquad \text{for} \qquad \Gamma_0 \le \Gamma \le C_1 \tag{8.147}$$

$$u_z = R \cdot \left(\frac{F \cdot R}{2 \cdot K_B^{(i+l+a)}} \right)^{\frac{1}{n}} \cdot \int_{\Gamma}^{1} \left(\Gamma - \frac{C_1^2}{\Gamma} \right)^{\frac{1}{n}} d\Gamma \qquad \text{for} \qquad C_1 \le \Gamma \le 1 \tag{8.148}$$

Where:

$$\Gamma = \frac{r}{R} \tag{8.149}$$

$$\Gamma_0 = \frac{R_0}{R} \tag{8.150}$$

List of symbols

Γ = the dimensionless radial coordinate, $[-]$

R_0 = the inner radius of the annulus, $[m]$

The boundary conditions:

At $\Gamma = \Gamma_0$ $\qquad u_z = 0$ (8.151)

At $\Gamma = 1$ $\qquad u_z = 0$ (8.152)

Both equations (8.147) and (8.148) must give the same value of the velocity at $\Gamma = C_1$. The constant of integration is determined as a function of Γ and $\frac{1}{n}$ from the equality of the two expressions for the velocity in equations (8.147) and (8.148):

$$\int_{\Gamma_0}^{C_1} \left(\frac{C_1^2}{\Gamma} - \Gamma \right)^{\frac{1}{n}} d\Gamma = \int_{C_1}^{1} \left(\Gamma - \frac{C_1^2}{\Gamma} \right)^{\frac{1}{n}} d\Gamma \tag{8.153}$$

This is the determining equation for C_1, which is a function of Γ_0 and $\frac{1}{n}$.

The volume rate of flow is determined by integrating the velocity distribution over the annular region:

$$\phi_{v,B}^{(i+l+a)} = 2\pi \cdot R^2 \cdot \int_{\Gamma_0}^{1} u_z \cdot \Gamma d\Gamma \tag{8.154}$$

Knowing C_1, equation (8.154) is easily integrated by Taylor series expansion to determine the volume rate of flow.

Equations (8.147) and (8.148) are substituted in equation (8.154) and one integration step is performed to give:

$$\phi_{v,B}^{(i+l+a)} = \pi \cdot R^3 \cdot \left(\frac{F \cdot R}{2 \cdot K_B^{(i+l+a)}} \right)^{\frac{1}{n}} \cdot \int_{\Gamma_0}^{1} \left| C_1^2 - \Gamma^2 \right|^{\frac{1}{n}+1} \cdot \Gamma^{-\frac{1}{n}} d\Gamma \tag{8.155}$$

$$\int_{\Gamma_0}^{1} \left| C_1^2 - \Gamma^2 \right|^{\frac{1}{n}+1} \cdot \Gamma^{-\frac{1}{n}} d\Gamma = \frac{n}{2n+1} \cdot \left[\left| C_1^2 - 1 \right|^{\frac{2n+1}{n}} - \Gamma_0^{-\frac{1}{n}} \cdot \left| C_1^2 - \Gamma^2 \right|^{\frac{2n+1}{n}} \right] \tag{8.156}$$

Replacing in equation (8.154):

$$\phi_{v,B}^{(i+l+a)} = \pi \cdot R^3 \cdot \left(\frac{F \cdot R}{2 \cdot K_B^{(i+l+a)}} \right)^{\frac{1}{n}} \cdot \frac{n}{2n+1} \cdot \left[\left| C_1^2 - \Gamma^2 \right|^{\frac{2n+1}{n}} - \Gamma_0^{-\frac{1}{n}} \cdot \left| C_1^2 - \Gamma_0^2 \right|^{\frac{2n+1}{n}} \right] \tag{8.157}$$

The expression of the flow is easily calculated once C_1 has been determined.

11. Physical properties for the simulation of the ice cream freezing model

Table 8.1. Overview of physical properties variables for the ice cream freezing model

Name		Symbol	Unit	Value
Density	Ice	$\rho^{(i)}$	$\left[kg/m^3\right]$	916.7
	Water	$\rho^{(w)}$	$\left[kg/m^3\right]$	999.8
	Sugar	$\rho^{(s)}$	$\left[kg/m^3\right]$	1600
	Fat	$\rho^{(f)}$	$\left[kg/m^3\right]$	900
	Other	$\rho^{(o)}$	$\left[kg/m^3\right]$	1996.6
Thermal conductivity	Ice	$\lambda^{(i)}$	$\left[W/m\cdot K\right]$	2.2
	Water	$\lambda^{(w)}$	$\left[W/m\cdot K\right]$	0.6
	Bulk	λ_B	$\left[W/m\cdot K\right]$	0.5
	Wall	$\lambda^{(wall)}$	$\left[W/m\cdot K\right]$	70
Heat transfer coefficient of coolant		$\alpha_{coolant}$	$\left[W/m^2\cdot K\right]$	12000
Specific heat	Ice	$C_p^{(i)}$	$\left[J/kg\cdot K\right]$	2000
	Water	$C_p^{(w)}$	$\left[J/kg\cdot K\right]$	4200
	Sugar	$C_p^{(s)}$	$\left[J/kg\cdot K\right]$	1100
	Fat	$C_p^{(f)}$	$\left[J/kg\cdot K\right]$	2100
	Other	$C_p^{(o)}$	$\left[J/kg\cdot K\right]$	1160
	Air	$C_p^{(a)}$	$\left[J/kg\cdot K\right]$	1000
Mass transfer coefficients	Ice in the B	$k_S^{(i)}$	$\left[m/s\right]$	10^{-6}
	Ice in the B due to temperature difference between B & FL	$k_{T,0}^{(i)}$	$\left[m/s\right]$	1
	Water from B to FL	$k_{B,w}^{(l)}$	$\left[m/s\right]$	10^4
Latent heat of crystallization		Δh_{cryst}	$\left[J/kg\right]$	$334\cdot10^3$
Standard melting temperature of water		T_m	$\left[K\right]$	273.15

12. The shrinking core model for the melting of an ice particle

The ice particle is submerged in a fluid with a higher temperature. The ice is surrounded by a stagnant (film) layer, while the rest of the fluid is turbulent.

From the pseudo-steady state energy balance around a spherical particle, the following result is obtained:

$$\frac{\partial}{\partial r}\left(r^2 \frac{\partial T}{\partial r} \right) = 0 \tag{8.158}$$

The boundary conditions for equation (8.158) are defined as:

a) At the interface between the particle and the fluid, $r = s^{(i)}$

$$T\Big|_{r=s^{(i)}} = T^{(i)} \tag{8.159}$$

b) At the interface between the fluid film and the fluid, $r = s^{(i)} + \delta$

$$T\Big|_{r=s^{(i)}+\delta} = T^{(f)} \tag{8.160}$$

By integration of equation (8.158) the temperature profile around a particle are obtained:

$$\frac{T - T^{(i)}}{T^{(f)} - T} = \left(\frac{1}{s^{(i)}} - \frac{1}{r} \right) \cdot \frac{\left(s^{(i)}\right)^2 + \delta \cdot s^{(i)}}{\delta} \tag{8.161}$$

The heat flow towards the surface of an ice particle is calculated as:

$$\phi_q = a^{(i)} \cdot \phi_q^*\Big|_{r=s^{(i)}} = 4 \cdot \pi \cdot \left(s^{(i)}\right)^2 \left(-\lambda^{(f)} \cdot \frac{dT}{dr}\Big|_{r=s^{(i)}} \right) \tag{8.162}$$

After differentiating equation (8.162) and substituting the result in equation (8.161), the following expression is obtained for the heat flow towards a single ice particle:

$$\phi_q = -4 \cdot \pi \cdot \lambda^{(f)} \cdot \frac{\left(s^{(i)}\right)^2 + \delta \cdot s^{(i)}}{\delta} \cdot \left(T - T^{(i)} \right) \tag{8.163}$$

It is common in modelling of crystallization processes to use a size dependent film layer:

$$\delta = s^{(i)} \tag{8.164}$$

When applying this size dependent layer the following equation is obtained:

$$\phi_q = -8 \cdot \pi \cdot \lambda^{(f)} \cdot s^{(i)} \cdot \left(T - T^{(i)} \right) \tag{8.165}$$

The melting rate for a single particle, determined under the assumption that all the heat is directed towards the particle meltdown, is determined from:

$$r_s^{(i)} = \frac{\phi_q}{\Delta h_{cryst}} \tag{8.166}$$

List of symbols

$T(r)$ = the temperature, $[K]$

r = the radial coordinate for a particle, $[m]$

$T^{(i)}$ = the temperature of the ice particle, $[K]$

$T^{(f)}$ = the temperature of the fluid, $[K]$

δ = the thickness of the fluid film, $[m]$

ϕ_q = heat flow towards a single particle, $[W]$

$a^{(i)}$ = surface area of a spherical particle, $[m^2]$

$\lambda^{(f)}$ = thermal conductivity of the fluid, $\left[W/m \cdot K \right]$

$r_s^{(i)}$ = melting rate for a single particle, $\left[kg/s \right]$

Δh_{cryst} = enthalpy of crystallization, $\left[J/kg \right]$

13. Mass conservation equations for the bulk domain expressed per unit length of freezer

Considering the definitions:

$$N_B^{(i)} = \bar{n}_B^{(i)} \cdot A_B \tag{8.167}$$

$$\Omega_{B,j}^{(l)} = \bar{\varepsilon}_B^{(l)} \cdot \bar{c}_{B,j}^{(l)} \cdot A_B \tag{8.168}$$

$$\Omega_B^{(a)} = \bar{\varepsilon}_B^{(a)} \cdot \bar{c}_B^{(a)} \cdot A_B \tag{8.169}$$

The equations of change are written in the following form:

$$\frac{\partial\left(N_B^{(i)}\right)}{\partial t}+\nabla_z\left(\bar{u}_z^{(i)}\cdot N_B^{(i)}\right)+\nabla_{s^{(i)}}\left(\bar{r}_s^{(i)}\cdot N_B^{(i)}\right)=\bar{B}_B^{(i)}\cdot A_B+\bar{R}_{t,FL\to B}^{(i)}\cdot S_B-\bar{D}_B^{(i)}\cdot A_B-\bar{R}_{t,B\to FL}^{(i)}\cdot S_B$$

$$\frac{\partial\left(\Omega_{B,j}^{(l)}\right)}{\partial t}+\nabla_z\left(\bar{u}_z^{(l)}\cdot\Omega_{B,j}^{(l)}\right)=-\bar{R}_{t,B\to FL,j}^{(l)}\cdot S_B+\bar{R}_{B,j}^{(l)}\cdot A_B \tag{8.170}$$

$$\frac{\partial\left(\Omega_B^{(a)}\right)}{\partial t}+\nabla_z\left(\bar{u}_z^{(a)}\cdot\Omega_B^{(a)}\right)=0$$

With the **initial conditions**:

$$\text{At } t=0 \qquad \begin{aligned} &N_B^{(i)}(0,z,s^{(i)})=N_{B,0}^{(i)}\left(z,s^{(i)}\right)\\ &\Omega_{B,j}^{(l)}\left(0,z\right)=\Omega_{B,j,0}^{(l)}\left(z\right)\\ &\Omega_B^{(a)}\left(0,z\right)=\Omega_{B,0}^{(a)}\left(z\right)\end{aligned} \tag{8.171}$$

The **boundary conditions**:

a) In axial direction

Continuity of fluxes:

$$\text{At } z=0 \qquad \begin{aligned} &\left(\bar{u}_z^{(i)}\cdot N_B^{(i)}\right)\Big|_{z=0}=\tilde{F}_B^{(i)}\left(t,s^{(i)}\right)\\ &\left(\bar{u}_z^{(l)}\cdot\Omega_{B,j}^{(l)}\right)\Big|_{z=0r}=F_{B,j,0}^{(l)}\left(t\right)\\ &\left(\bar{u}_z^{(a)}\cdot\Omega_B^{(a)}\right)\Big|_{z=0}=F_{B,0}^{(a)}\left(t\right)\end{aligned} \tag{8.172}$$

b) Along the internal coordinate

The boundary condition for the crystal size is put at the upper range of ice crystal size due to the size reduction by the melting of the particles

$$\text{At } s^{(i)}=s_{\max} \qquad N_B^{(i)}\left(t,z,s_{\max}\right)=N_{B,s_{\max}}^{(i)}\left(t,z\right) \tag{8.173}$$

$$N_{B,s_{\max}}^{(i)}\left(t,z\right)=0 \tag{8.174}$$

List of symbols

$N_{B,s_{\max}}^{(i)}$ = nucleation rate, $\left[\#/m\right]$

$\Omega_{B,j}^{(l)}$ = concentration of component j in the liquid phase in the bulk, $\left[kg/m\right]$

$\Omega_B^{(a)}$ = concentration of air in the bulk, $\left[kg/m\right]$

14. Conservation property of the overall amount of water

Water is present as:

(1) liquid water in the bulk domain

(2) ice particles in the bulk domain

(3) solid ice in the frozen layer

The total amount of water does not change when there is no chemical reaction involving water.

$$F_B^{(i)}(t,z)+F_{B,w}^{(l)}(t,z)=F_B^{(i)}(t,0)+F_{B,w}^{(l)}(t,0)=F_{B,0}(t) \tag{8.175}$$

The amount of water (in solid and liquid phase) should be conserved if it is assumed there is no accumulation in the frozen layer. For the following, the conservation equations will be used in the form expressed per unit length of freezer, as defined in Appendix 13.

The mass of an ice particle is considered as an internal coordinate, $s^{(i)}=m^{(i)}$.

The conservation equations are written in the following form:

$$\frac{\partial\left(N_B^{(i)}\right)}{\partial t}+\nabla_z\left(\bar{u}_z^{(i)}\cdot N_B^{(i)}\right)+\nabla_{s^{(i)}}\left(\bar{r}_s^{(i)}\cdot N_B^{(i)}\right)=\bar{B}_B^{(i)}\cdot A_B+\bar{R}_{t,FL\to B}^{(i)}\cdot S_B-\bar{D}_B^{(i)}\cdot A_B-\bar{R}_{t,B\to FL}^{(i)}\cdot S_B \tag{8.176}$$

$$\frac{\partial\left(\Omega_{B,w}^{(l)}\right)}{\partial t}+\nabla_z\left(\bar{u}_z^{(l)}\cdot\Omega_{B,w}^{(l)}\right)=\bar{R}_{t,FL\to B,w}^{(l)}\cdot S_B-\bar{R}_{t,B\to FL,w}^{(l)}\cdot S_B+\bar{R}_{B,w}^{(l)}\cdot A_B \tag{8.177}$$

The concentration of ice particles is determined in the following way:

$$\Omega_B^{(i)}=\int_0^\infty\left(N_B^{(i)}\cdot dm^{(i)}\right)=\int_0^\infty\left(N_B^{(i)}\cdot\frac{dm^{(i)}}{ds^{(i)}}\cdot ds^{(i)}\right)=\frac{dm^{(i)}}{ds^{(i)}}\cdot\int_0^\infty\left(N_B^{(i)}\cdot ds^{(i)}\right) \tag{8.178}$$

The following relation is introduced:

$$\frac{dm^{(i)}}{ds^{(i)}}=1\left[\frac{1}{\#}\right] \tag{8.179}$$

The integration of equation (8.176) for the s - coordinate, term by term:

$$\int_0^\infty\left(N_B^{(i)}\cdot ds^{(i)}\right)=\Omega_B^{(i)}\cdot\frac{ds^{(i)}}{dm^{(i)}} \tag{8.180}$$

$$\int_0^\infty\left(\bar{u}_z^{(i)}\cdot N_B^{(i)}\cdot ds^{(i)}\right)=\bar{u}_z^{(i)}\cdot\Omega_B^{(i)}\cdot\frac{ds^{(i)}}{dm^{(i)}} \tag{8.181}$$

$$\int_0^\infty\frac{d}{ds^{(i)}}\left(\bar{r}_s^{(i)}\cdot N_B^{(i)}\cdot ds^{(i)}\right)=\bar{r}_s^{(i)}\cdot\Omega_B^{(i)}\Big|_0^\infty \tag{8.182}$$

For $s^{(i)} = s_{\max}^{(i)}$ $\qquad \bar{r}_s^{(i)} \cdot \Omega_B^{(i)} = 0$ (8.183)

It is assumed that particles with the size $s^{(i)} = 0$ cannot appear, hence:

$$\bar{r}_s^{(i)}\Big|_{s^{(i)}=0} = 0 \tag{8.184}$$

The rate of change of ice in the bulk should be equal with the rate of change of the water in the liquid phase in the bulk:

$$\int_0^{\infty} B_B^{(i)} \cdot ds^{(i)} - \int_0^{\infty} D_{m,B}^{(i)} \cdot ds^{(i)} - \int_0^{\infty} \frac{d}{ds^{(i)}}\left(\bar{r}_s^{(i)} \cdot N_B^{(i)} \cdot ds^{(i)}\right) + R_{B,w}^{(l)} = 0 \tag{8.185}$$

The frozen layer it is assumed to have a constant hold-up at each location. The particle fluxes in and out the frozen layer must be equal:

$$\int_0^{\infty} R_{t,FL\to B}^{(i)} \cdot ds^{(i)} - \int_0^{\infty} R_{t,B\to FL}^{(i)} \cdot ds^{(i)} + R_{t,FL\to B,w}^{(l)} - R_{t,B\to FL,w}^{(l)} = 0 \tag{8.186}$$

By adding the equations (8.176) and (8.177):

$$\frac{\partial\left(\Omega_B^{(i)} \cdot \frac{ds^{(i)}}{dm^{(i)}} + \Omega_{B,w}^{(l)}\right)}{\partial t} + \frac{\partial\left(\bar{u}_z^{(i)} \cdot \Omega_B^{(i)} \cdot \frac{ds^{(i)}}{dm^{(i)}} + \bar{u}_z^{(l)} \cdot \Omega_{B,w}^{(l)}\right)}{\partial z} = 0 \tag{8.187}$$

After taking into account equation (8.175):

$$\frac{\partial\left(\Omega_B^{(i)} + \Omega_{B,w}^{(l)}\right)}{\partial t} + \frac{\partial\left(\bar{u}_z^{(i)} \cdot \Omega_B^{(i)} + \bar{u}_z^{(l)} \cdot \Omega_{B,w}^{(l)}\right)}{\partial z} = 0 \tag{8.188}$$

Assuming steady state and integrating for the length of the freezer:

$$\int_0^{z}\left(\bar{u}_z^{(i)} \cdot \Omega_B^{(i)} + \bar{u}_z^{(l)} \cdot \Omega_{B,w}^{(l)}\right) dz = 0 \tag{8.189}$$

After the integration:

$$\bar{u}_z^{(i)} \cdot \Omega_B^{(i)}\Big|_{t,z} - \bar{u}_z^{(i)} \cdot \Omega_B^{(i)}\Big|_{t,0} + \bar{u}_z^{(l)} \cdot \Omega_{B,w}^{(l)}\Big|_{t,z} - \bar{u}_z^{(l)} \cdot \Omega_{B,w}^{(l)}\Big|_{t,0} = 0 \tag{8.190}$$

Considering the definitions of the flows:

$$\bar{u}_z^{(i)} \cdot \Omega_B^{(i)}\Big|_{t,0} = F_{B,0}^{(i)} \tag{8.191}$$

$$\bar{u}_z^{(l)} \cdot \Omega_{B,w}^{(l)}\Big|_{t,0} = F_{B,w,0}^{(l)} \tag{8.192}$$

$$\bar{u}_z^{(i)} \cdot \Omega_B^{(i)}\Big|_{t,z} = F_B^{(i)} \tag{8.193}$$

$$\bar{u}_z^{(l)} \cdot \Omega_{B,w}^{(l)} \Big|_{t,z} = F_{B,w}^{(l)} \tag{8.194}$$

Equation (8.175) is obtained.

15. Singular vectors for the SVD on the model parameters

15.1. Operational parameters

Table 8.2. Singular vectors for SVD on the operational parameters of the model

Input	Scaled singular vectors		Output
	u_1	v_1	
P_0	-2.2e-15	-0.44232	$T_{out}^{(ic)}$
$T_{B,0}$	0.086819	0.506063	$x_{out,w}^{(ic)}$
T_c	0.552294	-0.26831	$x_{out,i}^{(ic)}$
		-0.02409	$d_{4,3}^{(i)}$
$F_{in}^{(ic)}$	0.573117	-0.0303	$d_{3,2}^{(i)}$
		-0.6749	ΔP
ω_r	0.599142	-0.13886	Q_{tot}

15.2. Input parameters

Table 8.3. Singular vectors for SVD on the input parameters of the model

Input	Scaled singular vectors				Output
	u_1	u_2	v_1	v_2	
$x_{B,w,0}^{(l)}$	0.700519	0.324062	-0.41762	-0.36569	$T_{out}^{(ic)}$
$x_{B,s,0}^{(l)}$	0.072802	0.188483	0.38732	-0.23308	$x_{out,i}^{(ic)}$
$x_{B,f,0}^{(l)}$	0. 604682	0.098289	-0.16648	0.837098	$x_{out,w}^{(ic)}$
$x_{B,o,0}^{(l)}$	0.000188	0.00049	0.036041	-0.07859	$d_{4,3}^{(i)}$
Ovr	-0.02235	-0.39619	0.043712	-0.09815	$d_{3,2}^{(i)}$
M_s	0.371258	-0.83236	-0.75834	-0.19433	ΔP
			0.263771	-0.24008	Q_{tot}

15.3. Freezer design parameters

Table 8.4. Singular vectors for SVD on the freezer design parameters of the model

Input	Scaled singular vectors				Output
	u_1	u_2	v_1	v_2	
L	-0.08129	-0.60258	0.425611	-0.47097	$T_{out}^{(ic)}$
D	0.986003	0.057741	-0.41509	0.467772	$x_{out,w}^{(ic)}$
D_0	0.073692	-0.64664	0.220077	-0.24801	$x_{out,i}^{(ic)}$
			0.013769	0.009756	$d_{4,3}^{(i)}$
δ_{wall}	0.088767	-0.3282	0.017164	0.011687	$d_{3,2}^{(i)}$
			-0.74512	-0.66639	ΔP
δ_{blade}	0.088767	-0.3282	0.206008	-0.23142	Q_{tot}

15.4. Empirical parameters

Table 8.5. Singular vectors for SVD on the empirical parameters of the model

Input	Scaled singular vectors				Output
	u_1	u_2	v_1	v_2	
C_a	0.46419	-0.04306	-0.42951	-0.00524	$T_{out}^{(ic)}$
C_b	0.494268	-0.07836			
C_c	0.000224	5.44e-06	0.438453	0.000994	$x_{out,w}^{(ic)}$
Φ	-0.04759	0.008085			
C_γ	-0.00041	-0.00043	-0.23251	-0.00053	$x_{out,i}^{(ic)}$
c_1	0.231014	-0.02116			
c_2	0.464195	-0.04309	-0.01294	0.622092	$d_{4,3}^{(i)}$
n_ω	0.026641	0.553067			
k_ω	0.106593	0.43135	-0.01671	0.782451	$d_{3,2}^{(i)}$
Λ	00.494268	-0.07836	-0.72244	-0.02683	ΔP
Σ	0.026641	0.553067	-0.21627	0.00492	Q_{tot}
$\delta_{FL,min}$	0.109704	0.430891			

16. References

Bird, B.R., Stewart, W.E., Lightfoot, E.N. (2002). Transport phenomena, *John Wiley & Sons*

Fredrickson, A.G., Bird, R. B. (1958). Non-Newtonian Flow in Annuli, *Industrial and Engineering Chemistry* 50, 347

Hoffman, J. D. (2001). Numerical methods for engineers and scientists, 2nd Edition, *Marcel Dekker, Inc.*, New York

Curriculum Vitae

Bogdan Dorneanu was born in Medgidia, Romania, on the 21st of July 1981.

In 2000 he completed his high-school studies and graduated from the Nicolae Bălcescu Highschool (Medgidia) majoring in Mathematics and Physics. In the same year he started his university education at University Politehnica of Bucharest, Romania and in 2005 he received a degree in Chemical Engineering.

During his university studies he spent a 3-month internship at the Laboratoire de Génie des Procédés des Solides Divisés, at Ecole des Mines d'Albi-Carmaux, France, working on the experimental and modelling of the pyrolysis of cellulose.

In January 2006 he was appointed as PhD student for the Product and Process Engineering group at DelftChemTech, Faculty of Applied Sciences, at Delft University of Technology under the supervision of Prof. Johan Grievink and Dr. Costin Sorin Bildea. His research was carried on under a Marie Curie fellowship in the framework of the PRISM project.

During the PhD period, Bogdan attended several advanced courses on Plantwide Control, Separation Processes, Optimization and Control, Product and Process Design and Modelling, Computational Fluid Dynamics and Process Intesification in United Kingdom, Czech Republic, Spain, Denmark and The Netherlands. He also spent three months as a visiting researcher at the Jožef Stefan Institute, in Ljubljana, Slovenia, working on the improvement of a vinyl acetate polymerization reactor model.

The results of Bogdan's research have been preesented locally and internationally in CACE-symposia and congresses (NPS6 – 10, ESCAPE 17 – 21, NL-GUTS). For the last four years, he was additionally involved in the supervision of undergraduate students during their graduations projects.

Presently he works as a Post Doc researcher at the Joint Research Centre of the European Commission, at the Institute for the Protection and Security of the Citizen, the Security Technology Assessment Unit, in Ispra, Italy, on the modelling of critical infrastructures failures.

Publications

Journals and conference proceedings

1. Dorneanu, B., Bildea, C.S., Grievink, J. *On the application of model reduction to plantwide control*, Computer Aided Chemical Engineering, Vol. 24, 2007, 823
2. Dorneanu, B., Bildea, C.S., Grievink, J. *Model reduction techniques for dynamic optimization of chemical plants operation*, Computer Aided Chemical Engineering, Vol. 25, 2008, 337
3. Dorneanu, B., Bildea, C.S., Grievink, J. *On the application of model reduction to plantwide control*, Computers and Chemical Engineering, Vol. 33 (3), 2009, 699
4. Dorneanu, B., Bildea, C.S., Grievink, J., Bongers, P.M. *A first-principles model for the freezing step in ice cream manufacture*, Computer-Aided Chemical Engineering, Vol. 26, 2009, 171
5. Dorneanu, B., Bildea, C.S., Grievink, J., Bongers, P.M. *A reduced model for the freezing step in ice cream manufacture*, Computer-Aided Chemical Engineering, Vol. 28, 2010, 265
6. Dorneanu, B., Bildea, C.S., Grievink, J. Process modeling and model reduction for chemical engineering applications, 21st European Symposium on Computer-Aided Process Engineering, Greece, May 2011

Acknowledgement

This thesis is the result of my research during the period of 2006 to 2010 at the Delft University of Technology, on knowledge-based tools for process systems engineering. At this time, I wish to express my gratitude to all the people who have contributed to this thesis, although unfortunately I am able to mention just a few.

Firstly, I would like to thank my two supervisors, Johan Grievink, and Sorin Bildea for their support during this research project. Your support, advice and encouragement ensured the success of the work and the completion of this book. Although you often asked me to be careful not to be pushed in two opposite directions due to your different ways of thinking, I have realized that actually the path was somewhere in the middle… Now, every Tuesday afternoon it will be somewhat empty without our discussions and the green tea.

Secondly, I would like to thank all my colleagues and students at the Product and Process Engineering Group. My first (and part-time) office colleagues Marco and Peter: your presence was often greatly missed. It follows a long list of people that helped creating a special (and more social) atmosphere in the Proeffabriek: David, Malte, Renske, David, Nasim, Pietro, Bashar, Ivan, as well as the members of the "staff": Mark, Mojgan, Caroline, Ruud, Henk. Listing all the memories of the coffee breaks, barbecues, Sinterklaas or Christmas parties would require another thesis, not to mention the conferences, courses or workshops. I look happily back at the days at the office and I thank you all!

Un mulțumesc Olgăi, care s-a lăsat convinsă să aplice la Delft pentru a ajuta la creșterea numărului de români din Olanda. Ajută enorm când e cineva cu care te înțelegi într-un mediu nou. Discuțiile de pe mess, telefon și prânz au fost mereu extreme de… interesante. Ca să nu mai vorbim de micul dejun de la Scally's, duminca la 10:00.

Apoi, un mulțumesc părinților mei. Cei care au fost permanent alături de mine și care, în același timp, mi-au permis să îmi găsesc drumul de unul singur. Vă mulțumesc!

Finally, Jo, thank you for being next to me and for your understanding during the last year of my thesis work!

Bogdan